A Random Matrix Model for Two-Colour QCD at Non-Zero Quark Density

Michael James Phillips

Department of Mathematical Sciences

Brunel University

In partial fulfillment of the requirements for the degree of

Doctor of Philosophy

December 2010

Abstract

We solve a random matrix ensemble called the chiral Ginibre orthogonal ensemble, or chGinOE. This non-Hermitian ensemble has applications to modelling particular low-energy limits of two-colour quantum chromodynamics (QCD). In particular, the matrices model the Dirac operator for quarks in the presence of a gluon gauge field of fixed topology, with an arbitrary number of flavours of virtual quarks and a non-zero quark chemical potential.

We derive the joint probability density function (JPDF) of eigenvalues for this ensemble for finite matrix size N, which we then write in a factorised form. We then present two different methods for determining the correlation functions, resulting in compact expressions involving Pfaffians containing the associated kernel. We determine the microscopic large-N limits at strong and weak non-Hermiticity (required for physical applications) for both the real and complex eigenvalue densities. Various other properties of the ensemble are also investigated, including the skew-orthogonal polynomials and the fraction of eigenvalues that are real.

A number of the techniques that we develop have more general applicability within random matrix theory, some of which we also explore in this thesis.

Acknowledgements

First and foremost, I should like to thank my supervisor, Prof. Gernot Akemann, for all his help and encouragement over the last three or so years. The working relationship between a graduate student and his supervisor should always, ideally, be a close one, but I believe that I have been particularly fortunate; I feel that Gernot has treated me more as a co-worker than as a student, and has generously granted me almost unlimited access to his wisdom and experience.

I should also like to extend my thanks to three of our co-authors, namely Prof. Hans-Jürgen Sommers, Dr Leonid Shifrin and Dr Mario Kieburg, all of whom have been most patient in helping me to gain a deeper understanding of various aspects of Random Matrix Theory. Correspondence with two of our other collaborators, Mr Takuya Kanazawa and Prof. Tilo Wettig, together with Dr Jacques Bloch, has always been most enlightening.

Thanks are also due to my second supervisor at Brunel, Dr Dmitry Savin, and to my (now, sadly, former) colleague in the Mathematical Physics group, Dr Pierpaolo Vivo, for the many hours of interesting and stimulating conversations that we have had. I have also benefited greatly from the workshops and departmental seminars organised by Gernot and Dmitry, together with Dr Igor Krasovsky and Dr Igor Smolyarenko.

The support from Ms Kay Lawrence and the other members of the management and administration team in the Mathematics Department has been invaluable.

Finally, I am especially grateful to the Engineering and Physical Sciences Research Council (EPSRC) for providing the funding for my research through a doctoral training grant.

Previously Published Work

I have co-authored the following papers during my period of registration at Brunel University:

[Ake09a] G. Akemann, M.J. Phillips and H.-J. Sommers, *J. Phys.* **A 42** (2009) 012001.

[Ake09b] G. Akemann, M.J. Phillips and L. Shifrin, *J. Math. Phys.* **50** (2009) 063504.

[Ake09c] G. Akemann, E. Bittner, M.J. Phillips and L. Shifrin, *Phys. Rev.* **E 80** (2009) 065201 (R).

[Ake10a] G. Akemann, M.J. Phillips and H.-J. Sommers, *J. Phys.* **A 43** (2010) 085211.

[Ake10b] G. Akemann, M. Kieburg and M.J. Phillips, *J. Phys.* **A 43** (2010) 375207.

[Ake11] G. Akemann, T. Kanazawa, M.J. Phillips and T. Wettig, *JHEP* **1103** (2011) 066.

This thesis contains material published in [Ake09a; Ake10a; Ake10b; Ake11]; material from [Ake09b; Ake09c] is not included here. The correspondence between chapters in this thesis and the papers published is not one-to-one, and so we provide further details on page 174 of where particular results first appeared.

Contents

List of Tables

List of Figures

Chapter 1

Introduction

1.1 Overview

We solve a random matrix ensemble called the chiral Ginibre orthogonal ensemble (chGinOE), which has applications to modelling certain low-energy limits of two-colour quantum chromodynamics (QCD) in the presence of a non-zero quark chemical potential. The matrices in this ensemble have a particular off-diagonal ('chiral') block structure, with the matrix dimensions being characterised by two parameters, N (related to the volume of the physical system) and ν (the number of exactly-zero eigenvalues of the Dirac operator for the quarks in a certain topology of the gluon gauge field). The non-zero matrix elements are real, and can be written in terms of normally-distributed variables. However, the probability distribution may be further modified by the addition of extra factors to the weight function which correspond to the presence of virtual quarks. These factors take the form of determinants, or characteristic polynomials, involving the masses of the different types (flavours) of quark.

This ensemble may be considered as, equivalently,[1]

1. the chiral (or Wishart-Laguerre) extension of the Ginibre ensemble with Dyson index $\beta = 1$ (i.e. matrices with real-valued elements) known as the GinOE, with an arbitrary non-Hermiticity parameter and additional mass-dependent determinant factors, or

2. the non-Hermitian generalisation of the chiral Gaussian orthogonal ensemble (chGOE) introduced by Verbaarschot, or

[1] We give further details and references in the next chapter.

3. the $\beta = 1$ version of the non-Hermitian chiral ensembles previously introduced and solved by Osborn (chGinUE, with $\beta = 2$) and Akemann (chGinSE, with $\beta = 4$).

The solution of our ensemble therefore completes the programme of solving the chiral Gaussian ensembles at arbitrary non-Hermiticity.

Compared with the Ginibre ensembles for $\beta = 2$ and $\beta = 4$ (complex and quaternion-real elements respectively), the Ginibre $\beta = 1$ case has a number of difficult features (for example, a finite fraction of eigenvalues are real), and so was fully solved only very recently. Our ensemble inherits many of the properties of this ensemble, but with additional complexity due to the chiral structure and the additional factors dependent on the quark masses.

We derive the joint probability density function (JPDF) of eigenvalues for this ensemble for finite matrix size N, and compact expressions for the various correlation functions in terms of the associated kernel. We determine the large-N limits at strong and weak non-Hermiticity, for the densities of both real and complex eigenvalues; these large-N limits are required for physical applications.

In this work we focus on the mathematical properties of the random matrix ensemble, rather than on the physics. Work to compare our predictions for the eigenvalue densities with results from computer simulations of QCD (lattice gauge theory or LGT) is currently in progress, although that does not form part of this thesis. However, it is important to point out that, under certain circumstances (e.g. two-colour QCD with non-degenerate quark masses at non-zero chemical potential), numerical solutions of QCD may not be possible at all, due to the infamous 'sign problem', and so random matrix theory (RMT) is in a position to provide genuinely new insight into the nature of the solutions.

1.2 Outline of thesis

In Chapter 2 we give a brief historical review of random matrix theory (RMT), followed by an introduction to the application of RMT to the modelling of quantum chromodynamics (QCD). We then outline the specific physical arguments that lead to our model.

In Chapter 3 we derive the joint probability density function (JPDF) of eigenvalues for the chGinOE, starting from the JPDF of matrix elements. The chiral

nature of the ensemble, the non-Hermiticity and the reality of the matrix elements all present their own challenges.

In Chapter 4 we show how the JPDF can be written in a factorised form involving a skew-symmetric (i.e. anti-symmetric) bivariate weight function. Many of the properties of our ensemble, such as the correlation functions, can be written in terms of the kernel and the skew-orthogonal polynomials associated with this weight function, and so we discuss some of the more elementary general properties of skew-symmetric measures in §4.2. We then derive generic formulas for the correlation functions in terms of the kernel; these can be obtained in two different ways, and we present both.

In Chapter 5 we derive explicit formulas for the kernels and skew-orthogonal polynomials for the chGinOE at finite N. The unquenched quantities (i.e. for the case where we include the effects of virtual quarks) can be most conveniently expressed in terms of the corresponding quenched ones (where the virtual quarks are absent), as we demonstrate.

Chapters 6, 7 and 8 consider the quenched ensemble. Chapter 6 covers the finite-N densities, and we also investigate how the number of eigenvalues that are real depends on the matrix size N. We then look briefly at the macroscopic large-N limit.

In Chapter 7 we turn our attention to the first of two microscopic large-N limits, namely the strongly non-Hermitian limit, which has physical applications to QCD at very high quark density.

In Chapter 8 we look at a different microscopic large-N limit, that of weak non-Hermiticity, which has physical applications when the quark density is low. For the density of real eigenvalues, taking this limit poses a technical challenge because the limit operation for large N does not commute with the integral in the finite-N expression (as is also the case with the Hermitian chGOE).

Chapter 9 extends the previous three chapters to the case when virtual quarks are considered (i.e. the mass-dependent determinant factors are present in the weight function), also drawing on earlier results from Chapter 5. We show that, when the quark masses are not degenerate, then there may be regions of the complex plane where the eigenvalue density oscillates rapidly between extremely large positive and negative values. Using approximations for the various kernels, we identify the boundaries of these regions for the cases with one and two virtual quark flavours.

In Chapter 10 we present a brief numerical investigation into universality, by using Monte Carlo simulations to compare the densities of real eigenvalues at weak non-Hermiticity, for several different random matrix ensembles that all share the chiral block structure, and that all have real-valued elements.

Finally we present a conclusion in Chapter 11, where we summarise what we have achieved, and discuss some of the problems that still remain outstanding.

Appendix A presents some elementary results that are used in the rest of the text, and also provides an introduction to Grassmann variables and Berezin integration used in Chapter 5.

Appendix B gives a proof of some useful generic formulas for expressing skew-orthogonal polynomials as matrix expectations, valid for a wide range of ensembles.

The remaining two appendices show how some of the techniques that we have used for the $\beta = 1$ chiral ensemble can also be applied to other ensembles. In particular, Appendix C shows how the $\beta = 4$ chiral ensemble (chGinSE) has the same algebraic structure as the chGinOE discussed in Chapter 4, and hence how the correlation functions can be expressed in a similar way. And in Appendix D we use the techniques developed in Chapter 5 to derive the kernel and the skew-orthogonal polynomials for the (non-chiral) Ginibre $\beta = 1$ ensemble (GinOE).

Finally, on page 174, we provide specific details of which results in this thesis have been previously published by us (and in which paper), and which results are new.

Chapter 2

Background: RMT and QCD

2.1 Random matrix theory

Random matrix theory (RMT) is the branch of mathematics concerned with examining the properties of matrices whose elements are random variables. A particular interest is in the statistical properties – such as the correlation functions, spacing distributions, and so on – of the eigenvalues. RMT has many practical applications, especially in quantum physics where random matrices are often used to model the spectra of highly complex systems.

A key point is the concept of universality: In the limit of infinitely large matrix size, certain statistical properties of the eigenvalues are found to be independent of the precise probability distributions of the matrix elements, and depend only on the symmetries of the matrices. This is after a suitable rescaling (known as unfolding), so that the average eigenvalue separation is unity.

There are many excellent introductory and general reviews of RMT. For short overviews, we refer to [Ste01; For03], and to the seminal textbook [Meh04] for an introduction to many of the more important mathematical ideas. We refer to [Kho09] for an overview of non-Hermitian RMT (which is particularly relevant to this thesis), and to [Tra00] which provides a brief review of universality.

2.1.1 Early historical review

Some of the earliest known work on RMT was undertaken by Wishart [Wis28] who considered the probability distributions of the matrix $W = AA^T$, where the elements in a given column of the rectangular matrix A are real and have Gaussian

distributions (and are correlated). Recent extensions of this work are discussed in [Jan03].

However, interest in the field increased considerably some quarter of a century later, when Wigner (see e.g. [Wig51; Wig55; Wig58]) used random matrices to model certain statistical properties of the energy levels of excitations of heavy nuclei. Because the interactions within these nuclei are so complicated and so numerous, it is impossible to model them exactly. On a local scale (i.e. after unfolding), it makes more sense to consider the energy levels statistically, and so Wigner suggested replacing the Hamiltonian with a large random symmetric matrix. The observed energy levels appear to repel one another; after rescaling, the distribution of nearest-neighbour spacings obeys very closely the so-called Wigner distribution

$$p(s) = \frac{\pi}{2}\, s e^{-\pi s^2/4}. \tag{2.1}$$

This formula is a very good approximation for the spacing distribution of the eigenvalues of large random symmetric matrices (and in fact is exact for the 2-by-2 case). This is distinct from the Poisson distribution which would be expected if there were no correlations between eigenvalues. Furthermore, it appeared that the same random matrix model could be used for many different kinds of nuclei, implying that the eigenvalue spacing distributions may be universal.

Wigner also explored some of the so-called macroscopic properties of the eigenvalue distributions (i.e. under a rescaling such that the support of the eigenvalues remains finite as the matrix size $N \to \infty$), deriving the famous semi-circle distribution for the eigenvalues of certain ensembles.

Subsequent work by Mehta, Gaudin and des Cloizeaux [Meh60a; Meh60b; Gau61; desC73] verified the accuracy of the semi-circle law, but showed that the Wigner distribution does indeed only give an approximate spacing distribution for eigenvalues of matrices of large size.

It was Dyson [Dys62a; Dys62b; Dys62c; Dys62d; Dys62e] who undertook a more systematic study of the ensembles concerned. He showed that there are three distinct classes of ensemble, and related these to different symmetry patterns under time reversal of the corresponding quantum Hamiltonians.

2.1.2 Hermitian ensembles

Amongst the first ensembles to be systematically studied, and still arguably the most important, are the Hermitian random matrices with independently-distributed

Gaussian elements (referred to now as the Wigner-Dyson ensembles). The symmetries of quantum mechanical systems necessitate the use of real, complex or quaternion-real matrix elements, with β =1, 2 or 4 (real) degrees of freedom per matrix element respectively. These ensembles are known as the Gaussian orthogonal, unitary and symplectic ensembles respectively (GOE, GUE and GSE), because of their invariance under the corresponding transformations, and the parameter β is called the Dyson index.

The joint probability density function (JPDF) of eigenvalues for these (and many other) ensembles can generally be written as a product of weight functions multiplied by the Jacobian of the transformation (from matrix elements to eigenvalues), which has the form of the absolute value of the Vandermonde determinant to the power of β, where the Vandermonde determinant is defined as

$$\Delta_N(\{z\}) \equiv \det\left[z_i^{j-1}\right]_{1\leq i,j\leq N} = \prod_{1\leq i<j\leq N}(z_j - z_i). \tag{2.2}$$

The repulsion of adjacent eigenvalues can then be understood from this.

Let us be specific and consider the $\beta = 2$ case (the GUE) with N-by-N matrices, whose weight function $w(x) = \exp(-cx^2)$ for some scaling parameter c. The JPDF of the eigenvalues (which are all real) is then given by

$$P_N(x_1, x_2, \ldots, x_N) \propto |\Delta_N(\{x\})|^2 \prod_{i=1}^{N} w(x_i). \tag{2.3}$$

Using the orthogonal polynomial method (see [Meh04]), one first rewrites the Vandermonde determinant in terms of the set of polynomials that are orthogonal with respect to the weight. It is then possible to write the JPDF as a determinant of the associated kernels. Multiple application of Dyson's Integration Theorem (see §4.3.1) allows one to obtain the various correlation functions, also expressed as determinants of kernels. Finally, large-N limits of the correlation functions can be obtained by determining the asymptotic behaviour of the polynomials and kernels.

For the $\beta = 1$ and $\beta = 4$ ensembles, it is convenient to introduce quaternions (see e.g. [Dys70; Mah91; Meh04]) built from skew-orthogonal polynomials, and express the correlation functions in terms of so-called quaternion determinants (which are closely related to Pfaffians). We demonstrate this for the chGinOE in Chapter 4.

2.1.3 Non-Hermitian ensembles

The non-Hermitian Gaussian ensembles were first considered by Ginibre [Gin65]; this was originally out of mathematical interest, although more recently many practical applications have been found (we list a few in §2.1.5). As with the Hermitian case, there are three ensembles, labelled GinOE, GinUE and GinSE. Girko (see e.g. [Gir84]) discovered that the eigenvalues (now complex-valued) have circular support at large N, and that the density is constant within this circle.

Although Ginibre's original interest was in ensembles with maximal non-Hermiticity, it was not long before ensembles that interpolated between the Hermitian and maximally non-Hermitian cases were considered. Such ensembles are often termed the elliptic ensembles, because the complex eigenvalues lie in an ellipse (see [Somm88]).

A surprising fact is that, at large N, a new scaling regime actually lies between the Hermitian and the elliptic ensembles, where the non-Hermiticity is very weak [Fyo97a; Fyo97b]. The extent to which the behaviour is independent of the particular small deformation applied to the Hermitian matrices is considered in [Fyo98]; and for a more recent review, see [Fyo03].

Although Ginibre had solved the $\beta = 2$ (GinUE) and $\beta = 4$ (GinSE) ensembles at maximal Hermiticity, the $\beta = 1$ ensemble (GinOE) remained only partly solved. The difficulty here arose because a finite fraction of eigenvalues are real, or, equivalently, the weight function is singular on the real axis. Because of this problem, it took many more decades before a complete solution was found. Since the chGinOE presented in this thesis is, essentially, the chiral equivalent of the GinOE, we now briefly review the sequence of steps taken to solve the Ginibre case.

Ginibre himself had managed to show that when all the eigenvalues are real, then their distribution is the same as for the GOE. [Lehm91] derived the JPDF (for the elliptic case) but not in a form that allowed direct application of Dyson's Integration Theorem to generate expressions for the correlation functions. [Ede94] determined the expected number of eigenvalues that are real. The same author [Ede97] rediscovered the JPDF, and derived the density of complex eigenvalues at finite matrix size N, together with particular cases of the probability $p_{N,k}$ that k eigenvalues are real in an N-by-N matrix (including the probability that all the eigenvalues are real). However, his formulas were cumbersome, and [Kanz05; Ake07d] subsequently

derived more useable expressions for $p_{N,k}$, and, importantly, also showed that the complex correlations could be expressed as Pfaffians.

The key step of treating real and complex eigenvalues together was taken in [Sin06] who found expressions for the weighted average of some function of the eigenvalues. This is essentially an extension of the de Bruijn formulas [deB55].

Then, almost simultaneously, three independent groups of researchers made the final breakthrough; [Bor07] found the general formula for the correlations, expressed as a Pfaffian. [For07] introduced the specific skew-orthogonal polynomials that are required (with a later proof in [For08]), and [Somm07] derived the results in an alternative manner, further expanded in [Somm08].

The extension to odd matrix size N was analysed in [For09; Sin09], and work to understand certain scaling limits was presented in [Bor09].

2.1.4 Mathematical techniques[1]

A number of techniques have been adopted for solving RMT models. Apart from the method of orthogonal [Dei00; Meh04] and skew-orthogonal [Adl99; Eyn01; Gho02; Gho09] polynomials already mentioned, other techniques include the use of supersymmetry [Zuk94; Efe97a; Ver04], and the replica method [Kanz09].

2.1.5 Recent applications

Probably the most significant applications of RMT are in the field of quantum physics. For an in-depth review of such applications, see [Guh98].

In addition to modelling nuclear energy levels, it has been conjectured [Boh84] that RMT explains the eigenvalue statistics of quantum chaotic systems (the quantum analogues of systems that are classically chaotic), such as certain billiard systems (see [Sto99; Haa01]) including quantum dots. An explanation for the quantum chaos/RMT link was given in [Heu07].

Other quantum applications include disordered mesoscopic systems (e.g. universal conductance fluctuations in electronic transport problems, Anderson localisation, etc.; see [Efe97a]), 2D quantum gravity [DiF95], and modelling the Euclidean QCD Dirac operator (see §2.2).

[1] Some of the references in this section and the next are to review papers and textbooks.

An important purely mathematical application is in number theory, where the positions of the zeros of the Riemann zeta function appear to be described, statistically, by random matrix theory [Mon73]. For reviews, we refer to [Con00; Kea03].

And in finance, RMT can be used to model correlation matrices, see [Bou09] for a review.

Applications of non-Hermitian RMT include random neural networks [Somp88], directed quantum chaos [Efe97b], random quantum maps [Bru09], QCD in the presence of a quark chemical potential (see §2.2), and delayed time series in financial markets [Kwa06].

2.2 Random matrices and QCD

2.2.1 QCD essentials

In order to provide motivation for our work, it is useful to review very briefly some of the facets of quantum chromodynamics (QCD) that are particularly relevant. Our aim is certainly not to provide a comprehensive review of QCD, nor even a modest pedagogical introduction, and we do not provide references for results that are now considered standard. For further details, we suggest the following textbooks: [Smi01; Ynd06] on general aspects of QCD, [Now96; Rip97; Hos01] on issues concerning chiral symmetry, and [Shu04; Kog04; Rho08] on QCD under extreme conditions. There is, of course, much overlap in the material covered in these books.

QCD is the most generally accepted theory of the strong nuclear interaction, with compelling experimental evidence to support it. It describes how sub-atomic particles known as quarks (and their corresponding anti-particles) interact by the exchange of virtual[1] gluons, binding them into the hadrons (such as protons, neutrons and pions) which are observed in nature. QCD also indirectly explains the force *between* hadrons, responsible, for example, for binding protons and neutrons into atomic nuclei.

There are six types (or 'flavours') of quark ('up' and 'down', or u and d, being the most relevant to low energy physics, since they are the lightest). The interaction between quarks and gluons is governed by their chromodynamic charges, known simply as 'colours', of which there are three kinds.

[1] Virtual particles are short-lived particle states that may appear in the vacuum by virtue of the Heisenberg Uncertainty Principle.

As with all field theories, QCD is described by a Lagrangian, which incorporates the Dirac operator that describes the quarks. However, QCD is a highly complex, non-linear theory; whilst at high energies the interaction strength is small enough to allow the use of perturbation theory, at lower energies this is not possible.

If the up and down quarks are considered massless (which is a good approximation to reality), then the Lagrangian possesses a so-called global chiral symmetry, which means (very loosely speaking) that quarks of different spin states (chiralities) ought to behave as if they were distinct and independent types of particle.

In order to understand QCD, it can sometimes be instructive to modify (theoretically) the parameters of the theory in non-physical ways. For example, we can change the number of quark flavours (N_f) or the number of colours (N_c) from their physical values. We can modify the quark masses; for example, setting them to zero is known as taking the chiral limit, or making them very large is known as quenching, and is equivalent to ignoring them completely. We can also vary the number of space-time dimensions, or change the representations of the quantum fields. One can also introduce conjugate quarks, and modify the value of the QCD vacuum angle θ (a parameter in the Lagrangian).

Although originally formulated in (physical) Minkowskian space-time, there are certain advantages – both theoretical and practical – to mapping QCD to Euclidean space-time. For example, the Dirac operator becomes anti-Hermitian (with purely imaginary eigenvalues), and probability amplitudes (or 'weights'), which are in general complex numbers, may become real and positive, allowing for Monte Carlo simulations of QCD (lattice gauge theory, LGT) to be performed on computers. However, these properties are no longer true once a chemical potential has been introduced (see below).

QCD at low energies is characterised by two phenomena. First, we have colour confinement. We do not see free quarks and gluons, but only the hadrons which have no net colour charge, and which are considerably more massive that the sum of the masses of their constituent quarks. Second, below a critical temperature, the global chiral symmetry of the QCD Lagrangian is broken if there are two or more quark flavours ($N_f \geq 2$). This manifests itself in large mass differences between the pions and other low energy mesons that differ only in their spin states. If the quarks are considered massless, then this symmetry breaking is spontaneous; the vacuum state (the lowest energy state) has a lower symmetry than the Lagrangian. Low energy physics is consequently dominated by the resulting Goldstone bosons, identified as

the pions, which are weakly-interacting. In practice, because the quark masses are not exactly zero, we observe pseudo-Goldstone bosons that have non-zero, but nonetheless relatively small, masses.

The chiral condensate $\Sigma \equiv |\langle\bar{\psi}\psi\rangle|$ is an order parameter for chiral symmetry breaking, where ψ is the quark field operator. Loosely speaking, it is a measure of the degree of interaction between quark states of different chiralities in the vacuum. The Banks-Casher relation [Ban80] relates the chiral condensate to the average density of Euclidean Dirac eigenvalues near the origin (i.e. at low virtuality), in the case when there is no chemical potential μ:

$$\Sigma \equiv |\langle\bar{\psi}\psi\rangle| = \lim_{\substack{V\to\infty \\ m\to 0}} \frac{\pi}{V} \langle\rho(0)\rangle. \tag{2.4}$$

More generally, the chiral condensate is related to the discontinuity in the resolvent of the Dirac operator at the origin which may be caused either by an accumulation of eigenvalues (when $\mu = 0$) or by some other mechanism (e.g. when $\mu > 0$, discussed below).

The physical cause of chiral symmetry breaking, at least at $\mu = 0$, has been attributed to the presence of certain topological soliton-like solutions of the gluon fields, known as instantons, which result in the accumulation of the low-lying Dirac eigenvalues (the zero and almost-zero modes).

One particular area of interest is the consideration of extreme physical conditions, such as heavy ion collisions in particle accelerators, the properties of neutron stars and the early universe. For these, it is necessary to introduce temperature T and chemical potential μ (essentially, a measure of the density of quarks) into the model. It is expected that the states (phases) of matter change depending on T and μ, and this can be shown on a phase diagram.

When $\mu > 0$, the Dirac operator is no longer anti-Hermitian, and so its eigenvalues become complex, in general. This is the cause of the infamous sign problem with physical QCD that we mentioned in Chapter 1; essentially, the weights of configurations in the Euclidean framework become not merely non-positive, but complex-valued in general, thereby hampering the use of Monte Carlo LGT simulations.

One of the advantages of considering 2-colour QCD is that the sign problem is less severe than in physical, 3-colour QCD. The weights in 2-colour QCD will, at worst, become negative, but will always remain real. And, in fact, the theory does not have a sign problem at all if we have an even number N_f of quark flavours whose

masses are degenerate. One of the benefits of applying RMT to QCD is that we can quantify how serious the sign problem is expected to be as a function of the mass split (the difference between the masses of quarks of different flavours).

2.2.2 RMT and QCD

It is believed that the statistical properties of the low-lying (zero and near-zero) eigenvalues of the Euclidean QCD Dirac operator depend solely on the global symmetries of the operator, and so, being universal, can be described by any theory with similar symmetries, such as an appropriately constructed random matrix model. We should emphasize that the truth of this statement can, at the present time, be verified only by comparison with LGT, since there is no rigorous proof of this from first principles.

In the absence of a chemical potential, we can use Hermitian matrices $\mathcal{D}$ to model the Dirac operator $\mathcal{D}_{\mathrm{QCD}}$ (making the correspondence $\mathcal{D}_{\mathrm{QCD}} \leftrightarrow i\mathcal{D}$). The choice of Dyson index β (1, 2 or 4) in the random matrix model depends on the number N_c of colours and on the representations of the fields adopted; $\beta = 2$ corresponds to physical QCD, for example, and $\beta = 1$ to QCD with 2 colours (considered in this thesis).

One can consider RMT as a model of QCD in which the quarks are moving chaotically in a randomly-fluctuating gluon field. Equivalently, this can then be modelled by a Dirac operator that is itself random. But more precisely, RMT corresponds exactly to QCD in the so-called mesoscopic regime, where the RMT model is equivalent to the ϵ-regime of chiral perturbation theory (a low-energy effective field theory defined in a box of finite size). However, when we consider non-zero temperatures and quark densities (chemical potentials), then RMT models may also have phenomenological applications, giving qualitative information about the phase diagram that cannot be obtained by other methods.

A number of general review articles on the application of RMT to QCD have appeared over the last decade or so, all written by leading researchers in the field. For general reviews, see [Ver00; Dam02; Ver09], together with [Ake07c; Spl08] which specifically cover the case of non-zero chemical potential.

The idea of using RMT to model the low-lying eigenvalues of the Dirac operator in QCD was first proposed almost twenty years ago in [Shu93], in which the authors solved the $\beta = 2$ case (physical QCD) for the partition function $\mathcal{Z}^{(N_f)}(\{m\})$ and the

spectral sum rules (particular quantities related to the distribution of the eigenvalues). Soon after, an expression for the eigenvalue density itself was also obtained for this model [Ver93; Ver94a], although only given explicitly for the unquenched case when all the quark masses are zero.

This work was subsequently extended [Ver94b] to the $\beta = 1$ and $\beta = 4$ ensembles, presenting the JPDFs and the sum rules, and the spectrum for the $\beta = 1$ case was also explicitly obtained [Ver94c], but again only for the unquenched case with quark masses set to zero. Further results on spectral sum rules [Ver94e] and the derivation of effective theories from RMT [Hal95] followed shortly afterwards.

Encouraging comparisons of RMT results with the liquid instanton model (in which instantons are assumed to have a certain distribution) were made in [Ver94d] and [Ver94g], the latter paper also reviewing results to date. The behaviour of the chiral condensate as a function of the masses, which can be derived within the RMT framework, was also investigated [Ver96].

Further work continued to analyse in more detail various properties of these ensembles. For example, the unquenched microscopic densities with non-zero quark masses were determined in a sequence of papers [Dam98a; Wil98; Ake00; Nag00a; Nag00b; Ake01a], and distributions of individual eigenvalues were analysed in [Nis98; Dam01; Ake04a]. [Tou99] discusses the various patterns of symmetry breaking.

Much work was undertaken on the issue of universality, in other words, investigating whether probability distributions other than Gaussian will give identical results for microscopic spectral quantities. See [Nis96; Ake97; Sen98; Ake98a; Ber98; Dam98a; Kle00].

The incorporation of the effect of a quark chemical potential into the RMT model leads to matrices that are non-Hermitian. This was first undertaken by adding a *fixed* constant (multiplied by the identity matrix) to the matrix blocks of the Hermitian ensembles [Ste96]. This was entirely realistic, because the effect of a chemical potential is not random. The model was quickly extended [Hal97] to the $\beta = 1$ and $\beta = 4$ cases.

This one-matrix RMT model was able to provide the solution to a long-standing problem in QCD itself. At zero chemical potential, the quenched model (in which the effects of virtual quarks are ignored) is a good approximation for the unquenched case (where these effects are taken into account), as demonstrated by LGT results. But this does not seem to hold true when a chemical potential is added. The RMT model showed that the quenched case actually approximates an entirely different model,

the so-called phase-quenched ensemble, which has additional types of (hypothetical) quarks (known as conjugate quarks) and different symmetry breaking patterns.

Technically, however, it is rather difficult to find complete solutions for such an ensemble. Therefore, an alternative model was suggested [Ake02a; Ake03a], specified simply by its eigenvalue JPDF, without reference to any underlying matrix representation. Subsequent investigations [Ake03b; Ake04b] showed that the microscopic behaviours of this model and the original one-matrix model were very close at small chemical potential.

A third type of model was proposed [Osb04] not long after, originally for the $\beta = 2$ case. Not only did this model have the desirable property of being formulated in a matrix representation, but also it was entirely solvable analytically. The chemical potential was now incorporated by multiplying it by another *random* matrix, leading to a two-matrix model. Whilst chemical potential is clearly not stochastic, universality arguments imply that this model should actually have identical microscopic spectral properties to the original one-matrix model. A solution for the corresponding $\beta = 4$ ensemble was given in [Ake05b; Ake07a], and the $\beta = 1$ case is solved in this thesis.

As with the Hermitian ensembles, it is of significant practical importance to be able to derive the distributions of the individual eigenvalues, once an appropriate ordering scheme has been introduced, see [Ake08a; Ake08b], for example.

For the unquenched $\beta = 2$ case, it was noted [Ake05a] that the eigenvalue density can become highly oscillatory in certain regions of the complex plane. These oscillations were shown [Osb05] to be the cause, when $\mu > 0$, of the jump in the resolvent that leads to the non-zero chiral condensate. The condensate is μ-independent in the phase when chiral symmetry is broken [Osb08a], and, in fact, a physical interpretation of the oscillating region can be given [Osb08b].

The presence of these oscillations (and in particular, the existence of regions where the density is non-positive) is closely tied in with the infamous sign problem, which makes LGT simulations difficult if not impossible. RMT can be used to investigate the severity of this effect [Spl07; Han08; Blo09a; Blo09b].

RMT at non-zero chemical potential has two distinct types of application to QCD, the first being a precise mapping, typically at low chemical potential μ, and the second being a phenomenological application at larger μ and non-zero temperature T, in order to understand the phase diagram. However, a new exact mapping for 2-colour QCD was recently discovered [Kana10] which is actually valid at high

chemical potential, when matter is believed to condense into a new phase consisting of di-quarks.

Let us briefly discuss the nature of the precise mapping of RMT to QCD. This typically occurs in the ϵ-regime of chiral perturbation theory. One (mathematical) way of showing this equivalence for all correlation functions is to introduce additional 'dummy' types of quark into the models, such as bosonic quarks. For details, we refer to [Dam98b; Ake98b; Osb99; Dam99], and [Spl06; Bas07] for the non-Hermitian case.

We mention also that considering non-physical situations can also lead to greater insight. QCD in 3-dimensions was considered for $\beta = 2$ [Ver94f] and $\beta = 4$ [Mag00], for the unquenched case [Nag01], and with chemical potential [Ake01b]. We can also see what happens mathematically if the chemical potential in matrix models is taken to be imaginary rather than real [Ake07b; Lehn09].

It is often possible to use Monte Carlo simulations of lattice gauge theory to generate eigenvalue distributions for comparison with the predictions of RMT. However, there are many potential problems: for example, it is difficult to put quarks with small masses onto the lattice, and so simulations are often performed using the quenched approximation. There is also a technical problem in that, with certain techniques for implementing fermions (so-called staggered fermions), the symmetry classes are different on the lattice from those in the continuum. Another significant problem, also with the unquenched simulations, is of course the sign problem at non-zero chemical potential.

However, a number of tests against LGT data have been successfully carried out. These include comparisons of the eigenvalue densities, as well as investigations into the distributions of individual eigenvalues. The RMT models need to be appropriately scaled to match the data. Indeed, this scaling allows one to extract certain low energy parameters of QCD such as the chiral condensate. We refer to the review articles cited earlier for more details and references, e.g. [Ver09].

2.2.3 Statement of the chGinOE model

As indicated earlier, random matrix models are constructed using only global symmetries, and so we introduce a random matrix $i\mathcal{D}$, which will model the Euclidean QCD Dirac operator $\mathcal{D}_{\rm QCD} = \gamma_k(\partial_k + iA_k) + \mu\gamma_0$, where the γ_k (for space-time index $k = 0, 1, 2, 3$) are the Euclidean Dirac gamma matrices, and the A_k are the gluon

fields (with various other labels suppressed). For two-colour QCD with a chemical potential, the model that we will adopt is the non-Hermitian extension of the chGOE model [Ver94b; Ver94c] using a prescription similar to that given in [Osb04]. The matrix $\mathcal{D}$ is constructed as follows:

- The QCD Dirac operator possesses axial $U_A(1)$ symmetry (i.e. $\{\gamma_5, \mathcal{D}_{\mathrm{QCD}}\} = 0$ where $\gamma_5 \equiv \gamma_0\gamma_1\gamma_2\gamma_3$ is the chirality operator) which implies that all non-zero eigenvalues come in pairs $\pm\Lambda$. We wish to retain this property, and hence we write $\mathcal{D}$ as an off-diagonal block ('chiral') matrix.

- By the Atiyah-Singer index theorem, in a gauge (gluon) field of fixed topological charge ν the Dirac operator will have precisely $|\nu|$ eigenvalues that are exactly zero. Therefore, we will work in sectors of fixed topological charge, and use $N \times (N + \nu)$ matrices as the blocks in $\mathcal{D}$, where N corresponds to the volume of the system in QCD, and ν to the topological charge of the gluon fields.

- With no chemical potential present, $\mathcal{D}_{\mathrm{QCD}}$ is anti-Hermitian, and so $\mathcal{D}$ must be a Hermitian random matrix. For a non-zero chemical potential $\mu > 0$, we then add μ times a second random matrix (see the earlier discussion concerning universality) which must be anti-Hermitian; μ is assumed to be the same for all quark flavours.

- Since the fields in two-colour QCD are in representations of the Lie group $SU_c(2)$ which is pseudo-real, we can choose to write $\mathcal{D}$ in a basis with real matrix elements. Therefore, when $\mu = 0$, $\mathcal{D}$ will be symmetric, and for $\mu > 0$, we add an anti-symmetric matrix, so that $\mathcal{D}$ becomes asymmetric.

The matrix $\mathcal{D}$ is therefore given by

$$\mathcal{D} \equiv \left(\begin{array}{c|c} 0 & A \\ \hline B^T & 0 \end{array}\right) \equiv \left(\begin{array}{c|c} 0 & P + \mu Q \\ \hline P^T - \mu Q^T & 0 \end{array}\right) \tag{2.5}$$

where A, B, P and Q are all real-valued matrices of size $N \times (N + \nu)$, and $\mu \in [0, 1]$ is the non-Hermiticity parameter.

Universality arguments imply that the choice of distribution for matrix elements is arbitrary, and so we choose the simplest mathematically, which is the Gaussian

distribution. The partition function (from which we can read off the JPDF of the matrix elements of $\mathcal{D}$) is consequently given by

$$\mathcal{Z}_{N,\nu}^{(N_f)} = \left(\frac{1}{\sqrt{2\pi}}\right)^{2N(N+\nu)} \int dP\, dQ\, \exp\left[-\tfrac{1}{2}\operatorname{Tr}(PP^T + QQ^T)\right] \times \prod_{f=1}^{N_f} \det(\mathcal{D} + m_f \mathcal{I}), \quad (2.6)$$

where $dP \equiv \prod_{i,j} P_{ij}$, and similarly for dQ. The integral is over the $N(N+\nu)$ elements of each of P and Q, and is over $\mathbb{R}$ for each element. In order to simplify the notation, we have not included any N-dependency in the weight function at this stage (the N-dependent scaling is introduced in §6.2).

The product over the determinants in eq. (2.6) models the effects of virtual quarks, and corresponds to a similar factor in the QCD partition function once the (Grassmann-valued) quark fields have been integrated out at fixed gauge field configuration. $N_f \geq 0$ is the number of virtual quark flavours, and the $\{m_f\}$ are the individual quark masses ($1 \leq f \leq N_f$). Note that, numerically, when $N_f = 0$, we have $\mathcal{Z}_{N,\nu} = 1$; however, when $N_f > 0$, we have $\mathcal{Z}_{N,\nu} \equiv \mathcal{Z}_{N,\nu}(\{m_f\})$ which in general will not equal unity.

The partition function eq. (2.6) is valid in a sector of fixed topological charge ν, and so the complete QCD partition function at vacuum angle θ is given by

$$\mathcal{Z}_N^{(N_f)}(\theta) = \sum_{\nu=-\infty}^{\infty} e^{i\nu\theta} \mathcal{Z}_{N,\nu}^{(N_f)}. \quad (2.7)$$

All the results in this thesis are given for a fixed topology ν, and so we drop the subscript ν in the remainder of this thesis, always considering it to be fixed.

From a physics point of view, we will be interested in the limit $N \to \infty$. This limit can be taken in different ways, depending on how we scale the eigenvalues, quark masses and chemical potential with N.

The term 'massless' is somewhat ambiguous. Throughout this document we will use the term 'quenched' for the case where $N_f = 0$ (corresponding to large m_f when $N_f > 0$), and the term 'zero mass' for $m_f = 0$. The unquenched case is the more general case when $N_f > 0$. In the specific examples of the unquenched case given in Chapter 9, we will generally choose $N_f = 2$ (corresponding to the lightest u and d quarks). We will often consider the case of degenerate masses $m_1 = m_2 \equiv m$, so that the JPDF is real and positive for all values of the matrix elements. However, we will also consider non-degenerate masses, since this is physically realistic, and leads to interesting phenomena. Also, since $\mu = 0$ corresponds to a Hermitian (and

not an anti-Hermitian) matrix in our convention, we will mostly be interested in *imaginary* m_f for applications. However, in this document, we will also show some graphs where the m_f are taken to be real.

Chapter 3

From matrix representation to eigenvalue JPDF

Starting with the partition function of the chGinOE expressed as an integral over the matrix elements, we now show how to integrate out the angular degrees of freedom to arrive at the joint probability density function (JPDF) of the eigenvalues. We specified the ensemble for the general unquenched case ($N_f > 0$) in §2.2.3. However, the quenched case ($N_f = 0$) is easier to solve, since the elements of P and Q are independent, normally-distributed random variables $\sim N(0, 1)$. Furthermore, many of the unquenched results can actually be expressed in terms of the quenched results. Therefore it makes sense to solve the quenched case first.

Because the chGinOE is non-Hermitian, we cannot use a simple spectral decomposition to obtain a diagonal matrix of eigenvalues, but instead we must use a variant of the Schur transformation. Since the model has a chiral form involving two matrices, and not one, we actually require the QZ decomposition. And because the matrices in question all have real elements, we use the *real* QZ decomposition. After making the transformation, we can integrate out all of the degrees of freedom apart from the eigenvalues themselves, leaving the partition function expressed as an integral over the eigenvalue JPDF.

3.1 JPDF for quenched case

For $N_f = 0$, the partition function in eq. (2.6) reads

$$\mathcal{Z}_N = \left(\frac{1}{\sqrt{2\pi}}\right)^{2N(N+\nu)} \int dP\, dQ\, \exp\left[-\tfrac{1}{2}\operatorname{Tr}(PP^T + QQ^T)\right]. \tag{3.1}$$

Here, and throughout this thesis, we will usually drop the superscript '(N_f)' on all quantities for the case when $N_f = 0$. We wish to solve for the eigenvalue JPDF of the Dirac matrix $\mathcal{D}$ defined in eq. (2.5):

$$\mathcal{D} \equiv \left(\begin{array}{c|c} 0 & A \\ \hline B^T & 0 \end{array}\right) \equiv \left(\begin{array}{c|c} 0 & P+\mu Q \\ \hline P^T-\mu Q^T & 0 \end{array}\right).$$

In practice, it is easier to solve for the eigenvalues of the so-called Wishart matrix $W \equiv AB^T \equiv (P+\mu Q)(P^T-\mu Q^T)$, which is of size N-by-N. The eigenvalues of W are the squares of the (non-zero) eigenvalues of $\mathcal{D}$. This can be understood by considering the characteristic equation

$$0 = \det[\Lambda - \mathcal{D}] = \Lambda^\nu \det[\Lambda^2 - AB^T] = \Lambda^\nu \prod_{j=1}^{N} (\Lambda^2 - \Lambda_j^2). \tag{3.2}$$

The matrix $W \equiv AB^T$ has real elements, and so its eigenvalues can be grouped into pairs: either both eigenvalues in a pair will be real, or they will both be complex valued ($\in \mathbb{C}\backslash\mathbb{R}$) and complex conjugates of each other. For N odd, there will also be a final unpaired real eigenvalue. Hence, the non-zero eigenvalues of $\mathcal{D}$ come in real pairs ($\Lambda_j^2 > 0$), pure imaginary pairs ($\Lambda_j^2 < 0$), or complex quadruplets ($\pm\Lambda_j$, $\pm\Lambda_j^*$).

3.1.1 Change of variables to A and B

Our partition function eq. (3.1) is written as a multiple integral over independent matrices P and Q. We begin by changing variables from $\{P, Q\}$ to the matrix elements $\{A, B\}$, where $A \equiv P + \mu Q$ and $B \equiv P - \mu Q$, or equivalently $P = \frac{1}{2}(A+B)$ and $Q = \frac{1}{2\mu}(A-B)$, which has Jacobian

$$\mathcal{J}^{(N)} = (2\mu)^{-N(N+\nu)}. \tag{3.3}$$

In the exponent we have

$$\mathrm{Tr}(PP^T + QQ^T) = \mathrm{Tr}\left(\eta_+(AA^T + BB^T) - \eta_-(AB^T + BA^T)\right), \tag{3.4}$$

where we have defined

$$\eta_\pm \equiv \frac{1 \pm \mu^2}{4\mu^2}. \tag{3.5}$$

But $AB^T = W$, and $\mathrm{Tr}\, BA^T = \mathrm{Tr}(AB^T)^T = \mathrm{Tr}\, AB^T$. Therefore the weight becomes

$$\exp\left\{-\tfrac{1}{2}\,\mathrm{Tr}(PP^T + QQ^T)\right\} = \exp\{\eta_-\,\mathrm{Tr}\, W\}\, \exp\left\{-\frac{\eta_+}{2}\,\mathrm{Tr}(AA^T + BB^T)\right\}, \tag{3.6}$$

giving us the probability density function for matrices A and B as

$$P(A,B) = \frac{\mathcal{J}^{(N)}}{(2\pi)^{N(N+\nu)}}\, \exp\{\eta_-\,\mathrm{Tr}\, W\} \exp\left\{-\frac{\eta_+}{2}\,\mathrm{Tr}(AA^T + BB^T)\right\}. \tag{3.7}$$

3.1.2 QZ decomposition

3.1.2.1 Definition

We now undertake a variation of the transform known as the QZ decomposition[1] which is usually performed on two *square* matrices, A and B. If A and B have complex-valued elements, then we can write $A = QSZ^{-1}$ and $B = QTZ^{-1}$, where S and T are upper-triangular, and the transforming matrices Q and Z are unitary.

However, if A and B are real, and we wish to restrict ourselves to using real Q and Z (i.e. orthogonal and not just unitary transforming matrices), then the best we can achieve is that only one of S and T will be upper-triangular. The other will be of so-called almost-upper-triangular (AUT) form[2]. Such a matrix has 2-by-2 blocks down the diagonal (plus a single 1-by-1 block in the bottom right-hand corner if the matrix size N is odd), with all the entries below the block diagonal being zero. Since an ordinary upper-triangular matrix is, of course, a special case of an AUT matrix, we can consider both S and T to be AUT in what follows.

The precise transformation that we make is:

$$A = O_A(\Delta_A + \Lambda_A)O_B^T, \qquad B^T = O_B(\Delta_B + \Lambda_B)O_A^T. \tag{3.8}$$

Λ_A and Λ_B contain 2-by-2 blocks down the diagonal. When N is odd, there is also an additional entry in the bottom right-hand corner of Λ_A and Λ_B. We will describe Λ_A and Λ_B as being block-diagonal. Δ_A and Δ_B are zero except in elements strictly above the diagonal blocks (and so $\Delta_A + \Lambda_A$ and $\Delta_B + \Lambda_B$ are AUT), and we will describe Δ_A and Δ_B as being strictly AUT.

Note that O_A is of size $N \times N$, and O_B is of size $(N+\nu) \times (N+\nu)$. Δ_A and Λ_A are the same size as A itself, i.e. rectangular, $N \times (N+\nu)$, and Δ_B and Λ_B are the same size as B^T, i.e. rectangular, $(N+\nu) \times N$.

An important point is that, under this transformation, the Wishart matrix W transforms as follows:

$$W \equiv AB^T = O_A(\Delta_A + \Lambda_A)(\Delta_B + \Lambda_B)O_A^T \equiv O_A(\Delta_{AB} + L)O_A^T \tag{3.9}$$

where $L \equiv \Lambda_A\Lambda_B$ is block diagonal, and Δ_{AB} is strictly AUT. Clearly, $\Delta_{AB} + L$ has the same eigenvalues as W, since this is a similarity transformation; however, it is

[1] The QZ decomposition is a two-matrix generalisation of the Schur decomposition which involves a single matrix. We refer to Table A.1 where we list some matrix transformations.

[2] This is sometimes called quasi-upper-triangular form.

Before		After		
Matrix	Degrees of freedom	Matrix	Degrees of freedom	
			Even N	Odd N
A	$N(N+\nu)$	Λ_A	$2N$	$2N-1$
B	$N(N+\nu)$	Λ_B	$2N$	$2N-1$
		Δ_A	$\frac{1}{2}N^2 - N + \nu N$	$\frac{1}{2}(N^2+1) - N + \nu N$
		Δ_B	$\frac{1}{2}N^2 - N$	$\frac{1}{2}(N^2+1) - N$
		O_A	$\frac{1}{2}N^2 - N$	$\frac{1}{2}(N^2+1) - N$
		O_B	$\frac{1}{2}N^2 - N + \nu N$	$\frac{1}{2}(N^2+1) - N + \nu N$
Total	$2N(N+\nu)$	Total	$2N(N+\nu)$	$2N(N+\nu)$

Table 3.1: Degrees of freedom before and after the QZ decomposition.

also true that L has precisely the same eigenvalues as well (see Appendix A.2.5 (ii)). Furthermore, each 2-by-2 block of L 'contains' two eigenvalues, in the sense that the eigenvalues of the i-th block, L_i, are Λ_{2i-1}^2 and Λ_{2i}^2, and every pair of eigenvalues must either both be real, or be non-real and complex conjugates of each other. If N is odd, then the 1-by-1 block of L contains simply the unpaired, real eigenvalue Λ_N.

However, we still have freedom about how to order the blocks, and how to order the pairs within the blocks. We will discuss our particular choice later.

Because we are not diagonalising the 2-by-2 blocks in this step, and because A and B^T are not square, the set of orthogonal matrices O_A and O_B over which we will integrate is restricted as follows; for even N we have

$$O_A \in O(N)/O(2)^{N/2}, \qquad O_B \in O(N+\nu)/O(2)^{N/2}\,O(\nu) \tag{3.10}$$

and for odd N

$$O_A \in O(N)/O(2)^{(N-1)/2}\,O(1), \qquad O_B \in O(N+\nu)/O(2)^{(N-1)/2}\,O(1)\,O(\nu). \tag{3.11}$$

We can use the fact that $O(N)$ has $\frac{N(N-1)}{2}$ degrees of freedom to cross-check that the degrees of freedom before and after the transformation match (see Table 3.1).

Under the transformation, the weight changes as follows:

$$\exp\left\{-\frac{\eta_+}{2}\operatorname{Tr}(AA^T + BB^T)\right\} = \exp\left\{-\frac{\eta_+}{2}\operatorname{Tr}(\Lambda_A\Lambda_A^T + \Lambda_B\Lambda_B^T + \Delta_A\Delta_A^T + \Delta_B\Delta_B^T)\right\}, \tag{3.12}$$

and

$$\exp\{\eta_-\operatorname{Tr} W\} = \exp\{\eta_-\operatorname{Tr} L\} = \exp\{\eta_-\sum_i \Lambda_i^2\}. \tag{3.13}$$

3.1.2.2 Calculation of Jacobian

We are changing variables from $\{A, B^T\}$ to $\{\Lambda_A, \Lambda_B, \Delta_A, \Delta_B, O_A, O_B\}$, and will then integrate over all the new variables apart from Λ_A and Λ_B, whose product $L \equiv \Lambda_A \Lambda_B$ is block-diagonal, and 'contains' the eigenvalues of W.

To determine the Jacobian, we first differentiate eq. (3.8), to give

$$\begin{aligned} dA &= O_A\big[O_A^T dO_A(\Delta_A + \Lambda_A) - (\Delta_A + \Lambda_A)O_B^T dO_B + d\Delta_A + d\Lambda_A\big]O_B^T, \\ dB^T &= O_B\big[O_B^T dO_B(\Delta_B + \Lambda_B) - (\Delta_B + \Lambda_B)O_A^T dO_A + d\Delta_B + d\Lambda_B\big]O_A^T, \end{aligned} \tag{3.14}$$

where we also used result eq. (A.18). The matrices $O_A^T dO_A$ and $O_B^T dO_B$ are anti-symmetric (see eq. (A.19)), and so the elements are not independent.

In fact, we can omit the outside rotation factors in eq. (3.14) since these will not affect the Jacobian. This is because $\mathrm{Tr}(dA\, dA^T + dB\, dB^T)$ is invariant under this rotation, and so the corresponding Jacobian matrix is itself orthogonal; its determinant is therefore equal to unity. So, in component form, we have

$$(dA)_{ij} = \sum_{k=1}^{N} (O_A^T dO_A)_{ik}(\Delta_A + \Lambda_A)_{kj} - \sum_{k=1}^{N+\nu} (\Delta_A + \Lambda_A)_{ik}(O_B^T dO_B)_{kj} + (d\Delta_A)_{ij} + (d\Lambda_A)_{ij}, \tag{3.15}$$

$$(dB^T)_{ij} = \sum_{k=1}^{N+\nu} (O_B^T dO_B)_{ik}(\Delta_B + \Lambda_B)_{kj} - \sum_{k=1}^{N} (\Delta_B + \Lambda_B)_{ik}(O_A^T dO_A)_{kj} + (d\Delta_B)_{ij} + (d\Lambda_B)_{ij}. \tag{3.16}$$

We now give an ordering of the old and new variables that will lead to an almost lower-triangular Jacobian matrix, with variables dA and dB^T in the columns and $d\Lambda_A$, $d\Lambda_B$, $d\Delta_A$, $d\Delta_B$, $O_A^T dO_A$ and $O_B^T dO_B$ in the rows.

First, consider the differentials with respect to Δ_A, Δ_B, Λ_A and Λ_B:

$$\begin{aligned} \frac{\partial A_{ij}}{\partial(\Delta_A)_{pq}} &= \delta_{ip}\delta_{jq} = \delta_{(ij)(pq)}, & \frac{\partial B_{ij}^T}{\partial(\Delta_B)_{pq}} &= \delta_{ip}\delta_{jq} = \delta_{(ij)(pq)}, \\ \frac{\partial A_{ij}}{\partial(\Lambda_A)_{pq}} &= \delta_{ip}\delta_{jq} = \delta_{(ij)(pq)}, & \frac{\partial B_{ij}^T}{\partial(\Lambda_B)_{pq}} &= \delta_{ip}\delta_{jq} = \delta_{(ij)(pq)}. \end{aligned} \tag{3.17}$$

For any A_{ij} on or above the block-diagonal (OBD or ABD respectively), we will only get a single contribution, i.e. when we differentiate with respect to the element either of Δ_A or of Λ_A that occupies the matching position (i, j). Therefore, if we pair $(dA)_{ij}$ with $(d\Lambda_A)_{ij}$ or $(d\Delta_A)_{ij}$, as appropriate, and similarly for B^T, then we will get a resulting Jacobian sub-matrix that is simply the identity. We will put these

variables first, in any order. For A_{ij} and B^T_{ij} below the block-diagonal (BBD), these differentials will always be zero.

We now order the remaining (i.e. BBD) elements of dA and dB^T, along with the independent elements of $O_A^T dO_A$ and $O_B^T dO_B$. It is natural to choose the independent elements of $O_A^T dO_A$ and $O_B^T dO_B$ to be the BBD elements, with the ABD elements being dependent, because then there is also a very natural pairing of BBD $(dA)_{ij}$ with $(O_A^T dO_A)_{ij}$, and of BBD $(dB^T)_{ij}$ with $(O_B^T dO_B)_{ij}$.

We partition the BBD elements of dA, dB^T, $O_A^T dO_A$ and $O_B^T dO_B$ into blocks, as shown in Figure 3.1. For $N > 1$, we always find 2-by-2 blocks (shown in green). For N odd, we will also have a row of 1-by-2 blocks (blue). Whenever $\nu > 0$, there are also additional 1-by-2 blocks (yellow), and for odd N, 1-by-1 blocks (red). The figure shows the matrix dB^T; dA is similar, but has no yellow or red blocks, since it is of size N-by-$(N + \nu)$.

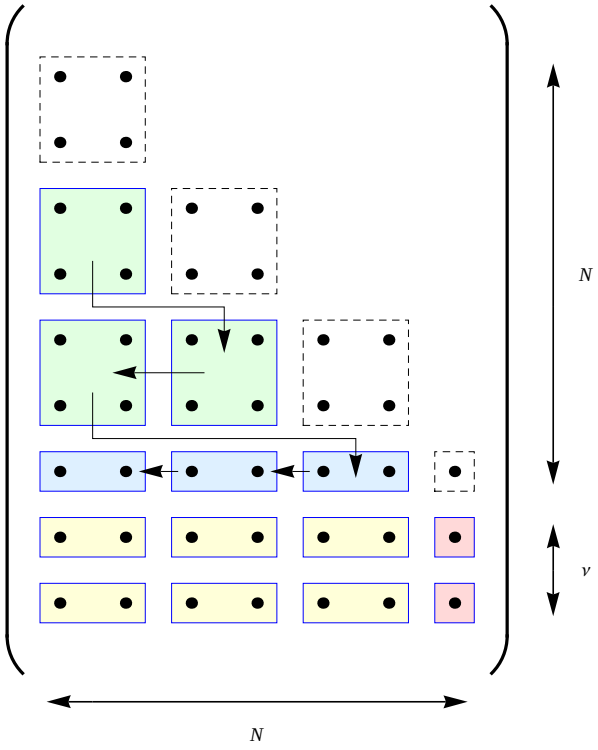

Figure 3.1: Partitioning of below-block-diagonal elements of matrices into sub-blocks.

We then order the blocks as shown in the diagram (the ordering of elements within each block is arbitrary); the green blocks come first, ordered from top to bottom

and right to left, followed by the blue blocks. Then we place the yellow blocks, and finally the red blocks. We shall now show that such an ordering (which is not unique) will lead to an almost-lower-triangular Jacobian matrix. The differentials, for all (i, j) but only for (p, q) BBD (i.e. the independent elements), are given by (see eq. (A.14) for details):

$$\begin{aligned} \frac{\partial A_{ij}}{(O_A^T \partial O_A)_{pq}} &= \delta_{ip}(\Delta_A + \Lambda_A)_{qj}, & \frac{\partial B_{ij}^T}{(O_A^T \partial O_A)_{pq}} &= -\delta_{jq}(\Delta_B + \Lambda_B)_{ip}, \\ \frac{\partial A_{ij}}{(O_B^T \partial O_B)_{pq}} &= -\delta_{jq}(\Delta_A + \Lambda_A)_{ip}, & \frac{\partial B_{ij}^T}{(O_B^T \partial O_B)_{pq}} &= \delta_{ip}(\Delta_B + \Lambda_B)_{qj}. \end{aligned} \tag{3.18}$$

The diagonal blocks in the Jacobian matrix arise from when (i, j) (which indexes an old variable) is in the same block as the block containing (p, q) (which indexes a new variable). Suppose now that (i, j) is in a block that comes after the block containing (p, q). The elements such as $\partial A_{ij}/(O_A^T \partial O_A)_{pq}$ will consequently lie above the diagonal blocks in the Jacobian matrix. To show that these are always zero, we consider the various possibilities:

- Case $i = p$: If j is odd, $j + 1 < q$ else $j < q$. Either way, all four differentials in eq. (3.18) equal zero.
- Case $i \neq p$: If i and p are in the same 'block row', then $j \neq q$. Otherwise, we must have $i > p + 1$ if p is odd, else $i > p$ if p is even. In all cases, again all four differentials equal zero.

So the above block-diagonal part of the Jacobian matrix is indeed empty. Since the matrix is therefore almost-lower-triangular, by using the second result from Appendix A.2.5, the determinant is merely the product of the determinants of the blocks that lie on the diagonal. As we noted above, these blocks arise from the cases when (i, j) and (p, q) both come from the same block, and hence they are of four types. Let us consider each of these in turn.

The 2-by-2 (green) blocks contain 4 elements (at positions $(2i - 1, 2j)$, $(2i - 1, 2j - 1)$, $(2i, 2j)$ and $(2i, 2j - 1)$) of each of dA and dB^T, and so this leads to 8-by-8 blocks (sub-matrices) down the diagonal of the Jacobian matrix. Each of these contains elements of Λ_A and Λ_B only. These blocks are of the form

$$\left(\begin{array}{c|c} \mathcal{S}_{ij} & \mathcal{T}_{ij} \\ \hline \mathcal{U}_{ij} & \mathcal{V}_{ij} \end{array}\right), \tag{3.19}$$

where

$$\mathcal{S}_{ij} \equiv \begin{pmatrix} (\Lambda_A)_{2j,2j} & -(\Lambda_B)_{2i-1,2i-1} & (\Lambda_A)_{2j,2j-1} & 0 \\ -(\Lambda_A)_{2i-1,2i-1} & (\Lambda_B)_{2j,2j} & 0 & (\Lambda_B)_{2j,2j-1} \\ (\Lambda_A)_{2j-1,2j} & 0 & (\Lambda_A)_{2j-1,2j-1} & -(\Lambda_B)_{2i-1,2i-1} \\ 0 & (\Lambda_B)_{2j-1,2j} & -(\Lambda_A)_{2i-1,2i-1} & (\Lambda_B)_{2j-1,2j-1} \end{pmatrix},$$

$$\mathcal{T}_{ij} \equiv \begin{pmatrix} 0 & -(\Lambda_B)_{2i,2i-1} & 0 & 0 \\ -(\Lambda_A)_{2i,2i-1} & 0 & 0 & 0 \\ 0 & 0 & 0 & -(\Lambda_B)_{2i,2i-1} \\ 0 & 0 & -(\Lambda_A)_{2i,2i-1} & 0 \end{pmatrix},$$

$$\mathcal{U}_{ij} \equiv \begin{pmatrix} 0 & -(\Lambda_B)_{2i-1,2i} & 0 & 0 \\ -(\Lambda_A)_{2i-1,2i} & 0 & 0 & 0 \\ 0 & 0 & 0 & -(\Lambda_B)_{2i-1,2i} \\ 0 & 0 & -(\Lambda_A)_{2i-1,2i} & 0 \end{pmatrix},$$

$$\mathcal{V}_{ij} \equiv \begin{pmatrix} (\Lambda_A)_{2j,2j} & -(\Lambda_B)_{2i,2i} & (\Lambda_A)_{2j,2j-1} & 0 \\ -(\Lambda_A)_{2i,2i} & (\Lambda_B)_{2j,2j} & 0 & (\Lambda_B)_{2j,2j-1} \\ (\Lambda_A)_{2j-1,2j} & 0 & (\Lambda_A)_{2j-1,2j-1} & -(\Lambda_B)_{2i,2i} \\ 0 & (\Lambda_B)_{2j-1,2j} & -(\Lambda_A)_{2i,2i} & (\Lambda_B)_{2j-1,2j-1} \end{pmatrix}. \tag{3.20}$$

We now show that, when we take the determinant of each of these sub-matrices eq. (3.19), then the result can be expressed in terms of two of the eigenvalues of W. We can easily verify (using the symbolic manipulation capabilities of Mathematica [Wol08], for example) that the modulus of the determinant of this is (algebraically) identical to

$$\mathcal{J}_{ij} = \left|(D_i - D_j)^2 + (S_i - S_j)(S_i D_j - S_j D_i)\right| \tag{3.21}$$

in which D_i is the determinant, and S_i is the trace, of the two-by-two matrix L_i given by $L_i \equiv A_i B_i$ where

$$A_i \equiv \begin{pmatrix} (\Lambda_A)_{2i-1,2i-1} & (\Lambda_A)_{2i-1,2i} \\ (\Lambda_A)_{2i,2i-1} & (\Lambda_A)_{2i,2i} \end{pmatrix} \qquad \text{and} \qquad B_i \equiv \begin{pmatrix} (\Lambda_B)_{2i-1,2i-1} & (\Lambda_B)_{2i-1,2i} \\ (\Lambda_B)_{2i,2i-1} & (\Lambda_B)_{2i,2i} \end{pmatrix}. \tag{3.22}$$

The 2-by-2 matrices A_i and B_i are the i-th 2-by-2 blocks along the diagonals of the block-diagonal matrices Λ_A and Λ_B respectively, and L_i is then the i-th 2-by-2 block along the diagonal of the block-diagonal matrix $L \equiv \Lambda_A \Lambda_B$. However, L_i has eigenvalues Λ_{2i-1}^2 and Λ_{2i}^2, and so D_i and S_i can be written as:

$$D_i = \Lambda_{2i-1}^2 \Lambda_{2i}^2 \quad \text{and} \quad S_i = \Lambda_{2i-1}^2 + \Lambda_{2i}^2. \tag{3.23}$$

Substituting these into eq. (3.21), and factorising, gives

$$\mathcal{J}_{ij} = \left|(\Lambda_{2i-1}^2 - \Lambda_{2j-1}^2)(\Lambda_{2i}^2 - \Lambda_{2j-1}^2)(\Lambda_{2i-1}^2 - \Lambda_{2j}^2)(\Lambda_{2i}^2 - \Lambda_{2j}^2)\right|. \tag{3.24}$$

So for each element (i,j) in the (green) 2-by-2 block, we have a factor $|\Lambda_i^2 - \Lambda_j^2|$.

When N is odd, in addition to the (green) 2-by-2 blocks, we have a row of (blue) 1-by-2 blocks. This leads to 4-by-4 blocks on the diagonal of the Jacobian. These are of the form

$$\begin{pmatrix} (\Lambda_A)_{2j,2j} & -(\Lambda_B)_{NN} & (\Lambda_A)_{2j,2j-1} & 0 \\ -(\Lambda_A)_{NN} & (\Lambda_B)_{2j,2j} & 0 & (\Lambda_B)_{2j,2j-1} \\ (\Lambda_A)_{2j-1,2j} & 0 & (\Lambda_A)_{2j-1,2j-1} & -(\Lambda_B)_{NN} \\ 0 & (\Lambda_B)_{2j-1,2j} & -(\Lambda_A)_{NN} & (\Lambda_B)_{2j-1,2j-1} \end{pmatrix}. \tag{3.25}$$

The modulus of the determinant of this is identically equal to

$$\mathcal{J}_{Nj} = \left| D_j - S_j \Lambda_N^2 + \Lambda_N^4 \right|, \tag{3.26}$$

where we used that $(\Lambda_A)_{NN}(\Lambda_B)_{NN} = \Lambda_N^2$ (no sums), and D_j and S_j were defined as before. But we can switch to writing D_j and S_j in terms of the eigenvalues of L_j, and this gives

$$\mathcal{J}_{Nj} = \left| (\Lambda_N^2 - \Lambda_{2j-1}^2)(\Lambda_N^2 - \Lambda_{2j}^2) \right|. \tag{3.27}$$

We see that this is of the same form as before.

Let us now consider the contribution to the Jacobian from the 'rectangular' part of dB^T (i.e. when $\nu > 0$). Suppose, for the moment, that N is even. We find that (yellow) 1-by-2 blocks are coupled in this case, leading to 2-by-2 diagonal blocks in the Jacobian matrix of the following form

$$\begin{pmatrix} (\Lambda_B)_{2j,2j} & (\Lambda_B)_{2j,2j-1} \\ (\Lambda_B)_{2j-1,2j} & (\Lambda_B)_{2j-1,2j-1} \end{pmatrix} \tag{3.28}$$

whose determinant is simply $\det B_j$. This is independent of i, and we have one of these for every i in the range $N+1 \leq i \leq N+\nu$. We therefore have a total contribution to the Jacobian of

$$\prod_{j=1}^{N/2} |\det B_j|^\nu. \tag{3.29}$$

Finally, when N is odd, we have the (red) 1-by-1 blocks in dB^T, which lead to ν 1-by-1 blocks on the diagonal of the Jacobian matrix, each being $(\Lambda_B)_{NN}$.

The total Jacobian is given by the modulus of the product of the determinants of the blocks on the diagonal:

$$\mathcal{J} = \prod_{i<j}{}' |\Lambda_j^2 - \Lambda_i^2| \times \begin{cases} \displaystyle\prod_{i=1}^{N/2} |\det B_i|^\nu & \text{for } N \text{ even}, \\ \displaystyle\prod_{i=1}^{(N-1)/2} |\det B_i|^\nu \, |(\Lambda_B)_{NN}|^\nu & \text{for } N \text{ odd} \end{cases} \tag{3.30}$$

Source	Even N	Odd N
Original pre-factor	$\dfrac{1}{(2\pi)^{N(N+\nu)}}$	Same
O_A	$\dfrac{VO(N)}{VO(2)^{N/2}}$	$\dfrac{VO(N)}{VO(2)^{(N-1)/2}\,VO(1)}$
O_B	$\dfrac{VO(N+\nu)}{VO(2)^{N/2}\,VO(\nu)}$	$\dfrac{VO(N+\nu)}{VO(2)^{(N-1)/2}\,VO(1)\,VO(\nu)}$
Δ_A	$\left(\sqrt{\dfrac{2\pi}{\eta_+}}\right)^{N^2/2-N+\nu N}$	$\left(\sqrt{\dfrac{2\pi}{\eta_+}}\right)^{(N^2+1)/2-N+\nu N}$
Δ_B	$\left(\sqrt{\dfrac{2\pi}{\eta_+}}\right)^{N^2/2-N}$	$\left(\sqrt{\dfrac{2\pi}{\eta_+}}\right)^{(N^2+1)/2-N}$

Table 3.2: Constants arising from integration of angular and off-diagonal variables.

in which the prime on the product symbol denotes that only those elements strictly below the blocks on the diagonal (BBD) are to be included.

Writing everything together, we have for the total measure

$$\begin{aligned} d\mu = {} & d\Lambda_A\, d\Lambda_B\, d\Delta_A\, d\Delta_B\, (O_A^T dO_A)\, (O_B^T dO_B)\, (2\pi)^{-N(N+\nu)}\, \mathcal{J}^{(N)} \prod_{i<j}{}' |\Lambda_j^2 - \Lambda_i^2| \\ & \times \exp\left\{\eta_- \sum_i \Lambda_i^2\right\} \exp\left\{-\frac{\eta_+}{2} \operatorname{Tr}(\Lambda_A\Lambda_A^T + \Lambda_B\Lambda_B^T + \Delta_A\Delta_A^T + \Delta_B\Delta_B^T)\right\} \\ & \times \begin{cases} \displaystyle\prod_{i=1}^{N/2} |\det B_i|^\nu & \text{for } N \text{ even}, \\ \displaystyle\prod_{i=1}^{(N-1)/2} |\det B_i|^\nu\, |(\Lambda_B)_{NN}|^\nu & \text{for } N \text{ odd}. \end{cases} \end{aligned} \tag{3.31}$$

3.1.3 Angular and off-diagonal integrations

We first integrate out $O_A^T dO_A$, $O_B^T dO_B$, Δ_A and Δ_B. These integrals are all decoupled, and so we get the contributions shown in Table 3.2. Here, $VO(n)$ is the volume of

the orthogonal group $O(n)$ which is given by

$$VO(n) = \prod_{d=0}^{n-1} S_d, \tag{3.32}$$

where S_d is the surface area of a d-sphere of unit radius (i.e. a sphere in $d+1$ dimensions whose surface is d-dimensional):

$$S_d = \frac{2\pi^{(d+1)/2}}{\Gamma\left(\frac{d+1}{2}\right)}. \tag{3.33}$$

Since $VO(1) = 2$ and $VO(2) = 4\pi$, we get a μ-independent total numeric factor

$$F_{N,\nu} = \begin{cases} \dfrac{1}{2^N\,(2\pi)^{N^2/2+2N+\nu N/2}}\,\dfrac{VO(N)\,VO(N+\nu)}{VO(\nu)} & \text{for } N \text{ even}, \\[2ex] \dfrac{1}{2^{N+1}\,(2\pi)^{N^2/2+2N+\nu N/2-3/2}}\,\dfrac{VO(N)\,VO(N+\nu)}{VO(\nu)} & \text{for } N \text{ odd}, \end{cases} \tag{3.34}$$

plus a μ-dependent scaling factor

$$G_{N,\nu,\mu} = \begin{cases} \eta_+^{-(N^2/2-N+\nu N/2)} & \text{for } N \text{ even}, \\ \eta_+^{-((N^2+1)/2-N+\nu N/2)} & \text{for } N \text{ odd}. \end{cases} \tag{3.35}$$

The measure is therefore

$$\begin{aligned} d\mu(\Lambda_A,\Lambda_B) &= d\Lambda_A\,d\Lambda_B\,F_{N,\nu}\,G_{N,\nu,\mu}\,\mathcal{J}^{(N)}\,{\prod_{i<j}}'|\Lambda_j^2-\Lambda_i^2|\,\exp\left\{\eta_-\sum_i\Lambda_i^2\right\} \\ &\quad\times\exp\left\{-\frac{\eta_+}{2}\,\mathrm{Tr}(\Lambda_A\Lambda_A^T+\Lambda_B\Lambda_B^T)\right\} \\ &\quad\times\begin{cases}\displaystyle\prod_{i=1}^{N/2}|\det B_i|^\nu & \text{for } N \text{ even}, \\ \displaystyle\prod_{i=1}^{(N-1)/2}|\det B_i|^\nu|(\Lambda_B)_{NN}|^\nu & \text{for } N \text{ odd}\end{cases} \\ &= F_{N,\nu}\,G_{N,\nu,\mu}\,\mathcal{J}^{(N)}\,{\prod_{i<j}}'|\Lambda_j^2-\Lambda_i^2|\,\exp\left\{\eta_-\sum_i\Lambda_i^2\right\} \\ &\quad\times\begin{cases}\displaystyle\prod_{i=1}^{N/2}\left(dA_i\,dB_i\,e^{-\frac{\eta_+}{2}\,\mathrm{Tr}(A_iA_i^T+B_iB_i^T)}\,|\det B_i|^\nu\right) & \text{for } N \text{ even}, \\ \displaystyle\prod_{i=1}^{(N-1)/2}\left(\text{ ditto }\right)_i\cdot\left(da\,db\,e^{-\frac{\eta_+}{2}(a^2+b^2)}\,|b|^\nu\right) & \text{for } N \text{ odd}. \end{cases} \end{aligned} \tag{3.36}$$

In the odd N case, we have written $a \equiv (\Lambda_A)_{NN}$ and $b \equiv (\Lambda_B)_{NN}$ for clarity.

We will now integrate out Λ_A and Λ_B at fixed $L \equiv \Lambda_A\Lambda_B$, and then we will integrate out L at fixed eigenvalues $\{\Lambda_i^2\}$. For the first of these steps, we have

$$d\mu(L) = \int d\mu(\Lambda_A, \Lambda_B)\delta(L - \Lambda_A\Lambda_B). \tag{3.37}$$

But since L, Λ_A and Λ_B are all block-diagonal, we see that

$$\delta(L - \Lambda_A\Lambda_B) = \begin{cases} \displaystyle\prod_{i=1}^{N/2} \delta^{(4)}(L_i - A_iB_i) & \text{for } N \text{ even}, \\ \\ \delta(\Lambda_N^2 - ab) \displaystyle\prod_{i=1}^{(N-1)/2} \delta^{(4)}(L_i - A_iB_i) & \text{for } N \text{ odd}. \end{cases} \tag{3.38}$$

Therefore each 2-by-2 block decouples, as does the 1-by-1 block for odd N, and so these steps can be performed separately on each block, which we do in §3.1.4 and §3.1.5. Everything is then recombined in §3.1.6.

3.1.4 Integration of the 2-by-2 diagonal blocks

In this section, our aim here is firstly to determine

$$\mathcal{P}(L_i) \equiv \int dA_i\, dB_i\, |\det B_i|^\nu \exp\left\{\frac{\eta_+}{2}\operatorname{Tr}(A_iA_i^T + B_iB_i^T)\right\} \delta^{(4)}(L_i - A_iB_i) \tag{3.39}$$

where A_i, B_i and L_i are 2-by-2 matrices[1]. We will then perform the necessary integrations to get $\mathcal{P}(\Lambda_{2i-1}^2, \Lambda_{2i}^2)$, where Λ_{2i-1}^2 and Λ_{2i}^2 are the two eigenvalues of L_i (and two of the eigenvalues of $W \equiv AB^T$). Note that $\mathcal{P}(L_i)$ is not strictly a probability density, because it is not normalised to unity.

For the remainder of §3.1.4, we will drop the subscript i on each of A_i, B_i and L_i. Furthermore, we will denote Λ_{2i-1}^2 and Λ_{2i}^2 as Λ_1^2 and Λ_2^2 respectively, otherwise the i-dependent notation becomes cumbersome.

3.1.4.1 Integration over A

First, we integrate out the matrix A. Formally, we make a change of variables from A to $F \equiv AB$. To determine the Jacobian, we write F and A as row vectors ($\tilde{F}$

[1]To pre-empt any confusion, we reiterate the B_i is a diagonal block of Λ_B which arises from the QZ decomposition of B^T (and not B), see eq. (3.8).

and $\tilde{A}$ respectively), and B as a 4-by-4 matrix operator ($\tilde{B}$), so that $\tilde{F} = \tilde{A}\tilde{B}$. In component form, this is

$$\begin{pmatrix} f_{11} & f_{12} & f_{21} & f_{22} \end{pmatrix} = \begin{pmatrix} a_{11} & a_{12} & a_{21} & a_{22} \end{pmatrix} \begin{pmatrix} b_{11} & b_{12} & 0 & 0 \\ b_{21} & b_{22} & 0 & 0 \\ 0 & 0 & b_{11} & b_{12} \\ 0 & 0 & b_{21} & b_{22} \end{pmatrix} \tag{3.40}$$

from which we can determine that the Jacobian $|\partial\{\tilde{A}\}/\partial\{\tilde{F}\}|$ is $|\det \tilde{B}|^{-1} = |\det B|^{-2}$. In the exponent, we have

$$\mathrm{Tr}(AA^T + BB^T) = \mathrm{Tr}(F^T F(B^T B)^{-1} + BB^T), \tag{3.41}$$

where we used the cyclic property of the trace operator. Making the variable change therefore gives

$$\mathcal{P}(L) = \int dB\, dF\, |\det B|^{\nu-2} \exp\left\{-\frac{\eta_+}{2}\, \mathrm{Tr}(F^T F(B^T B)^{-1} + BB^T)\right\} \delta^{(4)}(L - F). \tag{3.42}$$

We can now do the integrals over F, giving us

$$\mathcal{P}(L) = \int dB\, |\det B|^{\nu-2} \exp\left\{-\frac{\eta_+}{2}\, \mathrm{Tr}(L^T L(B^T B)^{-1} + BB^T)\right\}. \tag{3.43}$$

3.1.4.2 Diagonalisation of $L^T L$

Now $L^T L$ is symmetric (this is of course true for any L). Therefore, let us change variables from B to $B' = BO$, where O is the particular orthogonal matrix that diagonalises $L^T L$. The Jacobian for this transformation is unity. Then

$$L^T L(B^T B)^{-1} = L^T LO((B')^T B')^{-1} O^T. \tag{3.44}$$

We then take the trace of this; using the cyclic property of the trace operator we permute the final O^T to the front, to show that $L^T L$ has been replaced with the diagonal matrix D of its eigenvalues λ_1 and λ_2, which are both positive:

$$O^T L^T LO = \begin{pmatrix} \lambda_1 & 0 \\ 0 & \lambda_2 \end{pmatrix} \equiv D. \tag{3.45}$$

We now relabel B' as B.

3.1.4.3 Integration over B

On writing the matrix B in component form as $B \equiv \begin{pmatrix} a & b \\ c & d \end{pmatrix}$, then, since

$$D(B^T B)^{-1} = \frac{1}{(\det B)^2} \begin{pmatrix} \lambda_1(b^2+d^2) & \dots \\ \dots & \lambda_2(a^2+c^2) \end{pmatrix}, \tag{3.46}$$

we have for the first term in the exponent of eq. (3.43)

$$\mathrm{Tr}(D(B^T B)^{-1}) = h^{-2}\big((b^2+d^2)\lambda_1 + (a^2+c^2)\lambda_2\big), \tag{3.47}$$

in which

$$h \equiv \det B = ad - bc. \tag{3.48}$$

The second term is simply

$$\mathrm{Tr}(BB^T) = a^2 + b^2 + c^2 + d^2. \tag{3.49}$$

Now, the presence of h in eq. (3.47) means that the integrals over a, b, c and d in eq. (3.43) are not Gaussian. However, we can introduce a Dirac delta function and an additional integral, allowing us to treat the quantity h as being independent of a, b, c and d:

$$\mathcal{P}(L) = \int_{-\infty}^{\infty} dh\, |h|^{\nu-2} \int dB\, \delta(h - ad + bc) \times \exp\Big\{ -\frac{\eta_+}{2}\big[a^2 + b^2 + c^2 + d^2 + h^{-2}((b^2+d^2)\lambda_1 + (a^2+c^2)\lambda_2)\big]\Big\}. \tag{3.50}$$

In order to decouple h from a, b, c and d, we now replace the delta function with the integral representation

$$\delta(x) = \frac{1}{2\pi}\int_{-\infty}^{\infty} d\omega\, e^{-i\omega x}, \tag{3.51}$$

giving

$$\mathcal{P}(L) = \frac{1}{2\pi}\int_{-\infty}^{\infty} dh\, |h|^{\nu-2} \int_{-\infty}^{\infty} d\omega\, e^{-i\omega h} \times \int dB\, \exp\left\{-\frac{1}{2}(\phi_2[a^2+c^2] + \phi_1[b^2+d^2]) + i\omega(ad-bc)\right\}, \tag{3.52}$$

where

$$\phi_i \equiv \eta_+\left(1 + \frac{\lambda_i}{h^2}\right) \qquad \text{for } i = 1, 2. \tag{3.53}$$

Using eq. (A.3) we can perform the a, b, c and d integrals as two pairs, giving

$$\begin{aligned}\mathcal{P}(L) &= 2\pi \int_{-\infty}^{\infty} dh\, |h|^{\nu-2} \int_{-\infty}^{\infty} d\omega\, e^{-i\omega h} \frac{1}{\omega^2 + \phi_1\phi_2} \\ &= 4\pi \int_0^{\infty} dh\, h^{\nu-2} \int_{-\infty}^{\infty} d\omega\, e^{-i\omega h} \frac{1}{\omega^2 + \phi_1\phi_2}. \end{aligned} \tag{3.54}$$

Let us do an easy variable change from ω to $\tau = \omega h$, giving

$$\begin{aligned}\mathcal{P}(L) &= 4\pi \int_0^{\infty} dh\, h^{\nu-2} \int_{-\infty}^{\infty} \frac{d\tau}{h} \frac{e^{-i\tau}}{\frac{\tau^2}{h^2} + \phi_1\phi_2} \\ &= 4\pi \int_0^{\infty} dh\, h^{\nu-1} \int_{-\infty}^{\infty} d\tau \frac{e^{-i\tau}}{\tau^2 + \eta_+^2(h^2 + (\lambda_1+\lambda_2) + \lambda_1\lambda_2/h^2)}. \end{aligned} \tag{3.55}$$

Using the elementary result that, for $a > 0$,

$$\frac{1}{a} = \int_0^{\infty} e^{-at}\, dt \tag{3.56}$$

we have

$$\mathcal{P}(L) = 4\pi \int_0^{\infty} dh\, h^{\nu-1} \int_{-\infty}^{\infty} d\tau\, e^{-i\tau} \int_0^{\infty} dt\, e^{-(\tau^2 + \eta_+^2(h^2 + (\lambda_1+\lambda_2) + \lambda_1\lambda_2/h^2))t}. \tag{3.57}$$

This allows us to do the τ-integral, using the relationship eq. (A.2):

$$\mathcal{P}(L) = 4\pi \int_0^{\infty} dh\, h^{\nu-1} \int_0^{\infty} dt\, e^{-\eta_+^2(h^2 + (\lambda_1+\lambda_2) + \lambda_1\lambda_2/h^2)t} \sqrt{\frac{\pi}{t}} e^{-1/4t}. \tag{3.58}$$

To do the h-integral, let us change variables from h to $g = \dfrac{\eta_+^2\lambda_1\lambda_2 t}{h^2}$, so that

$$\begin{aligned}\mathcal{P}(L) &= 4\pi^{3/2} \int_0^{\infty} \frac{dg}{2\eta_+^2\lambda_1\lambda_2 t} \left(\frac{\eta_+^2\lambda_1\lambda_2 t}{g}\right)^{\nu/2+1} \int_0^{\infty} dt\, e^{-(\eta_+^4\lambda_1\lambda_2 t^2/g + \eta_+^2(\lambda_1+\lambda_2)t + g)} \frac{e^{-1/4t}}{\sqrt{t}} \\ &= 4\pi^{3/2}(\lambda_1\lambda_2)^{\nu/4} \int_0^{\infty} \frac{dt}{\sqrt{t}} \exp\left\{-\eta_+^2(\lambda_1+\lambda_2)t - \frac{1}{4t}\right\} \\ &\quad \times \frac{1}{2}(\eta_+^2\sqrt{\lambda_1\lambda_2}t)^{\nu/2} \int_0^{\infty} \frac{dg}{g^{\nu/2+1}}\, e^{-g - (\eta_+^2\sqrt{\lambda_1\lambda_2}t)^2/g}. \end{aligned} \tag{3.59}$$

We can now do the g-integral (i.e. the transformed h-integral) using eq. 8.432.6 of [Gra07] (for real z)

$$K_\nu(z) = \frac{1}{2}\left(\frac{z}{2}\right)^\nu \int_0^{\infty} \frac{e^{-t - z^2/4t}}{t^{\nu+1}}\, dt \tag{3.60}$$

where $K_\nu(z)$ is the modified Bessel function, which gives

$$\mathcal{P}(L) = 4\pi^{3/2}(\lambda_1\lambda_2)^{\nu/4} \int_0^{\infty} \frac{dt}{\sqrt{t}} \exp\left\{-\eta_+^2(\lambda_1+\lambda_2)t - \frac{1}{4t}\right\} K_{\frac{\nu}{2}}(2\eta_+^2\sqrt{\lambda_1\lambda_2}t). \tag{3.61}$$

To summarise, this gives us the probability density function for the 2-by-2 matrix L, expressed in terms of the two real, positive eigenvalues (λ_1 and λ_2) of $L^T L$.

3.1.4.4 Change variables to eigenvalues of L

We now switch from considering $L^T L$ (i.e. with its eigenvalues λ_1 and λ_2) to L itself, with eigenvalues Λ_1^2 and Λ_2^2. We do this in two steps, as follows.

In general, we can orthogonally transform any real matrix L to the form $\begin{pmatrix} \epsilon_1 & s \\ -s & \epsilon_2 \end{pmatrix}$, where ϵ_1, ϵ_2, s and the rotation parameter θ are also all real. This transformation is unique if an ordering of the epsilons is specified, and $0 \leq \theta < \pi$. In terms of these new variables, we have

$$\begin{aligned} \lambda_1 + \lambda_2 &= \mathrm{Tr}\, D \\ &= \epsilon_1^2 + \epsilon_2^2 + 2s^2, \qquad \text{and} \\ \lambda_1 \lambda_2 &= \det D \\ &= (\epsilon_1 \epsilon_2 + s^2)^2. \end{aligned} \tag{3.62}$$

Of course, ϵ_1 and ϵ_2 are not the eigenvalues of L; these are Λ_1^2 and Λ_2^2, and so we need to write the combinations $\lambda_1 + \lambda_2$ and $\lambda_1 \lambda_2$ in terms of $\{\Lambda_1^2, \Lambda_2^2, s, \theta\}$, rather than in terms of $\{\epsilon_1, \epsilon_2, s, \theta\}$. In fact, the relationship between the products of the eigenvalues follows immediately (we can by-pass the earlier parametrisation of L):

$$\lambda_1 \lambda_2 = \Lambda_1^4 \Lambda_2^4. \tag{3.63}$$

To determine $\lambda_1 + \lambda_2$, we will first determine an explicit relationship between the eigenvalues $\{\Lambda_1^2, \Lambda_2^2\}$ and the matrix parameters $\{\epsilon_1, \epsilon_2, s\}$. We have

$$\begin{aligned} 0 &= \begin{vmatrix} \epsilon_1 - \Lambda^2 & s \\ -s & \epsilon_2 - \Lambda^2 \end{vmatrix} \\ &= \Lambda^4 - (\epsilon_1 + \epsilon_2)\Lambda^2 + (\epsilon_1 \epsilon_2 + s^2) \end{aligned} \tag{3.64}$$

which has the solution

$$\Lambda_{1,2}^2 = \frac{\epsilon_1 + \epsilon_2}{2} \pm \sqrt{\frac{(\epsilon_1 - \epsilon_2)^2}{4} - s^2}. \tag{3.65}$$

This can be rearranged, to give

$$\epsilon_{1,2} = \frac{\Lambda_1^2 + \Lambda_2^2}{2} \pm \sqrt{\frac{(\Lambda_1^2 - \Lambda_2^2)^2}{4} + s^2}. \tag{3.66}$$

Therefore, after a few lines of elementary algebra, we find that

$$\begin{aligned} \lambda_1 + \lambda_2 &= \epsilon_1^2 + \epsilon_2^2 + 2s^2 \qquad \text{(from above)} \\ &= \Lambda_1^4 + \Lambda_2^4 + 4s^2. \end{aligned} \tag{3.67}$$

This then completes the change of variables (we calculate the Jacobian below). We have only to determine the range of s. Our parametrisation involves real ϵ_1 and ϵ_2, and so, from eq. (3.66),

$$\frac{(\Lambda_1^2-\Lambda_2^2)^2}{4}+s^2\geq 0 \tag{3.68}$$

and hence

$$s^2\geq -\frac{(\Lambda_1^2-\Lambda_2^2)^2}{4}. \tag{3.69}$$

There are two possibilities for the eigenvalues of a 2-by-2 real matrix: either both are real, or they are both complex, and complex conjugates of each other. Therefore we must have

$$s^2\geq s^2_{\min}(\Lambda_1^2,\Lambda_2^2)=\begin{cases} 0 & \text{if } \Lambda_{1,2}^2\in\mathbb{R},\\ -\dfrac{(\Lambda_1^2-\Lambda_2^2)^2}{4}>0 & \text{if } \Lambda_{1,2}^2\in\mathbb{C}\backslash\mathbb{R},\quad \Lambda_1^2=\Lambda_2^{2*}. \end{cases} \tag{3.70}$$

Let us evaluate the Jacobian; for the first step, we write the matrix L in component form as $\begin{pmatrix} l_{11} & l_{12}\\ l_{21} & l_{22}\end{pmatrix}$, and evaluate

$$\mathcal{J}_1=\left|\frac{\partial\{l_{11},l_{12},l_{21},l_{22}\}}{\partial\{\epsilon_1,\epsilon_2,s,\theta\}}\right|. \tag{3.71}$$

We have

$$\begin{pmatrix} l_{11} & l_{12}\\ l_{21} & l_{22}\end{pmatrix}=\begin{pmatrix} \cos\theta & -\sin\theta\\ \sin\theta & \cos\theta\end{pmatrix}\begin{pmatrix} \epsilon_1 & s\\ -s & \epsilon_2\end{pmatrix}\begin{pmatrix} \cos\theta & \sin\theta\\ -\sin\theta & \cos\theta\end{pmatrix} \tag{3.72}$$

giving

$$\begin{aligned} l_{11}&=\epsilon_1\cos^2\theta+\epsilon_2\sin^2\theta,\\ l_{12}&=(\epsilon_1-\epsilon_2)\sin\theta\cos\theta+s,\\ l_{21}&=(\epsilon_1-\epsilon_2)\sin\theta\cos\theta-s,\\ l_{22}&=\epsilon_1\sin^2\theta+\epsilon_2\cos^2\theta. \end{aligned} \tag{3.73}$$

Then

$$\mathcal{J}_1=\begin{vmatrix} \cos^2\theta & \sin^2\theta & 0 & -2\sin\theta\cos\theta(\epsilon_1-\epsilon_2)\\ \sin\theta\cos\theta & -\sin\theta\cos\theta & 1 & (\cos^2\theta-\sin^2\theta)(\epsilon_1-\epsilon_2)\\ \sin\theta\cos\theta & -\sin\theta\cos\theta & -1 & (\cos^2\theta-\sin^2\theta)(\epsilon_1-\epsilon_2)\\ \sin^2\theta & \cos^2\theta & 0 & 2\sin\theta\cos\theta(\epsilon_1-\epsilon_2)\end{vmatrix}=2\,|\epsilon_1-\epsilon_2|. \tag{3.74}$$

For the second step, we have to calculate $\mathcal{J}_2$, given by

$$\mathcal{J}_2=\left|\frac{\partial\{\epsilon_1,\epsilon_2\}}{\partial\{\Lambda_1^2,\Lambda_2^2\}}\right|. \tag{3.75}$$

Using eq. (3.66), we have

$$\mathcal{J}_2 = \begin{vmatrix} \frac{1}{2}\left(1+\frac{\Lambda_1^2-\Lambda_2^2}{\epsilon_1-\epsilon_2}\right) & \frac{1}{2}\left(1-\frac{\Lambda_1^2-\Lambda_2^2}{\epsilon_1-\epsilon_2}\right) \\ \frac{1}{2}\left(1-\frac{\Lambda_1^2-\Lambda_2^2}{\epsilon_1-\epsilon_2}\right) & \frac{1}{2}\left(1+\frac{\Lambda_1^2-\Lambda_2^2}{\epsilon_1-\epsilon_2}\right) \end{vmatrix} = \left|\frac{\Lambda_1^2-\Lambda_2^2}{\epsilon_1-\epsilon_2}\right|. \tag{3.76}$$

The total Jacobian for the change to L is therefore $\mathcal{J}_1\mathcal{J}_2 = 2\,|\Lambda_1^2 - \Lambda_2^2|$.

3.1.4.5 Integration over angle θ and variable s

We now integrate over θ and s:

$$\begin{aligned}\mathcal{P}(\Lambda_1^2,\Lambda_2^2) &= \int_0^\pi d\theta \int_{|s|\geq s_{\min}}^\infty ds\, \mathcal{P}(\Lambda_1^2,\Lambda_2^2,s,\theta) \\ &= 2\pi^3 \left|\Lambda_1^2-\Lambda_2^2\right| \,|\Lambda_1^2\Lambda_2^2|^{\nu/2}\, \frac{g(\Lambda_1^2,\Lambda_2^2)}{\eta_+}\end{aligned} \tag{3.77}$$

for Λ_1^2 and Λ_2^2 in some specified order, where

$$g(\Lambda_1^2,\Lambda_2^2) \equiv \frac{4\eta_+}{\sqrt{\pi}} \int_0^\infty \frac{dt}{\sqrt{t}} \exp\left\{-\eta_+^2(\Lambda_1^4+\Lambda_2^4)t - \frac{1}{4t}\right\} K_{\frac{\nu}{2}}(2\eta_+^2|\Lambda_1^2\Lambda_2^2|t) \int_{|s|\geq s_{\min}}^\infty ds\, e^{-4\eta_+^2 t s^2} \tag{3.78}$$

and the range of s was discussed earlier. The final integral is nothing more than the complementary error function, and so we have

$$g(\Lambda_1^2,\Lambda_2^2) = 2\int_0^\infty \frac{dt}{t} \exp\left\{-\eta_+^2(\Lambda_1^4+\Lambda_2^4)t - \frac{1}{4t}\right\} K_{\frac{\nu}{2}}(2\eta_+^2|\Lambda_1^2\Lambda_2^2|t)\ \mathrm{erfc}(2\eta_+\sqrt{t}\, s_{\min}). \tag{3.79}$$

3.1.4.6 Both eigenvalues real

For real Λ^2, $s_{\min} = 0$ and using the fact that $\mathrm{erfc}(0) = 1$, we have

$$g(\Lambda_1^2,\Lambda_2^2) = 2\int_0^\infty \frac{dt}{t} \exp\left\{-\eta_+^2(\Lambda_1^4+\Lambda_2^4)t - \frac{1}{4t}\right\} K_{\frac{\nu}{2}}(2\eta_+^2|\Lambda_1^2\Lambda_2^2|t). \tag{3.80}$$

We change variables $u = \frac{1}{2t}$ to give

$$g(\Lambda_1^2,\Lambda_2^2) = 2\int_0^\infty \frac{du}{u} \exp\left\{-\frac{\eta_+^2(\Lambda_1^4+\Lambda_2^4)}{2u} - \frac{u}{2}\right\} K_{\frac{\nu}{2}}\left(\frac{\eta_+^2|\Lambda_1^2\Lambda_2^2|}{u}\right). \tag{3.81}$$

We can now use eq. 6.653.2 of [Gra07] directly to do the integral:

$$\begin{aligned} g(\Lambda_1^2,\Lambda_2^2) &= 4K_{\frac{\nu}{2}}(\eta_+|\Lambda_1^2|)K_{\frac{\nu}{2}}(\eta_+|\Lambda_2^2|) \\ &\equiv g(\Lambda_1^2)\, g(\Lambda_2^2) \end{aligned} \tag{3.82}$$

where

$$g(x) = 2K_{\frac{\nu}{2}}(\eta_+|x|) \qquad \text{for } x \in \mathbb{R}. \tag{3.83}$$

We shall shortly extend this definition of $g(x)$ to complex argument, in a smooth, but not analytic, manner.

3.1.4.7 Both eigenvalues complex

When the Λ^2's are complex, we have $\Lambda_2^2 = (\Lambda_1^2)^*$. Writing $\Lambda_1^2 = x + iy$, we have

$$\Lambda_1^4 + \Lambda_2^4 = 2(x^2 - y^2) \qquad \text{and} \qquad |\Lambda_1^2 \Lambda_2^2| = x^2 + y^2. \tag{3.84}$$

Now,

$$s_{\min}^2 = -\frac{(\Lambda_1^2 - \Lambda_2^2)^2}{4} = y^2, \tag{3.85}$$

and so $s_{\min} = |y|$. We therefore write from eq. (3.79)

$$g(\Lambda_1^2, \Lambda_1^{*2}) = 2 \int_0^\infty \frac{dt}{t} \exp\left\{-2\eta_+^2 (x^2 - y^2)t - \frac{1}{4t}\right\} K_{\frac{\nu}{2}}(2\eta_+^2 (x^2 + y^2)t) \operatorname{erfc}(2\eta_+ \sqrt{t}\,|y|). \tag{3.86}$$

Since we will only require eq. (3.79) for the case when the two arguments are complex conjugates of each other, and since $g(\Lambda_1^2, \Lambda_1^{*2}) = g(\Lambda_1^{*2}, \Lambda_1^2)$, we can rewrite it in the more symmetric form

$$g(\Lambda_1^2, \Lambda_2^2) = g(\Lambda_1^2)\, g(\Lambda_2^2) \tag{3.87}$$

where

$$g(z) \equiv \sqrt{g(z, z^*)}. \tag{3.88}$$

This extends our earlier definition of $g(x)$ for real argument in eq. (3.83). $g(z)$ is continuous as $\Im\mathrm{m}\, z \to 0$, but is not an analytic function anywhere.

It is interesting to compare the form of the weight function in eq. (3.86) with the weight functions from other ensembles that have already been solved. We observe that the presence of an exponential is very much the signature of a Gaussian ensemble, arising of course from the original weight function in the matrix representation [Meh04]. Modified K-Bessel functions are seemingly ubiquitous in the weight functions for the (non-Hermitian) chiral ensembles (cf. chGinUE [Osb04] and chGinSE [Ake05b]). And the complementary error function is present in the non-Hermitian orthogonal ensemble (GinOE [Lehm91]). It is therefore reassuring to note that our representation for the weight function eq. (3.86) contains a combination of an exponential, a modified Bessel function and an error function.

3.1.5 Integration of the 1-by-1 diagonal block for odd N

When N is odd, we have an extra 1-by-1 block to integrate over in eq. (3.36), leading to the final unpaired eigenvalue Λ_N^2 which will always be real. We have

$$\mathcal{P}(\Lambda_N^2) = \int_{-\infty}^{\infty} da \int_{-\infty}^{\infty} db \exp\left\{-\frac{\eta_+}{2}(a^2 + b^2)\right\} |b|^\nu\, \delta(\Lambda_N^2 - ab). \tag{3.89}$$

If $\Lambda_N^2 < 0$, then we can change variables $a \to -a$, and so for arbitrary real Λ_N^2 we can write

$$\mathcal{P}(\Lambda_N^2) = \int_{-\infty}^{\infty} da \int_{-\infty}^{\infty} db \, \exp\left\{-\frac{\eta_+}{2}(a^2+b^2)\right\} \, |b|^\nu \delta(|\Lambda_N^2| - ab). \tag{3.90}$$

We can now trivially do the a-integral, and, because the integrand is symmetric in b, we have

$$\mathcal{P}(\Lambda_N^2) = 2\int_0^{\infty} db \, \exp\left\{-\frac{\eta_+}{2}\left(b^2 + \frac{|\Lambda_N^2|^2}{b^2}\right)\right\} \, b^{\nu-1}. \tag{3.91}$$

We can now do the b-integral by making an easy change of variables to $t = \dfrac{\eta_+|\Lambda_N^2|^2}{2b^2}$ and using eq. 8.432.6 of [Gra07]. The result is

$$\mathcal{P}(\Lambda_N^2) = 2|\Lambda_N^2|^{\nu/2} K_{\frac{\nu}{2}}(\eta_+|\Lambda_N^2|) = |\Lambda_N^2|^{\nu/2} g(\Lambda_N^2) \tag{3.92}$$

where $g(x)$ is the same function that was defined in eq. (3.83).

3.1.6 Joint probability density function

We now draw everything together from the previous two sections. For the i-th 2-by-2 block, we get a contribution from eq. (3.77) of

$$2\pi^3 \, |\Lambda_{2i-1}^2 - \Lambda_{2i}^2| \, |\Lambda_{2i-1}^2 \Lambda_{2i}^2|^{\nu/2} \, \frac{g(\Lambda_{2i-1}^2, \Lambda_{2i}^2)}{\eta_+}, \tag{3.93}$$

and when N is odd, we have an additional single contribution from eq. (3.92) of

$$|\Lambda_N^2|^{\nu/2} \, g(\Lambda_N^2). \tag{3.94}$$

Let us determine the overall numeric pre-factor in eq. (3.36), after doing the integrals in each block. For the even N case, there is an extra factor $2\pi^3$ per 2-by-2 block (of which there are $\frac{N}{2}$). The total numeric factor is therefore

$$(2\pi^3)^{N/2} F_{N,\nu} = \frac{1}{2^{2N}} \, \frac{1}{(2\pi)^{N(N+1+\nu)/2}} \, \frac{VO(N)VO(N+\nu)}{VO(\nu)} \tag{3.95}$$

where $F_{N,\nu}$ was defined in eq. (3.34). For odd N, we again have a factor $2\pi^3$ for each 2-by-2 block (of which there are $\frac{N-1}{2}$), plus a factor of unity for the 1-by-1 block, giving a total numeric factor

$$(2\pi^3)^{(N-1)/2} F_{N,\nu} = \frac{1}{2^{2N}} \, \frac{1}{(2\pi)^{N(N+1+\nu)/2}} \, \frac{VO(N)VO(N+\nu)}{VO(\nu)}. \tag{3.96}$$

We see that the overall numeric factor is the same regardless of whether N is even or odd. We also collect together powers of η_+ in the pre-factor, coming both from $G_{N,\nu,\mu}$ in eq. (3.35) and from eq. (3.93). This is also the same for both even and odd N. The total pre-factor can therefore be written as

$$c_N = \frac{C_N^2 \, k_\nu^{(N)} \, \mathcal{J}^{(N)}}{\eta_+^{N(N+\nu-1)/2}} \tag{3.97}$$

where

$$C_N \equiv 2^{-N} (2\pi)^{-N(N+1)/4} \, VO(N), \tag{3.98}$$

$$k_\nu^{(N)} \equiv (2\pi)^{-N\nu/2} \, \frac{VO(N+\nu)}{VO(N)VO(\nu)}, \tag{3.99}$$

and $\mathcal{J}^{(N)}$ was given in eq. (3.3). In our labelling we have suppressed the fact that c_N depends on μ and ν.

Finally, note that the quantities $|\Lambda_{2i-1}^2 - \Lambda_{2i}^2|$ for each $i = 1$ to $\frac{N}{2}$ (or $\frac{N-1}{2}$ for odd N) in eq. (3.93) will combine with the $\prod'_{i<j}$ in eq. (3.36) to make a true Vandermonde determinant (see eq. (2.2))

$$\prod_{i<j}^{N} |\Lambda_j^2 - \Lambda_i^2| \equiv \left|\Delta_N(\{\Lambda^2\})\right|. \tag{3.100}$$

So we end up with the modulus of a Vandermonde determinant to the power of unity, which is exactly what we would expect for an ensemble of real matrices (with Dyson index $\beta = 1$). Writing $z_i \equiv \Lambda_i^2$ for the squared eigenvalues, and defining our effective weight function as

$$w(z) \equiv |z|^{\nu/2} e^{\eta - z} g(z) \tag{3.101}$$

with $g(z)$ from eq. (3.88), we can write the JPDF as $c_N \left|\Delta_N(\{z\})\right| \prod_{k=1}^{N} w(z_k)$, for when the set of $\{z_1, \ldots, z_N\}$ contains zero or more pairs of complex conjugate values, and the remainder real, and where we have assumed that the $\{z_i\}$ have already been placed in some specified order. Otherwise the JPDF will be zero. This is indeed a properly normalised probability density, since its integral over all eigenvalues, i.e. $\mathcal{Z}_N$, was defined to be unity in eq. (2.6).

In fact, we can choose an ordering of the eigenvalues such that we can drop the modulus sign around the Vandermonde determinant. Our choice is as follows[1].

[1]Note that we choose a slightly different ordering here from that in [Ake10a].

Place the n complex eigenvalue pairs first, ordered with respect to increasing real part, and then with respect to decreasing imaginary part:

$$\begin{aligned}&(\Im\mathrm{m}\, z_1 > 0),\ (\Re\mathrm{e}\, z_2 = \Re\mathrm{e}\, z_1, \Im\mathrm{m}\, z_2 = -\Im\mathrm{m}\, z_1),\ (\Re\mathrm{e}\, z_3 \geq \Re\mathrm{e}\, z_2, \Im\mathrm{m}\, z_3 > 0), \ldots,\\ &(\Re\mathrm{e}\, z_{2n-1} \geq \Re\mathrm{e}\, z_{2n-2}, \Im\mathrm{m}\, z_{2n-1} > 0),\ (\Re\mathrm{e}\, z_{2n} = \Re\mathrm{e}\, z_{2n-1}, \Im\mathrm{m}\, z_{2n} = -\Im\mathrm{m}\, z_{2n-1}),\end{aligned} \tag{3.102}$$

and the $N - 2n$ real eigenvalues following in increasing order:

$$z_{2n+1} < z_{2n+2} < \ldots < z_N. \tag{3.103}$$

When a pair of eigenvalues is complex, we need to change variables once again, from z and z^* to $x = \Re\mathrm{e}\, z$ and $y = \Im\mathrm{m}\, z$; we then have $dz\, dz^* = (dx + i\, dy)(dx - i\, dy) = -2i\, dx\, dy \equiv -2i\, d^2z$.

Putting everything togther, we have for the partition function

$$\mathcal{Z}_N = \int_{\mathbb{C}} d^2z_1 \ldots \int_{\mathbb{C}} d^2z_N\, P_N(z_1, \ldots, z_N) \tag{3.104}$$

where the JPDF is given by

$$\begin{aligned}P_N(z_1, \ldots, z_N) = c_N \prod_{k=1}^{N} w(z_k) \Delta_N(\{z\}) \\ \times \sum_{n=0}^{[N/2]} \Big(\prod_{p=1}^{n} (2i)\, \delta^2(z_{2p-1} - z_{2p}^*) \Theta(\Im\mathrm{m}\, z_{2p-1}) \prod_{q=2}^{n} \Theta(\Re\mathrm{e}\, z_{2q-1} - \Re\mathrm{e}\, z_{2q-3}) \\ \times \prod_{r=2n+1}^{N} \delta(\Im\mathrm{m}\, z_r) \prod_{s=2n+2}^{N} \Theta(\Re\mathrm{e}\, z_s - \Re\mathrm{e}\, z_{s-1}) \Big).\end{aligned} \tag{3.105}$$

This is an eigenvalue representation for the partition function in which P_N is 'completely ordered', by which we mean that, for a given fixed set of squared eigenvalues $\{z_1, \ldots, z_N\}$, P_N is non-zero for (at most) one permutation of this set. In §4.1 we will derive an alternative form for the partition function which involves an integral over a factorised JPDF ($\hat{P}_N$), and in §4.3 we will introduce a symmetrised representation (P_N^{sym}).

3.2 JPDF for unquenched case

The modification needed for the unquenched case now follows easily. We have for each of the determinant factors in eq. (2.6)

$$\det(\mathcal{D} + m_f \mathcal{I}) = \prod_{j=1}^{2N+\nu} (\Lambda_j + m_f) \tag{3.106}$$

where the Λ_j are the eigenvalues of the Dirac matrix $\mathcal{D}$. Since the eigenvalues come in N pairs $\pm\Lambda$, and a further ν of them are exactly zero, we can write

$$\det(\mathcal{D} + m_f \mathcal{I}) = (-1)^N \, m_f^\nu \prod_{j=1}^{N} (z_j - m_f^2), \tag{3.107}$$

where the product runs over the N distinct, non-zero, squared eigenvalues $z_j \equiv \Lambda_j^2$. The partition function is therefore given by

$$\mathcal{Z}_N^{(N_f)} = (-1)^{N\,N_f} \prod_{f=1}^{N_f} m_f^\nu \prod_{k=1}^{N} \int_{\mathbb{C}} d^2 z_k \, P_N(z_1, \ldots, z_N) \prod_{g=1}^{N_f} \prod_{j=1}^{N} (z_j - m_g^2). \tag{3.108}$$

It should be noted that, for $m_f^2 \in \mathbb{R}$, these determinant factors are always real (since the z_j themselves are either real or come in complex conjugate pairs) but may not necessarily be positive, and so the same is true of the integrand in the partition function (the 'JPDF').

Chapter 4

Algebraic structure

In the previous chapter, we found the JPDF for the eigenvalues of the chGinOE, but this was expressed as a sum over distinct cases each with a fixed number of real and complex eigenvalues. Such a representation is difficult to work with directly, and so we begin this chapter by re-expressing the partition function as an integral involving a factorised, bivariate weight function. The structure of this is then somewhat closer to that of the other Gaussian ensembles (see eq. (2.3)), involving a Vandermonde determinant (to some power) and a product of weight functions, and therefore allows us to use a variant of the orthogonal polynomial method to derive the correlation functions.

In fact, we have to use the skew-orthogonal polynomials of the bivariate weight function, together with the associated kernel, and §4.2 is devoted to introducing these concepts and the relationships between them.

We then present two alternative methods of deriving the correlation functions for the eigenvalues. The first method involves writing the JPDF as a quaternion determinant (equivalent to a Pfaffian), which can then be repeatedly integrated using Dyson's Integration Theorem to obtain the correlation functions, also expressed as quaternion determinants. Conversely, the second method involves the functional differentiation of a generating function, which we perform explicitly for the density and two-point correlation functions by placing Dirac delta functions into the partition function.

As will be seen, many of the results that we derive in this chapter do not depend on the specific form of the weight function. Appendix C contains a discussion of how the symplectic ($\beta = 4$) ensemble also fits the same pattern.

Finally, we mention that we shall generally only consider the case of even matrix size N from now on, because our ultimate interest is in the large-N limits which are independent of the parity of N. The exception to this is in the next section (§4.1), where the odd N case follows easily from the even N case.

4.1 Factorisation of the JPDF

4.1.1 Quenched case

We start by finding a factorised representation of the quenched JPDF[1], although we note that this factorised JPDF can take negative values for certain combinations of arguments, and so is not a true probability density as such. Furthermore, in order to calculate the expectation of any observable quantity, it will be necessary to symmetrise the JPDF (see §4.3).

Let us consider the even N case first. Starting with the representation for the partition function in eqs. (3.104) and (3.105), we observe that, after interchanging two pairs of complex eigenvalues, and relabelling, then everything remains unchanged. Therefore, by summing over all such permutations and dividing by $n!$, we will have removed the ordering of the pairs (although still keeping the ordering within each pair the same). We therefore have

$$\begin{aligned}\mathcal{Z}_N = c_N \prod_{k=1}^{N} \int_{\mathbb{C}} d^2 z_k \, w(z_k) \Delta_N(\{z\}) \\ \times \sum_{n=0}^{N/2} \frac{1}{n!} \Big(\prod_{p=1}^{n} (2i) \, \delta^2(z_{2p-1} - z_{2p}^*) \Theta(\Im\mathrm{m}\, z_{2p-1}) \\ \times \prod_{r=2n+1}^{N} \delta(\Im\mathrm{m}\, z_r) \prod_{s=2n+2}^{N} \Theta(\Re\mathrm{e}\, z_s - \Re\mathrm{e}\, z_{s-1}) \Big). \end{aligned} \tag{4.1}$$

We now drop the ordering between different pairs of real eigenvalues, just keeping

[1]The author originally derived a proof of this factorisation starting from the generalised de Bruijn formula. However, the proof that we present here is based on that of Mario Kieburg, and the de Bruijn formula then follows as a consequence (see §4.4.1). We jointly published both proofs in [Ake10b].

each pair internally ordered as before. Using the result eq. (A.34), we have

$$\begin{aligned}\mathcal{Z}_N = c_N \prod_{k=1}^{N} \int_{\mathbb{C}} d^2 z_k \, w(z_k) \Delta_N(\{z\}) \\ \times \sum_{n=0}^{N/2} \frac{1}{n! \left(\frac{N}{2}-n\right)!} \Big(\prod_{p=1}^{n} (2i) \, \delta^2(z_{2p-1} - z_{2p}^*) \Theta(\Im\mathrm{m}\, z_{2p-1}) \\ \times \prod_{r=2n+1}^{N} \delta(\Im\mathrm{m}\, z_r) \prod_{t=n+1}^{N/2} \Theta(\Re\mathrm{e}\, z_{2t} - \Re\mathrm{e}\, z_{2t-1}) \Big). \end{aligned} \tag{4.2}$$

Finally, and by using further relabelling, we can now use the binomial summation formula

$$\sum_{n=0}^{L} \frac{1}{n!(L-n)!} A^n \, B^{L-n} = \frac{1}{L!} \prod_{j=0}^{L} (A+B) \tag{4.3}$$

to give

$$\mathcal{Z}_N = \frac{c_N}{\left(\frac{N}{2}\right)!} \prod_{k=1}^{N} \int_{\mathbb{C}} d^2 z_k \prod_{j=1}^{N/2} \mathcal{G}(z_{2j-1}, z_{2j}) \, \Delta_N(\{z\}), \tag{4.4}$$

where $\mathcal{G}(z_1, z_2)$ is an asymmetric weight

$$\mathcal{G}(z_1, z_2) \equiv w(z_1) w(z_2) \Big\{ \Theta(x_2 - x_1) \delta(y_1) \delta(y_2) + 2i \Theta(y_1) \delta^2(z_1 - z_2^*) \Big\}. \tag{4.5}$$

On relabelling once more, and adding (using the anti-symmetric property of the determinant), we can write

$$\mathcal{Z}_N = \int_{\mathbb{C}} d^2 z_1 \ldots \int_{\mathbb{C}} d^2 z_N \, \hat{P}(z_1, \ldots, z_N), \tag{4.6}$$

where $\hat{P}(z_1, \ldots, z_N)$ is our 'factorised' JPDF

$$\hat{P}(z_1, \ldots, z_N) = \frac{c_N}{\left(\frac{N}{2}\right)!} \prod_{j=1}^{N/2} \frac{\mathcal{F}(z_{2j-1}, z_{2j})}{2} \, \Delta_N(\{z\}) \tag{4.7}$$

and $\mathcal{F}(z_1, z_2)$ is the anti-symmetric function

$$\mathcal{F}(z_1, z_2) \equiv w(z_1) w(z_2) \Big\{ 2i \delta^2(z_1 - z_2^*) \, \mathrm{sgn}(y_1) + \delta(y_1) \delta(y_2) \, \mathrm{sgn}(x_2 - x_1) \Big\}. \tag{4.8}$$

$\mathcal{F}(z_1, z_2)$ plays a key role in the analysis of the chGinOE. However, in fact, we can write

$$\mathcal{Z}_N = \frac{c_N}{\left(\frac{N}{2}\right)!} \prod_{k=1}^{N} \int_{\mathbb{C}} d^2 z_k \prod_{j=1}^{N/2} \hat{\mathcal{F}}(z_{2j-1}, z_{2j}) \, \Delta_N(\{z\}) \tag{4.9}$$

for *any* $\hat{\mathcal{F}}(z_1, z_2)$ that satisfies

$$\hat{\mathcal{F}}(z_1, z_2) - \hat{\mathcal{F}}(z_2, z_1) = \mathcal{F}(z_1, z_2). \tag{4.10}$$

$\mathcal{G}$ is one possibility for $\hat{\mathcal{F}}$; another is of course simply

$$\hat{\mathcal{F}}(z_1, z_2) = \frac{\mathcal{F}(z_1, z_2)}{2}, \tag{4.11}$$

as in eq. (4.7).

For odd N, we would simply carry through an extra integral for the unpaired (and always real) eigenvalue:

$$\mathcal{Z}_N = \frac{c_N}{(\frac{N-1}{2})!} \prod_{k=1}^{N} \int_{\mathbb{C}} d^2 z_k \prod_{j=1}^{\frac{N-1}{2}} \hat{\mathcal{F}}(z_{2j-1}, z_{2j})\, w(z_N) \delta(\Im\mathrm{m}\, z_N)\, \Delta_N(\{z\}). \tag{4.12}$$

We should add that this factorisation result can also be applied to any other ensemble that can be cast into the form of eq. (3.104) for some weight function $w(z)$. Examples include the (non-chiral) GinOE and the symplectic ($\beta = 4$) cases. We refer to [Ake10b] for further details.

4.1.2 Unquenched case

Because the determinants in eq. (2.6) can be written in terms of the Wishart (squared) eigenvalues (see eq. (3.107)), we can easily write down the partition function for the unquenched case as an integral over eigenvalues as follows:

$$\mathcal{Z}_N^{(N_f)} = (-1)^{N N_f} \prod_{f=1}^{N_f} m_f^{\nu} \int_{\mathbb{C}} d^2 z_1 \ldots \int_{\mathbb{C}} d^2 z_N\, \hat{P}_N(z_1, \ldots, z_N) \prod_{g=1}^{N_f} \prod_{k=1}^{N} (z_k - m_g^2). \tag{4.13}$$

For even N, this is

$$\mathcal{Z}_N^{(N_f)} = \frac{c_N}{(\frac{N}{2})!} \prod_{f=1}^{N_f} m_f^{\nu} \int_{\mathbb{C}} d^2 z_1 \ldots \int_{\mathbb{C}} d^2 z_N\, \Delta_N(\{z\}) \prod_{j=1}^{N/2} \hat{\mathcal{F}}(z_{2j-1}, z_{2j}) \prod_{g=1}^{N_f} \prod_{k=1}^{N} (z_k - m_g^2), \tag{4.14}$$

where we used the representation in eq. (4.9). If we define the unquenched bivariate weight function $\hat{\mathcal{F}}^{(N_f)}(u, v)$ as

$$\hat{\mathcal{F}}^{(N_f)}(u, v) \equiv \hat{\mathcal{F}}(u, v) \prod_{g=1}^{N_f} (u - m_g^2)(v - m_g^2), \tag{4.15}$$

then the unquenched partition function has the form

$$\mathcal{Z}_N^{(N_f)} = \frac{c_N}{(\frac{N}{2})!} \prod_{f=1}^{N_f} m_f^\nu \int_{\mathbb{C}} d^2 z_1 \ldots \int_{\mathbb{C}} d^2 z_N \, \Delta_N(\{z\}) \prod_{k=1}^{N/2} \hat{\mathcal{F}}^{(N_f)}(z_{2k-1}, z_{2k}), \tag{4.16}$$

i.e. we see that the ensemble with virtual quarks (i.e. with the mass-dependent determinant factors) is structurally (i.e. algebraically) the same as the quenched ensemble, but with a modified bivariate weight.

Note that, for $N_f > 0$, $\mathcal{Z}_N^{(N_f)} \equiv \mathcal{Z}_N^{(N_f)}(\{m_f\}) \neq 1$. In order to be able to make a direct comparison between the unquenched and quenched cases, it is occasionally convenient to define a different partition function that is also numerically equal to unity (cf. eq. (4.9)):

$$\mathfrak{Z}_N^{(N_f)} = \frac{c_N^{(N_f)}}{(\frac{N}{2})!} \int_{\mathbb{C}} d^2 z_1 \ldots \int_{\mathbb{C}} d^2 z_N \, \Delta_N(\{z\}) \prod_{k=1}^{N/2} \hat{\mathcal{F}}^{(N_f)}(z_{2k-1}, z_{2k}). \tag{4.17}$$

The coefficient $c_N^{(N_f)}$ now depends on the masses in a way that ensures that $\mathfrak{Z}_N^{(N_f)} = 1$ always. For this to be the case, we must have that

$$c_N^{(N_f)} = \frac{c_N \prod_{f=1}^{N_f} m_f^\nu}{\mathcal{Z}_N^{(N_f)}}. \tag{4.18}$$

In fact, we will never need $\mathfrak{Z}_N^{(N_f)}$ itself in what follows. But when 'converting' a quenched result to an unquenched one, as in eq. (4.73) for example, we will merely replace c_N with $c_N^{(N_f)}$.

4.2 Skew-symmetric measures, kernels and skew-orthogonal polynomials

As mentioned in §2.1.2, the eigenvalue JPDF for the ensembles with Dyson index $\beta = 2$ will typically contain a product of (monovariate) weight functions, together with a Vandermonde determinant (to the power of 2). This structure allows us to introduce the orthogonal polynomials and the kernel corresponding to the weight function. We can then express the JPDF in the form of a determinant containing the kernel (written in terms of the orthogonal polynomials).

For the $\beta = 1$ case, where the weight function is bivariate and anti-symmetric (skew-symmetric), and the Vandermonde determinant appears to the power of 1, we

find that it is *skew*-orthogonal polynomials that are required, and we end up with Pfaffians (or quaternion determinants), rather than determinants, in the JPDF.

A further complication is that, for the chGinOE, it is difficult to find the skew-orthogonal polynomials starting from the weight function. We defer this problem until the next chapter, where our strategy will be to determine the kernel first (in §5.2), using an independent method, and then to extract the polynomials from the kernel (in §5.4.1).

For the remainder of this present chapter, we work at a more general level, and show how expressions for the correlation functions can be written in terms of the (as yet, unknown) kernel.

This section discusses the relationships between skew-symmetric measures, kernels and skew-orthogonal polynomials. It is essentially independent of random matrix theory as such. For an alternative introduction to skew-orthogonal polynomials, see, for example, [Gho02].

Let $\mathcal{F}(z_1, z_2)$ be a skew-symmetric measure (or weight function), by which we mean that $\mathcal{F}(z_1, z_2) = -\mathcal{F}(z_2, z_1)$, and

$$\mathcal{A}_{kl} \equiv \int_{\mathbb{C}^2} d^2z_1\, d^2z_2\, \mathcal{F}(z_1, z_2) z_1^k\, z_2^l < \infty \qquad \forall\, k, l \geq 0. \tag{4.19}$$

We can define a skew-symmetric inner product of two polynomials $p(z)$ and $q(z)$ as follows:

$$\begin{aligned} \langle p|q\rangle &\equiv \int_{\mathbb{C}^2} d^2z_1\, d^2z_2\, \mathcal{F}(z_1, z_2) p(z_1)\, q(z_2) \\ &= -\langle q|p\rangle. \end{aligned} \tag{4.20}$$

Using this notation, $\mathcal{A}_{kl} = \langle z^k|z^l\rangle$. Now, for every skew-symmetric function $\mathcal{F}(z_1, z_2)$, we can always find some (non-unique) $\hat{\mathcal{F}}(z_1, z_2)$, such that

$$\mathcal{F}(z_1, z_2) = \hat{\mathcal{F}}(z_1, z_2) - \hat{\mathcal{F}}(z_2, z_1). \tag{4.21}$$

We can write the inner product in terms of $\hat{\mathcal{F}}$ as follows; eq. (4.20) becomes

$$\begin{aligned} \langle p|q\rangle &= \int_{\mathbb{C}^2} d^2z_1\, d^2z_2 \left(\hat{\mathcal{F}}(z_1, z_2) - \hat{\mathcal{F}}(z_2, z_1)\right) p(z_1)\, q(z_2) \\ &= \int_{\mathbb{C}^2} d^2z_1\, d^2z_2\, \hat{\mathcal{F}}(z_1, z_2) \left(p(z_1)\, q(z_2) - q(z_1)\, p(z_2)\right) \\ &= \int_{\mathbb{C}^2} d^2z_1\, d^2z_2\, \hat{\mathcal{F}}(z_1, z_2)\, \det \begin{bmatrix} p(z_1) & q(z_1) \\ p(z_2) & q(z_2) \end{bmatrix}. \end{aligned} \tag{4.22}$$

We note that, in general, $\hat{\mathcal{F}}(z_1, z_2)$ itself will *not* be skew-symmetric.

We can now define the skew-symmetric kernel corresponding to $\mathcal{F}$ and $\hat{\mathcal{F}}$ as (for even $N \geq 2$)

$$\mathcal{K}_N(z_1, z_2) \equiv \sum_{k=0}^{N-1} \sum_{l=0}^{N-1} \mathcal{A}^{-1}_{kl}\, z_1^k\, z_2^l. \tag{4.23}$$

Importantly, if we replace each z^k with some polynomial $p_k(z)$, such that the $\{p_k(z)\}$ are linearly independent and each $p_k(z) = z^k + \mathcal{O}(z^{k-1})$, then

$$\mathcal{K}_N(z_1, z_2) = \sum_{k=0}^{N-1} \sum_{l=0}^{N-1} \hat{\mathcal{A}}^{-1}_{kl}\, p_k(z_1)\, p_l(z_2) \tag{4.24}$$

where

$$\hat{\mathcal{A}}_{kl} \equiv \int_{\mathbb{C}^2} d^2z_1\, d^2z_2\, \mathcal{F}(z_1, z_2) p_k(z_1)\, p_l(z_2), \tag{4.25}$$

i.e. the kernel is actually independent of the choice of $\{p_k(z)\}$. It is truly a property of the measure $\mathcal{F}(z_1, z_2)$ and not of the polynomials. In fact, there will always exist a particular choice (indeed, many choices) of polynomials, denoted $\{q_k(z)\}$, and known as the skew-orthogonal polynomials, such that (for integers $j, k \geq 0$)

$$\begin{aligned} \langle q_{2j} | q_{2k} \rangle &= 0, \\ \langle q_{2j+1} | q_{2k+1} \rangle &= 0, \\ \langle q_{2j} | q_{2k+1} \rangle &= h_j \delta_{jk}, \end{aligned} \tag{4.26}$$

where h_j is then the norm of the two skew-orthogonal polynomials q_{2j} and q_{2j+1}. Note that, if $q_{2k+1}(z)$ is an odd skew-orthogonal polynomial, then so is $q_{2k+1}(z) + c q_{2k}(z)$ for any choice of constant c. The inverse of the corresponding matrix $\hat{A}$, given by

$$\hat{A}_{kl} \equiv \int_{\mathbb{C}^2} d^2z_1\, d^2z_2\, \mathcal{F}(z_1, z_2) q_k(z_1)\, q_l(z_2), \tag{4.27}$$

can be easily determined, and so the kernel reduces to a single sum

$$\mathcal{K}_N(z_1, z_2) = \sum_{k=0}^{\frac{N}{2}-1} \frac{1}{h_k} \big(q_{2k+1}(z_1) q_{2k}(z_2) - q_{2k+1}(z_2) q_{2k}(z_1) \big). \tag{4.28}$$

Given the kernels $\mathcal{K}_N(z_1, z_2)$ for every even $N \geq 2$, it is possible to extract the skew-orthogonal polynomials as follows:

$$\begin{aligned} q_{2k}(z) &= \frac{h_k}{(2k+1)!} \frac{\partial^{2k+1}}{\partial u^{2k+1}} \mathcal{K}_{2k+2}(u, z) \\ &= h_k \lim_{u \to \infty} \frac{\mathcal{K}_{2k+2}(u, z)}{u^{2k+1}}, \end{aligned} \tag{4.29}$$

$$q_{2k+1}(z) = -\frac{h_k}{(2k)!} \frac{\partial^{2k}}{\partial u^{2k}} \mathcal{K}_{2k+2}(u, z)\Big|_{u=0} + c q_{2k}(z). \tag{4.30}$$

c is some arbitrary constant mentioned above, which we will often set to zero. These results can be proven by direct manipulation of eq. (4.28), and using the fact that $q_k(z) = z^k + \mathcal{O}(z^{k-1})$.

The skew-orthogonal polynomials can also be expressed as matrix averages of characteristic polynomials. A proof of this is given in Appendix B.

4.3 Correlation functions I: Dyson-Mehta method

The first method of deriving the correlation functions involves repeated integration of the symmetrised JPDF, defined by

$$P_N^{sym}(z_1, \ldots, z_N) \equiv \frac{1}{N!} \sum_{\sigma \in S_N} \hat{P}_N(z_{\sigma(1)}, \ldots, z_{\sigma(N)}) \tag{4.31}$$

where S_N is the set of all permutations of the integers from 1 to N, and $\hat{P}_N$ is the factorised JPDF from eq. (4.7). The n-point correlation function is then defined as

$$R_{n,N}(z_1, \ldots, z_n) \equiv \frac{N!}{(N-n)!} \int_{\mathbb{C}} d^2 z_{n+1} \ldots \int_{\mathbb{C}} d^2 z_N \, P_N^{sym}(z_1, \ldots, z_N). \tag{4.32}$$

The essence of the Dyson-Mehta method is to show that the JPDF (i.e. the integrand, P_N^{sym}) can be written as the determinant of a matrix with quaternion-valued elements that satisfy certain conditions. Consequently, Dyson's Integration Theorem (see below) can be used iteratively to perform the integrals in eq. (4.32), giving the result that each correlation function can also be written as a quaternion determinant. For an introduction to quaternions and quaternion determinants (denoted Qdet), we refer to [Meh04].

4.3.1 Dyson's Integration Theorem

Let us begin by stating Dyson's Integration Theorem for the quaternion case, which we take almost verbatim from Theorem 5.1.4 of [Meh04], where one will also find a proof.

> **Dyson's Integration Theorem:** *Let $K(x, y)$ be a quaternion-valued function, such that*
>
> $$\bar{K}(x, y) = K(y, x) \tag{4.33}$$

where $\bar{K}$ is the quaternion conjugate of K. Suppose further that

$$\int dy\, K(x,y)K(y,z) = K(x,z) + \lambda K(x,z) - K(x,z)\lambda \tag{4.34}$$

with λ a constant quaternion. Let $[K(x_i,x_j)]_N$ denote the $N \times N$ matrix with its (i,j) element equal to $K(x_i,x_j)$. Then

$$\int dx_N\ \mathrm{Qdet}[K(x_i,x_j)]_N = (c-N+1)\ \mathrm{Qdet}[K(x_i,x_j)]_{N-1} \tag{4.35}$$

where

$$c = \int dx\, K(x,x). \tag{4.36}$$

In the original theorem, x, y and z are real, and the integrals are over $\mathbb{R}$. However, the generalisation to complex variables and integrals over $\mathbb{C}$ is straightforward.

4.3.2 Quaternion kernel

We begin by defining the integrated skew-orthogonal polynomial

$$Q_i(v) \equiv \int_{\mathbb{C}} d^2u\, q_i(u)\, \mathcal{F}(u,v) \tag{4.37}$$

where $\mathcal{F}(u,v)$ is the anti-symmetric weight function in eq. (4.8) and $q_i(u)$ is the i-th skew-orthogonal polynomial with respect to $\mathcal{F}(u,v)$. It follows from this, by relabelling, that

$$Q_i(u) = -\int_{\mathbb{C}} d^2v\, \mathcal{F}(u,v)\, q_i(v) \tag{4.38}$$

since $\mathcal{F}(u,v)$ is anti-symmetric. The functions $\{Q_i(z)\}$ are, of course, not themselves polynomials; we will also use them later in Chapter 9. Inserting these definitions into eq. (4.26) (where we will only keep track of the even-odd case, since the odd-odd and the even-even cases are always zero) gives

$$\int_{\mathbb{C}} d^2z\, Q_{2j}(z)\, q_{2k+1}(z) = h_j\, \delta_{jk} \ = \ -\int_{\mathbb{C}} d^2z\, q_{2j}(z)\, Q_{2k+1}(z). \tag{4.39}$$

If we now define the complex quaternion $\chi_i(z)$ as (using the 2-by-2 matrix representation, see eq. 2.4.6 of [Meh04])

$$\chi_i(z) \equiv \begin{pmatrix} q_{2i}(z) & Q_{2i}(z) \\ -q_{2i+1}(z) & -Q_{2i+1}(z) \end{pmatrix} \tag{4.40}$$

with conjugate (for definition, see eq. 2.4.9 of [Meh04])

$$\bar{\chi}_i(z) \equiv \begin{pmatrix} -Q_{2i+1}(z) & -Q_{2i}(z) \\ q_{2i+1}(z) & q_{2i}(z) \end{pmatrix} \tag{4.41}$$

then these quaternions are orthogonal (i.e. rather than skew-orthogonal) in the sense that

$$\int_{\mathbb{C}} d^2z\, \chi_j(z)\, \bar{\chi}_k(z) = 2h_j\, \delta_{jk} \begin{pmatrix} 1 & 0 \\ 0 & 1 \end{pmatrix}. \tag{4.42}$$

This choice of $\{\chi_i(z)\}$ is not unique; there are other ways of constructing orthogonal quaternions from the $\{q_i(z)\}$ and $\{Q_i(z)\}$. However, we make this choice to be consistent with the earlier results that we published in [Ake10a]. Note also that the squared norm here is $2h_j$, and not h_j as for the skew-orthogonal polynomials.

Let us now define the bivariate quaternion $K_N^Q(u,v)$ as follows

$$K_N^Q(u,v) \equiv g_N^Q(u,v) - \mathcal{F}^Q(u,v), \tag{4.43}$$

where

$$g_N^Q(u,v) \equiv \sum_{k=0}^{\frac{N}{2}-1} \frac{1}{h_k}\, \bar{\chi}_k(u)\, \chi_k(v) \quad \text{and} \tag{4.44}$$

$$\mathcal{F}^Q(u,v) \equiv \begin{pmatrix} 0 & \mathcal{F}(u,v) \\ 0 & 0 \end{pmatrix}. \tag{4.45}$$

$K_N^Q(u,v)$ is said to qualify as a quaternion kernel, because it satisfies the following relations necessary for Dyson's Integration Theorem, i.e. quaternion duality eq. (4.33) and the projection property eq. (4.34) respectively:

$$\bar{K}_N^Q(u,v) = K_N^Q(v,u), \tag{4.46}$$

$$\int_{\mathbb{C}} d^2w\, K_N^Q(u,w)\, K_N^Q(w,v) = K_N^Q(u,v) + \lambda K_N^Q(u,v) - K_N^Q(u,v)\lambda \tag{4.47}$$

where λ is some fixed quaternion constant. In this case,

$$\lambda = \begin{pmatrix} -\frac{1}{2} & 0 \\ 0 & \frac{1}{2} \end{pmatrix}. \tag{4.48}$$

One may ask what $K_N^Q(u,v)$ looks like when explicitly written out in its 2-by-2 matrix representation. A little manipulation shows that

$$K_N^Q(u,v) = \begin{pmatrix} -G_N(v,u) & W_N(u,v) \\ \mathcal{K}_N(u,v) & -G_N(u,v) \end{pmatrix} \tag{4.49}$$

where

$$\mathcal{K}_N(u,v) = \sum_{k=0}^{\frac{N}{2}-1} \frac{1}{h_k} \big(q_{2k+1}(u)q_{2k}(v) - q_{2k}(u)q_{2k+1}(v)\big), \tag{4.50}$$

$$G_N(u,v) = -\int_{\mathbb{C}} d^2z\, \mathcal{K}_N(u,z)\, \mathcal{F}(z,v) \qquad \text{and} \tag{4.51}$$

$$W_N(u,v) = \int_{\mathbb{C}^2} d^2p\, d^2q\, \mathcal{F}(u,p)\, \mathcal{K}_N(p,q)\, \mathcal{F}(q,v) - \mathcal{F}(u,v). \tag{4.52}$$

$\mathcal{K}_N(u,v)$ is precisely the same skew-orthogonal kernel that we defined in eq. (4.28).

We note in passing that $\mathcal{K}_N(u,v)$ is sometimes referred to as the 'pre-kernel', and $K_N^Q(u,v)$ simply as the 'kernel'. See, for example, [Kanz02] when considering the symplectic ($\beta = 4$) ensemble. We adopt the terminology 'kernel' and 'quaternion kernel' respectively.

4.3.3 JPDF as a quaternion determinant

In this section, we show how the symmetrised eigenvalue JPDF defined in eq. (4.31) can be written as the quaternion determinant of an $N \times N$ matrix of quaternion kernels $K_N^Q(u,v)$, i.e.

$$P_N^{sym}(z_1,\ldots,z_N) = \frac{1}{N!}\, \mathrm{Qdet}[K_N^Q(z_i,z_j)]_{1\le i,j\le N}. \tag{4.53}$$

We can then use Dyson's Integration Theorem, eq. (4.35), iteratively to derive the correlation functions. The method here is based closely on that in [Meh04] for the non-chiral, Hermitian ensemble; however, there are a few significant differences, since we are now dealing with a non-Hermitian ensemble. Furthermore, our proof also uses the factorised product formula for the JPDF in eq. (4.7).

We shall now prove eq. (4.53), starting from the right-hand side and arriving at the JPDF. The first part of our proof follows §5.8.3 of [Meh04] quite closely, although later it becomes more specific to the non-Hermitian case. Recall again that N is even throughout.

First, we write the quaternion determinant on the right-hand side of eq. (4.53) as the Pfaffian of a $2N \times 2N$ matrix of ordinary elements. Define the $2N \times 2N$ block diagonal matrix Z as

$$Z \equiv \mathrm{diag}\underbrace{(\sigma,\ldots,\sigma)}_{N\text{times}} \tag{4.54}$$

where

$$\sigma \equiv \begin{pmatrix} 0 & 1 \\ -1 & 0 \end{pmatrix}. \tag{4.55}$$

Then we use a second theorem of Dyson (Theorem 5.1.2 in [Meh04]) to write

$$\begin{aligned}\mathrm{Qdet}[K_N^Q(z_i,z_j)]_{1\le i,j\le N} &= \mathrm{Pf}\left[Z\,K_N^Q(z_i,z_j)\right]_{1\le i,j\le N}\\ &= \mathrm{Pf}\left[\begin{array}{cc}\mathcal{K}_N(z_i,z_j) & -G_N(z_i,z_j)\\ G_N(z_j,z_i) & -W_N(z_i,z_j)\end{array}\right]_{1\le i,j\le N}\\ &= (-1)^{N/2}\,\mathrm{Pf}\left[\begin{array}{c|c}\mathcal{K}_N(z_i,z_j) & -G_N(z_i,z_j)\\ \hline G_N(z_j,z_i) & -W_N(z_i,z_j)\end{array}\right]_{1\le i,j\le N}. \end{aligned} \tag{4.56}$$

In the last line we reordered the rows and columns, so that we have four $N\times N$ blocks, rather than the N^2 2×2 blocks in the line before. We now use the same linearity argument as in [Meh04] to show that, almost surely,

$$\begin{aligned}\mathrm{Qdet}[K_N^Q(z_i,z_j)]_{1\le i,j\le N} &= (-1)^{N/2}\,\mathrm{Pf}\left[\begin{array}{c|c}\mathcal{K}_N(z_i,z_j) & 0\\ \hline 0 & \mathcal{F}_N(z_i,z_j)\end{array}\right]_{1\le i,j\le N}\\ &= (-1)^{N/2}\,\mathrm{Pf}\left[\mathcal{K}_N(z_i,z_j)\right]_{1\le i,j\le N}\times\mathrm{Pf}\left[\mathcal{F}(z_i,z_j)\right]_{1\le i,j\le N}.\end{aligned} \tag{4.57}$$

It is easy to see from eq. (4.50) that (for even N)

$$\left[\mathcal{K}_N(z_i,z_j)\right]_{1\le i,j\le N} = -\mathcal{Q}(\{z\})\,\mathcal{H}\,\mathcal{Q}^T(\{z\}) \tag{4.58}$$

where $\mathcal{Q}(\{z\})$ and $\mathcal{H}$ are $N\times N$ matrices defined as

$$\mathcal{Q}(\{z\}) \equiv \left[q_{j-1}(z_i)\right]_{1\le i,j\le N} \quad \text{and} \tag{4.59}$$

$$\mathcal{H} \equiv \mathrm{diag}\left(\frac{1}{h_0}\sigma,\ldots,\frac{1}{h_{\frac{N}{2}-1}}\sigma\right) \tag{4.60}$$

and σ is the 2-by-2 matrix defined in eq. (4.55). Hence

$$\mathrm{Pf}\left[\mathcal{K}_N(z_i,z_j)\right]_{1\le i,j\le N} = (-1)^{N/2}\,\mathrm{Pf}[\mathcal{H}]\,\det[\mathcal{Q}(\{z\})]. \tag{4.61}$$

But

$$\mathrm{Pf}[\mathcal{H}] = \prod_{k=0}^{\frac{N}{2}-1}\frac{1}{h_k} \tag{4.62}$$

and

$$\det[\mathcal{Q}(\{z\})] = \Delta_N(\{z\}) \tag{4.63}$$

i.e. the Vandermonde determinant in eq. (2.2), shown by taking linear combinations of rows and columns to recreate monomial elements. Hence

$$\mathrm{Qdet}[K_N^Q(z_i,z_j)]_{1\le i,j\le N} = \prod_{k=0}^{\frac{N}{2}-1}\frac{1}{h_k}\,\Delta_N(\{z\})\,\mathrm{Pf}\left[\mathcal{F}(z_i,z_j)\right]_{1\le i,j\le N}. \tag{4.64}$$

Our proof now diverges from that in [Meh04]. Using the result eq. (A.25) in Appendix A.2.6, we can write

$$\mathrm{Pf}\left[\mathcal{F}(z_i,z_j)\right]_{1\le i,j\le N} = \frac{1}{(\frac{N}{2})!}\sum_{\sigma\in S_N}\mathrm{sgn}(\sigma)\prod_{i=1}^{N/2}\hat{\mathcal{F}}(z_{\sigma(2i-1)},z_{\sigma(2i)}) \tag{4.65}$$

where $\hat{\mathcal{F}}(u,v)$ is any function that satisfies $\mathcal{F}(u,v) = \hat{\mathcal{F}}(u,v) - \hat{\mathcal{F}}(v,u)$ (as in eq. (4.10)), and S_N is the set of all permutations of the integers from 1 to N. So, on inserting eq. (4.65) into eq. (4.64),

$$\begin{aligned}\mathrm{Qdet}[K_N^Q(z_i,z_j)]_{1\le i,j\le N} &= \left[\left(\frac{N}{2}\right)!\prod_{k=1}^{\frac{N}{2}-1}h_k\right]^{-1}\Delta_N(\{z\})\sum_{\sigma\in S_N}\mathrm{sgn}(\sigma)\prod_{i=1}^{N/2}\hat{\mathcal{F}}(z_{\sigma(2i-1)},z_{\sigma(2i)})\\ &= \left[\left(\frac{N}{2}\right)!\prod_{k=1}^{\frac{N}{2}-1}h_k\right]^{-1}\\ &\qquad\times\sum_{\sigma\in S_N}\mathrm{sgn}(\sigma)\,\mathrm{sgn}(\sigma)\Delta_N(\{\sigma(z)\})\prod_{i=1}^{N/2}\hat{\mathcal{F}}(z_{\sigma(2i-1)},z_{\sigma(2i)}),\end{aligned} \tag{4.66}$$

where we used that $\Delta_N(\{z\}) = \mathrm{sgn}(\sigma)\,\Delta_N(\{\sigma(z)\})$. But $[\mathrm{sgn}(\sigma)]^2 = 1$, and so, using eq. (4.7) with the choice eq. (4.11),

$$\begin{aligned}\mathrm{Qdet}[K_N^Q(z_i,z_j)]_{1\le i,j\le N} &= \left[c_N\prod_{k=1}^{\frac{N}{2}-1}h_k\right]^{-1}\sum_{\sigma\in S_N}\hat{P}(\sigma(z))\\ &= \left[c_N\prod_{k=1}^{\frac{N}{2}-1}h_k\right]^{-1}N!\,P_N^{sym}(z_1,\ldots,z_N),\end{aligned} \tag{4.67}$$

where P_N^{sym} is the symmetrised JPDF, defined in eq. (4.31). All that remains now is to relate the normalisation constants.

We calculate the constant c that appears in Dyson's Integration Theorem (see eq. (4.36)). We evaluate

$$\begin{aligned}\int_{\mathbb{C}}d^2z\,K_N^Q(z,z) &= \sum_{j=0}^{\frac{N}{2}-1}\frac{1}{h_j}\int_{\mathbb{C}}d^2z\,\bar{\chi}_j(z)\,\chi_j(z)\\ &= \sum_{j=0}^{\frac{N}{2}-1}\frac{1}{h_j}\begin{pmatrix}2h_j & 0\\ 0 & 2h_j\end{pmatrix}\\ &= N\begin{pmatrix}1 & 0\\ 0 & 1\end{pmatrix}\end{aligned} \tag{4.68}$$

so we take the constant c to be equal to N. Therefore, N successive applications of Dyson's Theorem will give

$$\int_{\mathbb{C}} d^2 z_1 \ldots \int_{\mathbb{C}} d^2 z_N \, \mathrm{Qdet}[K_N^Q(z_i, z_j)]_{1 \leq i,j \leq N} = N! \tag{4.69}$$

But we also have

$$\int_{\mathbb{C}} d^2 z_1 \ldots \int_{\mathbb{C}} d^2 z_N P_N^{sym}(z_1, \ldots, z_N) = \mathcal{Z}_N, \tag{4.70}$$

where $\mathcal{Z}_N$ is the partition function. Since we defined $\mathcal{Z}_N$ to be numerically equal to unity (see the discussion in §2.2.3), it then follows that

$$c_N = \prod_{k=0}^{\frac{N}{2}-1} \frac{1}{h_k} \tag{4.71}$$

which represents an important relationship between the normalisation constant c_N in the partition function, and the norms of the skew-orthogonal polynomials. Our main result, eq. (4.53), now follows from eqs. (4.67) and (4.71).

It is useful to note that eq. (4.71) implies that for $k \geq 0$

$$h_k = \frac{c_{2k}}{c_{2k+2}}. \tag{4.72}$$

For the chGinOE, we already found c_N explicitly in eq. (3.97). So, perhaps surprisingly, we can determine the norms of the skew-orthogonal polynomials without knowing the polynomials themselves. Following from the discussion at the end of §4.1.2, the norms for the unquenched skew-orthogonal polynomials must be given by the analagous formula

$$h_k^{(N_f)} = \frac{c_{2k}^{(N_f)}}{c_{2k+2}^{(N_f)}}, \tag{4.73}$$

where $c_N^{(N_f)}$ was defined in eq. (4.18).

4.3.4 Correlation functions

So, to summarise, we insert the symmetrised JPDF expressed as a quaternion determinant eq. (4.53) into the definition of the correlation functions eq. (4.32), and use Dyson's Integration Theorem eq. (4.35) to perform the integrals. The correlation functions are therefore given by (for even N, as usual)

$$R_{n,N}(z_1, \ldots, z_n) = \mathrm{Qdet}[K_N^Q(z_i, z_j)]_{1 \leq i,j \leq n}. \tag{4.74}$$

Note that there is no N- or n-dependent pre-factor. We can also write this as the Pfaffian of a $2n$-by-$2n$ matrix:

$$R_{n,N}(z_1,\ldots,z_n) = \mathrm{Pf}\left[\begin{array}{cc} \mathcal{K}_N(z_i,z_j) & -G_N(z_i,z_j) \\ G_N(z_j,z_i) & -W_N(z_i,z_j) \end{array}\right]_{1\le i,j\le n}. \tag{4.75}$$

Using this, we see that the eigenvalue density (the 1-point correlation function) can be written explicitly as

$$R_{1,N}(z_1) = -G_N(z_1,z_1) = \int_{\mathbb{C}} d^2z\, \mathcal{K}_N(z_1,z)\,\mathcal{F}(z,z_1), \tag{4.76}$$

where we used the expression for $G_N(u,v)$ from eq. (4.51). If we insert the form of the weight function from eq. (4.8) into eq. (4.76), then we see that the density of squared eigenvalues separates into complex (i.e. non-real) and real parts as follows ($z = x + iy$):

$$R_{1,N}(z) = R^{\mathbb{C}}_{1,N}(z) + \delta(y) R^{\mathbb{R}}_{1,N}(x), \tag{4.77}$$

with

$$\begin{aligned} R^{\mathbb{C}}_{1,N}(z) &= -2i\, w(z)w(z^*)\,\mathrm{sgn}(\Im\mathrm{m}\, z)\mathcal{K}_N(z,z^*) && \text{for } z\in\mathbb{C}\backslash\mathbb{R}, \\ R^{\mathbb{R}}_{1,N}(x) &= w(x)\int_{\mathbb{R}} dx'\,\mathcal{K}_N(x,x')w(x')\,\mathrm{sgn}(x-x') && \text{for } x\in\mathbb{R}. \end{aligned} \tag{4.78}$$

It is a particular feature of the non-Hermitian ensembles with Dyson index $\beta = 1$ that a finite number of eigenvalues lie exactly on the real axis (and for the chiral ensemble, a finite number also lie on the imaginary axis). For the $\beta = 2$ and $\beta = 4$ ensembles, the probability of finding an eigenvalue precisely on one of the axes is zero.

The n-point correlation functions where all the arguments are complex (and different) also follow easily. Using eqs. (4.51) and (4.52), with $\mathcal{F}(u,v)$ given by eq. (4.8), we find, for $z_i, z_j \in \mathbb{C}\backslash\mathbb{R}$, $z_i \neq z_j$, $z_i \neq z_j^*$,

$$\begin{aligned} G_N(z_i,z_j) &= 2iw(z_j)w(z_j^*)\,\mathrm{sgn}(\Im\mathrm{m}\, z_j)\mathcal{K}_N(z_i,z_j^*), \\ W_N(z_i,z_j) &= 4w(z_i)w(z_i^*)w(z_j)w(z_j^*)\,\mathrm{sgn}(\Im\mathrm{m}\, z_i)\,\mathrm{sgn}(\Im\mathrm{m}\, z_j)\mathcal{K}_N(z_i^*,z_j^*), \end{aligned} \tag{4.79}$$

and hence from eq. (4.75)

$$R^{\mathbb{C}}_{n,N}(z_1,\ldots,z_n) = (-2i)^n \prod_{i=1}^{n} w(z_i)w(z_i^*)\,\mathrm{sgn}(\Im\mathrm{m}\, z_i)\ \mathrm{Pf}\left[\begin{array}{cc} \mathcal{K}_N(z_i,z_j) & \mathcal{K}_N(z_i,z_j^*) \\ \mathcal{K}_N(z_i^*,z_j) & \mathcal{K}_N(z_i^*,z_j^*) \end{array}\right]_{1\le i,j\le n}. \tag{4.80}$$

We will make use of this result in §5.1 where we show how to write the unquenched partition functions in terms of the quenched kernel.

4.4 Correlation functions II: Functional differentiation method

We now present a completely different derivation of the correlation functions eq. (4.75), by inserting Dirac delta functions into the partition function. This is essentially equivalent to the method of multiple functional differentiation of a suitable generating function (see [Somm07; Somm08]).

4.4.1 Generalised de Bruijn formula

As a prerequisite, it is necessary to show that the partition function $\mathcal{Z}_N$ can be written as a Pfaffian of double integrals[1]. This is merely an easy generalisation of the formulas of de Bruijn [deB55]. Starting with the partition function in its factorised form in eq. (4.9), we first rewrite the Vandermonde determinant as a sum over permutations

$$\begin{aligned}\mathcal{Z}_N &= \frac{c_N}{(\frac{N}{2})!}\prod_{i=1}^{N}\int_{\mathbb{C}} d^2 z_i \prod_{j=1}^{N/2}\hat{\mathcal{F}}(z_{2j-1},z_{2j})\,\Delta_N(\{z\}) \\ &= \frac{c_N}{(\frac{N}{2})!}\prod_{i=1}^{N}\int_{\mathbb{C}} d^2 z_i \prod_{j=1}^{N/2}\hat{\mathcal{F}}(z_{2j-1},z_{2j}) \sum_{\sigma\in S_N}\operatorname{sgn}(\sigma)\prod_{k=1}^{N} z_k^{\sigma(k)-1}, \end{aligned} \tag{4.81}$$

where S_N is the set of all permutations of the integers from 1 to N. On rearranging, we then have

$$\begin{aligned}\mathcal{Z}_N &= \frac{c_N}{(\frac{N}{2})!}\prod_{i=1}^{N}\int_{\mathbb{C}} d^2 z_i \prod_{j=1}^{N/2}\hat{\mathcal{F}}(z_{2j-1},z_{2j}) \sum_{\sigma\in S_N}\operatorname{sgn}(\sigma)\prod_{k=1}^{N/2}\left(z_{2k-1}^{\sigma(2k-1)-1} z_{2k}^{\sigma(2k)-1}\right) \\ &= \frac{c_N}{(\frac{N}{2})!}\sum_{\sigma\in S_N}\operatorname{sgn}(\sigma)\prod_{i=1}^{N/2}\int_{\mathbb{C}^2} d^2 z_{2i-1}\, d^2 z_{2i}\,\hat{\mathcal{F}}(z_{2i-1},z_{2i})\, z_{2i-1}^{\sigma(2i-1)-1} z_{2i}^{\sigma(2i)-1} \\ &= \frac{c_N}{(\frac{N}{2})!}\sum_{\sigma\in S_N}\operatorname{sgn}(\sigma)\prod_{i=1}^{N/2}\left\{\int_{\mathbb{C}^2} d^2 u\, d^2 v\,\hat{\mathcal{F}}(u,v)\, u^{\sigma(2i-1)-1} v^{\sigma(2i)-1}\right\} \\ &= c_N\ \mathrm{Pf}\left[\int_{\mathbb{C}^2} d^2 u\, d^2 v\,\hat{\mathcal{F}}(u,v)\,(u^{i-1}v^{j-1}-u^{j-1}v^{i-1})\right]_{1\le i,j\le N}, \end{aligned} \tag{4.82}$$

[1] In fact, Sinclair [Sin06] had derived the generalised de Bruijn formula for the corresponding (non-chiral) $\beta = 1$ Ginibre ensemble, starting from the (ordered) partition function, and his argument carries across to the chiral case with no significant change. We do not therefore claim that the result in this section is fundamentally new, although the direct derivation from a factorised JPDF would appear to be so.

where we used eq. (A.25) in the last step. Finally, from eq. (4.10), we arrive at

$$\mathcal{Z}_N = c_N \operatorname{Pf}\left[\int_{\mathbb{C}^2} d^2u\, d^2v\, \mathcal{F}(u,v)\, u^{i-1}v^{j-1}\right]_{1\le i,j\le N}. \tag{4.83}$$

We should note that this proof, as with much of this chapter, does not depend at all on the specific structure of $\mathcal{F}(z_1, z_2)$, and so it has more general applicability.

This result easily generalises to

$$\begin{aligned}\mathcal{Z}_N[f,g] &\equiv \frac{c_N}{(\frac{N}{2})!}\prod_{i=1}^{N}\int_{\mathbb{C}} d^2z_i \prod_{j=1}^{N/2}\hat{\mathcal{F}}(z_{2j-1}, z_{2j})\, f(z_{2j-1})g(z_{2j})\Delta_N(\{z\}) \\ &= c_N \operatorname{Pf}\left[\int_{\mathbb{C}^2} d^2u\, d^2v\, \mathcal{F}(u,v)\, f(u)g(v)\, u^{i-1}v^{j-1}\right]_{1\le i,j\le N}\end{aligned} \tag{4.84}$$

for arbitrary functions f and g (assuming that the integrals are well-defined). We will now use this quantity as a generating functional for the correlation functions (in fact, we only need the case when f and g are the same).

4.4.2 Correlation functions

We consider first the 1-point correlation function, i.e. the eigenvalue density[1]. We can write the density at a point z as the expectation of a Dirac delta function evaluated at z (note that we have to symmetrise the observable when using the factorised JPDF, $\hat{P}$)

$$\begin{aligned}R_{1,N}(z) &= \int_{\mathbb{C}} d^2z_1 \ldots \int_{\mathbb{C}} d^2z_N\, \hat{P}(z_1,\ldots,z_N)\sum_{i=1}^{N}\delta(z-z_i) \\ &= \frac{\partial}{\partial\epsilon}\Big|_{\epsilon=0}\int_{\mathbb{C}} d^2z_1 \ldots \int_{\mathbb{C}} d^2z_N\, \hat{P}(z_1,\ldots,z_N)\sum_{i=1}^{N}\epsilon\delta(z-z_i) \\ &= \frac{\partial}{\partial\epsilon}\Big|_{\epsilon=0}\int_{\mathbb{C}} d^2z_1 \ldots \int_{\mathbb{C}} d^2z_N\, \hat{P}(z_1,\ldots,z_N)\prod_{i=1}^{N}(1+\epsilon\delta(z-z_i)) \\ &= \frac{\partial}{\partial\epsilon}\Big|_{\epsilon=0}\operatorname{Pf}\left[\int_{\mathbb{C}^2} d^2u\, d^2v\, \mathcal{F}(u,v)\,(1+\epsilon\delta(z-u))(1+\epsilon\delta(z-v))\, u^{i-1}v^{j-1}\right]_{1\le i,j\le N} \\ &\equiv \frac{\partial}{\partial\epsilon}\Big|_{\epsilon=0}\operatorname{Pf} A,\end{aligned} \tag{4.85}$$

where we used our generalised de Bruijn formula eq. (4.84) in the last-but-one line. Now, by using the chain rule of partial differentiation

$$\frac{\partial \operatorname{Pf} A}{\partial\epsilon} = \sum_{p,q}\frac{\partial \operatorname{Pf} A}{\partial A_{pq}}\frac{\partial A_{pq}}{\partial\epsilon} \tag{4.86}$$

[1]Recall that the matrix size N is assumed even throughout.

and the differential of a Pfaffian from eq. (A.29)

$$\frac{\partial \operatorname{Pf} A}{\partial A_{pq}} = \tfrac{1}{2} \operatorname{Pf}[A]\,(A^{-1})_{qp}$$

we have

$$R_{1,N}(z) = \tfrac{1}{2} \left(\operatorname{Pf}[A] \sum_{p,q} (A^{-1})_{qp} \frac{\partial A_{pq}}{\partial \epsilon} \right) \Bigg|_{\epsilon=0}. \tag{4.87}$$

We easily evaluate the factors:

$$\operatorname{Pf} A\Big|_{\epsilon=0} = \mathcal{Z}_N = 1 \tag{4.88}$$

and

$$\frac{\partial A_{pq}}{\partial \epsilon}\Big|_{\epsilon=0} = \int_{\mathbb{C}} d^2u\, \mathcal{F}(u,z)\big(u^{p-1}z^{q-1} - u^{q-1}z^{p-1}\big). \tag{4.89}$$

Hence, on identifying A evaluated at $\epsilon = 0$ with the $\mathcal{A}$ that was used in the definition of the kernel in eq. (4.23), we find that

$$\begin{aligned} R_{1,N}(z) &= \tfrac{1}{2} \sum_{p,q} (A^{-1})_{qp} \int_{\mathbb{C}} d^2u\, \mathcal{F}(u,z)\big(u^{p-1}z^{q-1} - u^{q-1}z^{p-1}\big) \\ &= \tfrac{1}{2} \int_{\mathbb{C}} d^2u \sum_{p,q} (A^{-1})_{qp} \big(u^{p-1}z^{q-1} - u^{q-1}z^{p-1}\big) \mathcal{F}(u,z) \\ &= \int_{\mathbb{C}} d^2u\, \mathcal{K}_N(z,u)\, \mathcal{F}(u,z) \equiv -G_N(z,z). \end{aligned} \tag{4.90}$$

This, of course, matches eq. (4.76) which we derived using a completely different method.

Using this technique for higher correlation functions becomes rapidly more cumbersome, but we show the $n = 2$ case. The 2-point function can be written as

$$\begin{aligned} R_{2,N}(z,w) &= \int_{\mathbb{C}} d^2z_1 \ldots \int_{\mathbb{C}} d^2z_N\, \hat{P}_N(z_1,\ldots,z_N) \sum_{\substack{i,j \\ i\neq j}} \delta(z-z_i)\delta(w-z_j) \\ &= \frac{\partial^2}{\partial\alpha\,\partial\epsilon}\Big|_{\substack{\alpha=0\\ \epsilon=0}} \int_{\mathbb{C}} d^2z_1 \ldots \int_{\mathbb{C}} d^2z_N\, \hat{P}_N(z_1,\ldots,z_N) \prod_{i=1}^{N} \Big(1 + \epsilon\delta(z-z_i) + \alpha\delta(w-z_i)\Big) \\ &= \frac{\partial^2}{\partial\alpha\,\partial\epsilon}\Big|_{\substack{\alpha=0\\ \epsilon=0}} \operatorname{Pf}\Big[\int_{\mathbb{C}^2} d^2u\, d^2v\, \mathcal{F}(u,v)\, u^{i-1}v^{j-1} \\ &\qquad \times \Big(1 + \epsilon\delta(z-u) + \alpha\delta(w-u)\Big)\Big(1 + \epsilon\delta(z-v) + \alpha\delta(w-v)\Big)\Big]_{1\le i,j\le N} \\ &\equiv \frac{\partial^2}{\partial\alpha\,\partial\epsilon}\Big|_{\substack{\alpha=0\\ \epsilon=0}} \operatorname{Pf} A. \end{aligned} \tag{4.91}$$

(The matrix A here differs from the previous case in eq. (4.85).) We now use the chain rule of partial differentiation

$$\frac{\partial^2 \operatorname{Pf} A}{\partial\alpha\,\partial\epsilon} = \sum_{p,q}\sum_{m,n} \frac{\partial^2 \operatorname{Pf} A}{\partial A_{mn}\partial A_{pq}} \frac{\partial A_{mn}}{\partial\alpha} \frac{\partial A_{pq}}{\partial\epsilon} + \sum_{p,q} \frac{\partial \operatorname{Pf} A}{\partial A_{pq}} \frac{\partial^2 A_{pq}}{\partial\alpha\,\partial\epsilon} \tag{4.92}$$

together with eq. (A.30)

$$\frac{\partial^2}{\partial A_{ij}\partial A_{pq}} \operatorname{Pf} A = \operatorname{Pf} A \left\{ \tfrac{1}{4}(A^{-1})_{qp}(A^{-1})_{ji} - \tfrac{1}{2}(A^{-1})_{qi}(A^{-1})_{jp} \right\}$$

to differentiate the Pfaffian in eq. (4.91) twice. After a few lines of algebra (which we omit for space reasons), we arrive at the result

$$\begin{aligned} R_{2,N}(z,w) &= G_N(z,z)G_N(w,w) - G_N(z,w)G_N(w,z) + \mathcal{K}_N(z,w)W_N(z,w) \\ &= \operatorname{Pf} \begin{bmatrix} 0 & -G_N(z,z) & \mathcal{K}_N(z,w) & -G_N(z,w) \\ G_N(z,z) & 0 & G_N(w,z) & -W_N(z,w) \\ \mathcal{K}_N(w,z) & -G_N(w,z) & 0 & -G_N(w,w) \\ G_N(z,w) & -W_N(z,w) & G_N(w,w) & 0 \end{bmatrix}, \end{aligned} \tag{4.93}$$

which agrees with our earlier calculation (eq. (4.75) for the case when $n = 2$).

It is somewhat more difficult using this brute-force method to prove the general pattern. Since we have already given a full (and completely different) proof of the general even-N case in §4.3, we merely make the following observation: The real chiral ensemble is algebraically similar to the real Ginibre ensemble (GinOE), and so we can, in fact, use the method of [Somm07; Somm08] with minimal changes. Essentially, for pairwise distinct arguments $z_1 \neq z_2 \neq \ldots \neq z_n$, these authors showed that can write (with $R_{n,N}(z_1,\ldots,z_n)$ defined in eq. (4.32))

$$\begin{aligned} R_{n,N}(z_1,\ldots,z_n) &= \frac{\delta}{\delta f(z_1)} \cdots \frac{\delta}{\delta f(z_n)} \mathcal{Z}_N[f,f]\Big|_{f=1} \\ &= \operatorname{Pf} \begin{bmatrix} \mathcal{K}_N(z_i,z_j) & -G_N(z_i,z_j) \\ G_N(z_j,z_i) & -W_N(z_i,z_j) \end{bmatrix}_{1\leq i,j\leq n}. \end{aligned} \tag{4.94}$$

Here, $\mathcal{Z}_N[f,f]$ was defined in eq. (4.84), $\mathcal{K}_N(u,v)$ is the kernel, and $G_N(u,v)$ and $W_N(u,v)$ were defined in eqs. (4.51) and (4.52) respectively. Of course, this matches our earlier result eq. (4.75) exactly.

In Appendix C, we show that the $\beta = 4$ ensemble has a similar algebraic (or structural) form at the level of the JPDF, and so the correlation functions also have the same form as eq. (4.75). The $\beta = 2$ case is somewhat simpler, involving ordinary determinants of a symmetric kernel.

4.5 Unquenched ensembles

As we indicated earlier, both the proofs (in §4.3 and §4.4) of the correlation functions eq. (4.75) were independent of the particular weight function $\mathcal{F}$. Since the unquenched ensemble has the same form as the quenched case (compare the partition functions in eqs. (4.16) and (4.9)), the results that we have derived are immediately applicable to the unquenched ensembles with the substitution $\mathcal{F} \to \mathcal{F}^{(N_f)}$, i.e.

$$R_{n,N}^{(N_f)}(z_1, \ldots, z_n) = \mathrm{Pf} \left[\begin{array}{cc} \mathcal{K}_N^{(N_f)}(z_i, z_j) & -G_N^{(N_f)}(z_i, z_j) \\ G_N^{(N_f)}(z_j, z_i) & -W_N^{(N_f)}(z_i, z_j) \end{array} \right]_{1 \le i,j \le n}, \tag{4.95}$$

where all quantities are determined based on the unquenched weight function $\mathcal{F}^{(N_f)}(u, v)$ in eq. (4.15). As we will show in §5.3, the unquenched kernel $\mathcal{K}_N^{(N_f)}(u, v)$ can itself be written as a Pfaffian involving quenched kernels $\mathcal{K}_N(u, v)$.

Chapter 5

Finite-N kernel and skew-orthogonal polynomials

We have now derived expressions for the correlation functions for finite, even N (eqs. (4.75) and (4.95) for the quenched and unquenched cases respectively). However, these were expressed in terms of the kernels, which we do not yet know explicitly. The determination of these is the key result in this chapter.

However, we begin by considering the unquenched partition functions $\mathcal{Z}_N^{(N_f)}$, since these can be obtained directly from results that we already know; they also form building blocks for some of our subsequent proofs. Then we determine the quenched kernel itself, using a technique employing Grassmann variables and Berezin integration. After deriving the unquenched kernels in terms of the quenched one (and, sometimes, skew-orthogonal polynomials), we determine the skew-orthogonal polynomials explicitly, for both the quenched and the unquenched cases.

The methodology adopted in §5.2 and §5.4 can also be applied to the non-chiral (Ginibre) $\beta = 1$ ensemble (the GinOE); see Appendix D for further details.

5.1 Unquenched partition function

We begin by showing how we can write the unquenched partition functions for various numbers of quark flavours $N_f > 0$ in terms of the quenched kernels. We show this explicitly for the case of two quark flavours $N_f = 2$ (as per §4.1 of our paper [Ake10a]), and then we present the general even N_f and odd N_f cases. All results are for even matrix size N only.

5.1.1 $N_f = 2$

First, note that we can write the unquenched partition function with two quark flavours as $\mathcal{Z}_N^{(N_f=2)}(m_1, m_2) = \mathcal{H}_N(-m_1, -m_2)$, where $\mathcal{H}_N(\lambda, \gamma)$ is the expectation of the product of two characteristic polynomials

$$\mathcal{H}_N(\lambda, \gamma) \equiv \langle \det(\lambda - \mathcal{D}) \det(\gamma - \mathcal{D}) \rangle, \tag{5.1}$$

the expectation being taken over the ensemble of $(2N+\nu)$-by-$(2N+\nu)$ Dirac matrices $\mathcal{D}$.

Let us choose $\gamma = \lambda^* \in \mathbb{C}\backslash\mathbb{R}$, and then

$$\begin{aligned}\mathcal{H}_N(\lambda, \lambda^*) &= \int_{\mathbb{C}} d^2 z_1 \ldots \int_{\mathbb{C}} d^2 z_N \, \hat{P}_N(z_1, \ldots, z_N)(\lambda\lambda^*)^\nu \prod_{j=1}^{N} (\lambda^2 - z_j)(\lambda^{*2} - z_j) \\ &= \frac{\left(\frac{N}{2}+1\right)!}{\left(\frac{N}{2}\right)!} \frac{c_N}{c_{N+2}} \frac{(\lambda\lambda^*)^\nu}{iw(\lambda^2)w(\lambda^{*2}) \operatorname{sgn}(\Im\mathrm{m}\, \lambda^2)(\lambda^{*2} - \lambda^2)} \\ &\quad \times \int_{\mathbb{C}} d^2 z_1 \ldots \int_{\mathbb{C}} d^2 z_N \, \hat{P}_{N+2}(z_1, \ldots, z_N, \lambda^2, \lambda^{*2}).\end{aligned} \tag{5.2}$$

For the arguments of $\hat{P}_{N+2}$ in the last expression, we chose one particular permutation of the $\{z_i\}$ and the pair $\{\lambda^2, \lambda^{*2}\}$, i.e. with the latter pair placed at the end. However, we could equally have chosen to insert the pair $\{\lambda^2, \lambda^{*2}\}$ at other positions, as follows. To count the number of non-zero permutations, first we pair the $\{z_i\}$ working from left to right. Then, we insert the pair $\{\lambda^2, \lambda^{*2}\}$. This pair can go at the start, or at the end, or between a pair of (z_{2k-1}, z_{2k}); this gives $\frac{N}{2} + 1$ possibilities.

But the sum (over these permutations) of the integrals of $\hat{P}_{N+2}$ is merely *half* the density $R^{\mathbb{C}}_{1,N+2}(\lambda^2)$, the factor of one half arising because the density also involves the permutations where λ^{*2} comes before λ^2. If λ^2 and λ^{*2} are separated in the argument list, then there is a zero contribution. So

$$\mathcal{H}_N(\lambda, \lambda^*) = \frac{1}{2} \frac{c_N}{c_{N+2}} \frac{(\lambda\lambda^*)^\nu}{iw(\lambda^2)w(\lambda^{*2}) \operatorname{sgn}(\Im\mathrm{m}\, \lambda^2)(\lambda^{*2} - \lambda^2)} R^{\mathbb{C}}_{1,N+2}(\lambda^2). \tag{5.3}$$

But we already know from eq. (4.76) that

$$R_{1,N+2}(z) = \int_{\mathbb{C}} d^2 u \, \mathcal{K}_{N+2}(z, u) \mathcal{F}(u, z) \tag{5.4}$$

and so for the complex case ($z \in \mathbb{C}\backslash\mathbb{R}$)

$$R^{\mathbb{C}}_{1,N+2}(z) = \mathcal{K}_{N+2}(z, z^*) w(z) w(z^*) (2i) \operatorname{sgn}(\Im\mathrm{m}\, z^*). \tag{5.5}$$

Therefore, after analytic continuation in each argument (since $\mathcal{H}_N$ is analytic in both arguments), we have

$$\mathcal{H}_N(\lambda,\gamma) = -\frac{c_N}{c_{N+2}}\frac{(\lambda\gamma)^\nu}{\gamma^2-\lambda^2}\mathcal{K}_{N+2}(\lambda^2,\gamma^2), \tag{5.6}$$

and hence

$$\mathcal{Z}_N^{(N_f=2)}(m_1,m_2) = -\frac{c_N}{c_{N+2}}\frac{(m_1m_2)^\nu}{m_2^2-m_1^2}\mathcal{K}_{N+2}(m_1^2,m_2^2). \tag{5.7}$$

So the unquenched ($N_f = 2$) partition function is directly related to the quenched ($N_f = 0$) kernel. Note that, by using eq. (3.97), we can determine the ratio of the normalisation constants explicitly. It is

$$\frac{c_N}{c_{N+2}} = (8\pi)(4\mu^2)(1+\mu^2)^{2N+\nu+1}N!(N+\nu)! \tag{5.8}$$

which equals $h_{N/2}$ by eq. (4.72).

5.1.2 General even N_f

We next consider the case with more than two quark flavours ($N_f > 2$) but with N_f even. Our proof here follows along almost identical lines to the $N_f = 2$ case[1]. We write the partition function $\mathcal{Z}_N^{(N_f)}(m_1,\ldots,m_{N_f}) = \mathcal{H}_N(-m_1,\ldots,-m_{N_f})$ where

$$\mathcal{H}_N(\lambda_1,\ldots,\lambda_{N_f}) \equiv \left\langle \prod_{i=1}^{N_f} \det(\lambda_i - \mathcal{D}) \right\rangle. \tag{5.9}$$

We choose the arguments to be non-real, pairwise complex conjugates ($\lambda_{2i-1} = \alpha_i$, $\lambda_{2i} = \alpha_i^*$), with the additional requirement that all the arguments are different. Following the same steps as before, we have

$$\begin{aligned}&\mathcal{H}_N(\alpha_1,\alpha_1^*,\alpha_2,\alpha_2^*,\ldots)\\ &\quad= \frac{1}{2^{N_f/2}}\frac{c_N}{c_{N+N_f}}\frac{\prod_{i=1}^{N_f/2}(\alpha_i\alpha_i^*)^\nu\, R^{\mathbb{C}}_{N_f/2,N+N_f}(\alpha_1^2,\alpha_2^2,\ldots)}{\prod_{i=1}^{N_f/2} iw(\alpha_i^2)w(\alpha_i^{*2})\,\mathrm{sgn}(\Im\mathrm{m}\,\alpha_i^2)\,\Delta_{N_f}(\alpha_1^2,\alpha_1^{*2},\alpha_2^2,\alpha_2^{*2},\ldots)}.\end{aligned} \tag{5.10}$$

But the complex correlation function for (distinct) non-real arguments is, from eq. (4.80),

$$R^{\mathbb{C}}_{n,N}(u_i,\ldots,u_n) = (-2i)^n\prod_{i=1}^{n} w(u_i)w(u_i^*)\,\mathrm{sgn}(\Im\mathrm{m}\,u_i)\ \mathrm{Pf}[\mathcal{K}_N(v_i,v_j)]_{1\le i,j\le 2n} \tag{5.11}$$

[1] An alternative proof of this result was given in our paper [Ake10b], based on earlier results in [Kie10].

where $v_{2i-1} = u_i$ and $v_{2i} = u_i^*$. Since $\mathcal{H}$ is an analytic function of its arguments, we can then analytically continue in each argument. The result is that

$$\mathcal{Z}_N^{(N_f)}(\{m\}) = (-1)^{N_f/2} \frac{c_N}{c_{N+N_f}} \frac{\prod_{f=1}^{N_f} m_f^\nu}{\Delta_{N_f}(\{m^2\})} \operatorname{Pf}[\mathcal{K}_{N+N_f}(m_i^2, m_j^2)]_{1\le i,j\le N_f}. \tag{5.12}$$

We also note that the ratio of normalisation coefficients can be written as a product over the norms of the skew-orthogonal polynomials:

$$\frac{c_N}{c_{N+N_f}} = \prod_{j=N/2}^{(N+N_f)/2-1} h_j. \tag{5.13}$$

5.1.3 General odd N_f

The easiest way of determining the partition function for odd N_f is to 'quench' the partition function for the $N_f + 1$ (even) case, i.e. by making one of the masses infinitely large so that it decouples. So, for odd N_f, we have

$$\mathcal{Z}_N^{(N_f)}(\{m\}) = \lim_{M\to\infty} \frac{\mathcal{Z}_N^{(N_f+1)}(M \cup \{m\})}{M^{2N+\nu}}. \tag{5.14}$$

We evaluate this by expressing the partition function on the right-hand side in terms of the kernel using eq. (5.12). The Vandermonde determinant can be quenched as follows

$$\lim_{M\to\infty} \frac{\Delta_{N_f+1}(M^2 \cup \{m^2\})}{M^{2N_f}} = (-1)^{N_f}\, \Delta_{N_f}(\{m^2\}) = -\,\Delta_{N_f}(\{m^2\}) \tag{5.15}$$

and so we get

$$\mathcal{Z}_N^{(N_f)}(\{m\}) = (-1)^{(N_f-1)/2} \frac{c_N}{c_{N+N_f+1}} \frac{\prod_{f=1}^{N_f} m_f^\nu}{\Delta_{N_f}(\{m^2\})} \lim_{M\to\infty} \frac{\operatorname{Pf}\left[\mathcal{K}_{N+N_f+1}(w_i, w_j)\right]_{1\le i,j\le N_f+1}}{M^{2N+2N_f}}, \tag{5.16}$$

where we write $w_1 \equiv M^2$ and $w_i \equiv m_{i-1}^2$ for $2 \le i \le N_f + 1$. Since only the first row and column of the matrix of kernels depend on M, we can take the limit operation inside the Pfaffian, and use eq. (4.29) to show that

$$\mathcal{Z}_N^{(N_f)}(\{m\}) = (-1)^{(N_f-1)/2} \frac{c_N}{c_{N+N_f-1}} \frac{\prod_{f=1}^{N_f} m_f^\nu}{\Delta_{N_f}(\{m^2\})} \operatorname{Pf}\left[A_{ij}\right]_{1\le i,j\le N_f+1}, \tag{5.17}$$

in which

$$A_{ij} = -A_{ji} \equiv \begin{cases} 0 & \text{if } i = j, \\ q_{N+N_f-1}(w_j) & \text{if } j > i = 1, \\ \mathcal{K}_{N+N_f+1}(w_i, w_j) & \text{if } j > i > 1, \end{cases} \tag{5.18}$$

and where $q_{N+N_f-1}(z)$ is the (even) quenched skew-orthogonal polynomial. Finally, observe that we can also write

$$\frac{c_N}{c_{N+N_f-1}} = \prod_{j=N/2}^{(N+N_f-1)/2-1} h_j, \tag{5.19}$$

which parallels eq. (5.13) for the even N_f case.

5.2 Quenched kernel

We now turn to an explicit determination of the quenched kernel $\mathcal{K}_N(u,v)$ for the chGinOE. In order to evaluate the kernel directly from its definition in eq. (4.23), we would need to evaluate the matrix $\mathcal{A}$ defined in eq. (4.19) and its inverse directly; however, for our particular weight function eq. (4.8) with weight $w(z)$ from eq. (3.101), this is non-trivial, so an alternative method is required. We proceed as follows. We invert eq. (5.6) to get

$$\mathcal{K}_N(u,v) = \frac{c_N}{c_{N-2}} \frac{(u-v)\mathcal{H}_{N-2}(\sqrt{u},\sqrt{v})}{(uv)^{\nu/2}} \tag{5.20}$$

where $\mathcal{H}_N(\lambda,\gamma)$ was defined in eq. (5.1):

$$\mathcal{H}_N(\lambda,\gamma) \equiv \langle \det(\lambda - \mathcal{D}) \det(\gamma - \mathcal{D}) \rangle,$$

and then look for an alternative way of determining $\mathcal{H}_N(\lambda,\gamma)$ explicitly. Fortunately this can be done by using Grassmann variables. Appendix A.4 gives a brief introduction to the relevant concepts used in the next section.

5.2.1 Reduction to six integrals

We begin by replacing the determinants in eq. (5.1) with Berezin integrals over Grassmann variables, see eq. (A.39), which gives

$$\begin{aligned}\mathcal{H}_N(\lambda,\gamma) &= (2\pi)^{-N(N+\nu)} \int dP\, dQ \int d\eta\, d\psi\, d\zeta\, d\phi \\ &\quad \times \exp\Big\{ -\frac{1}{2}(P_{ij}^2 + Q_{ij}^2) - \lambda(\eta_i^*\eta_i + \psi_j^*\psi_j) - \gamma(\zeta_i^*\zeta_i + \phi_j^*\phi_j) \\ &\qquad + \eta_i^*(P_{ij} + \mu Q_{ij})\psi_j + \psi_j^*(P_{ji}^T - \mu Q_{ji}^T)\eta_i \\ &\qquad + \zeta_i^*(P_{ij} - \mu Q_{ij})\phi_j + \phi_j^*(P_{ji}^T + \mu Q_{ji}^T)\zeta_i \Big\} \\ &= (2\pi)^{-N(N+\nu)} \int dP\, dQ \int d\eta\, d\psi\, d\zeta\, d\phi \\ &\quad \times \exp\Big\{ -\frac{P_{ij}^2}{2} + P_{ij}(\eta_i^*\psi_j + \psi_j^*\eta_i + \zeta_i^*\phi_j + \phi_j^*\zeta_i) \\ &\qquad - \frac{Q_{ij}^2}{2} + \mu Q_{ij}(\eta_i^*\psi_j - \psi_j^*\eta_i - \zeta_i^*\phi_j + \phi_j^*\zeta_i) \\ &\qquad - \lambda(\eta_i^*\eta_i + \psi_j^*\psi_j) - \gamma(\zeta_i^*\zeta_i + \phi_j^*\phi_j) \Big\} \end{aligned} \tag{5.21}$$

where i runs from 1 to N, and j from 1 to $N+\nu$, and summation over i and j in the exponent is implicit. We have $d\eta \equiv \prod_{i=1}^N d\eta_i^* d\eta_i$, and so on. We can now complete the squares in P_{ij} and Q_{ij} using eq. (A.44), and integrate out these variables, so

$$\begin{aligned}\mathcal{H}_N(\lambda,\gamma) = \int d\eta\, d\psi\, d\zeta\, d\phi\, \exp\Big\{ &-\lambda(\eta_i^*\eta_i + \psi_j^*\psi_j) - \gamma(\zeta_i^*\zeta_i + \phi_j^*\phi_j) \\ &+ \frac{1}{2}(\eta_i^*\psi_j + \psi_j^*\eta_i + \zeta_i^*\phi_j + \phi_j^*\zeta_i)^2 \\ &+ \frac{\mu^2}{2}(\eta_i^*\psi_j - \psi_j^*\eta_i - \zeta_i^*\phi_j + \phi_j^*\zeta_i)^2 \Big\}. \end{aligned} \tag{5.22}$$

We now multiply out the squares, removing the terms which are identically zero. After reordering, we have

$$\begin{aligned}\mathcal{H}_N(\lambda,\gamma) = \int d\eta\, d\psi\, d\zeta\, d\phi\, \exp\Big\{ &-\lambda(\eta_i^*\eta_i + \psi_j^*\psi_j) - \gamma(\zeta_i^*\zeta_i + \phi_j^*\phi_j) \\ &- \delta_-^2(\eta_i^*\eta_i)(\psi_j^*\psi_j) - \delta_-^2(\eta_i^*\zeta_i^*)(\psi_j\phi_j) \\ &- \delta_+^2(\eta_i^*\zeta_i)(\phi_j^*\psi_j) - \delta_+^2(\zeta_i^*\eta_i)(\psi_j^*\phi_j) \\ &- \delta_-^2(\eta_i\zeta_i)(\psi_j^*\phi_j^*) - \delta_-^2(\zeta_i^*\zeta_i)(\phi_j^*\phi_j) \Big\}, \end{aligned} \tag{5.23}$$

where we introduced $\delta_\pm^2 \equiv 1 \pm \mu^2$ to simplify the notation. The six quartic terms can be removed by repeated application of the complex Hubbard-Stratonovich transfor-

mation in eq. (A.46):

$$\begin{aligned}\mathcal{H}_N(\lambda,\gamma) = \frac{1}{\pi^6}\int_{\mathbb{C}^6} d^2u\, d^2v\, d^2w\, d^2z\, d^2p\, d^2q\, e^{-|u|^2-|v|^2-|w|^2-|z|^2-|p|^2-|q|^2} \\ \times \int d\eta\, d\psi\, d\zeta\, d\phi\, \exp\Big\{ -\lambda(\eta_i^*\eta_i + \psi_j^*\psi_j) - \gamma(\zeta_i^*\zeta_i + \phi_j^*\phi_j) \\ + i\delta_-(u\eta_i^*\eta_i + \bar{u}\psi_j^*\psi_j + v\zeta_i^*\zeta_i + \bar{v}\phi_j^*\phi_j \\ + w\eta_i^*\zeta_i^* + \bar{w}\psi_j\phi_j + z\eta_i\zeta_i + \bar{z}\psi_j^*\phi_j^*) \\ + i\delta_+(p\eta_i^*\zeta_i + \bar{p}\phi_j^*\psi_j + q\zeta_i^*\eta_i + \bar{q}\psi_j^*\phi_j)\Big\}. \end{aligned} \tag{5.24}$$

The i and j factors now decouple, and we can perform the Berezin integrations. The only terms that will contribute are those containing the combinations $\eta_i^*\eta_i\zeta_i^*\zeta_i$ and $\psi_j^*\psi_j\phi_j^*\phi_j$. Hence

$$\begin{aligned}\mathcal{H}_N(\lambda,\gamma) &= \frac{1}{\pi^6}\int_{\mathbb{C}^6} d^2u\, d^2v\, d^2w\, d^2z\, d^2p\, d^2q\, e^{-|u|^2-|v|^2-|w|^2-|z|^2-|p|^2-|q|^2} \\ &\qquad \times [(i\delta_- u - \lambda)(i\delta_- v - \gamma) - (i\delta_- w)(i\delta_- z) - (i\delta_+ p)(i\delta_+ q)]^N \\ &\qquad \times [(i\delta_- \bar{u} - \lambda)(i\delta_- \bar{v} - \gamma) - (i\delta_- \bar{w})(i\delta_- \bar{z}) - (i\delta_+ \bar{p})(i\delta_+ \bar{q})]^{N+\nu}. \\ &= \frac{1}{\pi^6}\int_{\mathbb{C}^6} d^2u\, d^2v\, d^2w\, d^2z\, d^2p\, d^2q\, e^{-|u|^2-|v|^2-|w|^2-|z|^2-|p|^2-|q|^2} \\ &\qquad \times [(\lambda - i\delta_- u)(\gamma - i\delta_- v) + \delta_-^2 wz + \delta_+^2 pq]^N \\ &\qquad \times [(\lambda - i\delta_- \bar{u})(\gamma - i\delta_- \bar{v}) + \delta_-^2 \bar{w}\bar{z} + \delta_+^2 \bar{p}\bar{q}]^{N+\nu}. \end{aligned} \tag{5.25}$$

We can compactify this result somewhat if we define three anti-symmetric matrices σ, $\tilde{\sigma}$ and M as

$$\sigma = \begin{pmatrix} 0 & u & p & z \\ & 0 & w & q \\ & & 0 & v \\ & & & 0 \end{pmatrix}, \quad \tilde{\sigma} = \begin{pmatrix} 0 & \delta_- u & \delta_+ p & \delta_- z \\ & 0 & \delta_- w & \delta_+ q \\ & & 0 & \delta_- v \\ & & & 0 \end{pmatrix} \quad \text{and} \quad M = \begin{pmatrix} 0 & i\lambda & 0 & 0 \\ & 0 & 0 & 0 \\ & & 0 & i\gamma \\ & & & 0 \end{pmatrix} \tag{5.26}$$

(where we do not write below-diagonal entries for clarity). We then have

$$\begin{aligned}\mathcal{H}_N(\lambda,\gamma) &= \mathcal{Z}_N^{(N_f=2)}(-\lambda,-\gamma) \\ &\propto \int D\sigma\, D\sigma^\dagger\, \exp\Big\{-\tfrac{1}{2}\operatorname{Tr}[\sigma\sigma^\dagger]\Big\}\, (\operatorname{Pf}[\tilde{\sigma}+M])^N (\operatorname{Pf}[\tilde{\sigma}^\dagger - M])^{N+\nu}, \end{aligned} \tag{5.27}$$

where we drop an irrelevant overall normalisation constant. This is, of course, merely a change in notation, but it hints at how the formula may generalise for the expectation of the product of more than two characteristic polynomials. Furthermore, starting from this kind of matrix representation it is easier to investigate how the

symmetry of the model is broken in the various large-N limits, leading to so-called non-linear sigma models which can be compared with those arising from chiral perturbation theory (see, e.g. [Kana10]). We do not pursue such an approach in this thesis, although we do devote the next section to deriving one particular large-N limit explicitly.

The form eq. (5.27) is similar to that of the Hermitian case (see eq. 5.16 of [Hal95]). The $\beta = 2$ case is analogous, but contains determinants instead of Pfaffians (see eq. 3.5 of [Shu93]).

5.2.2 Saddle point method for large-N limit with $\mu = 1$

We will solve eq. (5.25) exactly for finite N in the next section. However, more typically with problems of this sort it is difficult to find an exact result for finite N, and so one must take the large-N limit as part of the process of evaluating the integrals. This section demonstrates this technique, partly for pedagogic reasons, and partly to enable us to cross-check one of our later results.

To simplify the calculations we consider only the case of maximal non-Hermiticity (i.e. with $\mu = 1$), and seek the large-N limit. With $\mu = 1$, we have $\delta_- = 0$ and $\delta_+^2 = 2$. The four integrals over u, v, w and z in eq. (5.25) then decouple and can be performed trivially, leading to (after a flip of the sign of p)

$$\mathcal{H}_N(\lambda, \gamma; \mu = 1) = \frac{1}{\pi^2} \int_{\mathbb{C}^2} d^2p\, d^2q\, e^{-|p|^2 - |q|^2} (\lambda\gamma - 2pq)^N (\lambda\gamma - 2\bar{p}\bar{q})^{N+\nu}. \tag{5.28}$$

We now change variables from $p, q \in \mathbb{C}$ to $t, \tau, \theta, \phi \in \mathbb{R}$

$$\begin{aligned} p &= \sqrt{t} \cos\left(\tfrac{\phi}{2}\right) e^{i(\tau - \theta)}, \\ q &= \sqrt{t} \sin\left(\tfrac{\phi}{2}\right) e^{i\theta}, \end{aligned} \tag{5.29}$$

with $0 \le t < \infty$, $0 \le \tau \le 2\pi$, $0 \le \theta \le 2\pi$ and $0 \le \phi \le \pi$. After performing the decoupled angular integration over τ, giving us a factor 2π, we arrive at

$$\mathcal{H}_N(\lambda, \gamma; 1) = \frac{1}{4\pi} \int_0^{2\pi} d\tau \int_0^{\pi} d\phi \sin\phi \int_0^{\infty} dt\, t\, e^{-t} (\lambda\gamma - t \sin\phi\, e^{i\tau})^N (\lambda\gamma - t \sin\phi\, e^{-i\tau})^{N+\nu}. \tag{5.30}$$

To evaluate the t-integral for large N, we use the saddle point method. Using eq. (A.13), we have

$$\begin{aligned} \mathcal{H}_N(\lambda, \gamma; 1) \sim{}& \frac{(-1)^\nu 2^{2N+\nu-1}}{\pi^{3/2}} \sqrt{N}\, N!\, (N+\nu)! \\ & \times \int_0^{2\pi} d\tau \int_0^{\pi} d\phi\, \sin\phi\, (\sin\phi)^{2N+\nu}\, e^{-i\nu\tau}\, \exp\left[-\lambda\gamma \frac{\cos\tau}{\sin\phi}\right] \end{aligned} \tag{5.31}$$

where the $\sim$ sign indicates asymptotic behaviour. Next we consider the ϕ-integral. Since, for $0 \leq \phi \leq \pi$, we have

$$\lim_{N\to\infty} \sqrt{N}\, \sin^{2N}\phi = \sqrt{\pi}\, \delta\left(\phi - \tfrac{\pi}{2}\right), \tag{5.32}$$

it follows that the ϕ-integral effectively collapses into a single direction when N is very large:

$$\mathcal{H}_N(\lambda, \gamma; 1) \sim \frac{(-1)^\nu\, 2^{2N+\nu-1}}{\pi}\, N!\, (N+\nu)! \int_0^{2\pi} d\tau\, e^{-i\nu\tau} e^{-\lambda\gamma\cos\tau}. \tag{5.33}$$

We make a simple change of variables ($\rho = \tau - \pi$), to get

$$\mathcal{H}_N(\lambda, \gamma; 1) \sim \frac{2^{2N+\nu-1}}{\pi} N!\, (N+\nu)! \int_{-\pi}^{\pi} d\rho\, \cos(\nu\rho)\, e^{\lambda\gamma\cos\rho} \tag{5.34}$$

where the corresponding integral involving $\sin(\nu\rho)$ has vanished because it is odd. On applying eq. 8.431.5 of [Gra07], we find

$$\mathcal{H}_N(\lambda, \gamma; 1) \sim 2^{2N+\nu}\, N!\, (N+\nu)!\, I_\nu(\lambda\gamma). \tag{5.35}$$

Eq. (5.20) gives the kernel in terms of $\mathcal{H}_N(\lambda, \gamma; \mu)$, with normalisation given by (for $\mu = 1$)

$$\frac{c_N}{c_{N-2}} = \frac{1}{2^{2N+\nu+2}\pi\, (N-2)!\, (N+\nu-2)!}. \tag{5.36}$$

Therefore, on inserting eqs. (5.35) and (5.36) into eq. (5.20), we arrive at our final result at large N

$$\mathcal{K}_N(u, v; \mu = 1) \sim \frac{1}{2^6\pi}\, \frac{(u-v)}{(uv)^{\nu/2}}\, I_\nu(\sqrt{uv}). \tag{5.37}$$

We shall reproduce this result later (see eq. (7.7)), by explicitly taking the large-N limit of the exact finite-N result, which we will now determine.

5.2.3 Exact solution for finite N

We return now to calculating the exact finite-N result for arbitrary non-Hermiticity parameter μ. We can expand the trinomials in eq. (5.25) using the result

$$(A+B+C)^N = N! \sum_{j=0}^{N} \frac{C^{N-j}}{(N-j)!} \sum_{k=0}^{j} \frac{A^k B^{j-k}}{k!(j-k)!}. \tag{5.38}$$

This gives $\mathcal{H}_N(\lambda,\gamma)$ as a quadruple sum over six integrals. We then evaluate the integrals over w, z, p and q, using eq. (A.9), which reduces to a double sum of double integrals

$$\begin{aligned}\mathcal{H}_N(\lambda,\gamma) = \frac{N!(N+\nu)!}{\pi^2}\sum_{j=0}^{N}\sum_{k=0}^{j}\frac{\delta_-^{4(j-k)}\delta_+^{4(N-j)}}{k!(k+\nu)!} \\ \times\int_{\mathbb{C}} d^2u\, e^{-|u|^2}(\lambda - i\delta_- u)^k(\lambda - i\delta_-\bar{u})^{k+\nu} \\ \times\int_{\mathbb{C}} d^2v\, e^{-|v|^2}(\gamma - i\delta_- v)^k(\gamma - i\delta_-\bar{v})^{k+\nu}.\end{aligned} \tag{5.39}$$

Finally, we use eq. (A.11) to perform the remaining integrals, and find that

$$\mathcal{H}_N(\lambda,\gamma) = N!(N+\nu)!\delta_+^{4N}(\lambda\gamma)^\nu\sum_{j=0}^{N}\left(\frac{\delta_-}{\delta_+}\right)^{4j}\sum_{k=0}^{j}\frac{k!}{(k+\nu)!}L_k^\nu\left(\frac{\lambda^2}{\delta_-^2}\right)L_k^\nu\left(\frac{\gamma^2}{\delta_-^2}\right), \tag{5.40}$$

where $L_k^\nu(z)$ is the generalised Laguerre polynomial[1]. We can now write down the quenched kernel itself using eq. (5.20)

$$\mathcal{K}_N(u,v) = \frac{\eta_-}{8\pi(4\mu^2\eta_+)^{\nu+1}}(u-v)\sum_{j=0}^{N-2}\left(\frac{\eta_-}{\eta_+}\right)^{2j}\sum_{k=0}^{j}\frac{k!}{(k+\nu)!}\,L_k^\nu\left(\frac{u}{4\mu^2\eta_-}\right)L_k^\nu\left(\frac{v}{4\mu^2\eta_-}\right), \tag{5.41}$$

or equivalently, after using the Christoffel-Darboux relationship (see eq. 8.974.1 of [Gra07]) to perform one of the sums

$$\begin{aligned}\mathcal{K}_N(u,v) = \frac{\eta_-}{8\pi(4\mu^2\eta_+)^{\nu+1}}\sum_{j=0}^{N-2}\left(\frac{\eta_-}{\eta_+}\right)^{2j}\frac{(j+1)!}{(j+\nu)!} \\ \times\left\{L_{j+1}^\nu\left(\frac{v}{4\mu^2\eta_-}\right)L_j^\nu\left(\frac{u}{4\mu^2\eta_-}\right) - (u\leftrightarrow v)\right\}.\end{aligned} \tag{5.42}$$

In the case of maximal non-Hermiticity ($\mu = 1$), using the fact that

$$\lim_{a\to 0} a^j L_j^\nu\left(\frac{z}{a}\right) = (-1)^j\frac{z^j}{j!}, \tag{5.43}$$

we see that the kernel simplifies to

$$\mathcal{K}_N(u,v;\mu=1) = \frac{u-v}{2^{\nu+4}\pi}\sum_{j=0}^{N-2}\frac{(uv)^j}{4^j j!(j+\nu)!}. \tag{5.44}$$

[1]It is, of course, the presence of these polynomials in the solutions of the chiral ensembles that gives the ensembles their alternative names (i.e. the Wishart-Laguerre ensembles).

5.3 Unquenched kernel

We have already established that the unquenched kernel is of key importance in deriving expressions for correlation functions of the unquenched ensembles, see eq. (4.95). For even N we have that, in analogy with eq. (5.20),

$$\mathcal{K}_N^{(N_f)}(u,v) = \frac{c_N^{(N_f)}}{c_{N-2}^{(N_f)}} \frac{(u-v)\langle \det(\mathcal{D}-u)\det(\mathcal{D}-v)\rangle_{N-2}^{(N_f)}}{(uv)^{\nu/2}}. \tag{5.45}$$

In principle, we could repeat the procedure of §5.2 (i.e. using Grassmann variables and Berezin integration) to determine this expectation. However, such a method would be fairly laborious; the following alternative is easier, and furthermore, it results in compact expressions which otherwise might not have been quite so obvious.

Starting from eq. (5.45), we first replace the expectation over characteristic polynomials with a ratio of partition functions:

$$\mathcal{K}_N^{(N_f)}(u,v) = \frac{c_N^{(N_f)}}{c_{N-2}^{(N_f)}} (u-v) \frac{\mathcal{Z}_{N-2}^{(N_f+2)}(\{m\},\sqrt{u},\sqrt{v})}{\mathcal{Z}_{N-2}^{(N_f)}(\{m\})}. \tag{5.46}$$

Using eq. (4.18), we replace the unquenched normalisation coefficients with their quenched counterparts

$$\begin{aligned}\mathcal{K}_N^{(N_f)}(u,v) &= \frac{c_N}{c_{N-2}} \frac{\mathcal{Z}_{N-2}^{(N_f)}(\{m\})}{\mathcal{Z}_N^{(N_f)}(\{m\})} (u-v) \frac{\mathcal{Z}_{N-2}^{(N_f+2)}(\{m\},\sqrt{u},\sqrt{v})}{\mathcal{Z}_{N-2}^{(N_f)}(\{m\})} \\ &= \frac{c_N}{c_{N-2}} (u-v) \frac{\mathcal{Z}_{N-2}^{(N_f+2)}(\{m\},\sqrt{u},\sqrt{v})}{\mathcal{Z}_N^{(N_f)}(\{m\})}. \end{aligned} \tag{5.47}$$

For even N_f: We use eq. (5.12) twice, to replace each of the unquenched partition functions with Pfaffians of quenched kernels:

$$\begin{aligned}\mathcal{K}_N^{(N_f)}(u,v) &= (v-u) \frac{\Delta_{N_f}(m_1^2,m_2^2,\ldots)}{\Delta_{N_f+2}(u,v,m_1^2,m_2^2,\ldots)} \frac{\mathrm{Pf}\left[\mathcal{K}_{N+N_f}(w_i,w_j)\right]_{1\le i,j\le N_f+2}}{\mathrm{Pf}\left[\mathcal{K}_{N+N_f}(m_i^2,m_j^2)\right]_{1\le i,j\le N_f}} \\ &= \frac{1}{\prod_{i=1}^{N_f}(u-m_i^2)(v-m_i^2)} \frac{\mathrm{Pf}\left[\mathcal{K}_{N+N_f}(w_i,w_j)\right]_{1\le i,j\le N_f+2}}{\mathrm{Pf}\left[\mathcal{K}_{N+N_f}(m_i^2,m_j^2)\right]_{1\le i,j\le N_f}}, \end{aligned} \tag{5.48}$$

where $w_1 \equiv u$, $w_2 \equiv v$ and $w_{i+2} \equiv m_i^2$ for $1 \le i \le N_f$.

For odd N_f: We use eq. (5.17) twice, to give

$$\mathcal{K}_N^{(N_f)}(u,v) = \frac{1}{\prod_{i=1}^{N_f}(u-m_i^2)(v-m_i^2)} \frac{\mathrm{Pf}\left[A_{ij}\right]_{1\le i,j\le N_f+3}}{\mathrm{Pf}\left[B_{ij}\right]_{1\le i,j\le N_f+1}} \tag{5.49}$$

where

$$A_{ij} = -A_{ji} \equiv \begin{cases} 0 & \text{if } i = j, \\ q_{N+N_f-1}(w_j) & \text{if } j > i = 1, \\ \mathcal{K}_{N+N_f-1}(w_i, w_j) & \text{if } j > i > 1, \end{cases} \tag{5.50}$$

where $w_2 \equiv u$, $w_3 \equiv v$ and $w_{i+3} \equiv m_i^2$ for $1 \leq i \leq N_f$, and

$$B_{ij} = -B_{ji} \equiv \begin{cases} 0 & \text{if } i = j, \\ q_{N+N_f-1}(m_{j-1}^2) & \text{if } j > i = 1, \\ \mathcal{K}_{N+N_f-1}(m_{i-1}^2, m_{j-1}^2) & \text{if } j > i > 1. \end{cases} \tag{5.51}$$

These results, in which we write the unquenched kernel in terms of the quenched one, play an important part in Chapter 9.

5.4 Skew-orthogonal polynomials

We can now extract the skew-orthogonal polynomials from the kernels, using eqs. (4.29) and (4.30).

5.4.1 Quenched case

Explicit forms of the quenched skew-orthogonal polynomials are needed for the unquenched correlation functions for an odd number N_f of quark flavours. We have already determined the norms of the quenched skew-orthogonal polynomials (see eq. (5.8)).

For the even skew-orthogonal polynomials, we use eq. (4.29) with the quenched kernel from eq. (5.41). Only a single term survives the limiting process, which we evaluate using the fact that

$$\lim_{u\to\infty} \frac{1}{u^N} L_N^\nu \left(\frac{u}{\delta_-^2}\right) = \frac{(-1)^N}{N!\,\delta_-^{2N}}. \tag{5.52}$$

Hence we have immediately

$$\begin{aligned} q_{2k}(z) &= (2k)!(2k+\nu)!\,\delta_+^{8k} \left(\frac{\delta_-}{\delta_+}\right)^{8k} \frac{(2k)!}{(2k+\nu)!} L_{2k}^\nu \left(\frac{z}{\delta_-^2}\right) \frac{1}{(2k)!\delta_-^{4k}} \\ &= \delta_-^{4k}\,(2k)!\,L_{2k}^\nu \left(\frac{z}{\delta_-^2}\right). \end{aligned} \tag{5.53}$$

For the odd skew-orthogonal polynomials, we use eq. (4.30). Only three terms survive the differentiation, which we evaluate using

$$\frac{d^n}{dz^n} L_n^\nu(z) = (-1)^n \qquad \text{and} \tag{5.54}$$

$$\frac{d^{n-1}}{dz^{n-1}} L_n^\nu(z) = (-1)^n (z - (n+\nu)). \tag{5.55}$$

After using the recurrence relation for the Laguerre polynomials

$$L_n^\nu(z) = \left(2 + \frac{\nu - 1 - z}{n}\right) L_{n-1}^\nu(z) - \left(1 + \frac{\nu - 1}{n}\right) L_{n-2}^\nu(z) \tag{5.56}$$

and simplifying, we arrive at

$$\begin{aligned} q_{2k+1}(z) = -\delta_-^{4k+2}\,(2k+1)!\,L_{2k+1}^\nu\left(\frac{z}{\delta_-^2}\right) + \delta_+^4\,(2k)(2k+\nu)\,\delta_-^{4k-2}\,(2k-1)!\,L_{2k-1}^\nu\left(\frac{z}{\delta_-^2}\right) \\ - cL_{2k}^\nu\left(\frac{z}{\delta_-^2}\right). \end{aligned} \tag{5.57}$$

If we define scaled Laguerre polynomials as

$$C_k^\nu(z) \equiv \delta_-^{2k}\,k!\,L_k^\nu\left(\frac{z}{\delta_-^2}\right) \tag{5.58}$$

then we can write the results in a more compact form as

$$\begin{aligned} q_{2k}(z) &= C_{2k}^\nu(z), \\ q_{2k+1}(z) &= -\Big[C_{2k+1}^\nu(z) - \delta_+^4\,(2k)(2k+\nu)C_{2k-1}^\nu(z) + cC_{2k}^\nu(z)\Big]. \end{aligned} \tag{5.59}$$

We reiterate here that c is an arbitrary constant.

5.4.2 Unquenched case

We do not use the unquenched skew-orthogonal polynomials in the remainder of this thesis. However, we derive them here to demonstrate the elegance of our method.

5.4.2.1 Norms $h_k^{(N_f)}$

Let us first determine a relationship for the unquenched norms in terms of the quenched norms (together with the kernel and skew-orthogonal polynomials). Inserting eq. (4.18) into eq. (4.73), we have

$$h_k^{(N_f)} = \frac{c_{2k}}{c_{2k+2}} \frac{\mathcal{Z}_{2k+2}^{(N_f)}}{\mathcal{Z}_{2k}^{(N_f)}}. \tag{5.60}$$

We now merely replace the unquenched partition functions with Pfaffians of quenched kernels, using the results from §5.1.

For even N_f: We use eq. (5.12) to give

$$h_k^{(N_f)} = h_{k+N_f/2} \frac{\mathrm{Pf}\left[\mathcal{K}_{2k+N_f+2}(m_i^2, m_j^2)\right]_{1\le i,j\le N_f}}{\mathrm{Pf}\left[\mathcal{K}_{2k+N_f}(m_i^2, m_j^2)\right]_{1\le i,j\le N_f}}. \tag{5.61}$$

For odd N_f: We use eq. (5.17) to give

$$h_k^{(N_f)} = h_{k+(N_f-1)/2} \frac{\mathrm{Pf}\left[A_{ij}\right]_{1\le i,j\le N_f+1}}{\mathrm{Pf}\left[B_{ij}\right]_{1\le i,j\le N_f+1}}, \tag{5.62}$$

where

$$\begin{aligned} A_{ij} = -A_{ji} &\equiv \begin{cases} 0 & \text{if } i=j, \\ q_{2k+N_f+1}(m_{j-1}^2) & \text{if } j>i=1, \\ \mathcal{K}_{2k+N_f+3}(m_{i-1}^2, m_{j-1}^2) & \text{if } j>i>1, \end{cases} \\ B_{ij} = -B_{ji} &\equiv \begin{cases} 0 & \text{if } i=j, \\ q_{2k+N_f-1}(m_{j-1}^2) & \text{if } j>i=1, \\ \mathcal{K}_{2k+N_f+1}(m_{i-1}^2, m_{j-1}^2) & \text{if } j>i>1. \end{cases} \end{aligned} \tag{5.63}$$

5.4.2.2 Even N_f

First, let us consider the even skew-orthogonal polynomials; we insert eq. (5.48) into eq. (4.29)

$$\begin{aligned} q_{2k}^{(N_f)}(z) &= h_k^{(N_f)} \lim_{u\to\infty} \frac{\mathcal{K}_{2k+2}^{(N_f)}(u,z)}{u^{2k+1}} \\ &= \frac{h_k^{(N_f)} \lim_{u\to\infty} u^{-(2k+N_f+1)} \mathrm{Pf}\left[\mathcal{K}_{2k+N_f+2}(w_i,w_j)\right]_{1\le i,j\le N_f+2}}{\prod_{i=1}^{N_f}(z-m_i^2)\ \mathrm{Pf}\left[\mathcal{K}_{2k+N_f+2}(m_i^2,m_j^2)\right]_{1\le i,j\le N_f}} \end{aligned} \tag{5.64}$$

where $w_1 \equiv u$, $w_2 \equiv z$ and $w_{i+2} \equiv m_i^2$ for $1 \le i \le N_f$. Now, only the top row and first column of the Pfaffian in the numerator depend on u. Therefore we can take the limit and the power of u inside the Pfaffian, and since (also by eq. (4.29))

$$\lim_{u\to\infty} \frac{\mathcal{K}_{2k+N_f+2}(u,z)}{u^{2k+N_f+1}} = \frac{q_{2k+N_f}(z)}{h_{k+N_f/2}}, \tag{5.65}$$

we have

$$q_{2k}^{(N_f)}(z) = \frac{h_k^{(N_f)}\ \mathrm{Pf}\left[A_{ij}\right]_{1\le i,j\le N_f+2}}{h_{k+N_f/2}\prod_{i=1}^{N_f}(z-m_i^2)\ \mathrm{Pf}\left[\mathcal{K}_{2k+N_f+2}(m_i^2,m_j^2)\right]_{1\le i,j\le N_f}} \tag{5.66}$$

in which

$$A_{ij} = -A_{ji} \equiv \begin{cases} 0 & \text{if } i = j, \\ q_{2k+N_f}(w_j) & \text{if } j > i = 1, \\ \mathcal{K}_{2k+N_f+2}(w_i, w_j) & \text{if } j > i > 1, \end{cases} \tag{5.67}$$

i.e. the unquenched skew-orthogonal polynomial can be written as a Pfaffian involving a combination of quenched skew-orthogonal polynomials and quenched kernels. We can now use eq. (5.61) to eliminate the norms completely:

$$q_{2k}^{(N_f)}(z) = \frac{\operatorname{Pf}\left[A_{ij}\right]_{1\le i,j\le N_f+2}}{\prod_{i=1}^{N_f}(z-m_i^2)\,\operatorname{Pf}\left[\mathcal{K}_{2k+N_f}(m_i^2,m_j^2)\right]_{1\le i,j\le N_f}}. \tag{5.68}$$

Note that, by a linearity argument, we can equivalently use $\mathcal{K}_{2k+N_f}$ rather than $\mathcal{K}_{2k+N_f+2}$ inside A_{ij} in eq. (5.67).

For the odd skew-orthogonal polynomials, the calculation becomes rather unwieldy if we try to insert the unquenched kernel eq. (5.48) directly into eq. (4.30); an alternative is to use the following extension of eq. (4.30). Because, for integers $m, n \ge 0$,

$$h_k \frac{\partial^{2k+m}}{\partial u^{2k+m}}\, u^n\, \mathcal{K}_{2k+2}(u,z)\Big|_{u=0} = \begin{cases} 0 & \text{if } n < m, \\ -(2k+m)!\, q_{2k+1}(z) & \text{if } n = m, \\ \text{some polynomial in } z & \text{if } n > m, \end{cases} \tag{5.69}$$

it follows that, for any constants $\{a_i\}$ with $1 \le i \le m$,

$$q_{2k+1}(z) = -\frac{h_k}{(2k+m)!}\frac{\partial^{2k+m}}{\partial u^{2k+m}}\left(\prod_{i=1}^{m}(u-a_i)\,\mathcal{K}_{2k+2}(u,z)\right)\Bigg|_{u=0} \tag{5.70}$$

(where we note that an arbitrary multiple of $q_{2k}(z)$ could also be added). By inserting eq. (5.48) into eq. (5.70) with the choice that $m = N_f$ and $a_i = m_i^2$, we find that the reciprocal of the polynomial in u in the former cancels with the product on the right-hand side of the latter, and we arrive at

$$\begin{aligned} q_{2k+1}^{(N_f)}(z) &= -\frac{h_k^{(N_f)}\,\frac{\partial^{2k+N_f}}{\partial u^{2k+N_f}}\,\operatorname{Pf}\left[\mathcal{K}_{2k+N_f+2}(w_i,w_j)\right]_{1\le i,j\le N_f+2}}{(2k+N_f)!\,\prod_{i=1}^{N_f}(z-m_i^2)\,\operatorname{Pf}\left[\mathcal{K}_{2k+N_f+2}(m_i^2,m_j^2)\right]_{1\le i,j\le N_f}} \\ &= \frac{h_k^{(N_f)}\,\operatorname{Pf}\left[B_{ij}\right]_{1\le i,j\le N_f+2}}{h_{k+N_f/2}\,\prod_{i=1}^{N_f}(z-m_i^2)\,\operatorname{Pf}\left[\mathcal{K}_{2k+N_f+2}(m_i^2,m_j^2)\right]_{1\le i,j\le N_f}} \end{aligned} \tag{5.71}$$

in which

$$B_{ij} = -B_{ji} \equiv \begin{cases} 0 & \text{if } i = j, \\ q_{2k+N_f+1}(w_j) & \text{if } j > i = 1, \\ \mathcal{K}_{2k+N_f+2}(w_i, w_j) & \text{if } j > i > 1. \end{cases} \tag{5.72}$$

In the final step, we took the differential inside the Pfaffian (recall that $w_1 \equiv u$), and then used eq. (4.30) to evaluate this differential in terms of the quenched skew-orthogonal polynomials. Finally, we can also eliminate the norms by using eq. (5.61), to get

$$q_{2k+1}^{(N_f)}(z) = \frac{\operatorname{Pf}\left[B_{ij}\right]_{1\le i,j\le N_f+2}}{\prod_{i=1}^{N_f}(z-m_i^2)\,\operatorname{Pf}\left[\mathcal{K}_{2k+N_f}(m_i^2,m_j^2)\right]_{1\le i,j\le N_f}}. \tag{5.73}$$

A comparison of eqs. (5.68) and (5.73) reveals that the even and odd cases have near-identical forms.

5.4.2.3 Odd N_f

The skew-orthogonal polynomials for odd N_f can be calculated along similar lines. Since we gave details in [Ake10b], we will merely state the results here. The even polynomials are given by

$$q_{2k}^{(N_f)}(z) = -\frac{h_{k+(N_f-1)/2}\operatorname{Pf}\left[\mathcal{K}_{2k+N_f+1}(w_i,w_j)\right]_{1\le i,j\le N_f+1}}{\prod_{i=1}^{N_f}(z-m_i^2)\operatorname{Pf}\left[C_{ij}\right]_{1\le i,j\le N_f+1}}, \tag{5.74}$$

where $w_1 \equiv z$ and $w_{i+1} \equiv m_i^2$ for $1 \le i \le N_f$, and

$$C_{ij} = -C_{ji} \equiv \begin{cases} 0 & \text{if } i = j, \\ q_{2k+N_f-1}(m_{j-1}^2) & \text{if } j > i = 1, \\ \mathcal{K}_{2k+N_f-1}(m_{i-1}^2, m_{j-1}^2) & \text{if } j > i > 1, \end{cases} \tag{5.75}$$

and the odd polynomials by

$$q_{2k+1}^{(N_f)}(z) = -\frac{\operatorname{Pf}\left[D_{ij}\right]_{1\le i,j\le N_f+3}}{\prod_{i=1}^{N_f}(z-m_i^2)\operatorname{Pf}\left[E_{ij}\right]_{1\le i,j\le N_f+1}}, \tag{5.76}$$

where

$$D_{ij} = -D_{ji} \equiv \begin{cases} 0 & \text{if } i = j, \text{ or } i = 1 \text{ and } j = 2, \\ q_{2k+N_f+1}(w_{j-2}) & \text{if } i = 1 \text{ and } j > 2, \\ q_{2k+N_f-1}(w_{j-2}) & \text{if } j > i = 2, \\ \mathcal{K}_{2k+N_f+1}(w_{i-2}, w_{j-2}) & \text{if } j > i > 2, \end{cases}$$

$$E_{ij} = -E_{ji} \equiv \begin{cases} 0 & \text{if } i = j, \\ q_{2k+N_f-1}(m_{j-1}^2) & \text{if } j > i = 1, \\ \mathcal{K}_{2k+N_f-1}(m_{i-1}^2, m_{j-1}^2) & \text{if } j > i > 1, \end{cases} \tag{5.77}$$

where $w_1 \equiv z$ and $w_{i+1} \equiv m_i^2$ for $1 \leq i \leq N_f$. As before, we can add an arbitrary multiple of $q_{2k}^{(N_f)}(z)$ to this result.

Chapter 6

Quenched densities I: Finite-N case and macroscopic large-N limit

We have now determined generic formulas for the correlation functions for both the quenched and the unquenched ensembles, together with explicit formulas for the kernels in each case. We now turn to investigating the specific behaviour of the eigenvalue densities in the quenched case. In particular, we give formulas for the densities of real and non-real eigenvalues, discuss their behaviour, and present a semi-rigorous proof for the fraction of eigenvalues that are real.

Then we look briefly at the macroscopic large-N limit, which has a bounded support of the eigenvalues. The average spacing of eigenvalues tends to zero in this case. We can be quite brief here, since this limit is not so important for applications to QCD.

6.1 Finite-N eigenvalue densities

6.1.1 Expressions for densities

The eigenvalue densities for the Wishart (squared) eigenvalues (for even matrix size N) are given by eq. (4.78); inserting the finite-N kernel from eq. (5.42) and the specific form of the weight function from eq. (4.8) and $w(z)$ from eq. (3.101), we find

that the density of complex eigenvalues ($z \in \mathbb{C}\backslash\mathbb{R}$) is given by

$$R^{\mathbb{C}}_{1,N}(z) = -2i\ \mathrm{sgn}(\Im\mathrm{m}\ z)\, 2\int_0^\infty \frac{dt}{t}\, e^{-\eta_+^2 t(z^2+z^{*2})-\frac{1}{4t}} K_{\frac{\nu}{2}}(2\eta_+^2 t|z|^2)\ \mathrm{erfc}(2\eta_+\sqrt{t}|\Im\mathrm{m}\ z|) \\ \times \frac{\eta_-|z|^\nu e^{2\eta_-\Re\mathrm{e}\ z}}{8\pi(4\mu^2\eta_+)^{\nu+1}} \sum_{j=0}^{N-2}\left(\frac{\eta_-}{\eta_+}\right)^{2j}\frac{(j+1)!}{(j+\nu)!}\left\{L^\nu_{j+1}\left(\frac{z^*}{4\mu^2\eta_-}\right)L^\nu_j\left(\frac{z}{4\mu^2\eta_-}\right) - \mathrm{c.c.}\right\} \tag{6.1}$$

(where c.c. denotes the complex conjugate) and the density of real eigenvalues ($x \in \mathbb{R}$) by

$$R^{\mathbb{R}}_{1,N}(x) = \frac{\eta_-}{8\pi(4\mu^2\eta_+)^{\nu+1}}\int_{-\infty}^\infty dx'\ \mathrm{sgn}(x-x')\,|xx'|^{\nu/2}e^{\eta_-(x+x')}2K_{\frac{\nu}{2}}(\eta_+|x|)2K_{\frac{\nu}{2}}(\eta_+|x'|) \\ \times \sum_{j=0}^{N-2}\left(\frac{\eta_-}{\eta_+}\right)^{2j}\frac{(j+1)!}{(j+\nu)!}\left\{L^\nu_{j+1}\left(\frac{x'}{4\mu^2\eta_-}\right)L^\nu_j\left(\frac{x}{4\mu^2\eta_-}\right) - (x\leftrightarrow x')\right\}. \tag{6.2}$$

Both these equations are valid for even N only.

We can convert from Wishart (squared) eigenvalues ($z = \Lambda^2$) to Dirac eigenvalues (Λ) as follows:

$$R^{\mathbb{C}}_{1,\mathrm{Dirac}}(z) = 4\,|z|^2\,R^{\mathbb{C}}_1(z^2), \tag{6.3}$$

$$R^{\mathbb{R}}_{1,\mathrm{Dirac}}(x) = 2\,|x|\,R^{\mathbb{R}}_1(x^2). \tag{6.4}$$

Since these formulas are also applicable for the infinite-N limits, we drop the subscript N here. It is worth mentioning that, since $R^{\mathbb{R}}_{1,N}(x) \neq R^{\mathbb{R}}_{1,N}(-x)$ in general, the densities of real and imaginary Dirac eigenvalues will not be the same.

In Figure 6.1, we show the density of complex Dirac eigenvalues at finite N ($N = 10$) for $\mu^2 = 0.95$ (close to maximal non-Hermiticity) and for an intermediate value of $\mu^2 = 0.5$. Because the Dirac densities are symmetric under reflection in both the x- and y-axes, we show just one quadrant of the complex plane $\mathbb{C}$. For the case with μ close to unity, we see an almost circular 'support', although a repulsion of the eigenvalues from both axes is clearly visible. When we consider a lower value of μ, then we see that the 'support' becomes more elliptical.

Figure 6.2 shows the densities of real (in blue) and imaginary (in red, dashed) eigenvalues, again for high and intermediate values of μ. As the Dirac densities here are symmetric in x for the real eigenvalues, or in y for the imaginary ones, we only show the positive half-axes. At μ close to unity, there is a close similarity between the real and imaginary densities, whereas when we decrease μ, the number

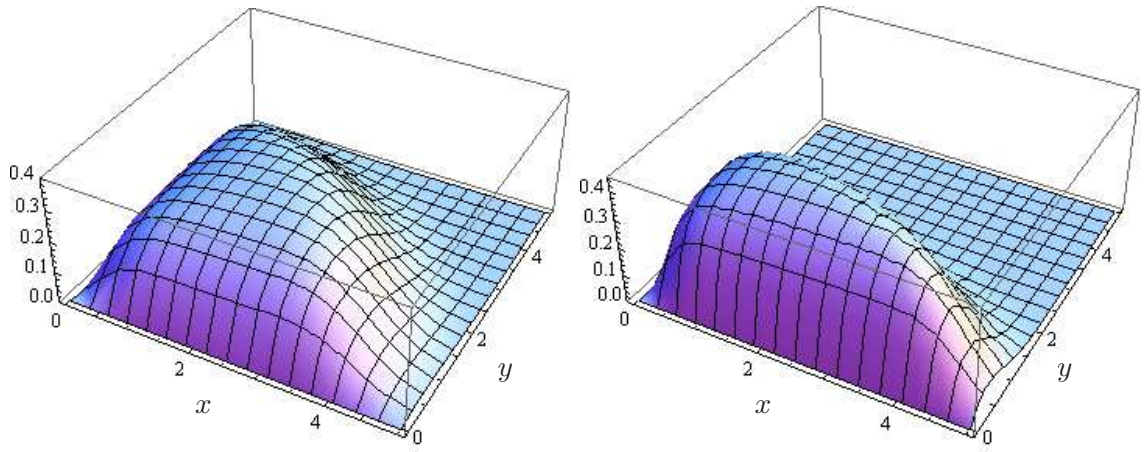

Figure 6.1: The densities of complex Dirac eigenvalues $R^{\mathbb{C}}_{1,N,\mathrm{Dirac}}(z)$ for $N = 10$ at $\mu^2 = 0.95$ (left) and $\mu^2 = 0.5$ (right); $\nu = 0$ in both cases.

of imaginary eigenvalues decreases, and there is a gradual build-up of eigenvalues on the real axis.

Figure 6.3 demonstrates the effect of increasing the topology parameter ν, whilst keeping the other parameters fixed. As we increase ν, there is additional repulsion of the eigenvalues from the origin, as would have been expected from an observation of the JPDF.

6.1.2 Hermitian limit ($\mu \to 0$) of density

We now verify explicitly that the Hermitian limit (i.e. $\mu \to 0$) of the density of real eigenvalues agrees with the formula given in [Ver94c] where the corresponding Hermitian model (chGOE) was originally introduced. Note that what happens for our $\beta = 1$ ensemble is that $R^{\mathbb{C}} \to 0$ and $R^{\mathbb{R}} \to$ the Hermitian limit smoothly as $\mu \to 0$; this is quite unlike the $\beta = 2$ and 4 cases, in which all eigenvalues are complex for any $\mu > 0$, and $R^{\mathbb{C}}$ 'collapses down' to a Dirac delta function on the real axis only when μ reaches zero. In fact, for the $\beta = 1$ case, when μ is very small (but non-zero) most of the eigenvalues will already lie exactly on the real axis.

Let us consider the limit $\mu \to 0$ of eq. (6.2). We have $4\mu^2\eta_+ \to 1$, $4\mu^2\eta_- \to 1$, $\eta_-/\eta_+ \to 1$ and $e^{\eta_- x} = e^{-x/2}e^{\eta_+ x}$. Using the fact that

$$\lim_{k\to\infty} \sqrt{k}\, e^{kx}\, K_\nu(k|x|) = \sqrt{\frac{\pi}{2x}}\, \Theta(x), \tag{6.5}$$

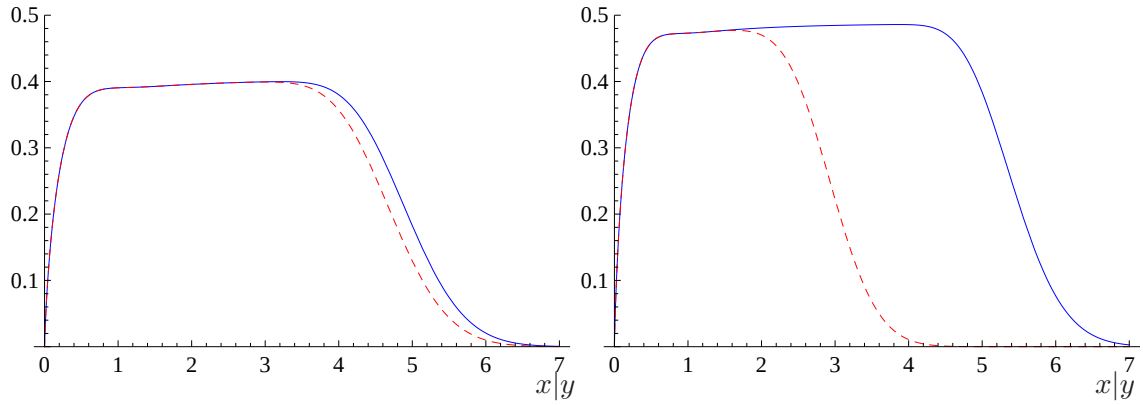

Figure 6.2: The densities of real (blue) and imaginary (red, dashed) Dirac eigenvalues, $R^{\mathbb{R}}_{1,N,\mathrm{Dirac}}(x)$ and $R^{\mathbb{R}}_{1,N,\mathrm{Dirac}}(iy)$ respectively, for $N = 10$ at $\mu^2 = 0.95$ (left) and $\mu^2 = 0.5$ (right); $\nu = 0$ in both cases.

(proven using eq. 8.451.6 of [Gra07]) where $\Theta(x)$ is the Heaviside step function, and putting $k = 1/4\mu^2$ gives, after a little simplification,

$$\lim_{\mu\to 0} R^{\mathbb{R}}_{1,N}(x) = \frac{\Theta(x)}{4}\, x^{(\nu-1)/2} e^{-x/2} \int_0^\infty dx'\, \mathrm{sgn}(x-x')\,(x')^{(\nu-1)/2} e^{-x'/2}\, S_N(x,x';\nu) \quad (6.6)$$

where

$$S_N(x,x';\nu) \equiv \sum_{j=0}^{N-2} \frac{(j+1)!}{(j+\nu)!} \left\{ L^\nu_{j+1}(x') L^\nu_j(x) - L^\nu_{j+1}(x) L^\nu_j(x') \right\}. \quad (6.7)$$

Let us simplify this sum. First we add and subtract two equal terms, and then we use eq. 8.971.5 of [Gra07] as follows:

$$\begin{aligned} S_N(x,x';\nu) &= \sum_{j=0}^{N-2} \frac{(j+1)!}{(j+\nu)!} \left\{ (L^\nu_{j+1}(x') - L^\nu_j(x')) L^\nu_j(x) - (L^\nu_{j+1}(x) - L^\nu_j(x)) L^\nu_j(x') \right\} \\ &= \sum_{j=0}^{N-2} \frac{(j+1)!}{(j+\nu)!} \left\{ L^{\nu-1}_{j+1}(x') L^\nu_j(x) - L^{\nu-1}_{j+1}(x) L^\nu_j(x') \right\}. \end{aligned} \quad (6.8)$$

Next, we relabel the sum, so that it runs from 1 to $N-1$:

$$S_N(x,x';\nu) = \sum_{j=1}^{N-1} \frac{j!}{(j+\nu-1)!} \left\{ L^{\nu-1}_j(x') L^\nu_{j-1}(x) - L^{\nu-1}_j(x) L^\nu_{j-1}(x') \right\}. \quad (6.9)$$

Now, using eq. 8.971.2 from [Gra07], we have

$$\begin{aligned} S_N(x,x';\nu) &= \sum_{j=1}^{N-1} \frac{j!}{(j+\nu-1)!} \left\{ -L^{\nu-1}_j(x') \frac{d}{dx} L^{\nu-1}_j(x) + L^{\nu-1}_j(x) \frac{d}{dx'} L^{\nu-1}_j(x') \right\} \\ &= \left(\frac{\partial}{\partial x'} - \frac{\partial}{\partial x} \right) \sum_{j=1}^{N-1} \frac{j!}{(j+\nu-1)!} L^{\nu-1}_j(x) L^{\nu-1}_j(x'). \end{aligned} \quad (6.10)$$

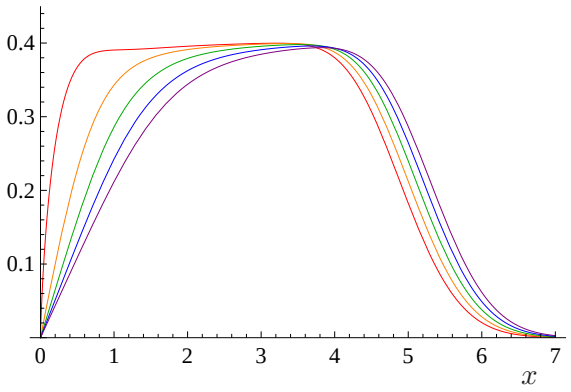

Figure 6.3: The densities of real Dirac eigenvalues $R^{\mathbb{R}}_{1,N,\mathrm{Dirac}}(x)$ for $N = 10$ at $\mu^2 = 1$, for a sequence of topologies: $\nu = 0$ (red), $\nu = 1$ (orange), $\nu = 2$ (green), $\nu = 3$ (blue) and $\nu = 4$ (purple).

Since the differential of a constant vanishes, we can start the sum from zero:

$$S_N(x, x'; \nu) = \left(\frac{\partial}{\partial x'} - \frac{\partial}{\partial x}\right) \sum_{j=0}^{N-1} \frac{j!}{(j+\nu-1)!} L_j^{\nu-1}(x) L_j^{\nu-1}(x'). \tag{6.11}$$

We now apply the Christoffel-Darboux formula (eq. 8.974.1 of [Gra07]), to arrive at

$$S_N(x, x'; \nu) = \frac{N!}{(N+\nu-2)!} \left(\frac{\partial}{\partial x'} - \frac{\partial}{\partial x}\right) \frac{L_{N-1}^{\nu-1}(x) L_N^{\nu-1}(x') - L_{N-1}^{\nu-1}(x') L_N^{\nu-1}(x)}{x - x'}. \tag{6.12}$$

Eqs. (6.6) and (6.12), when taken together, are essentially the same as eqs. 5.21 and 5.22 in [Ver94c], after changing to the same scaling convention.

Because there is no N-dependency in the exponents of the weight functions in eq. (2.6), we actually arrive at something that is 'mid-way' between the macroscopic and the microscopic scalings of the chGOE. Essentially, we see a density that is close to the semi-circle distribution of Wigner (but with a hole at the origin for topology $\nu > 0$). The support is approximately $[-2\sqrt{N}, 2\sqrt{N}]$, and the maximum height of the distribution is approximately $2\sqrt{N}/\pi$, i.e. both support and height tend to infinity with increasing matrix size N.

6.1.3 Number of real eigenvalues for $\mu = 1$

The non-Hermitian Gaussian random matrix ensembles with Dyson index $\beta = 1$ are characterised by the fact that, for finite matrix size N, the average number of real eigenvalues is non-zero. Furthermore, although the *fraction* of real eigenvalues does

tend to zero as we take the limit $N \to \infty$, the *absolute number* of real eigenvalues remains non-zero, and, perhaps surprisingly, also tends to infinity. This was explicitly proven for the non-chiral (GinOE) ensemble with arbitrary non-Hermiticity by Forrester and Nagao [For08], who showed by integrating the density function that the number of real eigenvalues is, to leading order, proportional to $\sqrt{N}$ at large N. This extended the earlier result of Edelman *et al* [Ede94] at maximal non-Hermiticity. We show now that a similar result is also true for the chiral ensemble.

The technique used for the non-chiral ensemble in [For08] relies on the fact that each odd skew-orthogonal polynomial can be written in terms of an exact differential involving an even skew-orthogonal polynomial. This does not appear to be true for the chiral case, and so we are reduced to presenting a semi-rigorous proof, and only for the case of maximal non-Hermiticity (i.e. for $\mu = 1$). Furthermore, our proof is just for the $\nu = 0$ case, although it can easily be generalised for $\nu > 0$, giving in fact the same answer (to leading order).

Let us now set ν to zero in eq. (6.2), and take the limit $\mu \to 1$. The Laguerre polynomials become monomials in this limit, see eq. (5.43), and, after some simplification, we have (for even N)

$$R^{\mathbb{R}}_{1,N}(x) = \frac{1}{16\pi} K_0\left(\frac{|x|}{2}\right) \int_{-\infty}^{\infty} dx' \, K_0\left(\frac{|x'|}{2}\right) \operatorname{sgn}(x - x') \times \sum_{j=0}^{N-2} \frac{1}{2^{2j}(j!)^2} \left\{x^{j+1}(x')^j - x^j(x')^{j+1}\right\}. \tag{6.13}$$

The total number of real squared eigenvalues is therefore given by integrating this over all $x \in \mathbb{R}$:

$$n_{\text{real}} = \frac{1}{16\pi} \sum_{j=0}^{N-2} \frac{1}{2^{2j}(j!)^2} \int_{-\infty}^{\infty} dx \, K_0\left(\frac{|x|}{2}\right) \int_{-\infty}^{\infty} dx' \, K_0\left(\frac{|x'|}{2}\right) \operatorname{sgn}(x - x') \times \left\{x^{j+1}(x')^j - x^j(x')^{j+1}\right\}, \tag{6.14}$$

which can of course also be written as

$$n_{\text{real}} = \frac{1}{16\pi} \sum_{j=0}^{\frac{N}{2}-1} \frac{1}{2^{4j}((2j)!)^2} \int_{-\infty}^{\infty} dx \, K_0\left(\frac{|x|}{2}\right) \int_{-\infty}^{\infty} dx' \, K_0\left(\frac{|x'|}{2}\right) \operatorname{sgn}(x - x') \times \left\{q_{2j}(x')q_{2j+1}(x) - q_{2j}(x)q_{2j+1}(x')\right\} \tag{6.15}$$

where the $q_j(x)$ are the skew-orthogonal polynomials (for $j \geq 0$) obtained by taking $\mu \to 1$ in eq. (5.59)

$$\begin{aligned} q_{2j}(x) &= x^{2j}, \\ q_{2j+1}(x) &= x^{2j+1} - 4(2j)^2\, x^{2j-1}. \end{aligned} \tag{6.16}$$

Let us consider a single term in the sum in eq. (6.14):

$$\begin{aligned} T(j) \equiv \frac{1}{16\pi}\frac{1}{2^{2j}(j!)^2} \int_{-\infty}^{\infty} dx\, K_0\left(\frac{|x|}{2}\right) \int_{-\infty}^{\infty} dx'\, K_0\left(\frac{|x'|}{2}\right) \operatorname{sgn}(x-x') \\ \times \left\{x^{j+1}(x')^j - x^j(x')^{j+1}\right\}. \end{aligned} \tag{6.17}$$

For large j, the interplay between the polynomials and the exponentially-decaying modified Bessel functions means that the dominant contribution to the integrals comes from regions of x and x' where we can use the large-argument asymptotic limit of the Bessel function:

$$K_0(x) \sim \sqrt{\frac{\pi}{2x}}\, e^{-x} \qquad \text{as} \qquad x \to \infty. \tag{6.18}$$

Therefore, for large j,

$$T(j) \sim \frac{1}{8}\frac{1}{2^{2j}(j!)^2} \int_{-\infty}^{\infty} dx \int_{-\infty}^{\infty} dx'\, \frac{e^{-|x|/2}}{\sqrt{|x|}}\, \frac{e^{-|x'|/2}}{\sqrt{|x'|}}\, \operatorname{sgn}(x-x')\, x^{j+1}(x')^j. \tag{6.19}$$

We can perform the integrals over x and x' by splitting the xx'-plane into six regions, and using eqs. 3.381.1 and 6.455.1 from [Gra07]. After simplification, the result is that

$$T(j) \sim \frac{1}{(j!)^2}\left\{\left(1+(-1)^j\right)\Gamma(j+\tfrac{1}{2})\Gamma(j+\tfrac{3}{2}) - \frac{\Gamma(2j+2)\,{}_2F_1(1,2j+2;j+\tfrac{5}{2};\tfrac{1}{2})}{2^{2j}(3+2j)}\right\}. \tag{6.20}$$

This contains the hypergeometric function which is defined for $|z| < 1$ as (see eq. 9.100 of [Gra07])

$${}_2F_1(a,b;c;z) \equiv \sum_{n=0}^{\infty} \frac{(a)_n (b)_n}{(c)_n\, n!}\, z^n \tag{6.21}$$

(and elsewhere by analytic continuation) where

$$(a)_n \equiv a(a+1)(a+2)\cdots(a+n-1) \tag{6.22}$$

is the Pochhammer symbol. We can now take the large-j limit of eq. (6.20), term-by-term. After a number of cancellations, we find simply that

$$T(j) \sim (-1)^j + \frac{1}{\sqrt{\pi j}}. \tag{6.23}$$

Finally, therefore, when N is large, the number of squared (Wishart) eigenvalues that are real is given by

$$n_{\text{real}} = \sum_{j=0}^{N-2} T(j) \approx \int_0^N dy \, \frac{1}{\sqrt{\pi y}} = \frac{2}{\sqrt{\pi}} \sqrt{N}. \tag{6.24}$$

So, when we map back to Dirac eigenvalues, we will have a total of $2N$ eigenvalues, of which $\frac{2}{\sqrt{\pi}}\sqrt{N}$ will be real, and the same number $\frac{2}{\sqrt{\pi}}\sqrt{N}$ pure imaginary (since $\mu = 1$). The fraction of Dirac eigenvalues that are real is therefore

$$f_{\text{real}} = \frac{1}{\sqrt{\pi N}}. \tag{6.25}$$

This is the same behaviour as for the non-chiral case (GinOE), although the constant factor is different; for the Ginibre case, the fraction of real eigenvalues at large N is $\sqrt{\frac{2}{\pi N}}$ [Ede94; For08].

6.1.4 Number of real eigenvalues for arbitrary μ

The authors of [Hal97] cite a (slightly) earlier formula of Efetov [Efe97b] for the fraction of real eigenvalues in a non-chiral $\beta = 1$ ensemble with a small perturbation from Hermiticity. The authors of [Hal97] reasoned that a similar formula may also apply to the chiral ensemble (at least, with a fixed perturbing matrix), supporting their claims with Monte Carlo results. For large N and small μ, the fraction of eigenvalues that are real is predicted to be

$$\mathfrak{F}_{real}(N, \mu) = \int_{-2}^{2} \rho_{sc}(\lambda) \, d\lambda \int_0^1 dt \, \exp\left\{-N[2\pi\mu\rho_{sc}(\lambda)]^2 t^2\right\} \tag{6.26}$$

where

$$\rho_{sc}(\lambda) = \frac{\sqrt{4 - \lambda^2}}{2\pi} \tag{6.27}$$

is the Wigner semi-circle distribution. Of course, this formula is not expected to be exact, especially at finite N and non-small μ.

However, now that we have derived an analytic formula for the density eq. (6.2), our aim in this short section is to demonstrate that Efetov's formula eq. (6.26) does indeed work rather well in practice for the chiral ensemble, even at finite N and moderate μ. We note that the asymptotic limit of eq. (6.26) at *fixed* μ and large N is

$$\mathfrak{F}_{real}(N, \mu) \sim \frac{1}{\mu\sqrt{\pi N}} \tag{6.28}$$

which is consistent with our previous result eq. (6.25) for the $\mu = 1$ case.

For our numerical checks of the accuracy of eq. (6.26) for finite N, we used Mathematica [Wol08] to perform the numerical integration of the density given in eq. (6.2). We show these results in Figure 6.4.

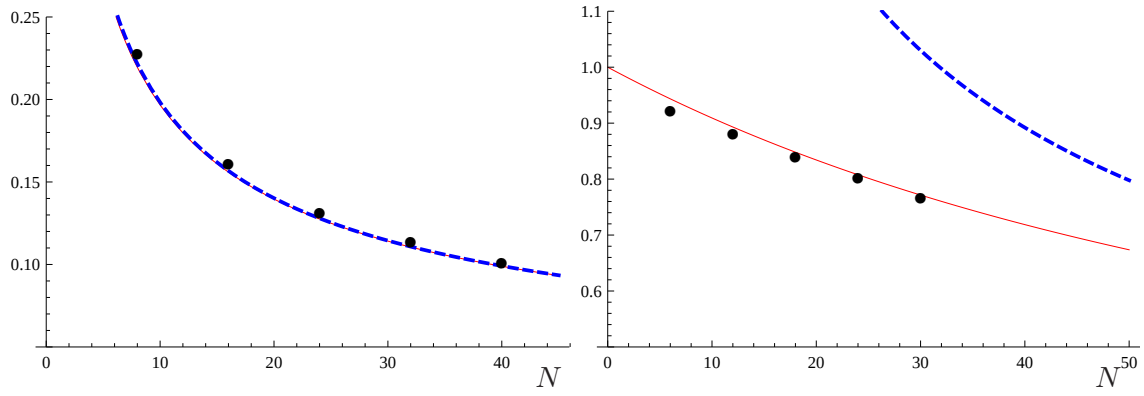

Figure 6.4: Comparison of fraction of real Dirac eigenvalues (black dots) with the Efetov formula (red) and the asymptotic limit of the Efetov formula (blue, dashed) for $\mu = 0.9$ (left) and $\mu = 0.1$ (right). In the left-hand graph, the asymptotic limit is indistinguishable from the Efetov formula.

For the case of $\mu = 0.9$ (Figure 6.4, left), we find that the Efetov formula eq. (6.26) is not exact at finite N, but is nevertheless quite close. Furthermore, even for these relatively moderate values of N, both the Efetov formula and our integrated results are already close to the asymptotic limit eq. (6.28) (the blue dashed curve appears to lie on top of the red curve).

We also considered a smaller $\mu = 0.1$ (Figure 6.4, right). Again, we find a close, but not exact, match to the Efetov formula. However, for the values of N considered, both the Efetov formula and our results are far from the asymptotic limit eq. (6.28). Indeed, the fraction of eigenvalues that are real for low values of N is closer to $\mathcal{O}(1)$, and it is only at much higher N that we find that the behaviour is closer to $\frac{1}{\mu\sqrt{\pi N}}$.

We will assume that the limiting behaviour eq. (6.28) is correct, when deriving the eigenvalue support in the next section. Otherwise we will make no further use of the Efetov formula, apart from at the end of Chapter 8 where we use it as a consistency check.

6.1.5 Approximate eigenvalue supports

We will establish in §7.3 that the finite-N densities (for both complex and real eigenvalues) converge pointwise to the strongly non-Hermitian large-N limits, which are essentially flat far away from the axes. We also see these plateaux for large, but finite, values of N, although for finite N, the densities must naturally tend to zero again at sufficiently large $|z|$.

We can therefore use the strong-limit densities from §7.3 as proxies for the finite-N densities in the plateau regions, and thereby estimate the approximate 'supports' of the eigenvalues in the finite-N case. We also need expressions for the numbers of real and complex eigenvalues. For the real case, we will use the asymptotic form of the Efetov formula eq. (6.28); for the complex case, we will assume that, for large N, all the eigenvalues (to leading order) are complex.

For the real case, the density of Dirac eigenvalues in the plateau region is given by eq. (7.18), and the number of real Dirac eigenvalues is estimated, from the asymptotic limit of Efetov's formula, to be

$$n_{real} \sim \frac{2}{\mu}\sqrt{\frac{N}{\pi}}. \tag{6.29}$$

Therefore, the approximate support must be the interval

$$\left[-2\sqrt{\frac{N}{1+\mu^2}}, 2\sqrt{\frac{N}{1+\mu^2}}\right] \tag{6.30}$$

on the real axis. Whilst most eigenvalues lie within this interval, a small number will lie outside (the true support is not bounded).

For the complex case, we have the Dirac density of the plateau given by eq. (7.15), and the number of complex Dirac eigenvalues $\sim 2N$, to leading order. Assuming that the eigenvalues lie in an ellipse (a reasonable assumption, cf. Girko's elliptical law, see [Gir84]), and that one axis of the ellipse must, by continuity, be the same as the support of the real eigenvalues eq. (6.30), then the other axis of the ellipse is the interval

$$\left[-2\mu^2\sqrt{\frac{N}{1+\mu^2}}i, 2\mu^2\sqrt{\frac{N}{1+\mu^2}}i\right] \tag{6.31}$$

on the imaginary axis. Eqs. (6.30) and (6.31) then specify the elliptical region that contains most of the complex eigenvalues.

6.2 Macroscopic large-N limit

We can define the macroscopic scaling for the complex and real Dirac eigenvalue densities as

$$\begin{aligned} R^{\mathbb{C}\,M}_{1,N,\mathrm{Dirac}}(z) &\equiv N\, R^{\mathbb{C}}_{1,N,\mathrm{Dirac}}(\sqrt{N}\, z), \\ R^{\mathbb{R}\,M}_{1,N,\mathrm{Dirac}}(x) &\equiv \sqrt{N}\, R^{\mathbb{R}}_{1,N,\mathrm{Dirac}}(\sqrt{N}\, x). \end{aligned} \tag{6.32}$$

These are the Dirac densities that we would have obtained if we had introduced an extra factor of N into the weight function of eq. (2.6), giving

$$\mathcal{Z}_N^{(N_f)} \sim \int dP\, dQ\, \exp\left[-\frac{N}{2}\,\mathrm{Tr}(PP^T + QQ^T)\right] \times \prod_{f=1}^{N_f} \det(\mathcal{D} + m_f \mathcal{I}). \tag{6.33}$$

In fact, this scaling is often adopted by RMT practitioners, since the support of the eigenvalue density remains bounded as $N \to \infty$. The N-dependent normalisations in eq. (6.32) are chosen such that the integrals of these densities (over $\mathbb{C}$ or $\mathbb{R}$ respectively) still correspond to the total numbers of complex and real/imaginary eigenvalues; consequently, $R^{\mathbb{C}\,M}_{1,N,\mathrm{Dirac}}(z)$ and $R^{\mathbb{R}\,M}_{1,N,\mathrm{Dirac}}(x)$ both diverge at large N for fixed z and x respectively.

To establish (non-divergent) macroscopic large-N limits, one must also introduce normalisations dependent on the number of eigenvalues that are complex, and the number that are real/imaginary. At large N, we conjectured in §6.1.4 that these $\sim 2N$ and $\sim \dfrac{2\sqrt{N}}{\mu\sqrt{\pi}}$ respectively, and so we would expect the following large-N limits to exist:

$$\begin{aligned} R^{\mathbb{C}\,M}_{1,\mathrm{Dirac}}(z) &\equiv \lim_{N\to\infty} \frac{1}{2N}\, R^{\mathbb{C}\,M}_{1,N,\mathrm{Dirac}}(z), \\ R^{\mathbb{R}\,M}_{1,\mathrm{Dirac}}(x) &\equiv \lim_{N\to\infty} \frac{\mu\sqrt{\pi}}{2\sqrt{N}}\, R^{\mathbb{R}\,M}_{1,N,\mathrm{Dirac}}(x). \end{aligned} \tag{6.34}$$

The N-dependency in the normalisations cancels the normalising pre-factors in eq. (6.32), and so we can write

$$R^{\mathbb{C}\,M}_{1,\mathrm{Dirac}}(z) = \tfrac{1}{2} \lim_{N\to\infty} R^{\mathbb{C}}_{1,N,\mathrm{Dirac}}(\sqrt{N}\, z), \tag{6.35}$$

$$R^{\mathbb{R}\,M}_{1,\mathrm{Dirac}}(x) = \tfrac{1}{2}\mu\sqrt{\pi} \lim_{N\to\infty} R^{\mathbb{R}}_{1,N,\mathrm{Dirac}}(\sqrt{N}\, x). \tag{6.36}$$

We have not (to date) been able to derive analytic formulas for these macroscopic densities eq. (6.34) at arbitrary μ, due to the complexity of the integrals involved.

However, we expect that the macroscopic behaviour is the same as that of the non-chiral case, where the complex Dirac density is constant within an ellipse, and zero outside, and the real and imaginary Dirac densities are constant on a fixed interval, and zero outside.

In the absence of analytical formulas, we shall merely content ourselves with demonstrating the (probable) existence of macroscopic limits for various non-Hermiticities μ, by showing a sequence of finite-N results (for $N = 10$, 20 and 30) (see Figure 6.5). We concentrate here on the densities of real eigenvalues (since it is easier to display several curves on the same chart) and fix $\nu = 0$ in all cases. Note that the effect of the normalisation in eq. (6.36) is that the area under the curve will tend to unity as $N \to \infty$.

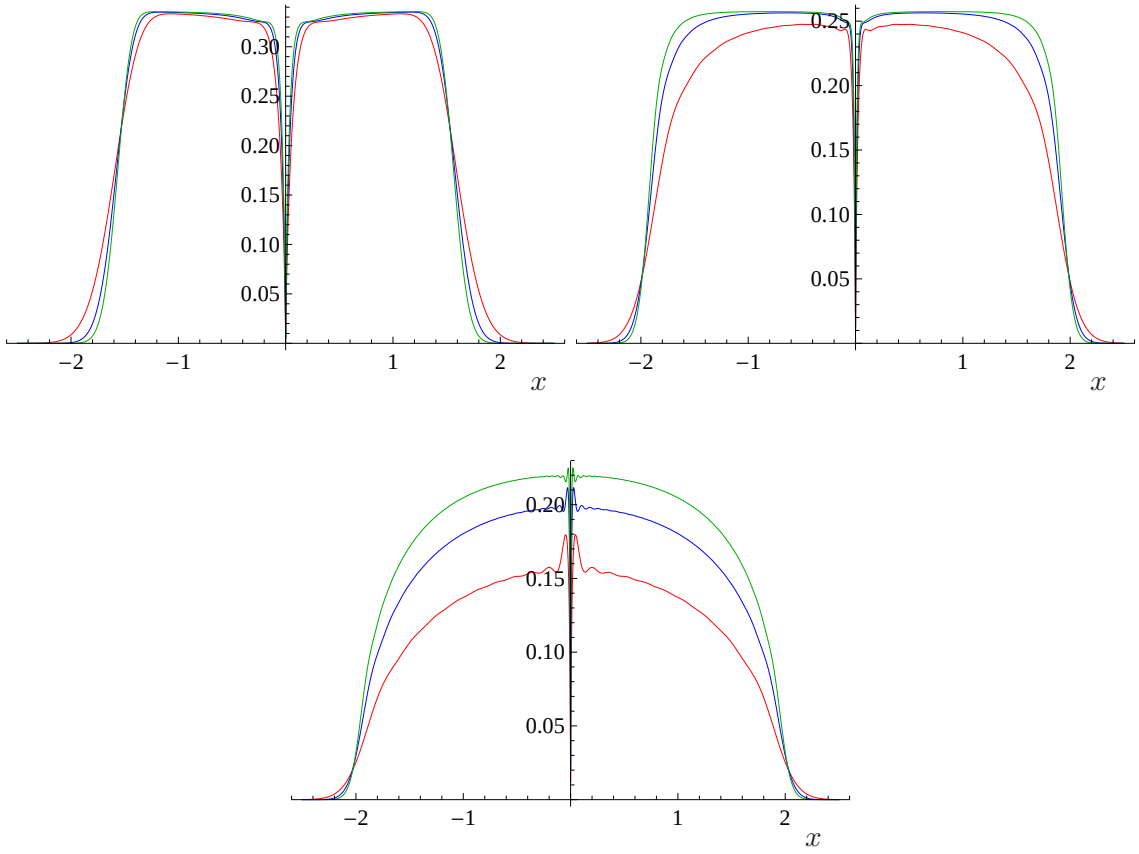

Figure 6.5: The macroscopic densities of real Dirac eigenvalues $\frac{1}{2}\mu\sqrt{\pi}R^{\mathbb{R}\,M}_{1,N,\mathrm{Dirac}}(x)$ for $N = 10$ (red), $N = 20$ (blue) and $N = 30$ (green) for $\mu = 0.9$ (top, left), $\mu = 0.25$ (top, right) and $\mu = 0.1$ (bottom); $\nu = 0$ in all cases.

For $\mu = 0.9$, we see rather rapid convergence to a step function, as expected. For

an intermediate value of μ (we chose $\mu = 0.25$), we also see rapid convergence to a step function, although for very low N, the density is perhaps closer to a semi-circle. For small μ (but still strictly positive – we chose $\mu = 0.1$), convergence is evidently much slower, and at the low values of N that we plot, the densities in fact all appear to be closer to semi-circles than to step functions (although we still expect that the large-N limit will be a step function).

Finally, we mention that, for finite N, the eigenvalue density at the origin will always be zero. Only in the large-N limit does the gap close, giving us a completely flat plateau.

Chapter 7

Quenched densities II: Strongly non-Hermitian microscopic large-N limit

We now consider the first of the two distinct microscopic scaling regimes for non-Hermiticity. Microscopic regimes are scaling regimes where the expected distance between neighbouring eigenvalues remains finite (and non-zero) as the matrix size $N \to \infty$. This is in contrast to the macroscopic regime introduced in §6.2, where the eigenvalue support remains finite in the large-N limit, and so adjacent eigenvalues become closer together on average. The particular limit considered in this chapter is the microscopic limit at strong non-Hermiticity, which has recently found applications in high-density QCD [Kana10].

7.1 Definition of the limit

In the so-called strongly non-Hermitian regime, the non-Hermiticity parameter μ (corresponding physically to the chemical potential) remains constant (cf. the weakly non-Hermitian regime which will be introduced in Chapter 8, where $\mu \to 0$ as $N \to \infty$).

Effectively, under microscopic scaling, we magnify the macroscopic density around a particular point; since we will choose the origin because of its applicability to physics, it turns out that the strong scaling of Dirac eigenvalues is in fact just the same as the finite-N scaling, and so we can take the large-N limits without any

change to the normalisation:

$$R_1^S(z) \equiv \lim_{N\to\infty} R_{1,N}(z). \tag{7.1}$$

We can take the corresponding large-N limits of the kernel and the weight functions separately (both of which exist), and then determine the large-N density functions (for real and complex argument).

7.2 Strong kernel

In §5.2.2 we derived the strongly non-Hermitian large-N limit of the kernel at maximal non-Hermiticity $\mu = 1$ using the saddle point method. Here, we explicitly take the large-N limit of the finite-N result, generating an expression valid for arbitrary μ. The finite-N kernel is given by eq. (5.42). Because the only N-dependency in this is in the upper limit of the sum, it is quite straightforward to take $N \to \infty$.

For generalised Laguerre polynomials, we can use a recurrence relation to show that

$$\begin{aligned}(j+1)\left\{L_{j+1}^\nu(x)L_j^\nu(y) - (x \leftrightarrow y)\right\} &= \left(x\frac{d}{dx}L_j^\nu(x) + (j+\nu+1-x)L_j^\nu(x)\right)L_j^\nu(y) - (x \leftrightarrow y) \\ &= \left(x\frac{\partial}{\partial x} - y\frac{\partial}{\partial y} - (x-y)\right)L_j^\nu(x)L_j^\nu(y).\end{aligned} \tag{7.2}$$

The finite-N kernel therefore becomes

$$\begin{aligned}\mathcal{K}_N(z_1,z_2;\mu) = \frac{\eta_-}{8\pi(4\mu^2\eta_+)^{\nu+1}} \sum_{j=0}^{N-2}\left(\frac{\eta_-}{\eta_+}\right)^{2j}\frac{j!}{(j+\nu)!} \\ \times\left\{\left(x\frac{\partial}{\partial x} - y\frac{\partial}{\partial y} - (x-y)\right)L_j^\nu(x)L_j^\nu(y)\Big|_{\substack{x=z_1/4\mu^2\eta_- \\ y=z_2/4\mu^2\eta_-}}\right\}.\end{aligned} \tag{7.3}$$

Differentiating eq. 8.976.1 of [Gra07] (the analogue of Mehler's formula), i.e.

$$S(x,y,z) \equiv \sum_{j=0}^{\infty}\frac{j!}{(j+\nu)!}L_j^\nu(x)L_j^\nu(y)z^j = \frac{(xyz)^{-\nu/2}}{1-z}\exp\left(\frac{-z(x+y)}{1-z}\right)I_\nu\left(\frac{2\sqrt{xyz}}{1-z}\right) \tag{7.4}$$

gives us

$$x\frac{\partial S}{\partial x} - y\frac{\partial S}{\partial y} = -\frac{z}{1-z}(x-y)\,S(x,y,z). \tag{7.5}$$

Hence the limit of the kernel as $N \to \infty$ is easily seen to be

$$\begin{aligned}\mathcal{K}^S(z_1, z_2; \mu) &\equiv \lim_{N\to\infty} \mathcal{K}_N(z_1, z_2; \mu) \\ &= \frac{\eta_+^3}{8\pi}(z_1 - z_2)\, e^{-\eta_-(z_1+z_2)}\, (z_1 z_2)^{-\nu/2}\, I_\nu\left(2\eta_+\sqrt{z_1 z_2}\right). \end{aligned} \tag{7.6}$$

When $\mu = 1$, this gives

$$\mathcal{K}^S(z_1, z_2; \mu = 1) = \frac{1}{64\pi}\,(z_1 - z_2)\,(z_1 z_2)^{-\nu/2}\, I_\nu\left(\sqrt{z_1 z_2}\right) \tag{7.7}$$

which is in perfect agreement with eq. (5.37).

7.3 Eigenvalue density

The weight function eq. (3.101) is independent of N, and so we can now write down the densities. For $z \in \mathbb{C}\backslash\mathbb{R}$, we have

$$\begin{aligned} R_1^{\mathbb{C}\,S}(z) = \mathrm{sgn}(\Im\mathrm{m}\ z)(-2i)(z - z^*)\frac{\eta_+^3}{8\pi} I_\nu(2\eta_+|z|) \\ \times\, 2\int_0^\infty \frac{dt}{t} \exp\left\{-\eta_+^2(z^2 + z^{*2})t - \frac{1}{4t}\right\} K_{\frac{\nu}{2}}(2\eta_+^2|z|^2 t)\,\mathrm{erfc}(2\eta_+\sqrt{t}|\Im\mathrm{m}\ z|), \end{aligned} \tag{7.8}$$

and for $x \in \mathbb{R}$, we have

$$R_1^{\mathbb{R}\,S}(x) = \frac{\eta_+^3}{8\pi} 2K_{\frac{\nu}{2}}(\eta_+|x|)\int_{-\infty}^{\infty} dx'\,[\mathrm{sgn}(xx')]^{-\nu/2}|x - x'|\,2K_{\frac{\nu}{2}}(\eta_+|x'|) I_\nu(2\eta_+\sqrt{xx'}). \tag{7.9}$$

Note how the η_--dependent factors have cancelled. As a consequence, the densities at arbitrary μ are related to those at maximal non-Hermiticity ($\mu = 1$) by a simple scaling of the eigenvalues by $2\eta_+$.

We show some plots of the densities of complex and real eigenvalues in Figures 7.1 and 7.2 respectively. The former figure shows the effect on the complex density of changing the topological parameter ν. Essentially, a larger value of ν leads to an increased depletion of the density in the vicinity of the origin; otherwise, little changes. The latter figure shows (left) how the finite-N density converges to the strong limit, and (right) the effect of increasing ν.

We observe that, away from the axes [origin], the densities of the complex [real] Dirac eigenvalues are, essentially, flat. Let us estimate the height of these plateaux. First, consider the function $g^2(z)$, given by eqs. (3.86) and (3.88):

$$g^2(z) = 2\int_0^\infty \frac{dt}{t}\,\exp\left\{-2\eta_+^2(x^2 - y^2)t - \frac{1}{4t}\right\}\, K_{\frac{\nu}{2}}(2\eta_+^2(x^2 + y^2)t)\,\mathrm{erfc}(2\eta_+|y|\sqrt{t}) \tag{7.10}$$

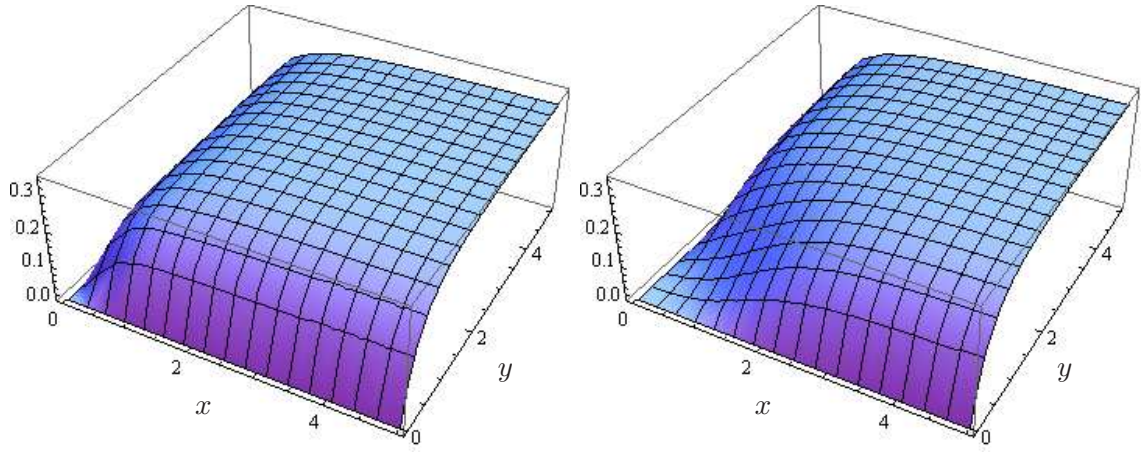

Figure 7.1: The densities of complex Dirac eigenvalues $R^{\mathbb{C}\,S}_{1,\mathrm{Dirac}}(z)$ in the strongly non-Hermitian limit with $\mu = 1$, and $\nu = 0$ (left) and $\nu = 4$ (right).

where $z = x + iy$. For large argument, we can replace the complementary error function with its asymptotic limit

$$\mathrm{erfc}(x) \sim \frac{e^{-x^2}}{\sqrt{\pi}\, x}. \tag{7.11}$$

Therefore, at sufficiently large y, we have

$$g^2(z) \approx \frac{1}{\sqrt{\pi}\,\eta_+|y|} \int_0^\infty \frac{dt}{t^{3/2}} \exp\left\{-2\eta_+^2(x^2+y^2)t - \frac{1}{4t}\right\} K_{\frac{\nu}{2}}(2\eta_+^2(x^2+y^2)t). \tag{7.12}$$

On making a simple change of variables $u = t^{-1}$, we can use eq. 6.654 of [Gra07] to perform the integral exactly, giving

$$g^2(z) \approx \frac{4}{\eta_+|y|} K_\nu\left(2\eta_+|z|\right). \tag{7.13}$$

The complex density in the strongly non-Hermitian limit is therefore

$$\begin{aligned} R_1^{\mathbb{C}\,S}(z) &\approx \frac{2\eta_+^2}{\pi} I_\nu\left(2\eta_+|z|\right) K_\nu\left(2\eta_+|z|\right) \\ &\approx \frac{\eta_+}{2\pi|z|} \end{aligned} \tag{7.14}$$

where we used the large-argument asymptotics for both the I- and K-Bessel functions in the last step. Finally, mapping to Dirac eigenvalues, we have for the density

$$R^{\mathbb{C}\,S}_{1,\mathrm{Dirac}}(z) \approx \frac{2\eta_+}{\pi}, \tag{7.15}$$

sufficiently far away from both the x- and y-axes. This is independent of z, as we observed in the plots.

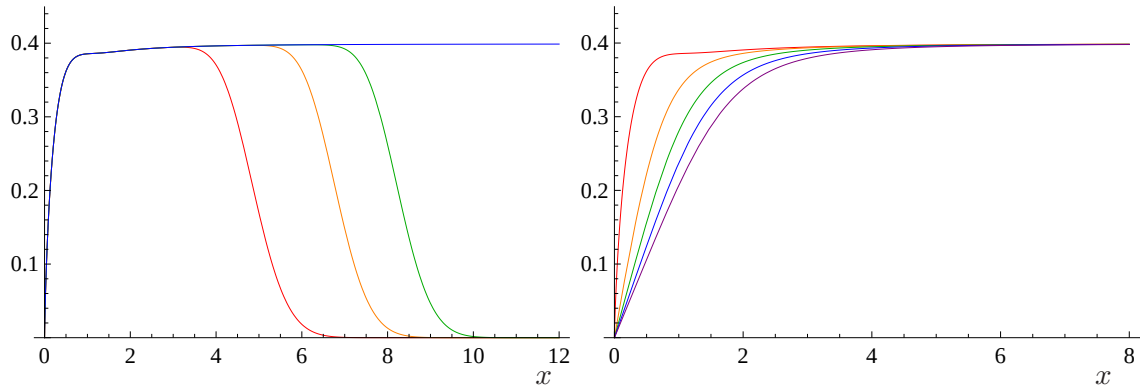

Figure 7.2: Left: The densities of real Dirac eigenvalues $R^{\mathbb{R}}_{1,N,\mathrm{Dirac}}(x)$ at $\mu = 1$ for $N = 10$ (red), $N = 20$ (orange), $N = 30$ (green) and in the strongly non-Hermitian limit $R^{\mathbb{R}\,S}_{1,\mathrm{Dirac}}(x)$ (blue); $\nu = 0$ in all cases. Right: The strongly non-Hermitian limit $R^{\mathbb{R}\,S}_{1,\mathrm{Dirac}}(x)$ at $\mu = 1$ for $\nu = 0$ (red), $\nu = 1$ (orange), $\nu = 2$ (green), $\nu = 3$ (blue) and $\nu = 4$ (purple).

For the density of real eigenvalues, we consider large, positive x in eq. (7.9). The dominant contribution to the integral can be shown to come from the region where $x' \sim x \gg 0$. We can therefore replace the three Bessel functions with their asymptotic forms, and change the lower limit of the integral from $-\infty$ to 0. After a change of variables from x' to $t = \sqrt{x'/x}$, we have

$$R_1^{\mathbb{R}\,S}(x) \approx \frac{\eta_+^{3/2}}{4\sqrt{\pi}} \int_0^\infty dt \, \sqrt{\frac{x}{t}} \, |1 - t^2| \, \exp\left\{-\eta_+ x (1-t)^2\right\}. \tag{7.16}$$

The dominant contribution to the integral is in the region where $t \approx 1$. However, we cannot use the usual saddle point formula, since the factor $|1 - t^2|$ is zero at $t = 1$. (In fact, the integrand has the form of two adjacent (disjoint) peaks, touching at $t = 1$.) However, because the integrand is greatest in the region close to (but not at) $t = 1$, we can make the following approximations (which become more accurate the greater x is): Because the two peaks are approximately the same size, we can integrate over just one of them, and double the result. And close to $t = 1$, we write

$1-t^2 = (1+t)(1-t) \approx 2(1-t)$, and put $\sqrt{t} \approx 1$ in the denominator. This then gives

$$\begin{aligned} R_1^{\mathbb{R}\,S}(x) &\approx \frac{\eta_+^{3/2}}{\sqrt{\pi}} \int_1^\infty dt\, \sqrt{x}\,(t-1)\, \exp\left\{-\eta_+ x(1-t)^2\right\} \\ &= \frac{1}{2}\sqrt{\frac{\eta_+}{\pi x}}\, \Big[-\exp\left\{-\eta_+ x(1-t)^2\right\} \Big]_1^\infty \\ &= \frac{1}{2}\sqrt{\frac{\eta_+}{\pi x}}. \end{aligned} \tag{7.17}$$

The Dirac density is therefore given by

$$R_{1,\mathrm{Dirac}}^{\mathbb{R}\,S}(x) \approx \sqrt{\frac{\eta_+}{\pi}} \tag{7.18}$$

which is independent of x, again in agreement with our observations.

We used eqs. (7.15) and (7.18) in the last chapter, since these are also good proxies for the densities at finite N, when considering the eigenvalues that lie within the approximate supports.

Chapter 8

Quenched densities III: Weakly non-Hermitian microscopic large-N limit

A precise map of RMT to chiral perturbation theory (χPT) can only be made in the epsilon regime, which requires that we rescale the chemical potential with $1/\sqrt{N}$. The resulting ensemble is therefore only weakly non-Hermitian. We also scale the eigenvalues as we would for the Hermitian case, obtaining a microscopic density. The rather surprising fact that we do not just end up with the Hermitian limit, but with a genuinely different limit, was originally discovered for the non-chiral Ginibre ensembles by [Fyo97a; Fyo97b].

However, unlike the cases with Dyson indices $\beta = 2$ and 4, for $\beta = 1$ we have a significant number of both complex and real eigenvalues in the weakly non-Hermitian limit. In fact, we can infer from Efetov's formula eq. (6.26) that the number of real eigenvalues and the number of complex eigenvalues both grow with $\sim N$ at large N, with the ratio of the two tending to some (finite and non-zero) constant.

In this chapter, we find explicit formulas for the densities of complex and real eigenvalues at weak non-Hermiticity where the parameter α will measure the degree of non-Hermiticity. The complex case is straightforward. However, the real case is more subtle; the large-N limit and the integral in the expression for the density do not commute, and so the density cannot be written purely in terms of a weak kernel and a rescaled weight function. This is also true for the Hermitian chGOE.

After we derive the correct solution, we show that the eigenvalue density of the chGOE can be recovered by taking the limit $\alpha \to 0$, an important consistency check.

8.1 Definition of the limit

In the weakly non-Hermitian case, we scale the chemical potential μ and the Dirac eigenvalue z with N as follows

$$\mu = \frac{\alpha}{\sqrt{2N}} \qquad \text{and} \qquad z = \frac{\hat{z}}{2\sqrt{N}}, \tag{8.1}$$

where the eigenvalue scaling is given with respect to the finite-N case in §6.1. For the densities of the Wishart (squared Dirac) eigenvalues, the weakly non-Hermitian limits are given by

$$\begin{aligned} R_1^{\mathbb{C}\,W}(z;\alpha) &\equiv \lim_{N\to\infty} \frac{1}{(4N)^2}\, R_{1,N}^{\mathbb{C}}\left(\frac{z}{4N}; \mu = \frac{\alpha}{\sqrt{2N}}\right), \\ R_1^{\mathbb{R}\,W}(x;\alpha) &\equiv \lim_{N\to\infty} \frac{1}{4N}\, R_{1,N}^{\mathbb{R}}\left(\frac{x}{4N}; \mu = \frac{\alpha}{\sqrt{2N}}\right). \end{aligned} \tag{8.2}$$

8.2 Complex eigenvalue density

So, for the complex case $z \in \mathbb{C}\backslash\mathbb{R}$, we have

$$R_1^{\mathbb{C}\,W}(z;\alpha) = -2i\,\mathrm{sgn}(\Im\mathrm{m}\, z) \lim_{N\to\infty} \left[\frac{1}{(4N)^2}\mathcal{K}_N\left(\frac{z}{4N}, \frac{z^*}{4N}\right) w\left(\frac{z^*}{4N}\right) w\left(\frac{z}{4N}\right)\right], \tag{8.3}$$

with the finite-N kernel from eq. (5.42) and the weight $w(z)$ from eq. (3.101). If we want to consider well-defined large-N limits of the kernel and the weight function separately, then we must make a split as follows:

$$R_1^{\mathbb{C}\,W}(z;\alpha) = -2i\,\mathrm{sgn}(\Im\mathrm{m}\, z)\, \mathcal{K}^W(z, z^*)\mathcal{W}(z, z^*) \tag{8.4}$$

in which we have defined the weak kernel and weight function as

$$\mathcal{K}^W(u,v) \equiv \lim_{N\to\infty} \left[\frac{1}{(4N)^2}\left(\frac{uv}{(4N)^2}\right)^{\nu/2} \mathcal{K}_N\left(\frac{u}{4N}, \frac{v}{4N}\right)\right], \tag{8.5}$$

$$\begin{aligned} \mathcal{W}(z, z^*) &\equiv \lim_{N\to\infty} \left[\left(\frac{(4N)^2}{zz^*}\right)^{\nu/2} w\left(\frac{z}{4N}\right) w\left(\frac{z^*}{4N}\right)\right] \\ &= \lim_{N\to\infty} \left[\exp\left[\frac{\eta_-(z+z^*)}{4N}\right] g\left(\frac{z}{4N}, \frac{z^*}{4N}\right)\right], \end{aligned} \tag{8.6}$$

and $g(z, z^*)$ is given in eq. (3.86). It must be remembered that μ also now depends on N through eq. (8.1) and that $\mathcal{K}_N(u,v)$ and $w(u)$ depend on μ.

We only need to evaluate the weight function $\mathcal{W}(z, z^*)$ for arguments which are complex conjugates of each other, which we shall do in §8.2.2; however, since we will need to use the weak kernel $\mathcal{K}^W(u,v)$ in the calculation of the real density in §8.3, we will evaluate it for arbitrary arguments in the next part.

8.2.1 Weak kernel

To determine the weak kernel, it is somewhat simpler if we first rewrite the finite-N kernel eq. (5.42) so that the generalised Laguerre polynomials are of the same degree. We use

$$nL_n^\nu(x) = (n+\nu)L_{n-1}^\nu(x) - xL_{n-1}^{\nu+1}(x) \tag{8.7}$$

(eq. 8.971.2 of [Gra07]) to show that

$$\begin{aligned}(n+1)\left\{L_{n+1}^\nu(u)\,L_n^\nu(v) - (u\leftrightarrow v)\right\} &= \left((n+1+\nu)L_n^\nu(u) - uL_n^{\nu+1}(u)\right)\,L_n^\nu(v) - (u\leftrightarrow v)\\ &= vL_n^{\nu+1}(v)\,L_n^\nu(u) - (u\leftrightarrow v).\end{aligned} \tag{8.8}$$

The finite-N kernel eq. (5.42) then becomes

$$\begin{aligned}\mathcal{K}_N(u,v) = \frac{1}{8\pi(4\mu^2\eta_+)^{\nu+1}4\mu^2}\sum_{j=0}^{N-2}\left(\frac{\eta_-}{\eta_+}\right)^{2j}\frac{j!}{(j+\nu)!}\\ \times\left\{uL_j^{\nu+1}\left(\frac{u}{4\mu^2\eta_-}\right)L_j^\nu\left(\frac{v}{4\mu^2\eta_-}\right) - (u\leftrightarrow v)\right\}.\end{aligned} \tag{8.9}$$

In the large-N limit, we will replace the sum with an integral over the variable $t \equiv \frac{j}{N} \in [0,1]$. We have several parts to consider; in each case, we take $N\to\infty$ for fixed t (and not for fixed j). The following are quite straightforward:

$$\lim_{N\to\infty}\sum_{j=0}^{N-2}\frac{1}{N} = \int_0^1 dt, \tag{8.10}$$

$$\lim_{\substack{N\to\infty\\ j=[tN]}}\left(\frac{1-\frac{\alpha^2}{2N}}{1+\frac{\alpha^2}{2N}}\right)^{2j} = \exp[-2\alpha^2 t], \tag{8.11}$$

$$\lim_{\substack{N\to\infty\\ j=[tN]}}\frac{j!}{(j+\nu)!}\,N^\nu = t^{-\nu}, \tag{8.12}$$

where $[x]$ denotes the integer part of x. For the limit of the Laguerre polynomials, we have that, from eq. 8.978.2 of [Gra07],

$$\lim_{N\to\infty}\left[N^{-\nu}\,L_N^\nu\left(\frac{x}{N}\right)\right] = x^{-\nu/2}\,J_\nu(2\sqrt{x}), \tag{8.13}$$

where ν is some real constant. Now, we choose some fixed $t\in[0,1]$. Then

$$\begin{aligned}\lim_{N\to\infty}\left[N^{-\nu}\,L_{[tN]}^\nu\left(\frac{x}{N}\right)\right] &= t^\nu\lim_{N\to\infty}\left[([tN])^{-\nu}\,L_{[tN]}^\nu\left(\frac{xt}{[tN]}\right)\right]\\ &= t^\nu(xt)^{-\nu/2}\,J_\nu(2\sqrt{xt})\\ &= t^{\nu/2}x^{-\nu/2}\,J_\nu(2\sqrt{xt}).\end{aligned} \tag{8.14}$$

Therefore,

$$\lim_{\substack{N\to\infty \\ j=[tN]}} \frac{1}{N^{\nu+1}} L_j^{\nu+1}\left(\frac{x}{4N(1-\frac{\alpha^2}{2N})}\right) = \lim_{N\to\infty} \frac{1}{N^{\nu+1}} L_{[tN]}^{\nu+1}\left(\frac{x}{4N}\right)$$
$$= \left(\frac{2\sqrt{t}}{\sqrt{x}}\right)^{\nu+1} J_{\nu+1}(\sqrt{xt}). \tag{8.15}$$

On assembling all the components, and after changing variables to $s = \sqrt{t}$, we have the weak kernel

$$\mathcal{K}^W(u,v) = \frac{1}{256\pi\alpha^2} \int_0^1 ds\, s^2\, e^{-2\alpha^2 s^2} \{\sqrt{u} J_{\nu+1}(s\sqrt{u}) J_\nu(s\sqrt{v}) - (u \leftrightarrow v)\}, \tag{8.16}$$

which cannot be simplified any further analytically.

8.2.2 Weight and density

It is straightforward to determine that the large-N limit of the weight function defined in eq. (8.6) under the scalings eq. (8.1) is

$$\mathcal{W}(z,z^*) = \exp\left[\frac{1}{8\alpha^2}\, 2\Re\mathrm{e}\, z\right]$$
$$\times\, 2\int_0^\infty \frac{dt}{t}\, \exp\left[-\frac{t}{64\alpha^4}(z^2+z^{*2}) - \frac{1}{4t}\right] K_{\frac{\nu}{2}}\left(\frac{t}{32\alpha^4}|z|^2\right) \operatorname{erfc}\left(\frac{\sqrt{t}}{4\alpha^2}|\Im\mathrm{m}\, z|\right), \tag{8.17}$$

and so we can immediately write down the density of complex eigenvalues ($z \in \mathbb{C}\backslash\mathbb{R}$) at weak non-Hermiticity from eq. (8.4) as

$$R_1^{\mathbb{C}\,W}(z) = -2i\,\mathrm{sgn}(\Im\mathrm{m}\, z) \exp\left[\frac{1}{8\alpha^2}\, 2\Re\mathrm{e}\, z\right]$$
$$\times\, 2\int_0^\infty \frac{dt}{t}\, \exp\left[-\frac{t}{64\alpha^4}(z^2+z^{*2}) - \frac{1}{4t}\right] K_{\frac{\nu}{2}}\left(\frac{t}{32\alpha^4}|z|^2\right) \operatorname{erfc}\left(\frac{\sqrt{t}}{4\alpha^2}|\Im\mathrm{m}\, z|\right)$$
$$\times \frac{1}{256\pi\alpha^2} \int_0^1 ds\, s^2\, e^{-2\alpha^2 s^2} \{\sqrt{z} J_{\nu+1}(s\sqrt{z}) J_\nu(s\sqrt{z^*}) - \text{c.c.}\}. \tag{8.18}$$

In Figure 8.1, we plot the density of complex Dirac eigenvalues for various values of the non-Hermiticity parameter α. The complex eigenvalues are seen to lie (predominantly) in a strip parallel to the real axis. We can estimate the width of this strip as follows. For the finite-N case, we know that the complex eigenvalues lie approximately in an ellipse whose axis on the imaginary axis has (half-)length given by eq. (6.31). Using this result, it is easy to show that, under the weak scaling eq.

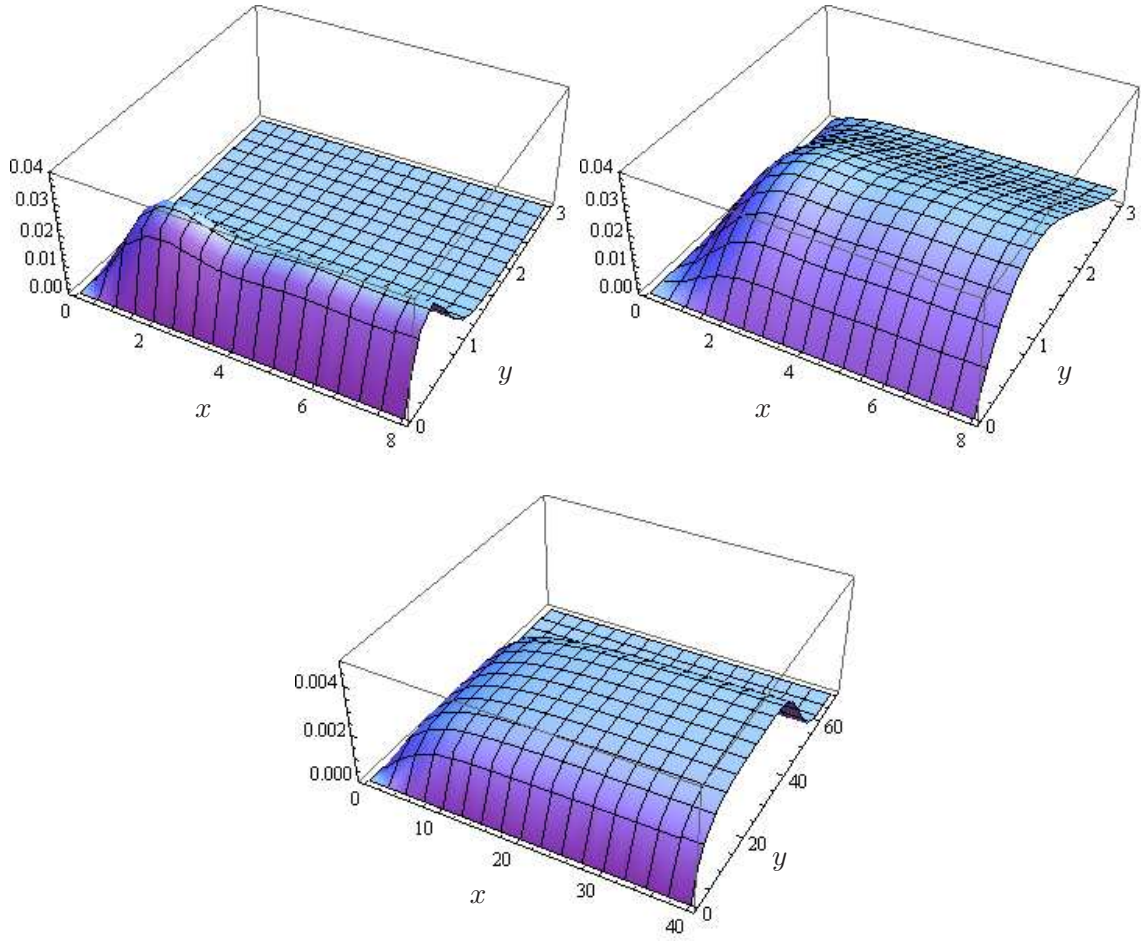

Figure 8.1: Densities of complex Dirac eigenvalues $R^{\mathbb{C}W}_{1,\mathrm{Dirac}}(z)$ in the weakly non-Hermitian limit, for $\alpha = \sqrt{0.2}$ (top, left), $\alpha = 1$ (top, right) and $\alpha = 5$ (bottom); $\nu = 0$ in all cases.

(8.1), the (half-)width of the strip of eigenvalues is $2\alpha^2$. When we say half-width, we mean that the strip is between $-2\alpha^2 i$ and $+2\alpha^2 i$, so the full width is actually $4\alpha^2$. We caution that the strip evidently does not have a sharp edge (indeed, strictly speaking, it has no edge at all), and so this width is only an approximate indicator of the edge of the 'support' of the complex eigenvalues.

8.2.3 Limiting cases

8.2.3.1 Hermitian limit ($\alpha \to 0$)

As $\alpha \to 0$, the height of the density function of complex eigenvalues tends to zero. We demonstrate this numerically in Figure 8.2, where we take a cross-section through

the density of complex eigenvalues at fixed $x = 6$, where x is chosen sufficiently large that the cross-section becomes essentially x-independent for the range of α considered.

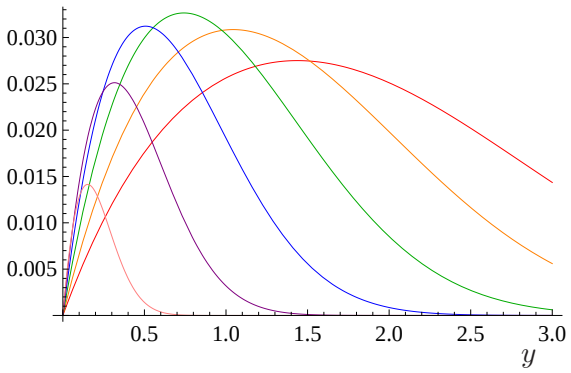

Figure 8.2: Cross-sections at $x = 6$ through the density of complex Dirac eigenvalues $R^{\mathbb{C}W}_{1,\text{Dirac}}(6 + iy)$ at weak non-Hermiticity, for $\alpha = 1.2$ (red), $\alpha = 1$ (orange), $\alpha = 0.8$ (green), $\alpha = 0.6$ (blue), $\alpha = 0.4$ (purple) and $\alpha = 0.2$ (pink); $\nu = 0$ in all cases.

8.2.3.2 Strongly non-Hermitian limit ($\alpha \to \infty$)

We now show that we can retrieve the strongly non-Hermitian microscopic density derived in §7.3 by taking the limit $\alpha \to \infty$ and suitably rescaling the eigenvalues. We begin with the weak kernel eq. (8.16). Using eq. 8.472.2 of [Gra07], we have

$$\mathcal{K}^W(u,v) = \frac{1}{128\pi\alpha^2}\left(v\frac{\partial}{\partial v} - u\frac{\partial}{\partial u}\right)\int_0^1 ds\, s\, e^{-2\alpha^2 s^2} J_\nu(s\sqrt{u})J_\nu(s\sqrt{v}). \tag{8.19}$$

We now define the following scaling of the weak kernel

$$\begin{aligned}
\mathcal{K}^+(z_1,z_2) &\equiv \lim_{\alpha\to\infty}(8\eta_+\alpha^2)^2\,\mathcal{K}^W(8\eta_+\alpha^2 z_1, 8\eta_+\alpha^2 z_2)\\
&= \frac{\eta_+^2}{2\pi}\lim_{\alpha\to\infty}\alpha^2\left(z_2\frac{\partial}{\partial z_2} - z_1\frac{\partial}{\partial z_1}\right)\int_0^1 ds\, s\, e^{-2\alpha^2 s^2}\, J_\nu(2\sqrt{2\eta_+}\alpha\sqrt{z_1}s)J_\nu(2\sqrt{2\eta_+}\alpha\sqrt{z_2}s)\\
&= \frac{\eta_+^2}{4\pi}\left(z_2\frac{\partial}{\partial z_2} - z_1\frac{\partial}{\partial z_1}\right)\lim_{\alpha\to\infty}\int_0^{\sqrt{2}\alpha} dt\, t\, e^{-t^2} J_\nu(2\sqrt{\eta_+ z_1}t)J_\nu(2\sqrt{\eta_+ z_2}t)\\
&= \frac{\eta_+^3}{8\pi}(z_1 - z_2)e^{-\eta_+(z_1+z_2)}I_\nu(2\eta_+\sqrt{z_1 z_2}),
\end{aligned} \tag{8.20}$$

where we used eq. 6.633.2 of [Gra07] to do the integral, and then we performed the two partial differentials and simplified the result. This is an exact result, although

note that $\mathcal{K}^+(z_1, z_2)$ is not the same as the strong kernel in eq. (7.6): Apart from the (minor) fact that we defined it not to include the factor $(z_1 z_2)^{-\nu/2}$, more significant is the fact that there is an η_+ in the exponent, and not an η_-. We now take the limit $\alpha \to \infty$ of the weight function eq. (8.17) with the same rescaling of eigenvalues as for the kernel:

$$\begin{aligned}\mathcal{W}^+(z, z^*) &\equiv \lim_{\alpha\to\infty} \mathcal{W}(8\eta_+\alpha^2 z, 8\eta_+\alpha^2 z^*) \\ &= \exp\{2\eta_+ \,\Re\mathrm{e}\, z\} \\ &\qquad \times 2\int_0^\infty \frac{dt}{t} \exp\left\{-\eta_+^2(z^2 + z^{*2})t - \frac{1}{4t}\right\} K_{\frac{\nu}{2}}(2\eta_+^2|z|^2 t)\,\mathrm{erfc}(2\eta_+\sqrt{t}|\Im\mathrm{m}\, z|).\end{aligned} \tag{8.21}$$

Combining eqs. (8.20) and (8.21) to obtain the limit of the density at large α, we find

$$\begin{aligned}\lim_{\alpha\to\infty}\left[(8\eta_+\alpha^2)^2\, R_1^{\mathbb{C}\,W}(8\eta_+\alpha^2 z)\right] &= -2i\,\mathrm{sgn}(\Im\mathrm{m}\, z)\mathcal{K}^+(z, z^*)\mathcal{W}^+(z, z^*) \\ &= R_1^{\mathbb{C}\,S}(z) \quad \text{at } \eta_+.\end{aligned} \tag{8.22}$$

So, although we cannot reconstruct either the strong kernel or the strong weight function individually from the weakly non-Hermitian limit, it turns out that we *can* obtain the density of complex eigenvalues at strong non-Hermiticity, for arbitrary μ.

From numerical investigations, we observe that convergence in eq. (8.22) is quite fast for moderately large α and when the Dirac eigenvalue $\sqrt{z}$ lies well within the strip determined in §8.2.2. So in practice the weakly non-Hermitian density may be described quite well by the formulas for the strongly non-Hermitian density under these circumstances.

8.2.4 Weak kernel revisited

We now investigate the behaviour of the weakly non-Hermitian kernel in some more detail. The results from this section will be needed in the next chapter when we come to investigate the behaviour of the unquenched ensembles at weak non-Hermiticity. They can also be used, for example, to understand the width of the strip of complex eigenvalues, and the probability of finding complex eigenvalues outside the strip.

Our aim is to find approximations for the weak kernel, to clarify precisely when these approximations are valid and to investigate how accurate they are likely to

be. We already determined a limit for the weak kernel in the limit $\alpha \to \infty$ for fixed arguments (see §8.2.3.2). Here, we look at the same problem from a different perspective, and consider α fixed and investigate the kernel for various arguments. Our approach is perhaps a little less rigorous than before, but the insights that we gain are deeper.

Let us recall the weak kernel from eq. (8.16)

$$\mathcal{K}^W(u,v) = \frac{1}{256\pi\alpha^2}\int_0^1 ds\, s^2\, e^{-2\alpha^2 s^2}\{\sqrt{u}J_{\nu+1}(s\sqrt{u})J_\nu(s\sqrt{v}) - (u \leftrightarrow v)\}.$$

We write this for Dirac eigenvalues on the positive, imaginary axis ($u, v > 0$):

$$\mathcal{K}^W\big((iu)^2,(iv)^2\big) = \frac{1}{256\pi\alpha^2}\int_0^1 ds\, s^2\, e^{-2\alpha^2 s^2}\{iuJ_{\nu+1}(isu)J_\nu(isv) - (u \leftrightarrow v)\}. \tag{8.23}$$

It is perhaps clearer if we switch to modified Bessel functions using eq. 8.406.3 of [Gra07]

$$J_\nu(iz) = i^\nu\, I_\nu(z), \tag{8.24}$$

and furthermore assume that the dominant contribution to the integral comes from a region where we can use the asymptotic form

$$I_\nu(z) \sim \frac{e^z}{\sqrt{2\pi z}} \tag{8.25}$$

as a reasonable approximation. This then gives

$$\mathcal{K}^W\big((iu)^2,(iv)^2\big) \approx \frac{(-1)^{\nu+1}}{2\pi}\,\frac{1}{256\pi\alpha^2}\,\frac{u-v}{\sqrt{uv}}\int_0^1 ds\, s\, e^{-2\alpha^2 s^2} e^{s(u+v)}. \tag{8.26}$$

We now change variables to $t = 2\alpha^2 s$, and complete the square in the exponent, giving

$$\mathcal{K}^W\big((iu)^2,(iv)^2\big) \approx \frac{(-1)^{\nu+1}}{2048\pi^2\alpha^6}\,\frac{u-v}{\sqrt{uv}}\, e^{\gamma^2/2\alpha^2}\int_0^{2\alpha^2} dt\, t\, \exp\left\{-\frac{(t-\gamma)^2}{2\alpha^2}\right\}, \tag{8.27}$$

where we have defined $\gamma \equiv \frac{u+v}{2}$ to be the average of the two (Dirac) arguments. We note that the integration domain depends on the square of α, but the Gaussian part of the integrand has a width which is $\sim \alpha$. We show this schematically in Figure 8.3 for α sufficiently large.

Let us now consider the first of two regimes: For $k\alpha < \gamma < 2\alpha^2 - k\alpha$, where k is some constant $\mathcal{O}(1)$ (for practical purposes, one could take k to be a low integer, perhaps 2 or 3), we can argue that the Gaussian peak is almost completely contained

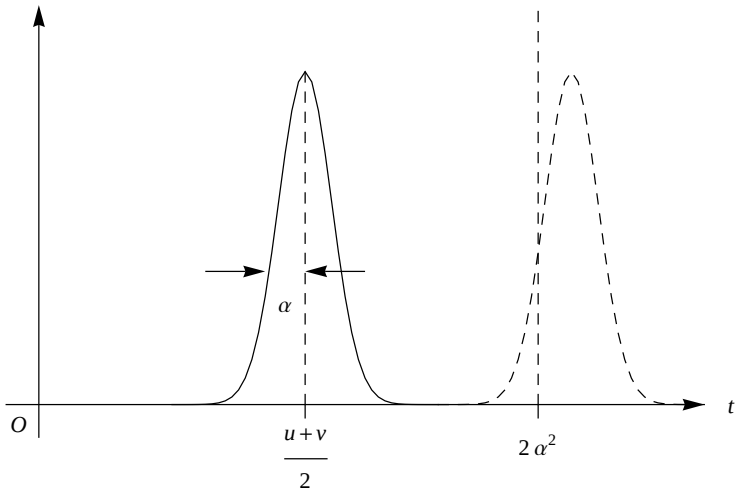

Figure 8.3: Schematic plot of the integrand of the weak kernel.

within the integration region (the solid peak in Figure 8.3). For such a regime to exist, we require $\alpha > k$. Therefore, we can switch the integration limits from $[0, 2\alpha^2]$ to $(-\infty, \infty)$ without losing much accuracy, and replace the t in the integrand with its value at the centre of the peak (i.e. γ). We then integrate over the Gaussian, to give

$$\mathcal{K}^W\big((iu)^2, (iv)^2\big) \approx \frac{(-1)^{\nu+1}}{2048\pi\alpha^5\sqrt{2\pi}} \frac{(u^2-v^2)}{\sqrt{uv}} \exp\left\{\frac{(u+v)^2}{8\alpha^2}\right\} \tag{8.28}$$

$$= \frac{(-1)^{\nu+1}}{2048\pi\alpha^5} (u^2-v^2)\, e^{(u^2+v^2)/8\alpha^2} \frac{e^{uv/4\alpha^2}}{\sqrt{2\pi uv}}$$

$$\approx \frac{(-1)^{\nu+1}}{4096\pi\alpha^6} (u^2-v^2)\, e^{(u^2+v^2)/8\alpha^2} I_\nu\left(\frac{uv}{4\alpha^2}\right). \tag{8.29}$$

This final form eq. (8.29) is given to show consistency with eq. (8.20), although eq. (8.28) will suffice in the following.

The second regime of interest is where $\gamma > 2\alpha^2 + k\alpha$, where k was discussed earlier. In this regime, the peak lies predominantly outside the integration region (the dashed peak in Figure 8.3). But rather than approximating the integral as zero, we wish to capture the tail that still lies inside the integration domain, and so will proceed as follows. The t in the integrand of eq. (8.27) can be replaced with its value at the edge of the integration domain (i.e. $2\alpha^2$). The integral is then equivalent to a complementary error function, which in turn we approximate with its asymptotic

limit, to give

$$\mathcal{K}^W\big((iu)^2,(iv)^2\big) \approx \frac{(-1)^{\nu+1}}{1024\pi^2\alpha^2}\,\frac{u-v}{\sqrt{uv}}\left[\frac{u+v}{2}-2\alpha^2\right]^{-1}\exp\left\{-2\alpha^2+u+v\right\} \tag{8.30}$$

$$= \frac{(-1)^{\nu+1}}{512\pi\alpha^2}\,(u-v)\left[\frac{u+v}{2}-2\alpha^2\right]^{-1} e^{-2\alpha^2}\frac{e^u}{\sqrt{2\pi u}}\,\frac{e^v}{\sqrt{2\pi v}}$$

$$\approx \frac{(-1)^{\nu+1}}{512\pi\alpha^2}\,(u-v)\left[\frac{u+v}{2}-2\alpha^2\right]^{-1} e^{-2\alpha^2} I_\nu(u) I_\nu(v). \tag{8.31}$$

(Note, incidentally, that if u, say, is taken to be very large whilst keeping v fixed, then

$$(u-v)\left[\frac{u+v}{2}-2\alpha^2\right]^{-1} \to 2, \tag{8.32}$$

and so the kernel is seen to factorise completely into the product of a u-dependent part and a v-dependent part.)

What is significant is that both approximations eqs. (8.28) and (8.30) would appear to be very good in their respective domains, and, compared with the width of the unquenched strip, $2\alpha^2$, the crossover region (where neither approximation is so good) is quite small, being only $\sim\mathcal{O}(\alpha)$.

Although we do not give details and proofs, we argue that the previous two approximations can also be extended to the more general case when the arguments of $\mathcal{K}^W(w,z)$ are no longer real and negative, although one must be particularly careful to handle the square root signs correctly (this can sometimes result in sign flips in the exponents). For example, one can show that, when the arguments are complex conjugates, then the kernel inside the strip has the behaviour

$$\mathcal{K}^W(z,z^*) \approx \frac{1}{2048\pi\alpha^5\sqrt{2\pi}}\,\frac{2iy}{\sqrt{|z|}}\,\exp\left\{\frac{-x+|z|}{4\alpha^2}\right\} \tag{8.33}$$

or equivalently in Dirac eigenvalues as

$$\mathcal{K}^W(z^2,z^{*2}) \approx \frac{1}{2048\pi\alpha^5\sqrt{2\pi}}\,\frac{4ixy}{\sqrt{x^2+y^2}}\,\exp\left\{\frac{y^2}{2\alpha^2}\right\}. \tag{8.34}$$

We have written $x\equiv\Re\mathrm{e}\,z$ and $y\equiv\Im\mathrm{m}\,z$. The weak weight function eq. (8.17) has the following approximate behaviour almost everywhere (both inside and outside the strip, except close to the axes), as can be established by using the large-argument approximation for eq. (7.13) under weak scaling:

$$\mathcal{W}(z,z^*) \approx \frac{32\sqrt{2\pi}\,\alpha^3}{|y|\,\sqrt{|z|}}\,\exp\left\{\frac{x-|z|}{4\alpha^2}\right\} \tag{8.35}$$

or in Dirac eigenvalues

$$\mathcal{W}(z^2, z^{*2}) \approx \frac{16\sqrt{2\pi}\,\alpha^3}{|xy|\,\sqrt{x^2+y^2}} \exp\left\{-\frac{y^2}{2\alpha^2}\right\}. \tag{8.36}$$

Hence, one can calculate the eigenvalue density within the strip as

$$\begin{aligned} R^{\mathbb{C}\,W}_{1,\mathrm{Dirac}}(z) &= 4\,|z|^2\,\{\,-2i\,\mathcal{K}^W(z^2, z^{*2})\mathcal{W}(z^2, z^{*2})\,\mathrm{sgn}(\Im\mathrm{m}\,z^2)\} \\ &\approx \frac{1}{4\pi\alpha^2}. \end{aligned} \tag{8.37}$$

We define the following scaling of the eigenvalues

$$\rho^{\mathbb{C}\,W}_{1,\mathrm{Dirac}}(z) \equiv 2\alpha^2\, R^{\mathbb{C}\,W}_{1,\mathrm{Dirac}}(2\alpha^2 z), \tag{8.38}$$

and in Figure 8.4 we show cross-sections through the strip of this scaled function for a sequence of increasing α; it is highly probable that the profile is converging to a step function of width 1, and of height $\frac{1}{2\pi}$, exactly as predicted from our discussion of the strip width in §8.2.2 and from eq. (8.37).

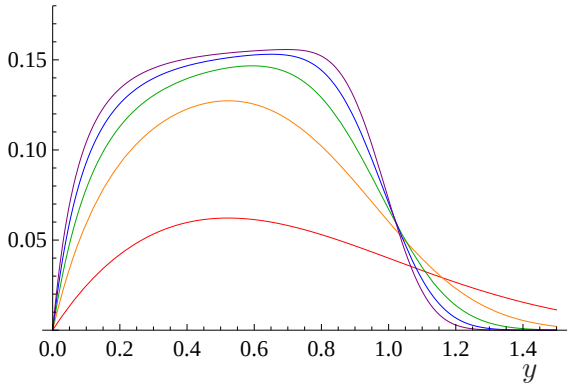

Figure 8.4: Cross-sections at $x = 3$ through the scaled density of complex Dirac eigenvalues $\rho^{\mathbb{C}\,W}_{1,\mathrm{Dirac}}(3+iy)$ at weak non-Hermiticity, for $\alpha = 1$ (red), $\alpha = 2$ (orange), $\alpha = 3$ (green), $\alpha = 4$ (blue) and $\alpha = 5$ (purple); $\nu = 0$ in all cases.

We clarify the difference between the earlier Figure 8.2 and Figure 8.4. The former shows behaviour at low α (roughly $\alpha \leq 1$), where the density profile decreases as α tends to zero. The latter shows behaviour at higher α (roughly $\alpha \geq 1$), where the density profile also tends to zero, but as α tends to infinity (although we have rescaled the vertical axis here to demonstrate the existence of a non-zero limit).

What will be of most interest to us in the next chapter is the behaviour of the exponential parts of eqs. (8.28) and (8.30), which will be much more significant than the constant and polynomial (etc.) factors. We therefore write simply

$$\mathcal{K}^W\big((iu)^2,(iv)^2\big) = \begin{cases} p_1(u,v)\exp\left\{\dfrac{(u+v)^2}{8\alpha^2}\right\} & \text{for } u+v<4\alpha^2, \\ p_2(u,v)\exp\left\{u+v-2\alpha^2\right\} & \text{for } u+v\geq 4\alpha^2, \end{cases} \tag{8.39}$$

where $p_{1,2}(u,v)$ grow more slowly than exponential. Because the exponent (and, indeed, its derivative as well) is actually continuous at the crossover point $u+v=4\alpha^2$, we have removed the k-dependency for the two regions of validity, giving a function that is defined everywhere.

Of course, the change of behaviour of the logarithm of the kernel beyond the strip edge (essentially from square to linear behaviour), together with the fact that the logarithm of the weight function eq. (8.36) is negative square everywhere, explains why the density is exponentially suppressed beyond the strip edge (the decaying weight function dominates).

8.3 Real eigenvalue density

For the weakly non-Hermitian limit of the density of real eigenvalues, we can write from eq. (8.2)

$$\begin{aligned} R_1^{\mathbb{R}\,W}(x;\alpha) &= \lim_{N\to\infty}\frac{1}{4N}\int_{-\infty}^{\infty} dy\,\mathcal{K}_N\left(\frac{x}{4N},y;\frac{\alpha}{\sqrt{2N}}\right) w\left(\frac{x}{4N}\right) w(y)\,\mathrm{sgn}\left(\frac{x}{4N}-y\right) \\ &= \lim_{N\to\infty}\frac{1}{(4N)^2}\,w\left(\frac{x}{4N}\right)\int_{-\infty}^{\infty} dy\,\mathcal{K}_N\left(\frac{x}{4N},\frac{y}{4N};\frac{\alpha}{\sqrt{2N}}\right) w\left(\frac{y}{4N}\right)\mathrm{sgn}(x-y) \end{aligned} \tag{8.40}$$

where $\mathcal{K}_N(x,y;\mu)$ is the finite-N kernel from eq. (5.42). However, in this case, we cannot switch the limiting process and the integral, and so we cannot express the density $R_1^{\mathbb{R}\,W}(x;\alpha)$ as an integral over the weak kernel and the limit of the weight function.

Recall that from eq. (4.76)

$$R_{1,N}^{\mathbb{R}}(x;\mu) = -\,G_N(x,x;\mu) \qquad \text{for } x\in\mathbb{R}, \tag{8.41}$$

where $G_N(x,x')$ was originally defined in eq. (4.51). In the next chapter, we will actually need the weak limit of $G_N(x,x';\mu)$ for $x\neq x'$, and so it makes sense to

determine this slightly more general limit here. The weakly non-Hermitian large-N limit is given by

$$\begin{aligned} G^W(x,x';\alpha) &\equiv \lim_{N\to\infty} \frac{1}{4N}\,\frac{x^{\nu/2}}{(x')^{\nu/2}}\,G_N\left(\frac{x}{4N},\frac{x'}{4N};\frac{\alpha}{\sqrt{2N}}\right) \\ &= -\lim_{N\to\infty}\frac{1}{(4N)^2}\,\frac{x^{\nu/2}}{(x')^{\nu/2}}\,w\left(\frac{x'}{4N}\right)\int_{-\infty}^{\infty} dy\,\mathcal{K}_N\left(\frac{x}{4N},\frac{y}{4N};\frac{\alpha}{\sqrt{2N}}\right) w\left(\frac{y}{4N}\right)\mathrm{sgn}(x'-y) \\ &= -\frac{\hat{h}(x')}{[\mathrm{sgn}(x')]^{\nu/2}}\lim_{N\to\infty}\frac{1}{(4N)^2}\left(\frac{x}{4N}\right)^{\nu/2}\int_{-\infty}^{\infty} dy\,\mathcal{K}_N\left(\frac{x}{4N},\frac{y}{4N};\frac{\alpha}{\sqrt{2N}}\right) w\left(\frac{y}{4N}\right)\mathrm{sgn}(x'-y), \end{aligned} \tag{8.42}$$

where the scaled real weight function is given by

$$\hat{h}(x) \equiv \lim_{N\to\infty}\left|\frac{4N}{x}\right|^{\nu/2} w\left(\frac{x}{4N}\right) = e^{x/8\alpha^2}\,2K_{\frac{\nu}{2}}\left(\frac{|x|}{8\alpha^2}\right). \tag{8.43}$$

We handle the sign function by using the fact that

$$\int_{-\infty}^{\infty} dy\;\mathrm{sgn}(x'-y)\,f(y) = \left(\int_{-\infty}^{0} dy + 2\int_{0}^{x'} dy - \int_{0}^{\infty} dy\right) f(y), \tag{8.44}$$

and so we can correspondingly write $G^W(x,x';\alpha)$ as the sum of three parts:

$$G^W(x,x';\alpha) = -\frac{\hat{h}(x')}{[\mathrm{sgn}(x')]^{\nu/2}}\Big[A(x;\alpha) + 2B(x,x';\alpha) - C(x;\alpha)\Big]. \tag{8.45}$$

For A and B, we find that actually it *is* possible to interchange the limit and the integral without problem, and so we have simply

$$A(x;\alpha) = (-i)^{\nu}\int_{-\infty}^{0} dy\,\mathcal{K}^W(x,y)\hat{h}(y), \tag{8.46}$$

$$B(x,x';\alpha) = \frac{1}{[\mathrm{sgn}(x')]^{\nu/2}}\int_{0}^{x'} dy\,\mathcal{K}^W(x,y)\hat{h}(y), \tag{8.47}$$

where the weak kernel was given in eq. (8.16). The main problem is then reduced to determining the third term $C(x;\alpha)$, where the non-commutativity issue remains. Using some semi-rigorous analytic methods, we will now determine a suitable expression for $C(x;\alpha)$.

8.3.1 Solution for $C(x;\alpha)$

8.3.1.1 Initial manipulation

Inserting the explicit form of the finite-N kernel from eq. (8.9), we have

$$C(x;\alpha) = \frac{x^{\nu/2}}{32\pi\alpha^2}\lim_{N\to\infty} D_N(x;\alpha), \tag{8.48}$$

where

$$D_N(x;\alpha) \equiv \frac{1}{(4N)^{2+\nu}} \int_0^\infty dy\, \exp\left(\frac{(1-\frac{\alpha^2}{2N})y}{8\alpha^2}\right) K_{\frac{\nu}{2}}\left(\frac{(1+\frac{\alpha^2}{2N})y}{8\alpha^2}\right) y^{\nu/2} \times \sum_{j=0}^{N-2} \left(\frac{1-\frac{\alpha^2}{2N}}{1+\frac{\alpha^2}{2N}}\right)^{2j} \frac{j!}{(j+\nu)!} \times \left\{ x\, L_j^{\nu+1}\left(\frac{x}{4N(1-\frac{\alpha^2}{2N})}\right) L_j^\nu\left(\frac{y}{4N(1-\frac{\alpha^2}{2N})}\right) - (x \leftrightarrow y) \right\}. \tag{8.49}$$

Since N is finite, we can switch the integral and the sum. We will also split the two terms in the curly brackets, writing $D_N(x;\alpha) = D_N^+(x;\alpha) - D_N^-(x;\alpha)$, where

$$D_N^+(x;\alpha) \equiv \frac{1}{(4N)^{2+\nu}} \sum_{j=0}^{N-2} \left(\frac{1-\frac{\alpha^2}{2N}}{1+\frac{\alpha^2}{2N}}\right)^{2j} \frac{j!}{(j+\nu)!}\, x\, L_j^{\nu+1}\left(\frac{x}{4N(1-\frac{\alpha^2}{2N})}\right) P(j,N,\alpha) \tag{8.50}$$

with

$$P(j,N,\alpha) \equiv \int_0^\infty dy\, \exp\left(\frac{(1-\frac{\alpha^2}{2N})y}{8\alpha^2}\right) K_{\frac{\nu}{2}}\left(\frac{(1+\frac{\alpha^2}{2N})y}{8\alpha^2}\right) L_j^\nu\left(\frac{y}{4N(1-\frac{\alpha^2}{2N})}\right) y^{\nu/2}, \tag{8.51}$$

and

$$D_N^-(x;\alpha) \equiv \frac{1}{(4N)^{2+\nu}} \sum_{j=0}^{N-2} \left(\frac{1-\frac{\alpha^2}{2N}}{1+\frac{\alpha^2}{2N}}\right)^{2j} \frac{j!}{(j+\nu)!} L_j^\nu\left(\frac{x}{4N(1-\frac{\alpha^2}{2N})}\right) Q(j,N,\alpha) \tag{8.52}$$

with

$$Q(j,N,\alpha) \equiv \int_0^\infty dy\, \exp\left(\frac{(1-\frac{\alpha^2}{2N})y}{8\alpha^2}\right) K_{\frac{\nu}{2}}\left(\frac{(1+\frac{\alpha^2}{2N})y}{8\alpha^2}\right) L_j^{\nu+1}\left(\frac{y}{4N(1-\frac{\alpha^2}{2N})}\right) y^{\nu/2+1}. \tag{8.53}$$

Our plan is to try to evaluate the large-N limits of eqs. (8.50) and (8.52) in a manner similar to the way we calculated the weak kernel in §8.2.1. This involves taking the limit for large j and N, with $j = tN$ and $t \in [0,1]$ fixed, of each of the factors inside the sums in eqs. (8.50) and (8.52), and replacing the sums with integrals. So, in the present case, our most important outstanding task is to determine appropriate large-N limits of $P(j,N,\alpha)$ and $Q(j,N,\alpha)$.

It turns out that for $D_N^+(x;\alpha)$, this method works in a relatively straightforward manner. However, for $D_N^-(x;\alpha)$, we also find an extra contribution that does not involve an integral. This arises from a different large-N leading order behaviour of $Q(j,N,\alpha)$.

8.3.1.2 Alternative representations for $P(j,N,\alpha)$ and $Q(j,N,\alpha)$

For finite N and non-zero α, $P(j,N,\alpha)$ and $Q(j,N,\alpha)$ are both entirely well-defined (i.e. the integrals are convergent). However, since part of our analysis is supported by numerical considerations[1], it is useful to rewrite $P(j,N,\alpha)$ and $Q(j,N,\alpha)$ in a way that will make them easier to evaluate numerically, since attempting numerical work directly with the integral representations eqs. (8.51) and (8.53) leads to large errors (or long computation times) even for moderate values of j and N.

We proceed as follows. We make a simple change of variables

$$u = \frac{y}{4N\left(1-\frac{\alpha^2}{2N}\right)} \tag{8.54}$$

and replace the generalised Laguerre polynomial with its power series representation eq. (A.8). Then, after switching the sum and integral, we use eq. 6.621.3 in [Gra07] to give

$$\begin{aligned} P(j,N,\alpha) = 2^{3+2\nu}\sqrt{\pi}\,\frac{N^{\nu+1}}{\alpha^{\nu}}\,(j+\nu)!\,\left(1+\frac{\alpha^2}{2N}\right)^{\nu/2} \\ \times\sum_{k=0}^{j}\frac{1}{(j-k)!\,\Gamma(k+\frac{\nu}{2}+\frac{3}{2})}\left(\frac{-2}{1-\frac{\alpha^2}{2N}}\right)^{k} \\ \times {}_2F_1\left(k+\nu+1,\tfrac{\nu}{2}+\tfrac{1}{2};k+\tfrac{\nu}{2}+\tfrac{3}{2};-\frac{2N}{\alpha^2}\right) \end{aligned} \tag{8.55}$$

and

$$\begin{aligned} Q(j,N,\alpha) = 2^{6+2\nu}\sqrt{\pi}\,\frac{N^{\nu+2}}{\alpha^{\nu}}\,(j+\nu+1)!\,\left(1+\frac{\alpha^2}{2N}\right)^{\nu/2} \\ \times\sum_{k=0}^{j}\frac{k+1}{(j-k)!\,\Gamma(k+\frac{\nu}{2}+\frac{5}{2})}\left(\frac{-2}{1-\frac{\alpha^2}{2N}}\right)^{k} \\ \times {}_2F_1\left(k+\nu+2,\tfrac{\nu}{2}+\tfrac{1}{2};k+\tfrac{\nu}{2}+\tfrac{5}{2};-\frac{2N}{\alpha^2}\right), \end{aligned} \tag{8.56}$$

where ${}_2F_1(a,b;c;z)$ is the hypergeometric function, defined earlier in eq. (6.21). We can now use Mathematica [Wol08] to evaluate $P(j,N,\alpha)$ and $Q(j,N,\alpha)$ to arbitrary precision, for rational α and for much larger j and N than was possible before.

[1] In particular, we compared (numerically) the finite-N case for several values of N with the claimed limits, at various intermediate steps in this proof.

8.3.1.3 Determination of limits of $P(j,N,\alpha)$ and $D_N^+(x;\alpha)$

Let us start with eq. (8.51). First, we use eq. 8.432.3 from [Gra07] to replace the Bessel function with an integral, giving

$$P(j,N,\alpha) = \frac{\sqrt{\pi}}{\Gamma\left(\frac{\nu+1}{2}\right)} \left(\frac{1+\frac{\alpha^2}{2N}}{16\alpha^2}\right)^{\nu/2} \int_0^\infty dy \int_1^\infty du\,(u^2-1)^{(\nu-1)/2}\, e^{-by}\, L_j^\nu\left(\frac{y}{c}\right) y^\nu \tag{8.57}$$

where

$$b \equiv \tfrac{1}{8}\left(\frac{u-1}{\alpha^2} + \frac{u+1}{2N}\right) \qquad \text{and} \tag{8.58}$$

$$c \equiv 4N\left(1-\frac{\alpha^2}{2N}\right). \tag{8.59}$$

We interchange the order of integrations, and perform the integral over y using the result eq. (A.7), which gives us

$$\begin{aligned} P(j,N,\alpha) &= \frac{\sqrt{\pi}}{\Gamma\left(\frac{\nu+1}{2}\right)} \left(\frac{1+\frac{\alpha^2}{2N}}{16\alpha^2}\right)^{\nu/2} \frac{(-1)^j\,(j+\nu)!}{j!\,c^j} \int_1^\infty du\,(u^2-1)^{(\nu-1)/2}\, \frac{(1-bc)^j}{b^{j+\nu+1}} \\ &= \frac{2^{\nu+3}\alpha^{\nu+2}\sqrt{\pi}}{\Gamma\left(\frac{\nu+1}{2}\right)} \frac{(j+\nu)!}{j!} \frac{\left(1+\frac{\alpha^2}{2N}\right)^{\nu/2}}{\left(1-\frac{\alpha^2}{2N}\right)^j} \\ &\quad \times \int_1^\infty du\, \frac{(u+1)^{(\nu-1)/2}}{(u-1)^{(\nu+3)/2}} \frac{\left(1-\frac{\alpha^2}{N\,(u-1)} - \frac{\alpha^4(u+1)}{4N^2(u-1)}\right)^j}{\left(1+\frac{\alpha^2}{2N}\,\frac{(u+1)}{(u-1)}\right)^{j+\nu+1}}. \end{aligned} \tag{8.60}$$

We now wish to set $j = tN$, and take the large-N limit keeping t fixed. In fact, j should remain an integer, so we will set $j = [tN]$, where the square brackets denote the integer part.

In order to take the limit, it is necessary to split $P(j,N,\alpha)$ into two parts, $P_1(j,N,\alpha)$ where the integral runs over the range $1 \le u < 1+\alpha^2/N$, and $P_2(j,N,\alpha)$ where the integral is over the range $1+\alpha^2/N \le u < \infty$. For $P_1(j,N,\alpha)$, we write $u+1 = 2+\mathcal{O}(N^{-1})$, and then make a change of variables to

$$s = 1 - \frac{\alpha^2}{N(u-1)} \tag{8.61}$$

with the result that (dropping the $\mathcal{O}(N^{-1})$ which will vanish when the limit is taken)

$$\int_1^{1+\alpha^2/N} du\,\ldots = \frac{(-1)^j\,2^{(\nu-1)/2}\,N^{(\nu+1)/2}}{\alpha^{\nu+1}} \int_0^\infty ds\, \frac{s^j\,(1+s)^{(\nu-1)/2}}{(2+s)^{j+\nu+1}} \left(1-\frac{\alpha^2(1-s)}{2N\,s}\right)^j. \tag{8.62}$$

It is important to note that the overall sign depends on whether j is an even or an odd integer. This implies that no single limit of $P_1(j, N, \alpha)$ will exist. To evaluate the integral on the right-hand side of eq. (8.62), we change variables to $u = j/s$, leading to

$$\int_0^\infty ds \ldots = \frac{1}{j^{(\nu+1)/2}} \int_0^\infty du \left\{ j^{(\nu+3)/2} \frac{u^{(\nu-1)/2}\,(u+j)^{(\nu-1)/2}}{(2u+j)^{\nu+1}\left(1+\frac{2u}{j}\right)^j} \left(1 - \frac{\alpha^2(u-j)}{2N\,j}\right)^j \right\}. \tag{8.63}$$

In fact, we are only interested in the large-N limit of this integral, with $j = [tN]$ and t fixed. As $N \to \infty$, the integrand in the curly brackets converges to an integrable function in a manner that allows us to interchange the limit and the integral. Therefore, on determining the limit of the integrand,

$$\begin{aligned} \lim_{\substack{N\to\infty \\ j=[tN]}} j^{(\nu+1)/2} \int_0^\infty ds \ldots &= e^{\alpha^2 t} \int_0^\infty du\, u^{(\nu-1)/2}\, e^{-2u} \\ &= \frac{\Gamma\left(\frac{\nu+1}{2}\right)}{2^{(\nu+1)/2}}\, e^{\alpha^2 t}. \end{aligned} \tag{8.64}$$

Combining everything, we have

$$\lim_{\substack{N\to\infty \\ j=[tN]}} \frac{P_1(j, N, \alpha)}{N^\nu} = (-1)^j\, 2^{\nu+2}\, \sqrt{\pi}\, \alpha\, t^{(\nu-1)/2}\, e^{\alpha^2 t}. \tag{8.65}$$

Note that we have been somewhat imprecise with our notation; there are actually two limits, depending on whether j steps through the even or the odd integers.

We now turn to consider the limit of $P_2(j, N, \alpha)$, for which we can write

$$\int_{1+\alpha^2/N}^\infty du \ldots = \int_1^\infty du\, \Theta\left(u - \left[1 + \frac{\alpha^2}{N}\right]\right) \ldots \tag{8.66}$$

(where $\Theta(x)$ is the Heaviside step function) and use the Monotone Convergence Theorem (MCT) to show that

$$\begin{aligned} \lim_{\substack{N\to\infty \\ j=[tN]}} \frac{P_2(j, N, \alpha)}{N^\nu} &= \frac{2^{\nu+3}\sqrt{\pi}\alpha^{\nu+2}t^\nu}{\Gamma\left(\frac{\nu+1}{2}\right)} \int_1^\infty du \frac{(u+1)^{(\nu-1)/2}}{(u-1)^{(\nu+3)/2}} \exp\left[-\frac{2\alpha^2 t}{u-1}\right] \\ &= \frac{(2\alpha)^{\nu+2}\sqrt{\pi}}{\Gamma\left(\frac{\nu+1}{2}\right)}\, t^\nu\, e^{\alpha^2 t}\, E_{\frac{1-\nu}{2}}(\alpha^2 t) \end{aligned} \tag{8.67}$$

where we used a change of variables $s = \dfrac{u+1}{u-1}$ in the last step, and $E_n(x)$ is the exponential integral defined by

$$E_n(x) \equiv \int_1^\infty dt\, \frac{e^{-xt}}{t^n}. \tag{8.68}$$

For the special case of $\nu = 0$, this reduces to

$$\lim_{\substack{N\to\infty \\ j=[tN]}} P_2(j, N, \alpha; \nu = 0) = 4\sqrt{\pi}\,\alpha^2 \left\{ \frac{e^{\alpha^2 t}\,\mathrm{erfc}(\alpha\sqrt{t})}{\alpha\sqrt{t}} \right\}, \tag{8.69}$$

where erfc(x) is the complementary error function. Our formula for the limit of $P(j, N, \alpha)$ is therefore

$$\lim_{\substack{N\to\infty \\ j=[tN]}} \frac{P(j, N, \alpha)}{N^\nu} = 2^{\nu+2}\,\sqrt{\pi}\,e^{\alpha^2 t} \left\{ \frac{\alpha^{\nu+2}\,t^\nu\,E_{\frac{1-\nu}{2}}(\alpha^2 t)}{\Gamma\left(\frac{\nu+1}{2}\right)} + (-1)^j\,\alpha\,t^{(\nu-1)/2} \right\} \tag{8.70}$$

where we reiterate that there are different limits depending on whether j takes even or odd values.

We now turn to the limit of $D_N^+(x;\alpha)$. Because of the two different limits of $P(j, N, \alpha)$, technically we should now split the sum in eq. (8.50) into odd and even parts, and treat each separately. However, because of the way that everything combines, it is completely equivalent if we merely use the 'average' limit over even and odd j:

$$\left\langle \lim_{\substack{N\to\infty \\ j=[tN]}} \frac{P(j, N, \alpha)}{N^\nu} \right\rangle = \frac{2^{\nu+2}\,\sqrt{\pi}}{\Gamma\left(\frac{\nu+1}{2}\right)}\,e^{\alpha^2 t}\,\alpha^{\nu+2}\,t^\nu\,E_{\frac{1-\nu}{2}}(\alpha^2 t) \tag{8.71}$$

where it should be understood that this is the average limit over a small interval around t which includes (an infinite number of) both even and odd terms in j.

We can now proceed along lines similar to the proof of the weak kernel. Hence

$$\lim_{N\to\infty} D_N^+(x;\alpha) = \frac{\sqrt{\pi}}{2\Gamma\left(\frac{\nu+1}{2}\right)}\,\frac{\sqrt{x}}{x^{\nu/2}}\,\alpha^{\nu+2} \int_0^1 dt\,e^{-\alpha^2 t}\,t^{(\nu+1)/2}\,E_{\frac{1-\nu}{2}}(\alpha^2 t)\,J_{\nu+1}(\sqrt{xt}) \tag{8.72}$$

which becomes for $\nu = 0$

$$\lim_{N\to\infty} D_N^+(x;\alpha;\nu = 0) = \frac{\sqrt{\pi}}{2}\,\alpha\,\sqrt{x} \int_0^1 dt\,e^{-\alpha^2 t}\,\mathrm{erfc}(\alpha\sqrt{t})\,J_1(\sqrt{xt}). \tag{8.73}$$

8.3.1.4 Determination of limits of $Q(j, N, \alpha)$ and $D_N^-(x;\alpha)$

To understand why the treatment of $Q(j, N, \alpha)$ is different from that of $P(j, N, \alpha)$, it is instructive to consider how each of them scales with N. Let us compare eqs. (8.56) and (8.55) on a term-by-term basis:

- Outside the sum, we have an additional power of N in eq. (8.56) compared with eq. (8.55), and also a factor of $(j+\nu+1)!$ instead of $(j+\nu)!$, which gives another factor $\propto N$ (since $j = [tN]$).

- Inside the sum, we have $k+1$ in the numerator in eq. (8.56), whereas in eq. (8.55) we had unity, but in the denominator the arguments of the gamma function are also different. The result is that the net magnitudes are the same.
- The hypergeometric functions are of the same magnitude, both being close to unity.

So the overall difference is N^2, and we therefore expect the limit

$$\lim_{\substack{N\to\infty \\ j=[tN]}} \frac{Q(j,N,\alpha)}{N^{\nu+2}} \tag{8.74}$$

to exist. The key point is that there are *two* powers of N difference compared with the $P(j,N,\alpha)$ case, and not just one.

To minimise our work, we will proceed by expressing the limits of Q in terms of the limits of P that we have already determined. We begin by proving an easy (and exact) relationship. Using the recurrence relation (eq. 8.971.4 of [Gra07])

$$z\,L_j^{\nu+1}(z) = (j+1)\Big\{L_j^{\nu}(z) - L_{j+1}^{\nu}(z)\Big\} + L_j^{\nu}(z) \tag{8.75}$$

we can show that

$$\frac{Q(j,N,\alpha)}{N} = 4\left(1-\frac{\alpha^2}{2N}\right)\Big[(j+1)\Big\{P(j,N,\alpha) - P(j+1,N,\alpha)\Big\} + \nu\,P(j,N,\alpha)\Big] \tag{8.76}$$

which will be used in the following two parts.

8.3.1.4.1 Leading order contribution We use eqs. (8.70) and (8.76) to show that

$$\lim_{\substack{N\to\infty \\ j=[tN]}} \frac{Q(j,N,\alpha)}{N^{\nu+2}} = (-1)^j\,2^{\nu+5}\,\sqrt{\pi}\,\alpha\,t^{(\nu+1)/2}\,e^{\alpha^2 t}, \tag{8.77}$$

where the sign depends on whether j is even or odd. Note that the other terms from eqs. (8.70) and (8.76) are of smaller order, and so will vanish in the large-N limit.

Now let us consider the limit of $D_N^-(x;\alpha)$. The presence of the $N^{\nu+2}$ leading order behaviour for Q is the crucial difference compared with the P case, which scaled only with N^ν to leading order. Although the $N^{\nu+2}$ here can be 'matched' with the $N^{-(\nu+2)}$ pre-factor in eq. (8.52), this means that there is then no residual N^{-1} to make dt when we take the large-N limit (see eq. (8.10)), and so we will not get an integral.

However, because adjacent even and odd terms have opposite signs, we can take the large-N limit of the sum in eq. (8.52) by using the fact that, for a continuous function $f(t)$ on the interval $0 \le t \le 1$,

$$\lim_{N\to\infty} \sum_{j=0}^{N/2-1} \left\{ f\left(\frac{2j+1}{N}\right) - f\left(\frac{2j}{N}\right) \right\} = \tfrac{1}{2}\{f(1) - f(0)\}. \tag{8.78}$$

(Note that, because there is no N^{-1} on the left-hand side, the limit of the sum does not become an integral over $f(t)$.) This results in a contribution

$$\begin{aligned} \lim_{\substack{N\to\infty \\ \text{Regime 1}}} D_N^-(x;\alpha) &= \frac{\sqrt{\pi}}{x^{\nu/2}}\,\alpha\,\left[e^{-\alpha^2 t}\,\sqrt{t}\,J_\nu(\sqrt{xt})\right]_{t=0}^{t=1} \\ &= \frac{\sqrt{\pi}\,\alpha\,e^{-\alpha^2}}{x^{\nu/2}}\,J_\nu(\sqrt{x}). \end{aligned} \tag{8.79}$$

8.3.1.4.2 Next-to-leading order contribution There will also be a contribution from the next-to-leading term of Q. Here we *can* average even and odd terms (as we did for $P(j,N,\alpha)$ in eq. (8.71)), so the effective limit (over a small neighbourhood of t) is, from eq. (8.76),

$$\begin{aligned} \left\langle \lim_{\substack{N\to\infty \\ j=[tN]}} \frac{Q(j,N,\alpha)}{N^{\nu+1}} \right\rangle &= 4\left(-t\,\frac{\partial}{\partial t} + \nu\right) \left\langle \lim_{\substack{N\to\infty \\ j=[tN]}} \frac{P(j,N,\alpha)}{N^{\nu}} \right\rangle \\ &= \frac{\sqrt{\pi}}{\Gamma\left(\frac{\nu+1}{2}\right)}\,(2\alpha)^{4+\nu} t^{1+\nu} e^{\alpha^2 t} \left\{ E_{\frac{-1-\nu}{2}}(\alpha^2 t) - E_{\frac{1-\nu}{2}}(\alpha^2 t) \right\}, \end{aligned} \tag{8.80}$$

where we used eq. (8.71) and the differential of the exponential integral

$$\frac{d}{dx}\,E_n(x) = -\,E_{n-1}(x). \tag{8.81}$$

For the particular case $\nu = 0$, this gives

$$\left\langle \lim_{\substack{N\to\infty \\ j=[tN]}} \frac{Q(j,N,\alpha;\nu=0)}{N} \right\rangle = 8\alpha^2 \left(2 + \frac{\sqrt{\pi}\,(1-2\alpha^2 t)\,e^{\alpha^2 t}\,\operatorname{erfc}(\alpha\sqrt{t})}{\alpha\sqrt{t}}\right). \tag{8.82}$$

Hence

$$\begin{aligned} \lim_{\substack{N\to\infty \\ \text{Regime 2}}} D_N^-(x;\alpha) &= \frac{\sqrt{\pi}}{\Gamma\left(\frac{\nu+1}{2}\right)}\,\frac{1}{x^{\nu/2}}\,\alpha^{\nu+4} \\ &\quad \times \int_0^1 dt\, e^{-\alpha^2 t}\, t^{1+\nu/2} \left\{ E_{\frac{-1-\nu}{2}}(\alpha^2 t) - E_{\frac{1-\nu}{2}}(\alpha^2 t) \right\} J_\nu(\sqrt{xt}). \end{aligned} \tag{8.83}$$

For $\nu = 0$, this is

$$\lim_{\substack{N\to\infty \\ \text{Regime 2}}} D_N^-(x;\alpha,\nu=0) = \frac{\alpha^2}{2}\int_0^1 dt\, e^{-2\alpha^2 t}\left(2 + \frac{\sqrt{\pi}\,(1-2\alpha^2 t)\,e^{\alpha^2 t}\,\operatorname{erfc}(\alpha\sqrt{t})}{\alpha\sqrt{t}}\right) J_0(\sqrt{xt}). \tag{8.84}$$

We should add that any lower order terms of Q would not contribute to the integral when we take the large-N limit of the sum in eq. (8.52). Effectively, we would have contributions involving $\int (dt)^p$ for $p > 1$, which would be zero.

8.3.1.5 Final formulas

Pulling everything together and simplifying, we have for $C(x;\alpha)$ (defined in eq. (8.48))

$$\begin{aligned} C(x;\alpha) = \frac{1}{32\sqrt{\pi}}\Bigg\{ &-\frac{1}{\alpha}\,e^{-\alpha^2}\,J_\nu(\sqrt{x}) + \frac{\alpha^\nu}{\Gamma\left(\frac{\nu+1}{2}\right)}\int_0^1 dt\, e^{-\alpha^2 t} t^{(\nu+1)/2} \\ &\times\Bigg(\frac{\sqrt{x}}{2}\,E_{\frac{1-\nu}{2}}(\alpha^2 t)\,J_{\nu+1}(\sqrt{xt}) \\ &-\alpha^2\sqrt{t}\left(E_{\frac{-1-\nu}{2}}(\alpha^2 t) - E_{\frac{1-\nu}{2}}(\alpha^2 t)\right) J_\nu(\sqrt{xt})\Bigg)\Bigg\}, \end{aligned} \tag{8.85}$$

which for $\nu = 0$ is

$$\begin{aligned} C(x;\alpha,\nu=0) = \frac{1}{32\pi\alpha}\Bigg\{ &\frac{\sqrt{\pi}}{2}\sqrt{x}\int_0^1 dt\, e^{-\alpha^2 t}\operatorname{erfc}(\alpha\sqrt{t})\,J_1(\sqrt{xt}) \\ &-\int_0^1 dt\left(\alpha e^{-2\alpha^2 t} + \frac{\sqrt{\pi}\,(1-2\alpha^2 t)\,e^{-\alpha^2 t}\operatorname{erfc}(\alpha\sqrt{t})}{2\sqrt{t}}\right) J_0(\sqrt{xt}) \\ &-\sqrt{\pi}\,e^{-\alpha^2}\,J_0(\sqrt{x})\Bigg\}. \end{aligned} \tag{8.86}$$

The final formula for $G^W(x,x')$ itself, eq. (8.45), is then given by

$$\begin{aligned} G^W(x,x') = &-\frac{\hat{h}(x')}{[\operatorname{sgn}(x')]^{\nu/2}}\Bigg\{\left((-i)^\nu\int_{-\infty}^0 dy + \frac{2}{[\operatorname{sgn}(x')]^{\nu/2}}\int_0^{x'} dy\right)\mathcal{K}^W(x,y)\hat{h}(y) \\ &-\frac{1}{32\sqrt{\pi}}\Bigg[-\frac{1}{\alpha}\,e^{-\alpha^2}\,J_\nu(\sqrt{x}) + \frac{2\alpha^\nu}{\Gamma\left(\frac{\nu+1}{2}\right)}\int_0^1 ds\, e^{-\alpha^2 s^2} s^{\nu+2} \\ &\times\left(\frac{\sqrt{x}}{2}\,E_{\frac{1-\nu}{2}}(\alpha^2 s^2)\,J_{\nu+1}(s\sqrt{x}) - \alpha^2 s\left(E_{\frac{-1-\nu}{2}}(\alpha^2 s^2) - E_{\frac{1-\nu}{2}}(\alpha^2 s^2)\right) J_\nu(s\sqrt{x})\right)\Bigg]\Bigg\}, \end{aligned} \tag{8.87}$$

after making a simple change of variables $s = \sqrt{t}$.

8.3.2 Plots of the eigenvalue density

We plot the densities of real and imaginary Dirac eigenvalues in Figures 8.5 and 8.6. Figure 8.5 shows how the weakly non-Hermitian limit is reached, by showing a sequence of finite-N plots. For the imaginary case, convergence is so quick that we just display $N = 2$ and $N = 4$ along with the limit. Figure 8.6 shows real eigenvalues for a sequence of topologies ν, for two values of α.

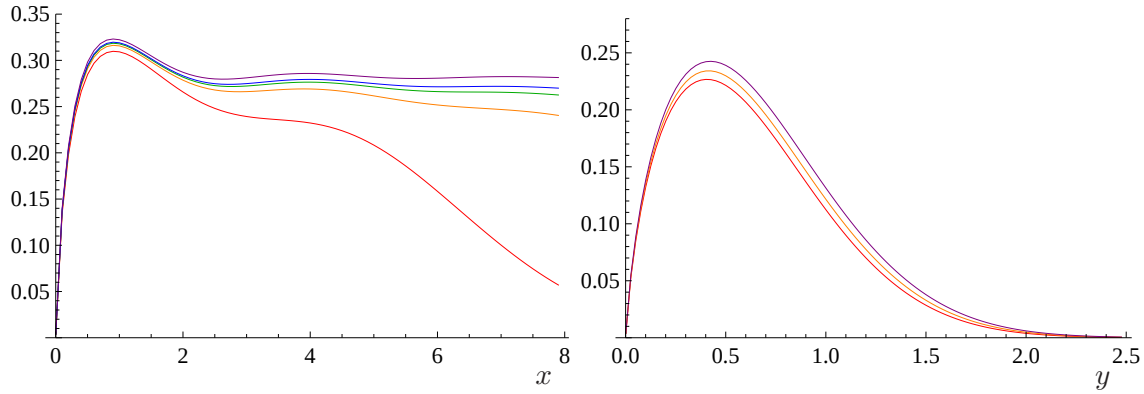

Figure 8.5: Densities of real (left) and imaginary (right) Dirac eigenvalues, for various (finite) N (under 'weak' scaling) and the weakly non-Hermitian limit. Left: $N = 2$ (red), $N = 4$ (orange), $N = 6$ (green), $N = 8$ (blue) and limit (purple). Right: $N = 2$ (red), $N = 4$ (orange) and limit (purple); $\alpha^2 = 0.2$ and $\nu = 0$ in all cases.

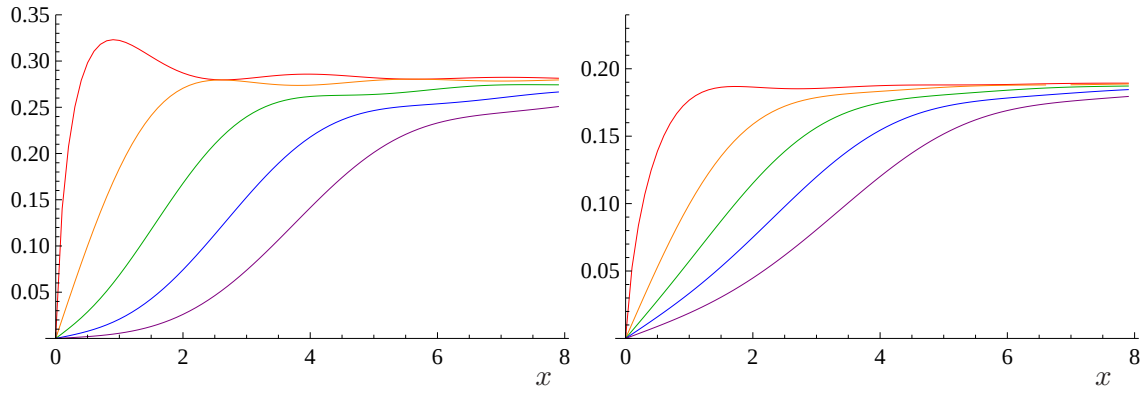

Figure 8.6: Densities of real Dirac eigenvalues $R^{\mathbb{R}\,W}_{1,\mathrm{Dirac}}(x)$ in the weakly non-Hermitian limit for $\alpha = \sqrt{0.2}$ (left) and $\alpha = 1$ (right), for $\nu = 0$ (red), $\nu = 1$ (orange), $\nu = 2$ (green), $\nu = 3$ (blue) and $\nu = 4$ (purple).

8.3.3 Hermitian limit ($\alpha \to 0$)

As $\alpha \to 0$, the chGinOE becomes equivalent to the Hermitian chGOE introduced in [Ver94c], and therefore the weakly non-Hermitian limit of the real eigenvalue density in this limit should be the same as the microscopic eigenvalue density (i.e. for real eigenvalues) for this other ensemble. Since $R_1^{\mathbb{R}\,W}(x) = -G^W(x,x)$, we can easily show using eq. (6.5) that the constituent parts of $G^W(x,x)$ have the following limits:

$$\lim_{\alpha\to 0} \frac{\hat{h}(x)}{[\mathrm{sgn}(x)]^{\nu/2}} A(x;\alpha) = 0, \tag{8.88}$$

$$\begin{aligned}\lim_{\alpha\to 0} \frac{\hat{h}(x)}{[\mathrm{sgn}(x)]^{\nu/2}} B(x,x;\alpha) \\ = \frac{\Theta(x)}{16} \int_0^x dy \int_0^1 ds\, s^2 \left\{ \frac{J_{\nu+1}(s\sqrt{x})J_\nu(s\sqrt{y})}{\sqrt{y}} - \frac{J_{\nu+1}(s\sqrt{y})J_\nu(s\sqrt{x})}{\sqrt{x}} \right\}.\end{aligned} \tag{8.89}$$

For the limit of $C(x;\alpha)$ given in eq. (8.85), we also need to use the fact that, for $\alpha > -1$,

$$\lim_{x\to 0} x^{\alpha+1} E_{-\alpha}(x) = \Gamma(\alpha+1), \tag{8.90}$$

which follows from an easy change of variables, and the result (for $\alpha > -1$)

$$\int_0^\infty du\, e^{-u}\, u^\alpha = \Gamma(\alpha+1). \tag{8.91}$$

Then we have

$$\begin{aligned}\lim_{\alpha\to 0} \frac{\hat{h}(x)}{[\mathrm{sgn}(x)]^{\nu/2}} C(x;\alpha) \\ = \frac{\Theta(x)}{8\sqrt{x}} \left\{ \int_0^1 dt \left(\frac{\sqrt{x}}{2} J_{\nu+1}(\sqrt{xt}) - \frac{\nu+1}{2\sqrt{t}} J_\nu(\sqrt{xt}) \right) - J_\nu(\sqrt{x}) \right\}.\end{aligned} \tag{8.92}$$

We can easily evaluate the integral by changing variables to $s = \sqrt{xt}$, and by using the recurrence relation for J-Bessel functions:

$$z\, J_{\nu+1}(z) - (\nu+1)\, J_\nu(z) = -\frac{d}{dz}\left[z\, J_\nu(z)\right]. \tag{8.93}$$

(To prove, we start with eq. 8.472.2 from [Gra07], and then

$$z\, J_{\nu+1}(z) - \nu J_\nu(z) = -z\frac{d}{dz} J_\nu(z). \tag{8.94}$$

Therefore

$$\begin{aligned} z\, J_{\nu+1}(z) - (\nu+1) J_\nu(z) &= -z\frac{d}{dz} J_\nu(z) - J_\nu(z) \\ &= -\frac{d}{dz}\left[z\, J_\nu(z)\right] \end{aligned} \tag{8.95}$$

as claimed.) This then gives the very simple result

$$\lim_{\alpha\to 0} \frac{\hat{h}(x)}{[\mathrm{sgn}(x)]^{\nu/2}} C(x;\alpha) = \frac{\Theta(x)}{8\sqrt{x}} \left\{-J_\nu(\sqrt{x}) - J_\nu(\sqrt{x})\right\} = -\frac{\Theta(x)}{4\sqrt{x}} J_\nu(\sqrt{x}). \tag{8.96}$$

So we see that, in the case of $\alpha \to 0$, the total result for C is precisely *twice* the value of the part coming from the integral, i.e. the contribution coming from the leading order term of D_N^- is exactly equal to the sum of the contributions from D_N^+ and from the next-to-leading order term of D_N^-, i.e. we find we get double the result that we would get from a naïve interchange of the limit and the integral, an observation made in [Ver94c]. Such a simple relationship is not true when $\alpha > 0$.

The result for the total density (of Wishart eigenvalues) is therefore

$$\begin{aligned}\lim_{\alpha\to 0} R_1^{\mathbb{R}\,W}(x;\alpha) &= 2\lim_{\alpha\to 0} \frac{\hat{h}(x)}{[\mathrm{sgn}(x)]^{\nu/2}} B(x,x;\alpha) - \lim_{\alpha\to 0} \frac{\hat{h}(x)}{[\mathrm{sgn}(x)]^{\nu/2}} C(x;\alpha) \\ &= \Theta(x)\left(\tfrac{1}{8}\int_0^x dy \int_0^1 ds\, s^2 \left\{\frac{J_{\nu+1}(s\sqrt{x})J_\nu(s\sqrt{y})}{\sqrt{y}} - \frac{J_{\nu+1}(s\sqrt{y})J_\nu(s\sqrt{x})}{\sqrt{x}}\right\} + \frac{1}{4\sqrt{x}} J_\nu(\sqrt{x})\right).\end{aligned} \tag{8.97}$$

If we switch to Dirac eigenvalues, and also change the integration variable to $u = \sqrt{y}$, then we can simplify this a little. For $x \in \mathbb{R}$,

$$\lim_{\alpha\to 0} R_{1,\mathrm{Dirac}}^{\mathbb{R}\,W}(x;\alpha) = \tfrac{1}{2}\int_0^x du \int_0^1 ds\, s^2 \Big\{x J_{\nu+1}(sx)J_\nu(su) - u J_{\nu+1}(su)J_\nu(sx)\Big\} + \tfrac{1}{2} J_\nu(x). \tag{8.98}$$

The integral over s can, in fact, be done exactly. Either of the following two results will suffice.

First, we have

$$\int_0^1 ds\, s^2 \Big\{a J_{\nu+1}(sa)J_\nu(sb) - b J_{\nu+1}(sb)J_\nu(sa)\Big\} = \frac{1}{(ab)^\nu}\left(\frac{1}{b}\frac{\partial}{\partial b} - \frac{1}{a}\frac{\partial}{\partial a}\right)\hat{K}_\nu(a,b), \tag{8.99}$$

where

$$\hat{K}_\nu(a,b) \equiv (ab)^{\nu+1}\left(\frac{bJ_{\nu+1}(a)J_\nu(b) - aJ_{\nu+1}(b)J_\nu(a)}{a^2-b^2}\right). \tag{8.100}$$

This is easily proved: Defining $\hat{K}_\nu(a,b)$ as above, eq. 6.521.1 from [Gra07] gives

$$\hat{K}_\nu(a,b) = (ab)^{\nu+1}\int_0^1 ds\, s\, J_{\nu+1}(as)\, J_{\nu+1}(bs). \tag{8.101}$$

We differentiate with respect to a using eq. 8.472.1 of [Gra07], and, after two terms cancel, we have

$$\frac{\partial}{\partial a}\,\hat{K}_\nu(a,b) = (ab)^{\nu+1}\,\int_0^1 ds\,s^2\,J_\nu(as)\,J_{\nu+1}(bs). \tag{8.102}$$

Repeating the same for b, eq. (8.99) then follows.

Second, we have

$$\int_0^1 ds\,s^2\left\{aJ_{\nu+1}(sa)J_\nu(sb) - bJ_{\nu+1}(sb)J_\nu(sa)\right\} = (ab)^\nu\,\left(\frac{1}{b}\,\frac{\partial}{\partial b} - \frac{1}{a}\,\frac{\partial}{\partial a}\right)\hat{\chi}_\nu(a,b), \tag{8.103}$$

where

$$\hat{\chi}_\nu(a,b) \equiv \frac{1}{(ab)^{\nu-1}}\,\left(\frac{bJ_{\nu-1}(a)J_{\nu-2}(b) - aJ_{\nu-1}(b)J_{\nu-2}(a)}{a^2-b^2}\right). \tag{8.104}$$

This is proven by a similar set of steps to the previous result, but using eq. 8.471.1 of [Gra07] in the final step.

Using the second of these, eq. (8.103), shows complete agreement with [Ver94c], who leaves the result expressed in terms of the 'kernel' eq. (8.104). However, we can be slightly more explicit, and perform the differentiations on the kernel, giving (after simplification):

$$\lim_{\alpha\to 0} R^{\mathbb{R}W}_{1,\mathrm{Dirac}}(x;\alpha) = \tfrac{1}{2}\,\int_0^x du\,D_\nu(x,u) + \tfrac{1}{2}\,J_\nu(x), \tag{8.105}$$

where

$$\begin{aligned} D_\nu(a,b) &\equiv (ab)^\nu\,\left(\frac{1}{b}\,\frac{\partial}{\partial b} - \frac{1}{a}\,\frac{\partial}{\partial a}\right)\hat{\chi}_\nu(a,b) \\ &= \frac{1}{(a^2-b^2)^2}\Bigg\{(b^4-a^4)J_\nu(a)J_\nu(b) - 2ab(a^2-b^2)J_{\nu-1}(a)J_{\nu-1}(b) \\ &\qquad + \Big(2b\big[a^2(\nu+1) - b^2(\nu-1)\big]J_\nu(a)J_{\nu-1}(b) - (a\leftrightarrow b)\Big)\Bigg\}. \end{aligned} \tag{8.106}$$

We now use numerical integration over u, and present graphs of the microscopic limit for a sequence of α tending towards zero, together with the limit itself (see Figure 8.7).

Finally we undertake a quick cross-check of the behaviour of the density of the real eigenvalues, assuming the correctness of the Efetov formula eq. (6.26) for the fraction of eigenvalues that are real. When α is large, the number of complex eigenvalues per unit length in the x-direction (sufficiently far away from the y-axis) is given by $\dfrac{1}{\pi}$, obtained by multiplying the plateau density eq. (8.37) by the strip

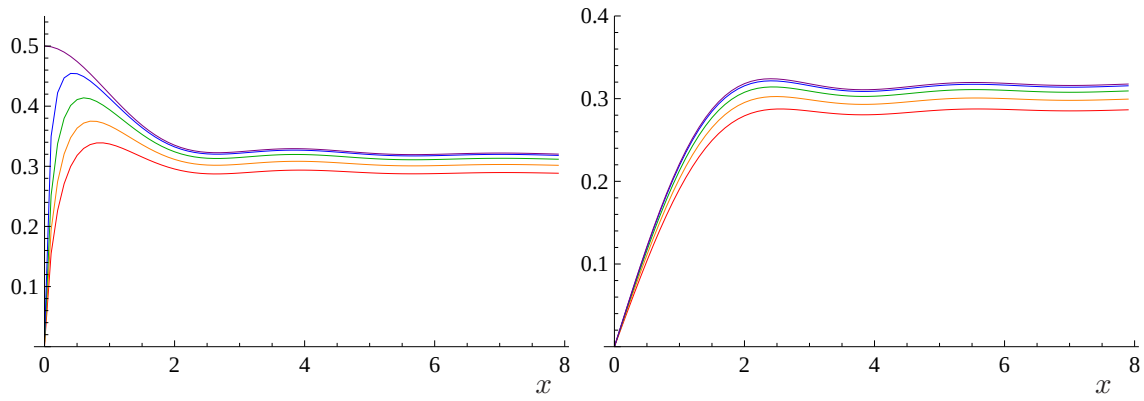

Figure 8.7: Densities of real Dirac eigenvalues $R^{\mathbb{R}\,W}_{1,\mathrm{Dirac}}(x)$ in the weakly non-Hermitian limit for $\nu = 0$ (left) and $\nu = 1$ (right), for a sequence of $\alpha \to 0$. We show $\alpha = 0.4$ (red), $\alpha = 0.3$ (orange), $\alpha = 0.2$ (green), $\alpha = 0.1$ (blue) and $\alpha = 0$ (purple).

width $4\alpha^2$ (counting complex eigenvalues on both sides of the x-axis). However, at large α, we expect almost all of the eigenvalues to be complex, and so this gives us an estimate of the *total* number of eigenvalues per unit length (along the x-direction) under the weak non-Hermiticity scaling. Now we turn to low α. At low $\alpha = \sqrt{2N}\,\mu$, the Efetov formula eq. (6.26) can easily be expanded in powers of α^2 as

$$\mathfrak{F}_{real}\left(N, \mu = \frac{\alpha}{\sqrt{2N}}\right) = 1 - \frac{\alpha^2}{2} + \dots\,, \tag{8.107}$$

and so the average density of real eigenvalues (i.e. the number per unit length along the x-direction, sufficiently far away from the y-axis) is

$$R^{\mathbb{R}\,W}_{1,\mathrm{Dirac}}(x;\alpha) = \frac{1}{\pi}\left\{1 - \frac{\alpha^2}{2} + \dots\right\}, \tag{8.108}$$

which appears to be consistent with the plateau heights in Figure 8.7.

Chapter 9

Unquenched partition functions and densities

When we add the determinant factors (which depend on the masses m_f of the N_f different flavours of quark) to the JPDF, the eigenvalue 'density' is no longer always positive. Indeed, to ensure positivity, we require that the quark masses appear in degenerate pairs (and that the squared masses are real). If the masses are not equal, or if N_f is odd, then the density, although still real, may be negative in certain regions, and possibly oscillating between positive and negative values. Large-N limits may not even exist in these latter cases, since the magnitude of the oscillations increases indefinitely with increasing matrix size N.

We have already determined the unquenched partition functions in §5.1, and so we can move immediately to consider the eigenvalue densities.

9.1 Finite-N densities

9.1.1 General N_f

As we established in §4.5, the correlation functions of (squared) eigenvalues for the unquenched cases are given by formulas that are similar to the quenched case, see eq. (4.95). For the density, for example, we have, analogous to eq. (4.76),

$$R_{1,N}^{(N_f)}(z) = \int_{\mathbb{C}} d^2z' \, \mathcal{K}_N^{(N_f)}(z, z') \, \mathcal{F}^{(N_f)}(z', z), \tag{9.1}$$

where the unquenched kernel $\mathcal{K}_N^{(N_f)}(z, z')$ was given in eqs. (5.48) and (5.49) for even and odd N_f respectively, and the unquenched weight function was given in eq. (4.15).

The matrix size N is even in all cases.

For even N_f: We can then write $R_{1,N}^{(N_f)}(z)$ as a ratio of Pfaffians involving the *quenched* kernel and weight function:

$$R_{1,N}^{(N_f)}(z) = \frac{\mathrm{Pf}\left[A_{ij}\right]_{1\le i,j\le N_f+2}}{\mathrm{Pf}\left[\mathcal{K}_{N+N_f}(m_i^2,m_j^2)\right]_{1\le i,j\le N_f}}, \tag{9.2}$$

where

$$A_{ij} = -A_{ji} \equiv \begin{cases} 0 & \text{if } i=j, \\ -G_{N+N_f}(w_j,z) & \text{if } j>i=1, \\ \mathcal{K}_{N+N_f}(w_i,w_j) & \text{if } j>i>1, \end{cases} \tag{9.3}$$

in which $w_2 \equiv z$ and $w_{i+2} \equiv m_i^2$ for $1 \le i \le N_f$, and from eq. (4.51)

$$\begin{aligned} G_N(u,v) &\equiv -\int_{\mathbb{C}} d^2z'\, \mathcal{K}_N(u,z')\mathcal{F}(z',v) \\ &= \begin{cases} 2i\mathcal{K}_N(u,v^*)w(v)w(v^*)\,\mathrm{sgn}(\Im\mathrm{m}\, v) & \text{for } v\in\mathbb{C}\backslash\mathbb{R}, \\ -w(v)\displaystyle\int_{\mathbb{R}} dx'\,\mathcal{K}_N(u,x')w(x')\,\mathrm{sgn}(v-x') & \text{for } v\in\mathbb{R}. \end{cases} \end{aligned} \tag{9.4}$$

For the particular case of two quark flavours $N_f = 2$, we can expand the Pfaffians, and noting that the first term then corresponds to the quenched density at matrix size $N+2$, we have

$$R_{1,N}^{(N_f=2)}(z) = R_{1,N+2}^{(N_f=0)}(z) + \frac{\mathcal{K}_{N+2}(z,m_2^2)G_{N+2}(m_1^2,z) - \mathcal{K}_{N+2}(z,m_1^2)G_{N+2}(m_2^2,z)}{\mathcal{K}_{N+2}(m_1^2,m_2^2)}. \tag{9.5}$$

When $z \in \mathbb{C}\backslash\mathbb{R}$, we can write the unquenched density as either an additive, or a multiplicative, correction to the quenched density as follows:

$$\begin{aligned} R_{1,N}^{\mathbb{C}\,(N_f=2)}(z) &= R_{1,N+2}^{\mathbb{C}\,(N_f=0)}(z) + 2iw(z)w(z^*)\,\mathrm{sgn}(\Im\mathrm{m}\, z) \\ &\qquad \times \left\{ \frac{\mathcal{K}_{N+2}(z,m_2^2)\mathcal{K}_{N+2}(m_1^2,z^*) - \mathcal{K}_{N+2}(z,m_1^2)\mathcal{K}_{N+2}(m_2^2,z^*)}{\mathcal{K}_{N+2}(m_1^2,m_2^2)} \right\} \\ &= R_{1,N+2}^{\mathbb{C}\,(N_f=0)}(z) \left\{ 1 - \frac{\mathcal{K}_{N+2}(z,m_2^2)\mathcal{K}_{N+2}(m_1^2,z^*) - \mathcal{K}_{N+2}(z,m_1^2)\mathcal{K}_{N+2}(m_2^2,z^*)}{\mathcal{K}_{N+2}(z,z^*)\mathcal{K}_{N+2}(m_1^2,m_2^2)} \right\}. \end{aligned} \tag{9.6}$$

It is interesting to note that, in the final formula, the multiplicative factor does not depend on the weight function. Such a representation does not exist for the real eigenvalues.

For odd N_f: We can use a similar argument, and find that

$$R_{1,N}^{(N_f)}(z) = \frac{\mathrm{Pf}\left[B_{ij}\right]_{1\le i,j\le N_f+3}}{\mathrm{Pf}\left[C_{ij}\right]_{1\le i,j\le N_f+1}}, \tag{9.7}$$

where

$$B_{ij} = -B_{ji} \equiv \begin{cases} 0 & \text{if } i = j, \\ -Q_{N+N_f-1}(z) & \text{if } i = 1, j = 2, \\ q_{N+N_f-1}(w_j) & \text{if } i = 1, j > 2, \\ -G_{N+N_f-1}(w_j, z) & \text{if } j > i = 2, \\ \mathcal{K}_{N+N_f-1}(w_i, w_j) & \text{if } j > i > 2, \end{cases} \tag{9.8}$$

in which $w_3 \equiv z$ and $w_{i+3} \equiv m_i^2$ for $1 \leq i \leq N_f$, and

$$C_{ij} = -C_{ji} \equiv \begin{cases} 0 & \text{if } i = j, \\ q_{N+N_f-1}(m_{j-1}^2) & \text{if } j > i = 1, \\ \mathcal{K}_{N+N_f-1}(m_{i-1}^2, m_{j-1}^2) & \text{if } j > i > 1. \end{cases} \tag{9.9}$$

We have also defined the integrated quenched skew-orthogonal polynomial, as in eq. (4.37):

$$\begin{aligned} Q_N(z) &\equiv \int_{\mathbb{C}} d^2z'\, q_N(z')\mathcal{F}(z', z) \\ &= \begin{cases} -2iq_N(z^*)w(z)w(z^*)\,\mathrm{sgn}(\Im\mathrm{m}\, z) & \text{for } z \in \mathbb{C}\backslash\mathbb{R}, \\ w(z)\displaystyle\int_{\mathbb{R}} dx'\, q_N(x')w(x')\,\mathrm{sgn}(z - x') & \text{for } z \in \mathbb{R}. \end{cases} \end{aligned} \tag{9.10}$$

For the particular case when $N_f = 1$, we have

$$R_{1,N}^{(N_f=1)}(z) = R_{1,N}^{(N_f=0)}(z) + \frac{q_N(z)G_N(m^2, z) - Q_N(z)\mathcal{K}_N(z, m^2)}{q_N(m^2)}. \tag{9.11}$$

After a few lines of algebra, this can be shown – using eq. (4.29) – to be the quenched version of the $N_f = 2$ case, i.e. by taking one of the two masses in eq. (9.5) to infinity.

As for the $N_f = 2$ case, when $z \in \mathbb{C}\backslash\mathbb{R}$, we can write the correction in two alternative ways:

$$\begin{aligned} R_{1,N}^{\mathbb{C}\,(N_f=1)}(z) &= R_{1,N}^{\mathbb{C}\,(N_f=0)}(z) + 2iw(z)w(z^*)\,\mathrm{sgn}(\Im\mathrm{m}\, z) \\ &\qquad \times \left\{ \frac{\mathcal{K}_N(z, m^2)q_N(z^*) - \mathcal{K}_N(z^*, m^2)q_N(z)}{q_N(m^2)} \right\} \\ &= R_{1,N}^{\mathbb{C}\,(N_f=0)}(z) \left\{ 1 - \frac{\mathcal{K}_N(z, m^2)q_N(z^*) - \mathcal{K}_N(z^*, m^2)q_N(z)}{\mathcal{K}_N(z, z^*)q_N(m^2)} \right\}. \end{aligned} \tag{9.12}$$

9.1.2 $N_f = 2$: Degenerate masses

Let us consider in a little more detail the case when we have two quark flavours, both with the same mass, i.e. $N_f = 2$ with $m_1 = m_2 \equiv m$. Our motivation is two-fold. First, this case has practical applications (there being two lighest quarks,

u and d, of almost equal mass). Second, if the masses are the same, then the eigenvalue density $R_{1,N}^{(N_f=2)}(z)$ will be positive everywhere, enabling Monte Carlo simulations to be performed. On the downside, we have a small amount of additional work to do, since the kernel in the denominator of eq. (5.48) vanishes when the arguments are the same. It is necessary to use l'Hôpital's Rule, which states that, if $\lim_{x\to c} f(x) = \lim_{x\to c} g(x) = 0$, then

$$\lim_{x\to c} \frac{f(x)}{g(x)} = \lim_{x\to c} \frac{f'(x)}{g'(x)}, \tag{9.13}$$

provided the right-hand side exists. Then we can write from eq. (9.5)

$$R_{1,N}^{(N_f=2)}(z) = R_{1,N+2}^{(N_f=0)}(z) - \frac{\mathcal{K}_{N+2}(z,m^2)U_{N+2}(m^2,z) - G_{N+2}(m^2,z)D_{N+2}(z,m^2)}{D_{N+2}(m^2,m^2)} \tag{9.14}$$

where $D_N(u,v)$ is the partial differential of the quenched kernel $\mathcal{K}_N(u,v)$ in eq. (5.42) with respect to its second argument:

$$\begin{aligned} D_N(u,v) &\equiv \frac{\partial}{\partial v}\mathcal{K}_N(u,v) \\ &= \frac{1}{32\pi\mu^2(4\mu^2\eta_+)^{\nu+1}} \sum_{j=0}^{N-2} \left(\frac{\eta_-}{\eta_+}\right)^{2j} \frac{(j+1)!}{(j+\nu)!} \\ &\quad \times \left\{ L_{j+1}^{\nu}\left(\frac{u}{4\mu^2\eta_-}\right) L_{j-1}^{\nu+1}\left(\frac{v}{4\mu^2\eta_-}\right) - L_j^{\nu+1}\left(\frac{v}{4\mu^2\eta_-}\right) L_j^{\nu}\left(\frac{u}{4\mu^2\eta_-}\right) \right\} \end{aligned} \tag{9.15}$$

and $U_N(u,v)$ is the integral of $D_N(u,v)$ with respect to the weight function (or the partial differential of $G_N(u,v)$ with respect to u)

$$\begin{aligned} U_N(u,v) &\equiv \int_{\mathbb{C}} d^2z'\, D_N(z',u)\mathcal{F}(z',v) = \frac{\partial}{\partial u} G_N(u,v) \\ &= \begin{cases} -2i\, D_N(v^*,u)w(v)w(v^*)\,\mathrm{sgn}(\Im\mathrm{m}\, v) & \text{for } v \in \mathbb{C}\backslash\mathbb{R}, \\ w(v)\displaystyle\int_{\mathbb{R}} dx'\, D_N(x',u)w(x')\,\mathrm{sgn}(v-x') & \text{for } v \in \mathbb{R}. \end{cases} \end{aligned} \tag{9.16}$$

For the complex Dirac eigenvalues $z \in \mathbb{C}\backslash\mathbb{R}$, this allows us to write eq. (9.14) as

$$R_{1,N}^{\mathbb{C}\,(N_f=2)}(z) = R_{1,N+2}^{\mathbb{C}\,(N_f=0)}(z) \left\{ 1 - \frac{\mathcal{K}_{N+2}(z,m^2)D_{N+2}(z^*,m^2) - \mathcal{K}_{N+2}(z^*,m^2)D_{N+2}(z,m^2)}{\mathcal{K}_{N+2}(z,z^*)D_{N+2}(m^2,m^2)} \right\}. \tag{9.17}$$

9.2 Strongly non-Hermitian microscopic large-N limit

9.2.1 General N_f

We begin by writing down generic formulas for an arbitrary number N_f of quark flavours for the partition function and the eigenvalue densities in the strongly non-Hermitian limit, before looking in detail at the $N_f = 2$ case with both degenerate and non-degenerate masses.

9.2.1.1 Partition function

For even N_f: We take the large-N limit of eq. (5.12) (after dropping the normalisation constant), giving

$$\begin{aligned}\mathcal{Z}^{S\,(N_f)}(\{m\}) &= (-1)^{N_f/2}\,\frac{\prod_{f=1}^{N_f} m_f^{\nu}}{\Delta_{N_f}(\{m^2\})}\,\mathrm{Pf}[\mathcal{K}^S(m_i^2,m_j^2)]_{1\le i,j\le N_f}\\ &\propto \frac{\prod_{f=1}^{N_f} e^{-\eta_- m_f^2}}{\Delta_{N_f}(\{m^2\})}\,\mathrm{Pf}[(m_i^2-m_j^2)\,I_\nu(2\eta_+ m_i m_j)]_{1\le i,j\le N_f},\end{aligned} \tag{9.18}$$

where we used the explicit form of the strong (quenched) kernel eq. (7.6) in the second step.

For odd N_f: This limit does not exist. We would have to take the large-N limit of eq. (5.17). However, that would include the large-N limit of $q_N(z)$, which does not exist.

9.2.1.2 Density

For even N_f: We can take the large-N limit of the finite-N result eq. (9.2), with no additional scaling, as we did for the quenched case. We can take the limit inside the Pfaffian (it operates only on elements in the first row and column), and there is no issue when changing the order of the limit and the integral:

$$R_1^{S\,(N_f)}(z) \equiv \lim_{N\to\infty} R_{1,N}^{(N_f)}(z) = \frac{\mathrm{Pf}\left[A_{ij}\right]_{1\le i,j\le N_f+2}}{\mathrm{Pf}\left[\mathcal{K}^S(m_i^2,m_j^2)\right]_{1\le i,j\le N_f}}, \tag{9.19}$$

where

$$A_{ij} = -A_{ji} \equiv \begin{cases} 0 & \text{if } i=j,\\ -G^S(w_j,z) & \text{if } j>i=1,\\ \mathcal{K}^S(w_i,w_j) & \text{if } j>i>1,\end{cases} \tag{9.20}$$

in which $w_2 \equiv z$ and $w_{i+2} \equiv m_i^2$ for $1 \leq i \leq N_f$, and where we define the limit of $G_N(u,v)$ in eq. (4.51):

$$\begin{aligned} G^S(u,v) &\equiv \lim_{N\to\infty} G_N(u,v) \\ &= -\lim_{N\to\infty} \int_{\mathbb{C}} d^2z'\, \mathcal{K}_N(u,z')\mathcal{F}(z',v) \\ &= -\int_{\mathbb{C}} d^2z' \lim_{N\to\infty} \mathcal{K}_N(u,z')\mathcal{F}(z',v) \\ &= -\int_{\mathbb{C}} d^2z' \mathcal{K}^S(u,z')\mathcal{F}(z',v) \\ &= \begin{cases} 2i\mathcal{K}^S(u,v^*)w(v)w(v^*)\,\mathrm{sgn}(\Im\mathrm{m}\, v) & \text{for } v \in \mathbb{C}\backslash\mathbb{R}, \\ -w(v)\displaystyle\int_{\mathbb{R}} dx'\, \mathcal{K}^S(u,x')w(x')\,\mathrm{sgn}(v-x') & \text{for } v \in \mathbb{R}. \end{cases} \end{aligned} \tag{9.21}$$

For the case with two quark flavours, this gives

$$R_1^{S\,(N_f=2)}(z) = R_1^{S\,(N_f=0)}(z) + \frac{\mathcal{K}^S(z,m_2^2)G^S(m_1^2,z) - \mathcal{K}^S(z,m_1^2)G^S(m_2^2,z)}{\mathcal{K}^S(m_1^2,m_2^2)}. \tag{9.22}$$

As for the finite-N case, when $z \in \mathbb{C}\backslash\mathbb{R}$, we can write this as a multiplicative correction to the quenched case as follows:

$$R_1^{\mathbb{C}\,S\,(N_f=2)}(z) = R_1^{\mathbb{C}\,S\,(N_f=0)}(z)\left\{1 - \frac{\mathcal{K}^S(z,m_2^2)\mathcal{K}^S(m_1^2,z^*) - \mathcal{K}^S(z,m_1^2)\mathcal{K}^S(m_2^2,z^*)}{\mathcal{K}^S(z,z^*)\mathcal{K}^S(m_1^2,m_2^2)}\right\}. \tag{9.23}$$

For $z \in \mathbb{R}$, we must use eq. (9.22) directly.

For odd N_f: This limit of eq. (9.7) does not exist, for the reason discussed above.

9.2.2 $N_f = 2$: Degenerate masses[1]

As for the finite-N case, the strongly non-Hermitian kernel is zero for identical arguments. Therefore we have

$$R_1^{S\,(N_f=2)}(z) = R_1^{S\,(N_f=0)}(z) - \frac{\mathcal{K}^S(z,m^2)U^S(m^2,z) - G^S(m^2,z)D^S(z,m^2)}{D^S(m^2,m^2)}, \tag{9.24}$$

[1]We assume for the examples in §9.2 that the masses are real. In fact, for a mapping to QCD, we actually require imaginary masses in the RMT model. However, because of the symmetry of the strongly non-Hermitian density, one can merely rotate the solutions by 90° in the complex plane to see the effect of imaginary masses.

in which $D^S(u,v)$ and $U^S(u,v)$ mirror their finite-N counterparts:

$$\begin{aligned} D^S(u,v) &\equiv \frac{\partial}{\partial v}\mathcal{K}^S(u,v) \\ &= \frac{\eta_+^3}{8\pi} e^{-\eta_-(u+v)}(uv)^{-\nu/2}(2v)^{-1} \\ &\quad \times \big\{\eta_+\sqrt{uv}(u-v)[I_{\nu-1}(2\eta_+\sqrt{uv}) + I_{\nu+1}(2\eta_+\sqrt{uv})] \\ &\quad - \big(\nu(u-v) + 2v(1+\eta_-(u-v))\big) I_\nu(2\eta_+\sqrt{uv})\big\} \end{aligned} \tag{9.25}$$

and

$$\begin{aligned} U^S(u,v) &\equiv \frac{\partial}{\partial u}G^S(u,v) \\ &= \begin{cases} -2i\, D^S(v^*,u)w(v)w(v^*)\,\mathrm{sgn}(\Im\mathrm{m}\, v) & \text{for } v \in \mathbb{C}\backslash\mathbb{R}, \\ w(v)\displaystyle\int_{\mathbb{R}} dx'\, D^S(x',u)w(x')\,\mathrm{sgn}(v-x') & \text{for } v \in \mathbb{R}. \end{cases} \end{aligned} \tag{9.26}$$

For $z \in \mathbb{C}\backslash\mathbb{R}$, we can write this as

$$R_1^{\mathbb{C}\,S\,(N_f=2)}(z) = R_1^{\mathbb{C}\,S\,(N_f=0)}(z)\left\{1 - \frac{\mathcal{K}^S(z,m^2)D^S(z^*,m^2) - \mathcal{K}^S(z^*,m^2)D^S(z,m^2)}{\mathcal{K}^S(z,z^*)D^S(m^2,m^2)}\right\}. \tag{9.27}$$

For $z \in \mathbb{R}$, we work from eq. (9.24) directly.

In Figure 9.1 we show plots for the strongly non-Hermitian unquenched limit, with two flavours of quark with degenerate masses $m_1 = m_2 = 2$. As with the earlier plots, we show only one quadrant of the complex plane $\mathbb{C}$, and only one half of each axis, since the densities are symmetric under reflection in the x- and y-axes. We see a depletion in the densities (of both real and complex eigenvalues) around the point $z = 2$, the 'location' of the masses, as if they were repelling the eigenvalues. However, the densities still remain real and positive. Since the masses are located on the real axis, the density of imaginary eigenvalues remains (almost) unaffected by their presence.

9.2.3 $N_f = 2$: Non-degenerate masses

In Figure 9.2, we show some plots of the densities of complex eigenvalues when the two masses are not the same. These were generated using eq. (9.23). For a moderate mass split $\Delta m \equiv |m_2 - m_1|$, we see that there is a depletion of eigenvalues around the 'location' of the masses, and a peak in the complex density elsewhere. As the mass split increases, we clearly see the formation of a circular region of oscillations, with the number and height of the oscillations both growing with the mass split.

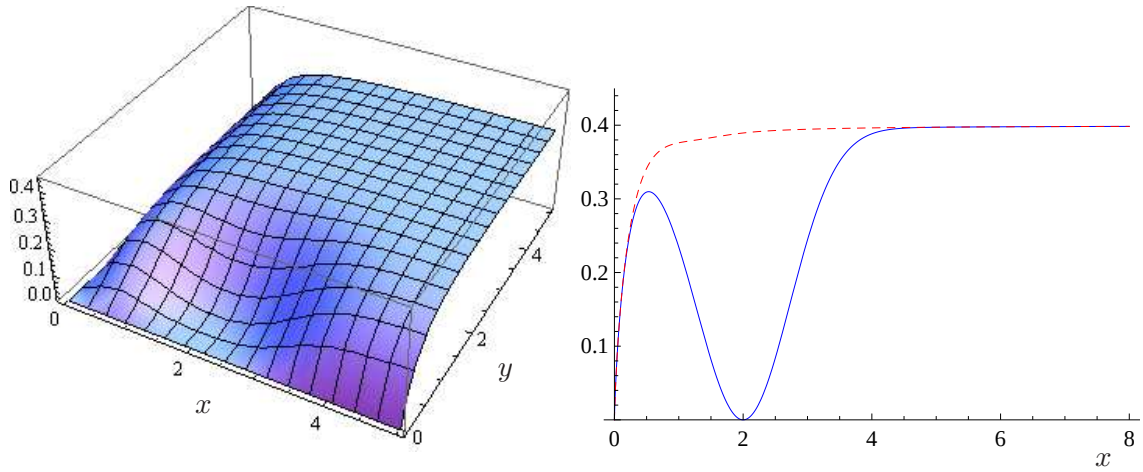

Figure 9.1: The densities of complex (left), real (right, blue) and imaginary (right, red, dashed) Dirac eigenvalues at strong non-Hermiticity with two degenerate masses $m_1 = m_2 = 2$; $\mu = 1$ and $\nu = 0$ in both cases.

(The graphs show just one quadrant of $\mathbb{C}$, with a semi-circular region of oscillations. In $\mathbb{C}$ itself, there are two circular regions of oscillations in total.)

Let us now investigate the reasons behind the oscillations. As we established in §7.3, the density of complex (Dirac) eigenvalues for the quenched case in the strongly non-Hermitian limit is, essentially, constant everywhere apart from close to the real and imaginary axes, where it vanishes. As we discussed earlier, the unquenched density can be written as a correction to the quenched case, see eq. (9.23), which is given by:

$$\begin{aligned}\Delta_1^{\mathbb{C}\,S}(z) &= \frac{-\mathcal{K}^S(z,m_1^2)\mathcal{K}^S(z^*,m_2^2)+\mathcal{K}^S(z^*,m_1^2)\mathcal{K}^S(z,m_2^2)}{\mathcal{K}^S(z,z^*)\mathcal{K}^S(m_1^2,m_2^2)}\,R_1^{\mathbb{C}\,S\,(N_f=0)}(z)\\ &= (-2i)\,\frac{\Im\mathrm{m}\,\{\mathcal{K}^S(z,m_1^2)\mathcal{K}^S(z^*,m_2^2)\}}{\mathcal{K}^S(z,z^*)\mathcal{K}^S(m_1^2,m_2^2)}\,R_1^{\mathbb{C}\,S\,(N_f=0)}(z),\end{aligned} \tag{9.28}$$

in which $\mathcal{K}^S(u,v)$ is the strong quenched kernel from eq. (7.6). We now switch to consider the correction to the density of Dirac eigenvalues:

$$\Delta_{1,\mathrm{Dirac}}^{\mathbb{C}\,S}(z) = (-2i)\,\frac{\Im\mathrm{m}\,\{\mathcal{K}^S(z^2,m_1^2)\mathcal{K}^S(z^{*2},m_2^2)\}}{\mathcal{K}^S(z^2,z^{*2})\mathcal{K}^S(m_1^2,m_2^2)}\,R_{1,\mathrm{Dirac}}^{\mathbb{C}\,S\,(N_f=0)}(z). \tag{9.29}$$

Next, we make the first of two approximations. For the quenched case, away from the axes, the Dirac density is almost flat, i.e. it is equal to some constant which we can determine exactly (see §7.3), but here we shall simply denote it by ρ_s. Hence

$$\Delta_{1,\mathrm{Dirac}}^{\mathbb{C}\,S}(z) \approx (-2i)\,\frac{\Im\mathrm{m}\,\{\mathcal{K}^S(z^2,m_1^2)\mathcal{K}^S(z^{*2},m_2^2)\}}{\mathcal{K}^S(z^2,z^{*2})\mathcal{K}^S(m_1^2,m_2^2)}\,\rho_s. \tag{9.30}$$

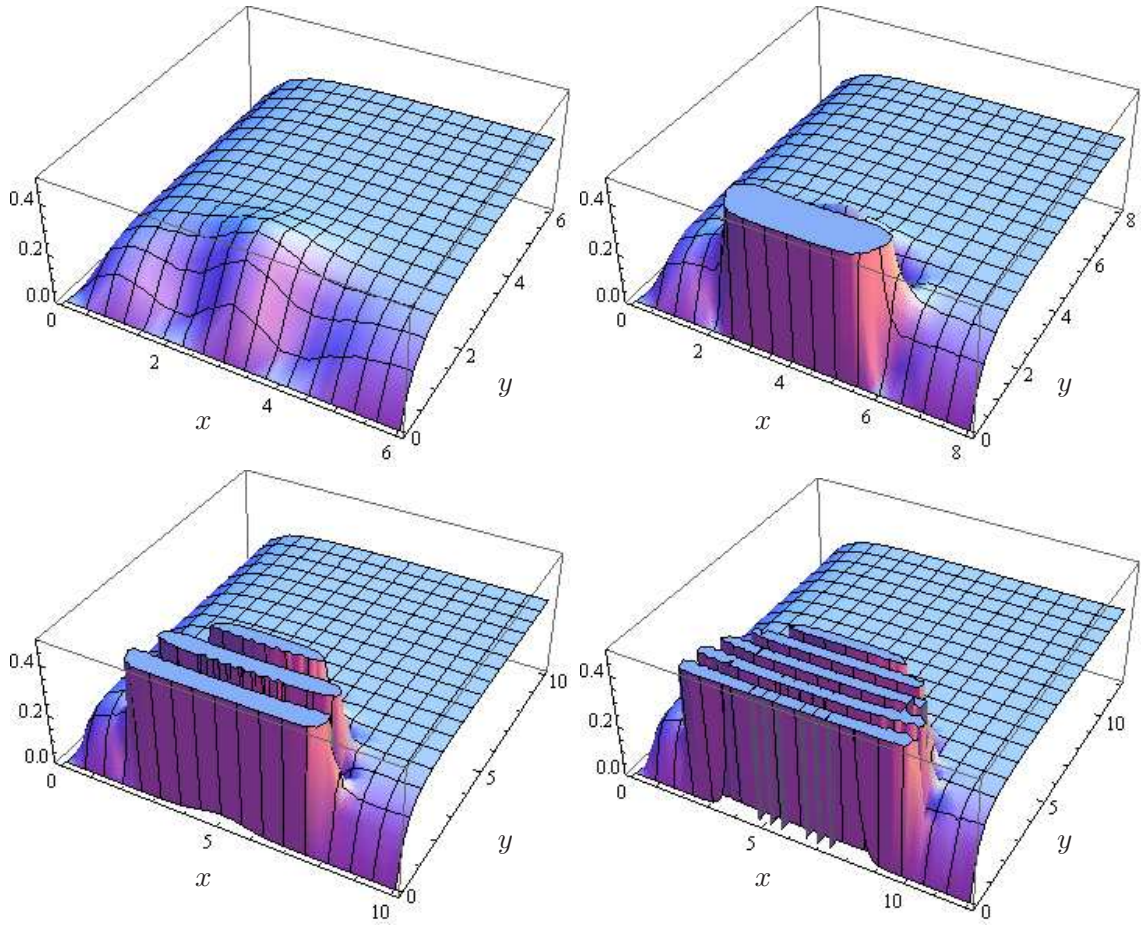

Figure 9.2: The densities of complex Dirac eigenvalues at strong non-Hermiticity with two non-degenerate real masses: $m_1 = 2$ in all cases, $m_2 = 4$ (top, left), $m_2 = 6$ (top, right), $m_2 = 8$ (bottom, left) and $m_2 = 10$ (bottom, right); $\mu = 1$ and $\nu = 0$ in all cases. The vertical scaling has been kept the same in all cases, with truncation of the peaks. Between these peaks, there are negative troughs (not visible) of comparable magnitude.

On inserting the explicit form of the strong kernel from eq. (7.6), we get (after noting that a number of factors cancel)

$$\Delta^{\mathbb{C}S}_{1,\text{Dirac}}(z) \approx (-2i)\,\frac{\Im\text{m}\,\left\{(z^2-m_1^2)(z^{*2}-m_2^2)I_\nu(2\eta_+ zm_1)I_\nu(2\eta_+ z^* m_2)\right\}}{(m_1^2-m_2^2)(z^2-z^{*2})I_\nu(2\eta_+ m_1 m_2)I_\nu(2\eta_+ zz^*)}\,\rho_s. \tag{9.31}$$

Our second approximation is to replace each I-Bessel function with its large-argument asymptotic limit

$$I_\nu(z) \sim \frac{e^z}{\sqrt{2\pi z}} \tag{9.32}$$

for $-\frac{\pi}{2} < \arg(z) < \frac{\pi}{2}$, i.e. in the right half-plane. After simplification, this gives (in the right half-plane, and sufficiently far away from the origin and from the axes)

$$\begin{aligned}\Delta^{\mathbb{C}\,S}_{1,\mathrm{Dirac}}(z) &\approx \frac{(-2i)\,\rho_S\, e^{-2\eta_+(m_1m_2+|z|^2)}}{(m_1^2-m_2^2)(z^2-z^{*2})}\,\Im\mathrm{m}\left\{(z^2-m_1^2)(z^{*2}-m_2^2)e^{2\eta_+(zm_1+z^*m_2)}\right\}\\ &= \frac{(-2i)\,\rho_S}{(m_1^2-m_2^2)(z^2-z^{*2})}\,\exp\left[2\eta_+\big((m_1+m_2)x-|z|^2-m_1m_2\big)\right]\\ &\quad\times\Im\mathrm{m}\Big\{(z^2-m_1^2)(z^{*2}-m_2^2)\\ &\qquad\times\Big(\cos(2\eta_+(m_1-m_2)y)+i\sin(2\eta_+(m_1-m_2)y)\Big)\Big\},\end{aligned}\tag{9.33}$$

where $x \equiv \Re\mathrm{e}\, z$ and $y \equiv \Im\mathrm{m}\, z$. We can regard this as being the product of an envelope (the exponential), some polynomials in z and z^*, and an oscillatory function of y. Let us consider each in turn.

To understand the behaviour of the exponential part, we can determine the contours in the z-plane where this part takes constant values. Equivalently, we can perform this analysis on the exponent. So we look for the solution of

$$(m_1+m_2)x - |z|^2 - m_1m_2 = k,\tag{9.34}$$

where k is some constant. Writing $|z|^2 = x^2+y^2$, and rearranging, we have

$$\left(x-\frac{m_1+m_2}{2}\right)^2 + y^2 = \left(\frac{m_1-m_2}{2}\right)^2 - k \;\equiv\; r^2.\tag{9.35}$$

This is, of course, the equation of a circle of radius r, centred on the point $z = (m_1+m_2)/2$. The exponential function equals unity when $k=0$, i.e. when the circle passes through the points $z=m_1$ and $z=m_2$. Crudely speaking, this marks the boundary of the region where the correction is 'significant' when compared with the quenched case (where the density equals ρ_S). Points inside this circle have $k>0$, so the circle marks the boundary of a peak (rather than a dip) in the complex plane. The maximal value of this peak is $\exp(2\eta_+ k_{\max})$, where

$$k_{\max} = \left(\frac{m_1-m_2}{2}\right)^2,\tag{9.36}$$

so the peak grows very rapidly indeed with the difference between m_1 and m_2. Of course, our approximations are not valid at the centre of the circle since this lies on the x-axis, and so this argument is merely indicative of the orders of magnitude that we might expect to observe in the density itself.

The polynomials $(z^2 - m_1^2)(z^{*2} - m_2^2)$ in eq. (9.33) result in a repulsion of eigenvalues from the points $\pm m_1$ and $\pm m_2$, similar to what we observed in the case of identical masses.

Finally, if we combine the oscillatory part of eq. (9.33) with the $(z^2 - z^{*2})^{-1}$ factor, then we get an oscillating function of y which is symmetric (even), and which has a constant 'wavelength'

$$\lambda = \frac{\pi}{\eta_+ \, |m_1 - m_2|}. \tag{9.37}$$

In other words, this constitutes a set of ridges and troughs parallel to the real axis.

Therefore, what we observe in the total density is a circular 'peak' of fairly dramatic oscillations, but these are almost completely suppressed elsewhere in the complex plane. There is also some repulsion from the location of the masses, although the exponential effect causing the peak is generally much more significant. The number of oscillations visible will therefore be given by

$$N_{\text{oscillations}} \approx \frac{\eta_+ \, (m_1 - m_2)^2}{\pi}, \tag{9.38}$$

and we can say that no oscillations will be seen at all if, roughly speaking,

$$|m_1 - m_2| < \sqrt{\frac{\pi}{\eta_+}}. \tag{9.39}$$

If we evaluate eq. (9.38) for the bottom right-hand plot of Figure 9.2, then we find that we would predict around 10 oscillations in the circular region; indeed, we see 5 oscillations in the half of the circle that is shown, in complete agreement.

In Figure 9.3 we show the real and imaginary Dirac eigenvalues when we have two non-degenerate masses. Although there are no oscillations in this case, the density of the real eigenvalues does turn negative in the region between the masses, and grows rapidly with the mass split. The density of the imaginary eigenvalues is essentially unaffected by the presence of the (real) masses, as for the earlier case with degenerate masses.

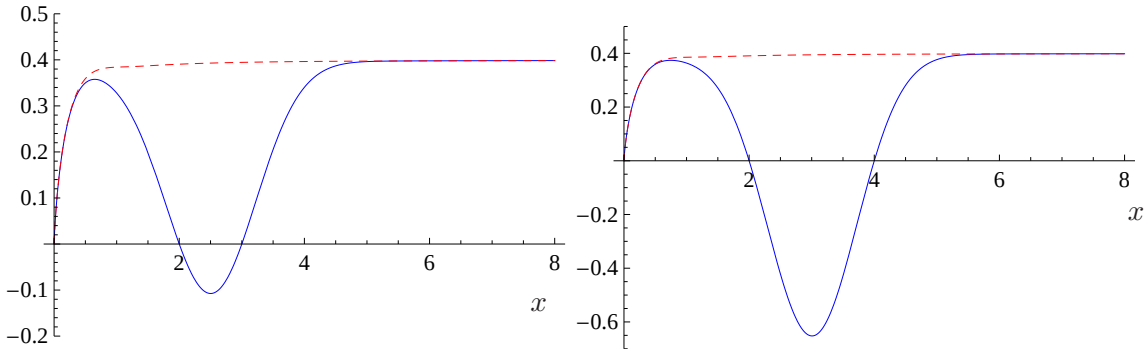

Figure 9.3: The densities of real (blue) and imaginary (red, dashed) Dirac eigenvalues at strong non-Hermiticity with two non-degenerate real masses. $m_1 = 2$ in both cases, $m_2 = 3$ (left) and $m_2 = 4$ (right); $\mu = 1$ and $\nu = 0$ in both cases.

9.3 Weakly non-Hermitian microscopic large-N limit

9.3.1 General N_f

We scale the chemical potential μ and the Dirac eigenvalue z as for the quenched case discussed in the previous chapter, but now we also have to scale the masses[1]:

$$\mu = \frac{\alpha}{\sqrt{2N}}, \qquad z = \frac{\hat{z}}{2\sqrt{N}} \qquad \text{and} \qquad m_i = \frac{\eta_i}{2\sqrt{N}}, \tag{9.40}$$

where z and $\hat{z}$ are Dirac eigenvalues. Equivalently, the Wishart eigenvalues and the *squared* masses scale as N^{-1}.

9.3.1.1 Partition function

For even N_f: Taking the limit of eq. (5.12) (multiplied by a suitable N-dependent scaling factor to guarantee that a limit exists) using eq. (8.5), we can immediately write down the partition function

$$\mathcal{Z}^{W\,(N_f)}(\{\eta\}) = \frac{(-1)^{N_f/2}}{\Delta_{N_f}(\{\eta^2\})} \operatorname{Pf}[\mathcal{K}^W(\eta_i^2, \eta_j^2)]_{1\le i,j\le N_f}, \tag{9.41}$$

with the quenched weak kernel $\mathcal{K}^W(u, v)$ which was given in eq. (8.16).
For odd N_f: Similarly, we take the limit of eq. (5.17) to give

$$\mathcal{Z}^{W\,(N_f)}(\{\eta\}) = \frac{(-1)^{(N_f-1)/2}}{\Delta_{N_f}(\{\eta^2\})} \operatorname{Pf}\left[A_{ij}\right]_{1\le i,j\le N_f+1}, \tag{9.42}$$

[1]One also has to scale the masses in the epsilon regime of chiral perturbation theory in order to exclude the propagating modes of the pions.

in which

$$A_{ij} = -A_{ji} \equiv \begin{cases} 0 & \text{if } i = j, \\ q^W(\eta_{j-1}^2) & \text{if } j > i = 1, \\ \mathcal{K}^W(\eta_{i-1}^2, \eta_{j-1}^2) & \text{if } j > i > 1, \end{cases} \tag{9.43}$$

and $q^W(z)$ is the limit of the (even) skew-orthogonal polynomial eq. (5.53) under the weak scaling, given by (N even)

$$\begin{aligned} q^W(z) &\equiv \lim_{N\to\infty} \frac{1}{(4N)^{\nu/2} N!} \left(\frac{z}{4N}\right)^{\nu/2} q_N\left(\frac{z}{4N}\right) \\ &= 2^{-\nu}\, e^{-\alpha^2/2} J_\nu(\sqrt{z}). \end{aligned} \tag{9.44}$$

There is some arbitrariness regarding the overall normalisation of the limit of the skew-orthogonal polynomial, since $q^W(z)$ is itself, of course, not a polynomial. Our choice ensures that the formulas for the large-N densities take the same forms as those for the finite-N case.

9.3.1.2 Density

Turning now to the eigenvalue densities, we simply take the limits of the appropriately scaled finite-N results from §9.1.1.

For even N_f: We have

$$\begin{aligned} R_1^{W\,(N_f)}(z;\alpha) &\equiv \lim_{N\to\infty} \frac{1}{4N} R_{1,N}^{(N_f)}\left(\frac{z}{4N}\right) \\ &= \frac{\operatorname{Pf}\left[A_{ij}\right]_{1\le i,j\le N_f+2}}{\operatorname{Pf}\left[\mathcal{K}^W(\eta_i^2,\eta_j^2)\right]_{1\le i,j\le N_f}}, \end{aligned} \tag{9.45}$$

where

$$A_{ij} = -A_{ji} \equiv \begin{cases} 0 & \text{if } i = j, \\ -G^W(w_j, z) & \text{if } j > i = 1, \\ \mathcal{K}^W(w_i, w_j) & \text{if } j > i > 1, \end{cases} \tag{9.46}$$

in which $w_2 \equiv z$ and $w_{i+2} \equiv \eta_i^2$ for $1 \le i \le N_f$, and

$$\begin{aligned} G^W(u,v) &\equiv \lim_{N\to\infty} \frac{1}{4N} \frac{u^{\nu/2}}{v^{\nu/2}} G_N\left(\frac{u}{4N}, \frac{v}{4N}\right) \\ &= -\lim_{N\to\infty} \frac{1}{4N} \frac{u^{\nu/2}}{v^{\nu/2}} \int_{\mathbb{C}} d^2z'\, \mathcal{K}_N\left(\frac{u}{4N}, z'\right) \mathcal{F}\left(z', \frac{v}{4N}\right) \\ &= \begin{cases} 2i\,\mathcal{K}^W(u, v^*)\mathcal{W}(v, v^*)\operatorname{sgn}(\Im\mathrm{m}\, v) & \text{for } v \in \mathbb{C}\backslash\mathbb{R}, \\ \text{see eq. (8.87)} & \text{for } v \in \mathbb{R}. \end{cases} \end{aligned} \tag{9.47}$$

As with the strongly non-Hermitian case, we took the limit inside the Pfaffian (it operates only on elements in the first row and column).

For two flavours $N_f = 2$, we can write out the formula eq. (9.45) explicitly:

$$R_1^{W\,(N_f=2)}(z) = R_1^{W\,(N_f=0)}(z) + \frac{\mathcal{K}^W(z,\eta_2^2)G^W(\eta_1^2,z) - \mathcal{K}^W(z,\eta_1^2)G^W(\eta_2^2,z)}{\mathcal{K}^W(\eta_1^2,\eta_2^2)}. \tag{9.48}$$

When $z \in \mathbb{C}\backslash\mathbb{R}$, we use eq. (9.47) to show that this becomes

$$R_1^{\mathbb{C}\,W\,(N_f=2)}(z) = R_1^{\mathbb{C}\,W\,(N_f=0)}(z) + 2i\mathcal{W}(z,z^*)\,\mathrm{sgn}(\Im\mathrm{m}\,z) \times \left\{\frac{\mathcal{K}^W(z,\eta_2^2)\mathcal{K}^W(\eta_1^2,z^*) - \mathcal{K}^W(z,\eta_1^2)\mathcal{K}^W(\eta_2^2,z^*)}{\mathcal{K}^W(\eta_1^2,\eta_2^2)}\right\} \tag{9.49}$$

$$= R_1^{\mathbb{C}\,W\,(N_f=0)}(z)\left\{1 - \frac{\mathcal{K}^W(z,\eta_2^2)\mathcal{K}^W(\eta_1^2,z^*) - \mathcal{K}^W(z,\eta_1^2)\mathcal{K}^W(\eta_2^2,z^*)}{\mathcal{K}^W(z,z^*)\mathcal{K}^W(\eta_1^2,\eta_2^2)}\right\}. \tag{9.50}$$

For simplicity, we will use the 'multiplicative form' eq. (9.50) when considering the case when the two masses both lie within the strip of quenched eigenvalues (since $R_1^{\mathbb{C}\,W\,(N_f=0)}(z)$ is almost constant in this region). However, when we consider the case when one of the masses lies outside the strip, where $R_1^{\mathbb{C}\,W\,(N_f=0)}(z)$ is typically negligible, then the 'additive form' eq. (9.49) is easier to use.

For odd N_f: We have

$$R_1^{W\,(N_f)}(z;\alpha) = \frac{\mathrm{Pf}\left[B_{ij}\right]_{1\le i,j\le N_f+3}}{\mathrm{Pf}\left[C_{ij}\right]_{1\le i,j\le N_f+1}}, \tag{9.51}$$

where

$$B_{ij} = -B_{ji} \equiv \begin{cases} 0 & \text{if } i=j, \\ -Q^W(z) & \text{if } i=1, j=2, \\ q^W(w_j) & \text{if } i=1, j>2, \\ -G^W(w_j,z) & \text{if } j>i=2, \\ \mathcal{K}^W(w_i,w_j) & \text{if } j>i>2, \end{cases} \tag{9.52}$$

in which $w_3 \equiv z$ and $w_{i+3} \equiv \eta_i^2$ for $1 \le i \le N_f$, and

$$C_{ij} = -C_{ji} \equiv \begin{cases} 0 & \text{if } i=j, \\ q^W(\eta_{j-1}^2) & \text{if } j>i=1, \\ \mathcal{K}^W(\eta_{i-1}^2,\eta_{j-1}^2) & \text{if } j>i>1. \end{cases} \tag{9.53}$$

We have the corresponding integrated skew-orthogonal polynomial given by

$$Q^W(z) \equiv \lim_{N\to\infty} \frac{4N}{N!}\frac{1}{z^{\nu/2}}\,Q_N\left(\frac{z}{4N}\right) = \lim_{N\to\infty} \frac{4N}{N!}\frac{1}{z^{\nu/2}}\int_{\mathbb{C}} d^2z'\,q_N(z')\mathcal{F}\left(z',\frac{z}{4N}\right). \tag{9.54}$$

For complex $z \in \mathbb{C}\backslash\mathbb{R}$, the integral contains a Dirac delta function, and so we can take the limit operator to act directly on q_N and $\mathcal{F}$, giving the product of the limiting cases of each:

$$Q^W(z) = -2i\, q^W(z^*)\mathcal{W}(z, z^*)\,\mathrm{sgn}(\Im\mathrm{m}\, z). \tag{9.55}$$

For real z we have, as with the real weak density, an issue when interchanging the limit and the integral. We find that

$$Q^W(x) = \frac{\hat{h}(x)}{[\mathrm{sgn}(x)]^{\nu/2}} \Bigg\{ \left((-i)^\nu \int_{-\infty}^{0} dy + \frac{2}{[\mathrm{sgn}(x)]^{\nu/2}} \int_0^x dy \right) q^W(y)\hat{h}(y) \\ - 2^{3-\nu}\sqrt{\pi} e^{\alpha^2/2} \left[\frac{\alpha^{\nu+2} E_{\frac{1-\nu}{2}}(\alpha^2)}{\Gamma\left(\frac{\nu+1}{2}\right)} + \alpha \right] \Bigg\}, \tag{9.56}$$

the proof of which follows along similar lines to that for $G^W(x, x')$ in §8.3, and which we therefore omit.

For $N_f = 1$, we have for the density of eigenvalues

$$R_1^{W\,(N_f=1)}(z) = R_1^{W\,(N_f=0)}(z) + \frac{q^W(z)G^W(\eta^2, z) - Q^W(z)\mathcal{K}^W(z, \eta^2)}{q^W(\eta^2)}. \tag{9.57}$$

When $z \in \mathbb{C}\backslash\mathbb{R}$, this can be written as

$$R_1^{\mathbb{C}\,W\,(N_f=1)}(z) = R_1^{\mathbb{C}\,W\,(N_f=0)}(z) + 2i\mathcal{W}(z, z^*)\,\mathrm{sgn}(\Im\mathrm{m}\, z) \left\{ \frac{\mathcal{K}^W(z, \eta^2)q^W(z^*) - \mathcal{K}^W(z^*, \eta^2)q^W(z)}{q^W(\eta^2)} \right\}. \tag{9.58}$$

9.3.2 $N_f = 2$: Degenerate masses

With our convention that $\mu = 0$ is Hermitian and not anti-Hermitian, the complex eigenvalues in the weakly non-Hermitian limit lie (predominantly) in a strip parallel to the real axis. We therefore take the masses η_i to be purely imaginary for the remainder of this chapter, in order to permit meaningful comparison with QCD results. Sometimes we will write $\eta_i = \mu_i i$, where $\mu_i \in \mathbb{R}^+$ (which should not be confused with the chemical potential μ).

When we have two quark flavours with masses that are degenerate $\eta_1 = \eta_2 \equiv \eta$, then

$$R_1^{W\,(N_f=2)}(z) = R_1^{W\,(N_f=0)}(z) - \frac{\mathcal{K}^W(z, \eta^2)U^W(\eta^2, z) - G^W(\eta^2, z)D^W(z, \eta^2)}{D^W(\eta^2, \eta^2)} \tag{9.59}$$

where $D^W(u,v)$ is determined by differentiating the quenched weak kernel eq. (8.16)

$$\begin{aligned} D^W(u,v) &\equiv \frac{\partial}{\partial v}\mathcal{K}^W(u,v) \\ &= \frac{1}{256\pi\alpha^2}\int_0^1 ds\, s^2\, e^{-2\alpha^2 s^2}\,(2v)^{-1}\Big\{\sqrt{v}J_{\nu-1}(s\sqrt{v})\Big[\nu J_\nu(s\sqrt{u}) - s\sqrt{u}J_{\nu-1}(s\sqrt{u})\Big] \\ &\qquad + J_\nu(s\sqrt{v})\Big[\nu\sqrt{u}J_{\nu-1}(s\sqrt{u}) - svJ_\nu(s\sqrt{u})\Big]\Big\}, \end{aligned} \tag{9.60}$$

and

$$U^W(u,v) = \frac{\partial}{\partial u}G^W(u,v). \tag{9.61}$$

We look in more detail at specific cases in the next two sections.

9.3.3 Complex eigenvalues

9.3.3.1 $N_f = 2$: Degenerate masses, both inside the strip

When we are considering complex eigenvalues $z \in \mathbb{C}\backslash\mathbb{R}$, the expressions for both $G^W(u,v)$ and $U^W(u,v)$ simplify. For the former, we refer to eq. (9.47); for the latter, we then have

$$U^W(u,v) = -2iD^W(v^*,u)\mathcal{W}(v,v^*)\,\mathrm{sgn}(\Im\mathrm{m}\, v), \tag{9.62}$$

and so we can write ($z \in \mathbb{C}\backslash\mathbb{R}$)

$$R_1^{\mathbb{C}\,W\,(N_f=2)}(z) = R_1^{\mathbb{C}\,W\,(N_f=0)}(z)\left\{1 - \frac{\mathcal{K}^W(z,\eta^2)D^W(z^*,\eta^2) - \mathcal{K}^W(z^*,\eta^2)D^W(z,\eta^2)}{\mathcal{K}^W(z,z^*)D^W(\eta^2,\eta^2)}\right\}. \tag{9.63}$$

Figure 9.4 shows the effect on the density of complex eigenvalues of adding two imaginary degenerate masses. The left-hand plot shows the quenched case; the two masses are added in the right-hand plot, and apart from a repulsion from the 'location' of the masses at $4i$, no other effect is seen.

9.3.3.2 $N_f = 2$: Non-degenerate masses, both inside the strip

We consider next the case when we have two non-degenerate masses, both located within the (quenched) eigenvalue strip ($|\Im\mathrm{m}\, z| < 2\alpha^2$). Since the densities depend on the squares of the masses, we take $\Im\mathrm{m}\,\eta_1 \geq 0$, $\Im\mathrm{m}\,\eta_2 \geq 0$, without loss of generality. The correction to the density of the complex eigenvalues is given by eq. (9.50). Since all arguments (η_1, η_2 and z) lie within the strip, we can use the approximation

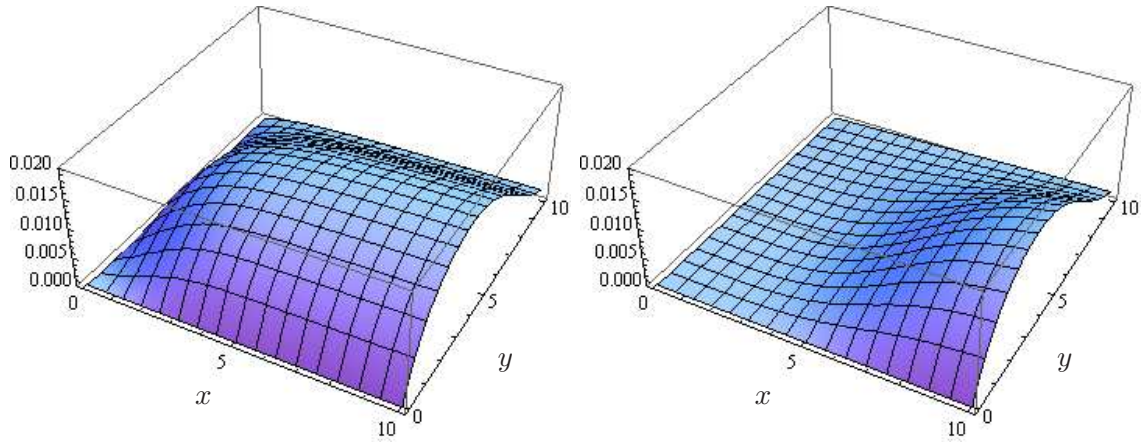

Figure 9.4: The densities of complex Dirac eigenvalues at weak non-Hermiticity for $\alpha = 2$ in the quenched case (left) and with two degenerate imaginary masses $\eta_1 = \eta_2 = 4i$ (right); $\nu = 0$ in both cases.

for the kernel from eq. (8.29)[1]. Because of the way everything combines and the various exponential factors cancel, we are, in fact, left with something identical to the *strongly* non-Hermitian unquenched case at $\mu = 1$, analysed in detail in §9.2.3, but with all the arguments (i.e. Dirac eigenvalues and masses) rescaled by a factor $1/2\alpha$ (and of course everything is also rotated by 90° in the complex plane). Consequently, all the results that we found for the strongly non-Hermitian case carry over directly, provided we make this rescaling.

In particular, we can say that there is a region of oscillations which is a circle (in fact, two circles, one on each side of the x-axis), and the oscillations are parallel to the y-axis. The circle in $\Im\mathrm{m}\, z \geq 0$ passes through η_1 and η_2. The wavelength of the oscillations is given by

$$\lambda = \frac{8\pi\alpha^2}{|\eta_2 - \eta_1|}, \tag{9.64}$$

and the number of oscillations visible in the circle is given roughly by

$$N_{\text{oscillations}} \approx \frac{|\eta_2 - \eta_1|^2}{8\pi\alpha^2}. \tag{9.65}$$

No oscillations will be seen until, approximately,

$$|\eta_2 - \eta_1| > 2\sqrt{2\pi}\alpha \approx 5\alpha. \tag{9.66}$$

[1]Actually, this may cease to be strictly true if the larger of the two masses lies very close to the edge of the strip, but we shall ignore any small correction here.

Indeed, since the strip width is $\approx 2\alpha^2$ (see §8.2.2), we therefore require $2\sqrt{2\pi}\alpha \leq 2\alpha^2$, i.e. $\alpha \geq \sqrt{2\pi}$, if any oscillations are to be seen. Finally, the height of the oscillations grows exponentially with the *square* of the mass difference, as for the strongly non-Hermitian unquenched case.

Figure 9.5 shows a typical case (both plots show the same situation). With $\alpha = 6$, the approximate edge of the strip lies at $y \approx 2\alpha^2 = 72$, so the masses at $10i$ and $70i$ both lie inside the strip. The number of oscillations is predicted from eq. (9.65) to be 3.98 which is entirely consistent with the four peaks that can be seen. The region of oscillations is indeed circular, to a very good degree of approximation.

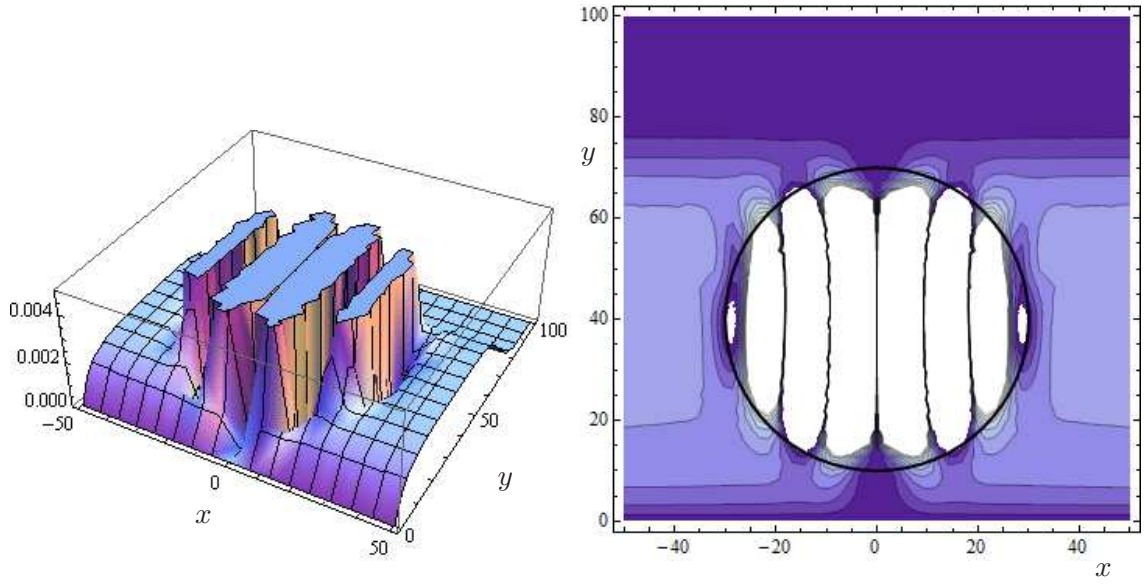

Figure 9.5: The densities of complex Dirac eigenvalues at weak non-Hermiticity for $\alpha = 6$ (and $\nu = 0$) with two masses $\eta_1 = 10i$ and $\eta_2 = 70i$, shown as a 3-dimensional plot (left) and as a contour plot (right). The peaks of the oscillations have been truncated. Between the positive peaks are negative peaks of similar size which are not visible in the left-hand plot. Each white band in the right-hand plot corresponds either to a positive or to a negative (truncated) oscillation. The predicted circular boundary of the region of oscillations has been superimposed in the right-hand plot (black line).

9.3.3.3 $N_f = 1$

The next simplest case is when we have just one (imaginary) mass which is located within the strip. (A single mass located outside the strip has almost no effect on

the quenched density.) The equation for the correction to the quenched density of complex eigenvalues is given in eq. (9.58). Let us denote the mass as $\eta = \mu i$ where $0 \leq \mu < 2\alpha^2$. We consider a point $z = x + iy$, such that $\frac{y+\mu}{2} < 2\alpha^2$, and so for both occurrences of the kernels we can use the first approximation in eq. (8.39). Note that z itself may lie outside the strip. For the Bessel functions that constitute the limiting skew-orthogonal polynomials, we use the large-argument asymptotic form, and for the weight function, we use the approximate form from eq. (8.36). If we substitute both these approximations into eq. (9.58), and isolate the real part of the exponent, then we arrive at an equation analogous to eq. (9.34) for the contours where the envelope of the oscillations is constant:

$$-x^2 - 3y^2 + \mu^2 + 2\mu y + 8\alpha^2 y - 8\alpha^2 \mu = k \tag{9.67}$$

where k is some constant. On choosing $k = 0$ (so that we find contours where the unquenched correction is unity), and rearranging, we arrive at

$$\frac{x^2}{\left(\frac{2}{\sqrt{3}}(2\alpha^2 - \mu)\right)^2} + \frac{\left(y - \frac{4\alpha^2+\mu}{3}\right)^2}{\left(\frac{2}{3}(2\alpha^2 - \mu)\right)^2} = 1. \tag{9.68}$$

This is the equation of an ellipse, with centre at $\left(\frac{4\alpha^2+\mu}{3}\right) i$, and passing through the mass $\eta = \mu i$ and the point $\left(\frac{8\alpha^2-\mu}{3}\right) i$ on the far side, which lies a distance $\frac{2\alpha^2-\mu}{3}$ outside the strip. Note that the average of this latter point and the mass is less than $2\alpha^2$, so our original choice of approximation for the kernel (the first approximation in eq. (8.39)) was indeed the correct one to use.

A region of oscillations also occurs in the $\beta = 2$ case [Ake05a], and, in fact, the formula for the boundary in that case is identical to the one for the $\beta = 1$ case (see [Osb08b], where the boundary was determined from an effective theory using an ansatz).

If we treat the point $\left(\frac{8\alpha^2-\mu}{3}\right) i$ as a 'dummy' second mass, and then use eq. (9.64) for the $N_f = 2$ case to estimate the wavelength of the oscillations (without rigorous justification), then we can obtain an approximate formula for the number of visible oscillations across the ellipse as

$$N_{\text{oscillations}} \approx \frac{2}{3\sqrt{3}\,\pi\alpha^2}\,(2\alpha^2 - \mu)^2. \tag{9.69}$$

In Figure 9.6 we show a typical case. The right-hand plot shows the predicted ellipse eq. (9.68) superimposed, demonstrating an impressive fit. Using eq. (9.69)

with the parameters in these plots ($\alpha = 6$ and $\mu = 10$), we find that 13.1 oscillations are predicted, entirely consistent with the 13 or 14 that are visible.

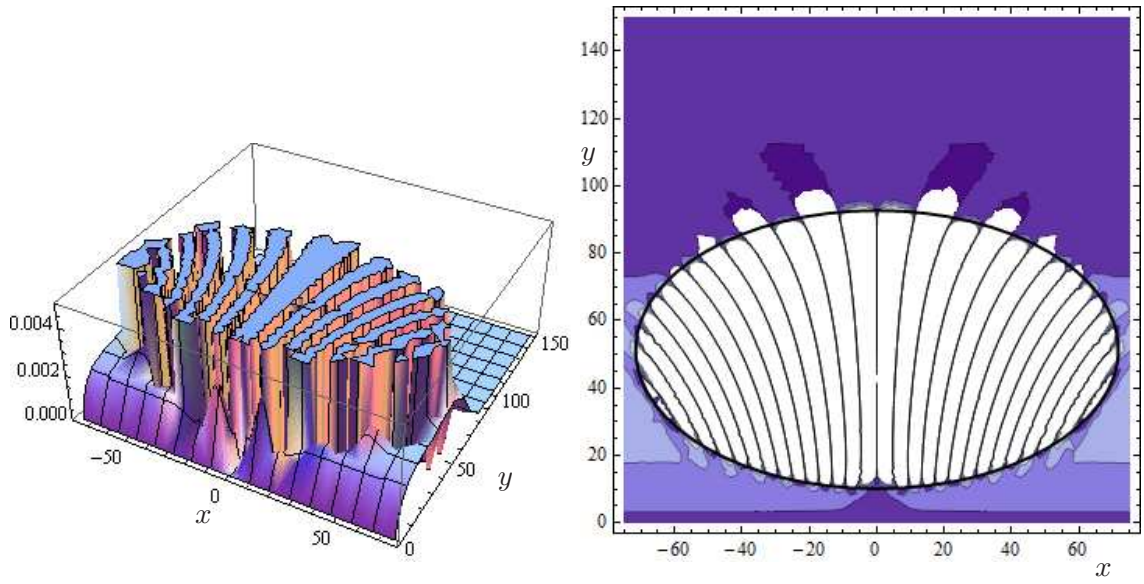

Figure 9.6: The densities of complex Dirac eigenvalues at weak non-Hermiticity for $\alpha = 6$ (and $\nu = 0$) with one mass $\eta = 10i$, shown as a 3-dimensional plot (left) and as a contour plot (right). The predicted elliptical boundary of the region of oscillations has been superimposed in the right-hand plot (black line). Some small errors in the numerical integration are clearly visible in certain places in the left-hand plot.

9.3.3.4 $N_f = 2$: Non-degenerate masses, one outside the strip

We now consider the case where $N_f = 2$, $\eta_1 = \mu_1 i$ and $\eta_2 = \mu_2 i$, with one mass inside the strip ($0 \leq \mu_1 < 2\alpha^2$) and the other mass outside the strip ($\mu_2 \geq 2\alpha^2$). We will use eq. (9.49) for the density, and will approximate each occurrence of the kernel in this expression by either the first or the second approximation in eq. (8.39), depending on the average of the two arguments. We omit the details of the calculation which are similar to those in the previous sections, and we just give the results.

First, if $2\alpha^2 \leq \mu_2 < 4\alpha^2 - \mu_1$, then, under our approximation, we find that the far boundary of the oscillating region is given by an ellipse (although different from the ellipse eq. (9.68) in the previous case), and the boundary closer to the real axis is given by a circle. Figure 9.7 shows such a case. We have superimposed the predicted circle and ellipse, each of which shows a good match in its region of applicability. Furthermore, we can derive the formula which gives the distance between the origin

and the furthest part of the region of oscillations:

$$d_{\text{far}} = \frac{4\alpha^2 + \mu_1}{3} + \sqrt{\frac{4(2\alpha^2 - \mu_1)^2}{9} - \frac{[4\alpha^2 - (\mu_1 + \mu_2)]^2}{3}}. \tag{9.70}$$

Second, if $\mu_2 \geq 4\alpha^2 - \mu_1$, then the weak kernel $\mathcal{K}^W(z, \eta_2^2)$ is always approximated by the second approximation in eq. (8.39), where it factorises into separate z- and μ_2-dependent parts[1]. The μ_2-dependent factors then completely cancel in the expression for the unquenched density eq. (9.49), and we get the same expression as for the $N_f = 1$ case. The quark with mass $\eta_2 = \mu_2 i$ can therefore be said to have decoupled from the system completely. Hence, $4\alpha^2 - \mu_1$ can be considered to be a critical value of μ_2.

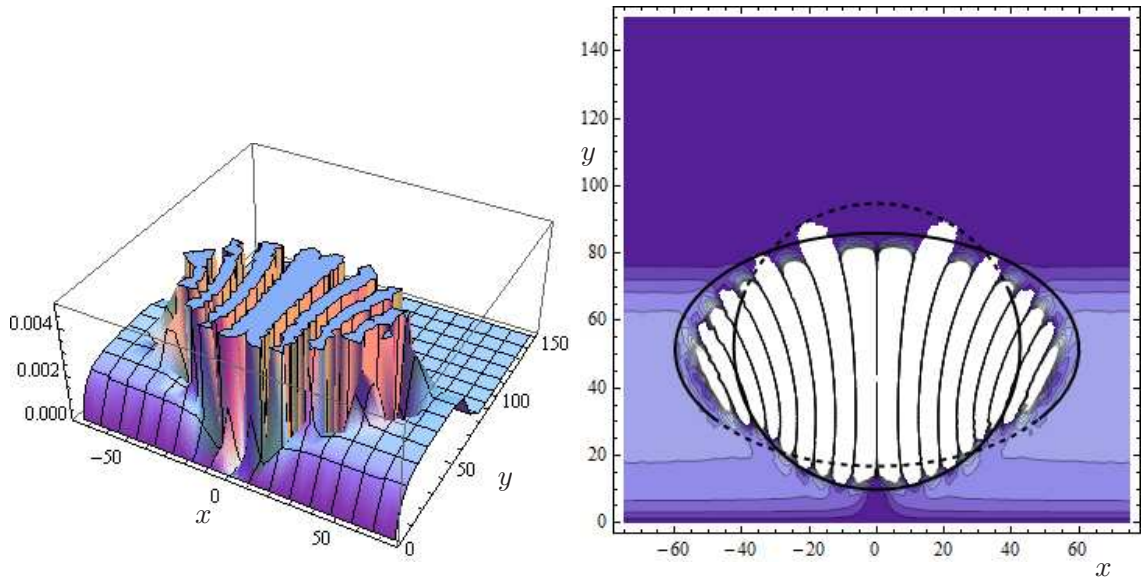

Figure 9.7: The densities of complex Dirac eigenvalues at weak non-Hermiticity for $\alpha = 6$ (and $\nu = 0$) with two masses $\eta_1 = 10i$ and $\eta_2 = 95i$, shown as a 3-dimensional plot (left) and as a contour plot (right). The predicted boundaries of the region of oscillations (an ellipse and a circle) have been superimposed in the right-hand plot (black lines).

9.3.3.5 Partially quenching the $N_f = 2$ case

We are now in a position to combine the results from the last three parts to gain an understanding of what happens to the $N_f = 2$ case as we take one of the masses to

[1] i.e. if we are just considering the exponential part which is the most relevant. Strictly speaking, complete factorisation does not occur until one of the arguments is infinitely big – see the comments after eq. (8.31).

be increasingly large. Assume that the lower mass, $\eta_1 = \mu_1 i$, is fixed, and lies within the strip ($0 \leq \mu_1 < 2\alpha^2$). The first regime corresponds to the case when the higher mass $\eta_2 = \mu_2 i$ also lies within the strip. We have a circular region of oscillations, extending from the lower mass $\mu_1 i$ to the higher mass $\mu_2 i$. The second regime is when $\mu_2 i$ lies outside the strip, but below the critical point. Here, the region of oscillations lies somewhere between a circle and an ellipse, and the far side of the oscillating region now lies outside the strip, but not as far outside as the second mass itself. For the third regime, $\mu_2 i$ lies beyond the critical point, and so the quark has effectively decoupled (and so this is the same as the $N_f = 1$ case). Here, the oscillating region is elliptical, and no longer shows any dependency on μ_2.

We can combine the previous results to extend the formula for the distance from the origin to the far side of the oscillating region:

$$d_{\text{far}}(\mu_2) = \begin{cases} \mu_2 & \text{for } 0 \leq \mu_1 \leq \mu_2 < 2\alpha^2 \\ \dfrac{4\alpha^2 + \mu_1}{3} + \sqrt{\dfrac{4(2\alpha^2 - \mu_1)^2}{9} - \dfrac{[4\alpha^2 - (\mu_1 + \mu_2)]^2}{3}} & \text{for } 2\alpha^2 \leq \mu_2 < 4\alpha^2 - \mu_1 \\ \dfrac{8\alpha^2 - \mu_1}{3} & \text{for } \mu_2 \geq 4\alpha^2 - \mu_1, \end{cases} \tag{9.71}$$

where α and μ_1 are considered fixed. We note that eq. (9.71) is continuous everywhere as a function of μ_2, as is its derivative, and this is illustrated in Figure 9.8. Although this figure is intended to be schematic, it was actually generated using $\mu_1 = 10$ and $\alpha = 6$, and so can be compared directly with the previous figures.

9.3.4 Real and imaginary eigenvalues

We now consider the real and imaginary Dirac eigenvalues. As in the previous section, we place the masses on the imaginary axis. We first consider a fairly low value of $\alpha = 2$. Figure 9.9 shows a sequence of graphs with one mass fixed, and varying the position of a second mass.[1] For the real eigenvalues, what we see is merely some additional repulsion coming from the location of the masses. For the imaginary eigenvalues, the density becomes negative in the region between the masses, but because of an exponential decay beyond the edge of the strip, the density remains bounded as the larger mass is taken to infinity, and so the $N_f = 1$ case is well-defined.

[1]For the case of real and imaginary Dirac eigenvalues when we have two quark flavours with degenerate masses, there is unfortunately no simple formula for $U^W(u, v)$ in eq. (9.61). It must be evaluated by differentiating eq. (8.87) term-by-term.

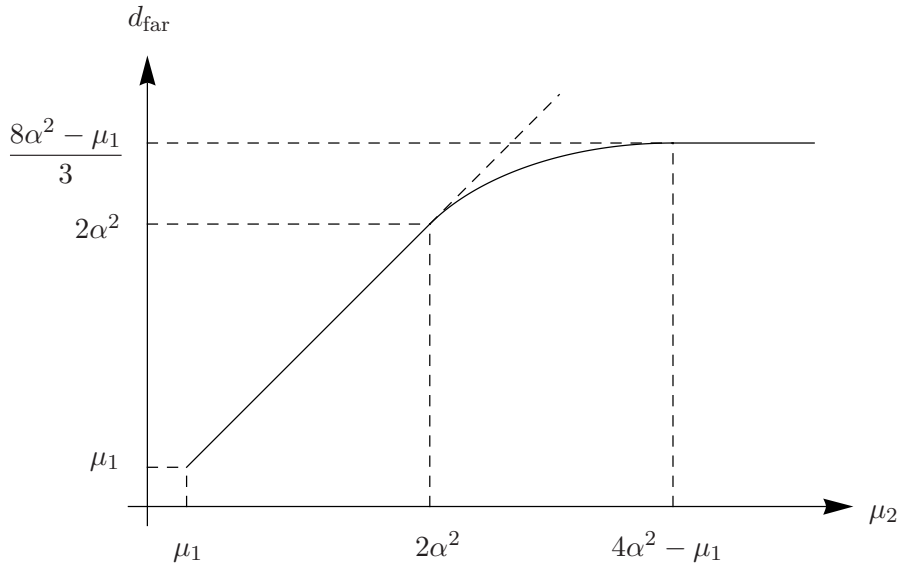

Figure 9.8: Schematic plot of the function $d_{\text{far}}(\mu_2)$ which gives the distance from the origin to the far side of the region of oscillations in the $N_f = 2$ case. The smaller mass $\eta_1 = \mu_1 i$ is considered fixed, and is within the strip ($\mu_1 < 2\alpha^2$). If $\eta_2 = \mu_2 i$ is also within the strip, then the oscillations lie within a circle, extending to $\mu_2 i$. If $\mu_2 i$ is beyond the critical point $(4\alpha^2 - \mu_1)i$, then it has no effect on the size of the oscillating region which is an ellipse extending to $\left(\frac{8\alpha^2-\mu_1}{3}\right) i$. Here, the quark can be considered to have decoupled completely, giving the $N_f = 1$ case. The graph also shows the transition regime, where $\mu_2 i$ is outside the strip, but below the critical mass. Here, the oscillating region lies somewhere between a circle and an ellipse, and does not extend as far as $\mu_2 i$.

We now consider a higher value of $\alpha = 3$ (recalling that we must have $\alpha > \sqrt{2\pi}$ if any oscillations are to be seen in the complex plane), see Figure 9.10. We see that the presence of the masses on the imaginary axis can induce oscillations in the density profile of the real eigenvalues, provided that the masses are sufficiently far apart, although the density still appears to remain positive, at least for this value of α.

We refer the interested reader to our paper [Ake11] for further examples with different choices of parameters, including graphs which directly compare the unquenched and quenched cases.

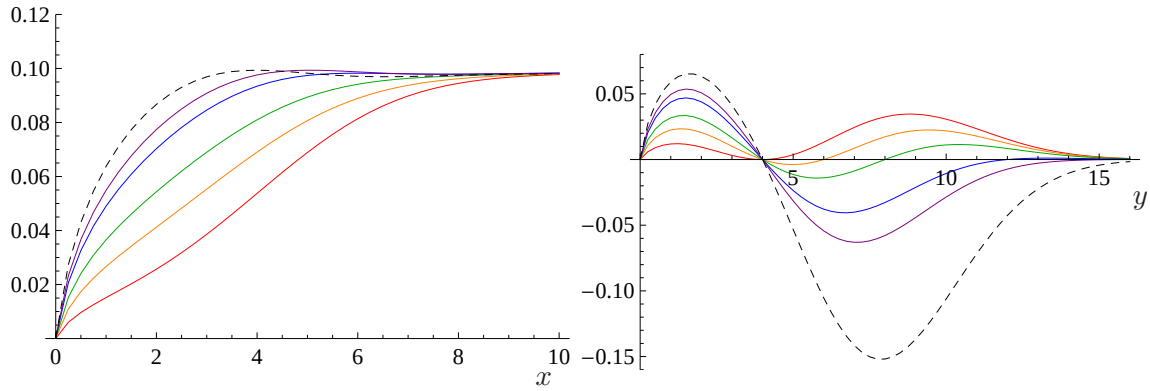

Figure 9.9: The densities of real (left) and imaginary (right) Dirac eigenvalues at weak non-Hermiticity for $\alpha = 2$, with one mass located at $\eta_1 = 4i$, and a second mass at $\eta_2 = 4i$ (red), $\eta_2 = 6i$ (orange), $\eta_2 = 8i$ (green), $\eta_2 = 12i$ (blue) and $\eta_2 = 16i$ (purple), plus the case with no second mass (black, dashed); $\nu = 0$ in all cases.

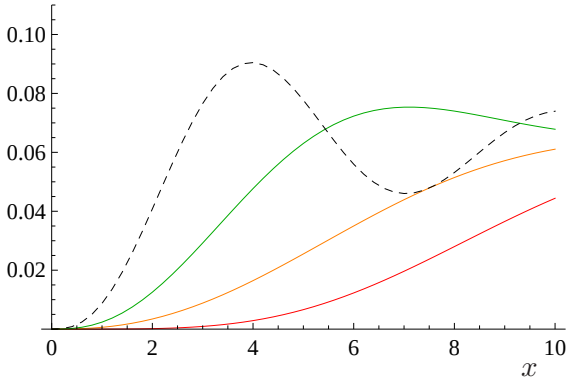

Figure 9.10: The densities of real Dirac eigenvalues at weak non-Hermiticity for $\alpha = 3$, with one mass located at $\eta_1 = 0$, and a second mass at $\eta_2 = 0$ (red), $\eta_2 = 9i$ (orange) and $\eta_2 = 18i$ (green), plus the case with no second mass (black, dashed); $\nu = 0$ in all cases.

Chapter 10

Universality

For certain Hermitian random matrix ensembles with independently distributed matrix elements, the macroscopic eigenvalue densities appear to depend only on the symmetries of the matrices, and not on the precise probability density functions of the individual elements. This is an example of a phenomenon called universality. Once correlations between elements are introduced, the macroscopic densities may no longer be universal, but it appears that microscopic densities (and other correlation functions) may still remain so. We refer to Appendix A.1 of [Meh04] for further background information, and to [Kho09] for a discussion of the non-Hermitian case, where universality may also be observed.

Universality is at the heart of the applicability of RMT to QCD, for example, and so it is interesting to explore the universal properties of the chiral ensembles. See §2.2.2 for some relevant references, and also [Ake02b] for a discussion of the non-Hermitian chiral case.

The purpose of this brief chapter is to investigate the apparent extent of the universality of non-Hermitian chiral ensembles, by showing the results of a series of Monte Carlo simulations for several different ensembles, and comparing the microscopic eigenvalue densities. We will consider here the weakly non-Hermitian limit, which perhaps has the greatest practical applicability. We will look at the density of real Dirac eigenvalues, since (i) there will be a large number of such eigenvalues, thereby reducing statistical errors, and (ii) because it is easier to compare 1-dimensional distributions visually. We will also look at the distribution of the lowest real eigenvalue which is not known analytically, even for the chGinOE.

We compare four ensembles, all of which involve 'chiral' block matrices with real elements; in all cases, we fix $N_f = 0$, $\nu = 0$ and the non-Hermiticity parameter

$\alpha = \sqrt{0.2}$. The ensembles are:

1. The chiral non-Hermitian ensemble presented in this thesis (the chGinOE) and defined by eqs. (2.5) and (2.6). This is chosen as a base case to cross-check our methodology, and to identify the size of the finite-N errors, since we already know the precise analytic form of the weak density (although not of the distribution of the lowest eigenvalue).

2. The Stephanov one-matrix model [Ste96] but with real matrix elements, where the matrix Q in eq. (2.5) is replaced with the identity matrix (multiplied by $\sqrt{N}$ under our choice of scaling convention). This model is, in some sense, closer to the physics than the chGinOE because the chemical potential is non-stochastic.

3. A modification of the chGinOE, where the Gaussian distribution of matrix elements is replaced with two Dirac delta functions as follows:

$$p(x) = \tfrac{1}{2}\big\{\delta(x-1) + \delta(x+1)\big\}. \tag{10.1}$$

   The mean and the variance of the matrix elements is hence the same as for the chGinOE (i.e. zero and unity respectively), and the matrix elements are still independent.

4. An alternative modification of the chGinOE, where we retain Gaussian distributions, but impose a fixed correlation ρ between all pairs of matrix elements. (This is effectively a single-factor model.) We choose $\rho = 0.5$. Although the Dirac matrix already contains correlated pairs of elements, here we are introducing a much stronger coupling between all the elements in the matrix.

We generated 100 000 random matrices of each type, with (Wishart) matrix size $N = 30$, then we compared all the results against the known large-N limit for the chGinOE given in Chapter 8.

Figure 10.1 shows the Monte Carlo results for each of the four cases, overlaid onto a plot of the analytic formula. For the third and fourth cases, it is necessary to rescale the analytic formula, so that the average eigenvalue spacings are consistent[1]. We do this by fitting to the plateau region $2 \leq x \leq 8$. We make another technical point: each histogram in Figure 10.1 may contain several eigenvalues from the same matrix

[1]This is a process known as unfolding, see [Guh98].

realisation, and so the histogram entries are not, strictly speaking, independent. However, the error bars are calculated on the assumption that they are, and hence should be treated as indicative only.

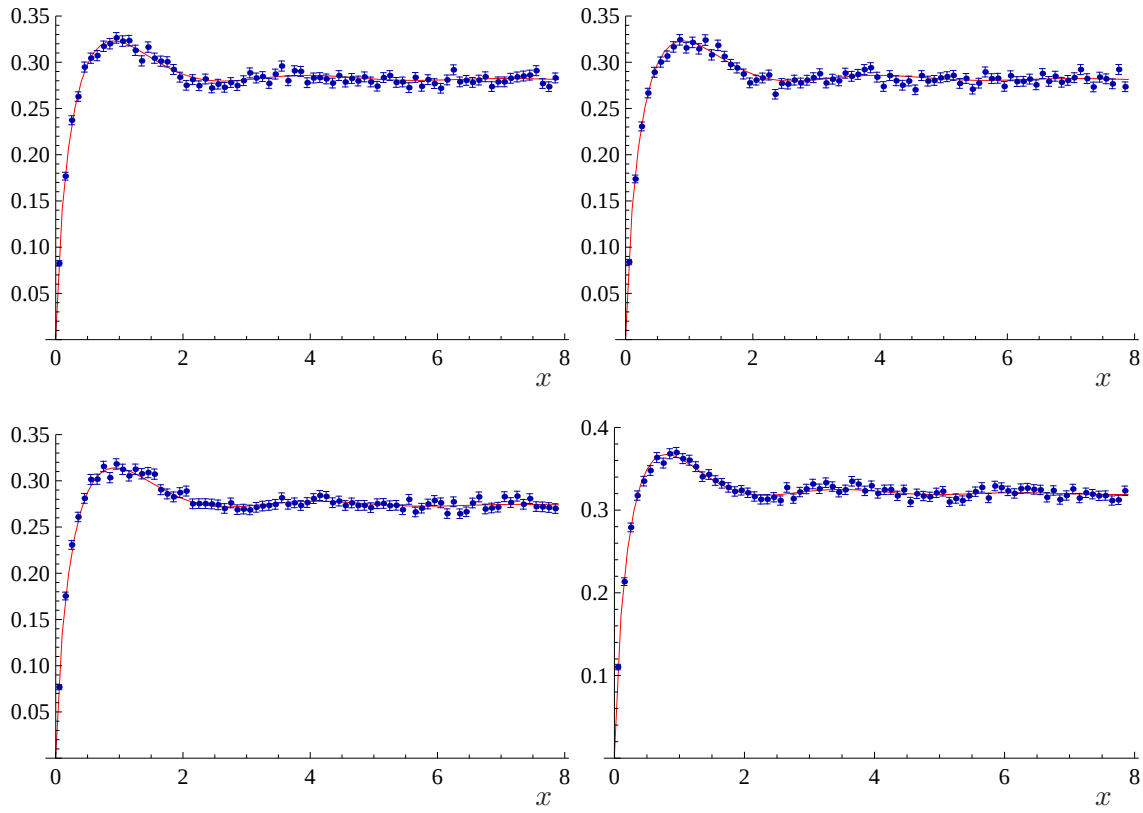

Figure 10.1: Densities of real Dirac eigenvalues at weak non-Hermiticity, with $\alpha^2 = 0.2$ and $\nu = 0$. Monte Carlo results (blue dots with error bars) for the chGinOE (top, left), Stephanov model (top, right), delta function distribution (bottom, left) and correlated Gaussians (bottom, right), all superimposed on the analytic result (scaled in bottom two cases) for the chGinOE density (red curve). See text for further details.

In the first plot, the Monte Carlo results and the analytical graph are for the same model, and so this demonstrates that finite-N effects are unlikely to cause significant problems[1] (although for a more conclusive statement concerning the other ensembles, one should repeat all the analysis for a higher value of N). The remaining three graphs show very impressive fits, indicating that universality is indeed highly likely

[1]See also Figure 8.5 on page 120 for an indication that the $N = 30$ result is likely to be very close to the large-N limit for the range of scaled eigenvalues x considered.

to be a feature in all these cases. We emphasize that the formula for the analytical curve is exceptionally non-trivial, and differs significantly near the origin from the Hermitian case (i.e. $\alpha = 0$, also with $\nu = 0$, see Figure 8.7, left).

Figure 10.2 shows the lowest eigenvalue distribution for the Stephanov model, overlaid on the corresponding distribution for the chGinOE. Both sets of data are from Monte Carlo, and the error bars in the latter case are not shown (but are expected to be of the same magnitude as those in the former case). Again, here, the arguments for universality are compelling.

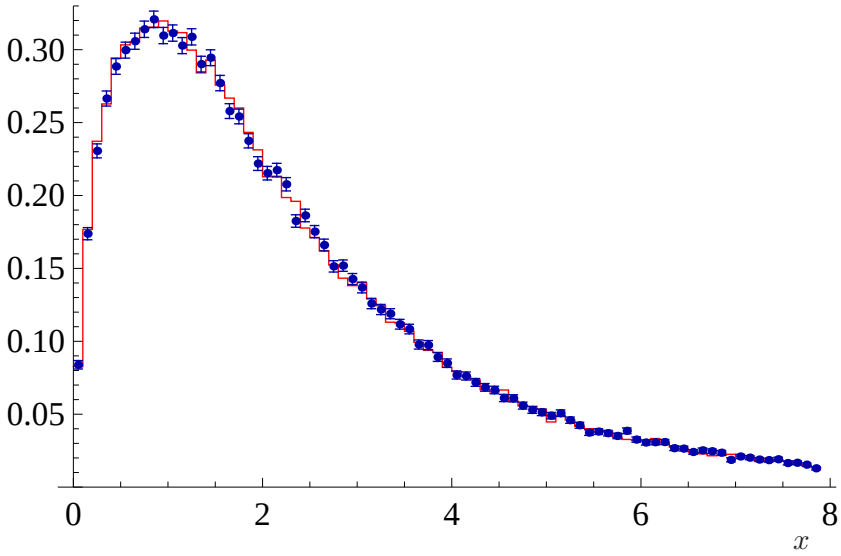

Figure 10.2: Lowest real Dirac eigenvalue distribution at weak non-Hermiticity, with $\alpha^2 = 0.2$ and $\nu = 0$. Monte Carlo results for the Stephanov model (blue dots with error bars), superimposed on Monte Carlo results for the chGinOE (red histogram, no error bars shown). See text for further details.

Although there is no intention to draw any definitive conclusions from the results in this chapter, we hope that they indicate that our analytical formulas for the chGinOE may indeed have the wider applicability that is anticipated. Whether two-colour QCD with chemical potential belongs to the same universality class is something that ultimately must be verified by comparison with results from lattice gauge theory.

Chapter 11

Conclusions

We have solved the $\beta = 1$ chiral Ginibre random matrix ensemble (chGinOE) for arbitrary non-Hermiticity parameter μ. We began by finding the joint probability density function for the eigenvalues, and then re-expressed this in a factorised form. We then derived compact expressions for the correlation functions, involving Pfaffians of kernels and skew-orthogonal polynomials, valid for an arbitrary number of flavours of virtual quarks. We also found analytical results for two large-N microscopic limits, at strong and weak non-Hermiticity. In the unquenched case, both of these limits can show interesting properties, such as regions of the complex plane containing large oscillations of the eigenvalue density function. We were able to determine where these regions are located, and how they depend on the masses of the virtual quarks.

From a mathematical viewpoint, we have demonstrated a new technique for determining the kernel and skew-orthogonal polynomials, by relating the kernel to an expectation of characteristic polynomials which we evaluate using a Berezin integral transform. This same method can be applied to the (non-chiral) $\beta = 1$ Ginibre ensemble as we showed, rederiving a result that was discovered only very recently.

However, there are many mathematical properties of the chGinOE that are, as yet, unknown. It would be interesting (both theoretically and practically) to derive analytic expressions for the distributions of individual eigenvalues, and the related gap probability distributions, extending our work in [Ake09b] for the chiral $\beta = 2$ and $\beta = 4$ ensembles. Such proofs are expected to be fairly complicated, especially since we do not yet have an elementary proof (i.e. using ordinary rather than Berezin integration) that the skew-orthogonal polynomials for the chGinOE

are indeed skew-orthogonal. Additionally, we have not yet considered in any detail the behaviour of the 2-point (and higher) correlation functions for the unquenched ensembles (although we did derive generic formulas for these). Nor did we investigate the scaling limits in parts of the spectrum other than in the vicinity of the origin, which may show new and interesting features.

We have only conjectured the extent to which our results may be universal, based on limited Monte Carlo analysis of some closely related ensembles. Further work in this direction (especially analytical) would be particularly challenging, although the results would be very illuminating.

Finally, we turn to the applications. In order to determine the validity of the chGinOE as a model for low-energy 2-colour QCD, it will be necessary to compare our results for the eigenvalue densities against those obtained from computer simulations of lattice gauge theory (LGT). This is possible for the quenched case, and also for the unquenched case where we have an even number of quark flavours whose masses come in degenerate pairs, thereby ensuring that the probabilities remain positive (and this is true of full 2-colour QCD at non-zero μ, and not just of RMT). The chGinOE can also be compared against lattice simulations of so-called adjoint QCD (a version of QCD in which the fermion fields are in the adjoint representation of $SU_c(3)$), when staggered fermions are used. Suitable LGT simulations are in fact already being undertaken at the time of writing, and preliminary results show excellent agreement; we look forward with interest to analysing the results in more detail.

Appendix A

Some useful preliminary results

In this appendix, we derive a number of elementary results that are used in the body of the text; in a few cases, where results are already well-known, we merely state them without proof.

A.1 Integrals

A.1.1 Some integrals on the real line

Firstly, we have the familiar result that, for real $\alpha > 0$,

$$\int_{-\infty}^{\infty} e^{-\alpha x^2} dx = \sqrt{\frac{\pi}{\alpha}}, \tag{A.1}$$

and so, for $\alpha > 0$,

$$\int_{-\infty}^{\infty} e^{-\alpha x^2 + \beta x} dx = \sqrt{\frac{\pi}{\alpha}}\, e^{\beta^2/4\alpha}. \tag{A.2}$$

It easily follows that ($\alpha > 0$, $\gamma > 0$, $\beta \in \mathbb{R}$)

$$\int_{-\infty}^{\infty} dx \int_{-\infty}^{\infty} dy \, \exp\left\{-\tfrac{1}{2}(\alpha x^2 + \gamma y^2) \pm i\beta xy\right\} = \frac{2\pi}{\sqrt{\alpha\gamma + \beta^2}}. \tag{A.3}$$

Using the power series representation of the physicists' Hermite polynomials

$$H_k(x) = k! \sum_{m=0}^{[k/2]} \frac{(-1)^m}{m!\,(k-2m)!} (2x)^{k-2m}, \tag{A.4}$$

with $[x]$ denoting the integer part of x, we can use eq. (A.1) to show that for $k \geq 0$

$$\int_{-\infty}^{\infty} dx\, e^{-x^2} (\lambda + icx)^k = \sqrt{\pi} \left(\frac{c}{2}\right)^k H_k\left(\frac{\lambda}{c}\right). \tag{A.5}$$

This result is also found as eq. 8.951 of [Gra07]. Now, we have

$$\int_0^\infty dy\, e^{-\beta y}\, y^\alpha = \frac{\Gamma(\alpha+1)}{\beta^{\alpha+1}} \tag{A.6}$$

for $\alpha > -1$ and $\beta > 0$. Therefore, for $\beta > 0$ and $\gamma > 0$:

$$\int_0^\infty dy\, e^{-\beta y}\, L_j^\nu\left(\frac{y}{\gamma}\right) y^\nu = (-1)^j\, \frac{(j+\nu)!}{j!}\, \frac{(1-\beta\gamma)^j}{\beta^{j+\nu+1}\gamma^j} \tag{A.7}$$

which follows from eq. (A.6) and the representation of the generalised Laguerre polynomials $L_j^\nu(u)$ as a power series

$$L_j^\nu(u) = \sum_{k=0}^{j} (-1)^k\, \frac{(j+\nu)!}{(j-k)!\, k!\, (k+\nu)!}\, u^k. \tag{A.8}$$

A.1.2 Some integrals in the complex plane

We begin with (for integers $p, q \geq 0$)

$$\int_{\mathbb{C}} \frac{d^2z}{\pi} e^{-|z|^2} z^p z^{*q} = p!\, \delta_{pq} \tag{A.9}$$

which is easily proved by switching to polar coordinates. Using this, we can deduce the following results:

$$\int_{\mathbb{C}} \frac{d^2z}{\pi} e^{-|z|^2} \left(|z|^2 + u\right)^k = k! \sum_{j=0}^{k} \frac{u^j}{j!} \tag{A.10}$$

and

$$\int_{\mathbb{C}} \frac{d^2z}{\pi} e^{-|z|^2} (iz+\lambda)^k (iz^*+\lambda)^{k+\nu} = (-1)^k \lambda^\nu k! L_k^\nu(\lambda^2) \tag{A.11}$$

where $L_k^\nu(x)$ is the generalised Laguerre polynomial. To prove the latter result, for example, it is merely necessary to expand the binomials to give a double sum. Application of eq. (A.9) then reduces this to a single sum, which can be identified with the power series representation of the Laguerre polynomials in eq. (A.8).

A.1.3 Saddle point method

The standard (real) saddle point formula (also known as Laplace's method) states that

$$\int_0^\infty dx\, f(x)\, e^{-Ng(x)} \sim \sqrt{\frac{2\pi}{Ng''(x_s)}}\, f(x_s)\, e^{-Ng(x_s)} \tag{A.12}$$

at large N, where $g(x)$ has a minimum at x_s. The proof follows by expanding $g(x)$ about its minimum, and integrating the second order contribution using eq. (A.1).

Using this, it is straightforward to show that, for large N, and real a, b and c,

$$\int_0^\infty dt\, t\, e^{-t}\, (a-bt)^N (a-ct)^{N+\nu} \sim \frac{(-1)^\nu 2^{2N+\nu+1}}{\sqrt{\pi}} \sqrt{N}\, N!\, (N+\nu)!\, b^N c^{N+\nu} \exp\left[-\frac{a}{2}\left(\frac{1}{b}+\frac{1}{c}\right)\right], \quad \text{(A.13)}$$

which is used in the text in §5.2.2.

A.2 Matrices

A.2.1 Differentiation of product of two matrices

Suppose we have the product of two matrices $A = BC$, or in component form, $A_{ij} = \sum_k B_{ik} C_{kj}$. Then the partial differentials are given by

$$\frac{\partial A_{ij}}{\partial B_{pq}} = \delta_{ip} C_{qj} \qquad \text{and} \qquad \frac{\partial A_{ij}}{\partial C_{pq}} = \delta_{jq} B_{ip}. \quad \text{(A.14)}$$

A.2.2 Differentiation of inverse of a matrix

We determine the partial differential of an element of the inverse of a square matrix with respect to an element of the matrix itself. Let M be any square matrix, and I the identity of the same size. Then

$$0 = dI = d(MM^{-1}) = dM\, M^{-1} + M\, d(M^{-1}). \quad \text{(A.15)}$$

Therefore

$$d(M^{-1}) = -M^{-1}\, dM\, M^{-1}. \quad \text{(A.16)}$$

It follows that

$$\begin{aligned} \frac{\partial (M^{-1})_{ij}}{\partial M_{mn}} &= -\sum_{s,t} (M^{-1})_{is} \frac{\partial M_{st}}{\partial M_{mn}} (M^{-1})_{tj} \\ &= -\sum_{s,t} (M^{-1})_{is} \delta_{sm} \delta_{nt} (M^{-1})_{tj} \\ &= -(M^{-1})_{im} (M^{-1})_{nj}. \end{aligned} \quad \text{(A.17)}$$

A.2.3 Some properties of orthogonal matrices

Let O be an orthogonal matrix. Then

$$O^T O = I \qquad \Rightarrow \qquad d(O^T O) = 0 \qquad \Rightarrow \qquad dO^T\, O = -O^T\, dO. \tag{A.18}$$

Furthermore,

$$O^T\, dO = -(O^T\, dO)^T, \tag{A.19}$$

i.e. $O^T\, dO$ is anti-symmetric. Now, O has $\frac{N(N-1)}{2}$ degrees of freedom, and so the same is true of $O^T\, dO$. But any anti-symmetric N-by-N matrix has $\frac{N(N-1)}{2}$ independent elements. Therefore, the strictly lower triangular elements of $O^T\, dO$ can be considered independent of each other. (Note that the same is not true of dO. All N^2 elements may be different, but they are not independent, since the number of degrees of freedom is smaller.) In fact, since we work with $O(N)/O(2)^{N/2}$ (when N is even), we can consider that the $\frac{N^2}{2} - N$ independent entries lie in the elements below the 2-by-2 blocks on the diagonal. A similar argument applies to the case when N is odd.

A.2.4 Similarity transformations

Suppose M is a square matrix with an eigenvalue λ, i.e. there exists some vector $\mathbf{v} \neq \mathbf{0}$, such that

$$M\mathbf{v} = \lambda\mathbf{v}. \tag{A.20}$$

Now consider the matrix SMS^{-1}, where S is some other non-singular square matrix of the same size as M. Then

$$(SMS^{-1})\,(S\mathbf{v}) = SM\mathbf{v} = S\lambda\mathbf{v} = \lambda(S\mathbf{v}). \tag{A.21}$$

Therefore, the matrix SMS^{-1} also has λ as an eigenvalue. S is known as a similarity transformation.

Some specific cases of similarity transformations which are mentioned in the text are listed (without proof) in Table A.1. All matrices are assumed to be square. An almost-upper-triangular matrix has 2-by-2 blocks down the diagonal (plus a 1-by-1 block if the matrix size N is odd), with all the entries below these blocks being zero.

Complex matrices		
Spectral decomposition	$H = U\Lambda U^{-1}$	H Hermitian, U unitary, Λ diagonal and real (containing eigenvalues)
Schur decomposition	$M = U\Delta U^{-1}$	M arbitrary, U unitary, Δ upper-triangular, eigenvalues on diagonal
QZ decomposition	$A = QSZ^{-1}$ $B = QTZ^{-1}$	A, B arbitrary, Q, Z unitary, S, T upper-triangular
Real matrices		
Spectral decomposition	$S = O\Lambda O^{-1}$	S symmetric, O orthogonal, Λ diagonal (containing eigenvalues)
Schur decomposition	$M = O\Delta O^{-1}$	M arbitrary, O orthogonal, Δ almost-upper-triangular
QZ decomposition	$A = QSZ^{-1}$ $B = QTZ^{-1}$	A, B arbitrary, Q, Z orthogonal, S almost-upper-triangular, T upper-triangular

Table A.1: Summary of similarity transformations referred to in the text.

A.2.5 Some properties of block diagonal matrices

Consider a block diagonal matrix M, i.e. a square matrix that is zero everywhere, apart from in square blocks down the diagonal. Then

(i) *The set of eigenvalues of M is the union of the set of eigenvalues of each of the blocks treated as matrices in their own right.*

(ii) *The eigenvalues of M remain unchanged if we make any of the element(s) above (or below, but not both) the block-diagonal non-zero.*

And, as simple corollaries,

(iii) *The determinant of M is simply the product of the determinants of the individual blocks.*

(iv) *The determinant of M remains unchanged if we make any element(s) above (or below, but not both) the block-diagonal non-zero.*

The proofs of these are straightforward, and are omitted.

A.2.6 Some properties of Pfaffians

For an anti-symmetric matrix $A = (A_{ij})$ of size N-by-N (where N is even), the Pfaffian is given by

$$\mathrm{Pf}\, A = \sum_{\pi \in P_N} \mathrm{sgn}(\pi) \prod_{i=1}^{N/2} A_{\pi(2i-1),\pi(2i)} \tag{A.22}$$

where P_N is the set of partitions into pairs of the integers from 1 to N, without regard either to the order of the two numbers making up each pair, or to the overall order of the pairs. In fact, this can be taken to be the definition of the Pfaffian, although an alternative definition as the square root of the determinant is more common. We use eq. (A.22) with $A_{ij} = M_{ij} - M_{ji}$ for arbitrary N-by-N matrix M, to write

$$\mathrm{Pf}(M - M^T) = \sum_{\pi \in P_N} \mathrm{sgn}(\pi) \prod_{i=1}^{N/2} (M_{\pi(2i-1),\pi(2i)} - M_{\pi(2i),\pi(2i-1)}). \tag{A.23}$$

We now perform two steps. First, we multiply out the product, giving

$$\mathrm{Pf}(M - M^T) = \sum_{\rho \in R_N} \mathrm{sgn}(\rho) \prod_{i=1}^{N/2} M_{\rho(2i-1),\rho(2i)} \tag{A.24}$$

where R_N is the set of partitions of pairs where we *do* now distinguish the order of the two items within a pair. Second, we also now wish to distinguish the overall ordering of the pairs, which merely introduces an additional factor of $(\frac{N}{2})!$. In fact, this is then simply equivalent to summing over all *permutations* of the integers from 1 to N:

$$\mathrm{Pf}(M - M^T) = \frac{1}{(\frac{N}{2})!} \sum_{\sigma \in S_N} \mathrm{sgn}(\sigma) \prod_{i=1}^{N/2} M_{\sigma(2i-1),\sigma(2i)}. \tag{A.25}$$

A.2.7 Differentiation of determinants and Pfaffians

We can differentiate the determinant of a square matrix with respect to any one of its elements as follows:

$$\frac{\partial}{\partial M_{ij}} \det M = \det M \, (M^{-1})_{ji}. \tag{A.26}$$

This can be proven by noting that

$$\frac{\partial}{\partial M_{ij}} \det M = C_{ij}, \tag{A.27}$$

which follows from the definition of the co-factor matrix C. But we also know that we can write the inverse of a matrix as

$$(M^{-1})_{ji} = \frac{1}{\det M}\,(C^T)_{ji}, \tag{A.28}$$

and so the result eq. (A.26) follows immediately.

Since $\det A = (\mathrm{Pf}\, A)^2$ for any N-by-N anti-symmetric matrix A with N even, it follows easily from eq. (A.26) that the differential of a Pfaffian is given by

$$\frac{\partial}{\partial A_{ij}}\,\mathrm{Pf}\, A = \tfrac{1}{2}\,\mathrm{Pf}\, A\,(A^{-1})_{ji}. \tag{A.29}$$

To differentiate again, we use eq. (A.29) itself, together with eq. (A.17), to show that

$$\frac{\partial^2}{\partial A_{ij}\partial A_{pq}}\,\mathrm{Pf}\, A = \mathrm{Pf}\, A\left\{\tfrac{1}{4}(A^{-1})_{qp}(A^{-1})_{ji} - \tfrac{1}{2}(A^{-1})_{qi}(A^{-1})_{jp}\right\}. \tag{A.30}$$

A.2.8 Some properties of characteristic polynomials

Let M be an m-by-m matrix. Then

$$\frac{\partial^{m-1}}{\partial u^{m-1}}\,\det(M-u)\Big|_{u=0} = (-1)^{m-1}\,(m-1)!\,\mathrm{Tr}\, M, \tag{A.31}$$

$$\frac{\partial^{m}}{\partial u^{m}}\,\det(M-u) = (-1)^{m}\,m!. \tag{A.32}$$

These can be proven by noting that only the diagonal elements of the matrix $M-u$ depend on u, and so the only terms in the determinant that survive differentiation by u at least $m-1$ times must contain the product of all the diagonal elements. Therefore,

$$\begin{aligned}\frac{\partial^{m-1}}{\partial u^{m-1}}\,\det(M-u) &= \frac{\partial^{m-1}}{\partial u^{m-1}}\,\prod_{j=1}^{m}(M_{jj}-u)\\ &= (-1)^{m-1}\,(m-1)!\,\mathrm{Tr}\, M + (-1)^m\,m!\,u,\end{aligned} \tag{A.33}$$

and both results follow immediately.

A.3 An integral over ordered variables

For even n, we have

$$\begin{aligned}&\int_{\mathbb{R}} dx_1 \ldots \int_{\mathbb{R}} dx_n \prod_{j=2}^{n}\Theta(x_j - x_{j-1}) \prod_{k=1}^{n} w(x_k)\,\Delta_n(\{x\})\\ &\quad= \frac{1}{(\frac{n}{2})!}\int_{\mathbb{R}} dx_1 \ldots \int_{\mathbb{R}} dx_n \prod_{j=1}^{n/2}\Theta(x_{2j} - x_{2j-1}) \prod_{k=1}^{n} w(x_k)\,\Delta_n(\{x\}),\end{aligned} \tag{A.34}$$

where $\Theta(x)$ is the Heaviside step function, $\Delta_n(\{x\})$ is the Vandermonde determinant (see eq. (2.2)) and $w(x)$ is any weight function for which the integrals exist.

The proof is straightforward, and uses the 'alternating variables' method (see §5.5 of [Meh04] for further details).

A.4 Grassmann variables

A.4.1 Definition

We present a brief introduction only to those concepts that we require in the text (specifically, in §5.2.1), and refer to textbooks such as [Efe97a; Sto99] for further details.

We define an algebra with generators η_i $(i = 1, \ldots, N)$ that anti-commute, i.e. $\{\eta_i, \eta_j\} \equiv \eta_i\eta_j + \eta_j\eta_i = 0$. Such an algebra is known as a Grassmann or exterior algebra. It follows that $\eta_i^2 = 0$ for all i. The algebra is a linear space of 2^N dimensions, with a general element of the form

$$\eta = c + \sum_{i=1}^{N} c_i\eta_i + \sum_{i<j}^{N} c_{ij}\eta_i\eta_j + \sum_{i<j<k}^{N} c_{ijk}\eta_i\eta_j\eta_k + \ldots + c_{1\ldots N}\eta_1\ldots\eta_N, \tag{A.35}$$

where the coefficients are either real or complex. Note that the basis elements may be partitioned into sets that either commute or anti-commute amongst themselves, although two arbitrary elements of the algebra will neither commute nor anti-commute with each other.

A.4.2 Berezin integration

We define the Berezin integral as follows:

$$\int d\eta = 0, \qquad \int \eta\, d\eta = 1. \tag{A.36}$$

This is not to be interpreted as integration in any classical sense, e.g. it is not the limit of a sequence of sums; it is merely a particular kind of mapping from functions of Grassmann variables to ordinary numbers. This mapping has certain properties (such as linearity) in common with classical integration. Since

$$\iint d\eta_1 d\eta_2\, \eta_1\eta_2 = \iint d\eta_2 d\eta_1\, \eta_2\eta_1 \tag{A.37}$$

by relabelling, but

$$\iint d\eta_2 d\eta_1 \, \eta_2\eta_1 = -\iint d\eta_2 d\eta_1 \, \eta_1\eta_2 \tag{A.38}$$

from the anti-commutivity of the Grassmann variables, it follows that $d\eta_1 d\eta_2 + d\eta_2 d\eta_1 = 0$, i.e. the differentials anti-commute as well. Indeed, for consistency, the differentials also have to anti-commute with the Grassmann variables.

A particularly useful result (and in fact the principal reason for introducing Grassmann variables and Berezin integration) is

$$\int d\eta \, \exp\Big\{ -\sum_{i,j}^{N} \eta_i^* M_{ij} \eta_j \Big\} = \det M, \tag{A.39}$$

where $d\eta \equiv d\eta_1^* d\eta_1 \ldots d\eta_N^* d\eta_N$, and M is some ordinary-valued N-by-N square matrix. Although a 'complex conjugation' operator (*) can be defined on the algebra, for our purposes the starred variables are simply another set of independent Grassmann variables. For a proof of eq. (A.39), we refer to textbooks.

A.4.3 Hubbard-Stratonovich transformations

Returning now to ordinary integration, we consider the integral

$$\mathcal{I} \equiv \int_{\mathbb{R}} dx \, \exp\left\{-x^2 + 2xA\right\} \tag{A.40}$$

where A is a commuting element of a Grassmann algebra. We can complete the square as follows:

$$\mathcal{I} = \exp\left\{A^2\right\} \int_{\mathbb{R}} dx \exp\Big\{-(x-A)^2\Big\}. \tag{A.41}$$

However, the question now is whether we can naïvely change variables in the integral over x, as if A were an ordinary (real) number.

In general, for commuting A, we can expand a function as a series as follows

$$f(x+A) = f(x) + f'(x)A + \frac{f''(x)}{2}A^2 + \ldots. \tag{A.42}$$

(Typically, this series will terminate. For example, if $A = \eta^*\eta$ for two basis elements of the algebra, then $A^n = 0$ for $n \geq 2$.) Hence

$$\int_a^b dx \, f(x-A) = \int_a^b dx \, f(x) - A\left[f(b) - f(a)\right] + \frac{A^2}{2}\left[f'(b) - f'(a)\right] + \ldots. \tag{A.43}$$

Now with $f(x) = e^{-x^2}$, $a = -\infty$ and $b = \infty$, we see that every term on the right-hand side, apart from the first one, is equal to zero[1]. Therefore

$$\begin{aligned}\mathcal{I} &\equiv \int_{\mathbb{R}} dx\, \exp\left\{-x^2 + 2xA\right\} \\ &= \exp\left\{A^2\right\} \int_{\mathbb{R}} dx\, e^{-x^2} \\ &= \sqrt{\pi}\, \exp\left\{A^2\right\}. \end{aligned} \tag{A.44}$$

So the naïve change of variables $x - A \to x$ works without any problem in this case. On introducing an additional scaling parameter $c \geq 0$, and rearranging, the previous result becomes

$$\exp(-cA^2) = \int_{\mathbb{R}} \frac{dx}{\sqrt{\pi}} \exp\{-x^2 \pm 2i\sqrt{c}xA\}, \tag{A.45}$$

which is known as the real Hubbard-Stratonovich transformation. This can be generalised to a complex version

$$\exp(-cAB) = \int_{\mathbb{C}} \frac{d^2z}{\pi} \exp\{-|z|^2 \pm i\sqrt{c}(zA + z^*B)\}, \tag{A.46}$$

where A and B are both arbitrary commuting elements of a Grassmann algebra. The complex case can be proved in a similar way to the real case.

We should add that, more generally, one can define the Hubbard-Stratonovich transformation for the case where both ordinary and Berezin integrals are involved (a key component of the supersymmetry method), although that is not needed here.

[1]Of course, this will not be true for arbitrary f, a and b. Any such terms that do not vanish are known as Efetov-Wegner boundary terms.

Appendix B

Skew-orthogonal polynomials from matrix expectations

In §4.2 we showed how to write the skew-orthogonal polynomials in terms of the kernel. However, the kernel can, in turn, be expressed in terms of expectations (over matrix ensembles) of characteristic polynomials (see eq. (5.20)). We show in this appendix how the kernel can then be 'eliminated', allowing the skew-orthogonal polynomials to be written directly in terms of matrix averages.[1]

Our result here in fact has more general applicability than to the chGinOE. For any ensemble of random matrices M whose JPDF has the form eq. (4.7) involving a bivariate weight function $\mathcal{F}(u,v)$ of the form eq. (4.8) for arbitrary weight $w(z)$, the skew-orthogonal polynomials of $\mathcal{F}(u,v)$ can be written as matrix expectations over M in the way that we show. In the case of the chGinOE, the matrix M corresponds to the Wishart matrix W, rather than to the Dirac matrix $\mathcal{D}$.

We begin by establishing some preliminary results. First, for a $2k$-by-$2k$ matrix M from any random matrix ensemble, we have the 'quenching' result that

$$\lim_{u\to\infty} \frac{(u-v)\langle \det(M-u)\,\det(M-v)\rangle}{u^{2k+1}} = \langle \det(M-v)\rangle. \tag{B.1}$$

Second, using the fact that, for some m-times differentiable function $F(u,v)$,

$$\frac{\partial^m}{\partial u^m}\Big\{(u-v)\,F(u,v)\Big\} = m\,\frac{\partial^{m-1}}{\partial u^{m-1}}F(u,v) + (u-v)\,\frac{\partial^m}{\partial u^m}F(u,v) \tag{B.2}$$

(which is not completely trivial, but is easy to prove by induction), we can establish

[1] We published alternative proofs of these results (due principally to Mario Kieburg) in [Ake10b].

that

$$\frac{\partial^{2k}}{\partial u^{2k}}\Big\{(u-v)\langle\det(M-u)\,\det(M-v)\rangle\Big\}\Big|_{u=0} = -(2k)!\Big\{\langle\det(M-v)\,\mathrm{Tr}\,M\rangle + v\,\langle\det(M-v)\rangle\Big\}, \tag{B.3}$$

where we also used some basic properties of determinants, see eqs. (A.31) and (A.32).

We can now determine the relationships between the skew-orthogonal polynomials and matrix expectations. Using eqs. (4.29), (5.20) and (B.1), we have

$$\begin{aligned} q_{2k}(z) &= h_k \lim_{u\to\infty} \frac{\mathcal{K}_{2k+2}(u,z)}{u^{2k+1}} \\ &= \lim_{u\to\infty} \frac{(u-z)}{u^{2k+1}} \langle\det(M-u)\det(M-z)\rangle_{2k} \\ &= \langle\det(M-z)\rangle_{2k}. \end{aligned} \tag{B.4}$$

Similarly, using eqs. (4.30), (5.20), (B.3) and (B.4), and setting $c = 0$,

$$\begin{aligned} q_{2k+1}(z) &= -\frac{h_k}{(2k)!}\frac{\partial^{2k}}{\partial u^{2k}}\mathcal{K}_{2k+2}(u,z)\Big|_{u=0} \\ &= -\frac{1}{(2k)!}\frac{\partial^{2k}}{\partial u^{2k}}\left((u-z)\langle\det(M-u)\det(M-z)\rangle_{2k}\right)\Big|_{u=0} \\ &= \langle\det(M-z)\;\mathrm{Tr}\,M\rangle_{2k} + z q_{2k}(z). \end{aligned} \tag{B.5}$$

Eqs. (B.4) and (B.5) extend the known results for the $\beta = 4$ ensemble [Kanz02].

Appendix C

The $\beta = 4$ chiral ensemble: algebraic structure

The $\beta = 4$ non-Hermitian chiral ensemble (chGinSE) was introduced in [Ake05b] where it was solved for the case with degenerate pairs of quark masses, and was revisited in [Ake07a] where the solution was extended to arbitrary sets of masses. We show here that this ensemble can be cast into the same (algebraic) form as that of the $\beta = 1$ case, a fact that has already been pointed out by various authors, e.g. [Kho09; Kie10].

The Dirac matrix here is given by

$$\mathcal{D} \equiv \left(\begin{array}{c|c} 0 & A \\ \hline B^T & 0 \end{array}\right) \equiv \left(\begin{array}{c|c} 0 & P + \mu Q \\ \hline P^T - \mu Q^T & 0 \end{array}\right) \tag{C.1}$$

and the partition function by

$$\mathcal{Z}_N^{(N_f)} \propto \int dP\, dQ\, \exp\left[-n\,\mathrm{Tr}(PP^T + QQ^T)\right] \times \prod_{f=1}^{N_f} \det(\mathcal{D} + m_f \mathcal{I}). \tag{C.2}$$

The elements of $\mathcal{D}$, A, B, P and Q are quaternion-real, rather than real; otherwise, these equations are identical to eqs. (2.5) and (2.6) respectively, except that we omit the overall normalisation of $\mathcal{Z}_N^{(N_f)}$ and have allowed for an arbitrary scaling n in the exponent.

Generally it is more convenient (and, indeed, necessary for physical interpretation) to replace the N-by-$(N + \nu)$ quaternion-valued matrices P and Q with $2N$-by-$(2N + 2\nu)$ complex-valued matrices (with certain constraints on the elements) and to consider the eigenvalues of these complex matrices instead.

It can be shown that the partition function can be written in terms of the (Wishart) eigenvalues as follows:

$$\mathcal{Z}_N^{(N_f)} \propto \prod_{j=1}^{N} \int_{\mathbb{C}} d^2 z_j \, w(z_j) \prod_{k<l} |z_l - z_k|^2 \, |z_l - z_k^*|^2 \prod_{h=1}^{N} |z_h - z_h^*|^2 \times \prod_{f=1}^{N_f} m_f^{2\nu} \prod_{m=1}^{N} (z_m - m_f^2)(z_m^* - m_f^2), \tag{C.3}$$

where the weight function is given by

$$w(z) = w(z^*) = |z|^{2\nu} K_{2\nu}\left(\frac{n(1+\mu^2)}{2\mu^2}\,|z|\right) \exp\left\{\frac{n(1-\mu^2)}{4\mu^2}\,(z+z^*)\right\}. \tag{C.4}$$

Compared with eqs. 2.4 and 2.5 of [Ake05b], we have written the partition function as integrals over squared (Wishart) variables. $w(z)$ is a non-analytic function of z, depending on z^* as well as z. We choose this notation to parallel what we have done for the $\beta = 1$ case in Chapter 3. We also point out the fact that the JPDF in eq. (C.3) is positive everywhere, and so this model does not have the 'sign problem' associated with the $\beta = 1$ and $\beta = 2$ ensembles.

We note that the Jacobian which arose from the QZ decomposition can be written as follows (see [Kanz02])

$$\prod_{k<l} |z_l - z_k|^2 \, |z_l - z_k^*|^2 \prod_{h=1}^{N} |z_h - z_h^*|^2 \propto \Delta_{2N}(\{z, z^*\}) \prod_{h=1}^{N} (z_h - z_h^*), \tag{C.5}$$

noting that we have been able to drop all the modulus signs. We can also change the N-fold integral to run over $2N$ variables, constraining the additional variables to be the complex conjugates of the first set by inserting Dirac delta functions. We then have

$$\mathcal{Z}_N^{(N_f)} \propto \prod_{f=1}^{N_f} m_f^{2\nu} \prod_{j=1}^{2N} \int_{\mathbb{C}} d^2 z_j \prod_{p=1}^{(2N)/2} \mathcal{F}(z_{2p-1}, z_{2p}) \prod_{m=1}^{2N} \prod_{g=1}^{N_f} (z_m - m_g^2) \, \Delta_{2N}(\{z\}) \tag{C.6}$$

where our effective weight function

$$\mathcal{F}(z_1, z_2) = w(z_1)\,(z_1 - z_2)\,\delta(z_1 - z_2^*) \tag{C.7}$$

incorporates part of the Jacobian. This now has essentially the same form as eq. (4.14), and so all the (algebraic) results that we derived in Chapter 4 will carry over. For example, the quenched density of (Wishart) eigenvalues is given by eq. (4.76)

$$\begin{aligned} R_{1,N}(z) &= \int_{\mathbb{C}} d^2 z' \, \mathcal{K}_{2N}(z, z') \mathcal{F}(z', z) \\ &= (z^* - z)\, w(z) \mathcal{K}_{2N}(z, z^*), \end{aligned} \tag{C.8}$$

matching eq. 2.10 of [Ake05b] (after switching to consistent notation). $\mathcal{K}_{2N}(u, v)$ is the kernel corresponding to the $\beta = 4$ weight function $\mathcal{F}(z_1, z_2)$ in eq. (C.7) which in [Ake05b] is expressed in terms of the skew-orthogonal polynomials whose skew-orthogonality is explicitly demonstrated.

Appendix D

The $\beta = 1$ Ginibre ensemble: kernel and skew-orthogonal polynomials

The techniques introduced in §5.2 and §5.4 can also be used to determine the kernel and skew-orthogonal polynomials of the corresponding (non-chiral) Ginibre ensemble (GinOE). These results are already known (see [For08]) but the derivations presented here are new.

Our first aim is to calculate the expectation of the product of two characteristic polynomials

$$\mathcal{H}_N(\lambda, \gamma) \equiv \langle \det(\lambda - M) \, \det(\gamma - M^T) \rangle_N \tag{D.1}$$

where the matrix $M = S + vA$, $v^2 = \dfrac{1-\tau}{1+\tau}$, $\tau \in [0, 1]$, and the probability density is given by

$$p(M)\, dM = \mathcal{Z}_N^{-1} \exp\left\{ -\frac{1}{2(1+\tau)} \operatorname{Tr}(SS^T + AA^T) \right\} dS\, dA. \tag{D.2}$$

S is a symmetric matrix, A anti-symmetric, and S, A and M are all of size N-by-N.

As with the chiral case, we begin by replacing the determinants with Berezin

integrals using eq. (A.39):

$$\begin{aligned}\mathcal{H}_N(\lambda,\gamma) &= \mathcal{Z}_N^{-1}\int dS\,dA\int d\zeta\,d\eta\,\exp\Bigg\{-\frac{1}{2(1+\tau)}\left[(S_{ij})^2+(A_{ij})^2\right]\\ &\qquad -\lambda\zeta_i^*\zeta_i-\gamma\eta_i^*\eta_i+\zeta_i^*(S_{ij}+vA_{ij})\zeta_j+\eta_i^*(S_{ij}-vA_{ij})\eta_j\Bigg\}\\ &= \mathcal{Z}_N^{-1}\int dS\,dA\int d\zeta\,d\eta\,\exp\Bigg\{-\lambda\zeta_i^*\zeta_i-\gamma\eta_i^*\eta_i\\ &\qquad -\frac{1}{2(1+\tau)}S_{ij}^2+\left(\frac{\zeta_i^*\zeta_j+\eta_i^*\eta_j+\zeta_j^*\zeta_i+\eta_j^*\eta_i}{2}\right)S_{ij}\\ &\qquad -\frac{1}{2(1+\tau)}A_{ij}^2+v\left(\frac{\zeta_i^*\zeta_j-\eta_i^*\eta_j-\zeta_j^*\zeta_i+\eta_j^*\eta_i}{2}\right)A_{ij}\Bigg\},\end{aligned}\tag{D.3}$$

where all the implicit sums run over all $1\le i,j\le N$ (and not just over the independent elements of A and S). We now complete the squares (see eq. (A.44)), and integrate out the matrix elements:

$$\begin{aligned}\mathcal{H}_N(\lambda,\gamma) &= \int d\zeta\,d\eta\,\exp\Bigg\{-\lambda\zeta_i^*\zeta_i-\gamma\eta_i^*\eta_i\\ &\qquad +\frac{\left(\zeta_i^*\zeta_j+\eta_i^*\eta_j+\zeta_j^*\zeta_i+\eta_j^*\eta_i\right)^2}{8/(1+\tau)}+\frac{v^2\left(\zeta_i^*\zeta_j-\eta_i^*\eta_j-\zeta_j^*\zeta_i+\eta_j^*\eta_i\right)^2}{8/(1+\tau)}\Bigg\}\\ &= \int d\zeta\,d\eta\,\exp\Bigg\{-\lambda\zeta_i^*\zeta_i-\gamma\eta_i^*\eta_i\\ &\qquad +\delta_-^2(\zeta_i^*\zeta_j)(\eta_i^*\eta_j)+\delta_-^2(\zeta_i^*\zeta_j)(\zeta_j^*\zeta_i)+\delta_+^2(\zeta_i^*\zeta_j)(\eta_j^*\eta_i)\\ &\qquad +\delta_+^2(\eta_i^*\eta_j)(\zeta_j^*\zeta_i)+\delta_-^2(\eta_i^*\eta_j)(\eta_j^*\eta_i)+\delta_-^2(\zeta_j^*\zeta_i)(\eta_j^*\eta_i)\Bigg\}\\ &= \int d\zeta\,d\eta\,\exp\Bigg\{-\lambda\zeta_i^*\zeta_i-\gamma\eta_i^*\eta_i\\ &\qquad -\delta_-^2\left[(\zeta_i^*\zeta_i)(\zeta_j^*\zeta_j)+(\eta_i^*\eta_i)(\eta_j^*\eta_j)\right]\\ &\qquad -2\delta_-^2(\zeta_i^*\eta_i^*)(\zeta_j\eta_j)+2\delta_+^2(\zeta_i^*\eta_i)(\eta_j^*\zeta_j)\Bigg\},\end{aligned}\tag{D.4}$$

where

$$\delta_\pm^2\equiv\frac{(1+\tau)(1\pm v^2)}{4}.\tag{D.5}$$

We now perform two real and two complex Hubbard-Stratonovich transforms (see

eqs. (A.45) and (A.46) respectively), giving

$$\mathcal{H}_N(\lambda,\gamma) = \frac{1}{\pi^3}\int_{\mathbb{C}^2} d^2z\, d^2w \int_{\mathbb{R}^2} dx\, dy\, e^{-|z|^2-|w|^2-x^2-y^2} \times \int d\zeta\, d\eta\, \exp\Bigg\{ -\lambda\zeta_i^*\zeta_i - \gamma\eta_i^*\eta_i - 2i\delta_-\left(x\zeta_i^*\zeta_i + y\eta_i^*\eta_i\right) + i\sqrt{2}\left(\delta_- z\zeta_i^*\eta_i^* + \delta_-\bar{z}\zeta_j\eta_j + \delta_+ w\zeta_i^*\eta_i + \delta_+\bar{w}\eta_j^*\zeta_j\right)\Bigg\}. \tag{D.6}$$

The Berezin integrals decouple, and only terms in $\zeta^*\zeta\eta^*\eta$ survive the integration:

$$\mathcal{H}_N(\lambda,\gamma) = \frac{1}{\pi^3}\int_{\mathbb{C}^2} d^2z\, d^2w \int_{\mathbb{R}^2} dx\, dy\, e^{-|z|^2-|w|^2-x^2-y^2} \times \Big[(\lambda+2i\delta_- x)(\gamma+2i\delta_- y) + 2\delta_-^2|z|^2 + 2\delta_+^2|w|^2\Big]^N. \tag{D.7}$$

We can now use eq. (A.10) twice, first for the w-integral, and then for the z-integral, to give (where we now write δ_+ and δ_- in terms of τ)

$$\mathcal{H}_N(\lambda,\gamma) = \frac{N!}{\pi}\sum_{j=0}^{N}\tau^j\sum_{k=0}^{j}\frac{1}{\tau^k k!}\int_{\mathbb{R}} dx\, e^{-x^2}(\lambda+i\sqrt{2\tau}x)^k \int_{\mathbb{R}} dy\, e^{-y^2}(\gamma+i\sqrt{2\tau}y)^k. \tag{D.8}$$

Finally, we perform the two real integrals using eq. (A.5):

$$\mathcal{H}_N(\lambda,\gamma) = N!\sum_{j=0}^{N}\tau^j\sum_{k=0}^{j}\frac{1}{2^k k!}H_k\left(\frac{\lambda}{\sqrt{2\tau}}\right)H_k\left(\frac{\gamma}{\sqrt{2\tau}}\right), \tag{D.9}$$

where the $H_k(z)$ are the (physicists') Hermite polynomials. Because the Ginibre and chiral ensembles have similar algebraic structures, we can immediately write down the kernel for even N in terms of $\mathcal{H}_N(\lambda,\gamma)$ as (cf. eq. (5.20))

$$\mathcal{K}_N(u,v) = \frac{1}{h_{N/2-1}}(u-v)\,\mathcal{H}_{N-2}(u,v). \tag{D.10}$$

It is now straightforward to determine the skew-orthogonal polynomials for this ensemble. For the even case, we use eq. (4.29), and find that, as with the chiral case, only one term in the double sum survives the limiting process:

$$\begin{aligned} q_{2k}(z) &= h_k \lim_{u\to\infty}\frac{\mathcal{K}_{2k+2}(u,z)}{u^{2k+1}} \\ &= \lim_{u\to\infty}\frac{(u-z)\mathcal{H}_{2k}(u,z)}{u^{2k+1}} \\ &= \left(\frac{\tau}{2}\right)^k H_{2k}\left(\frac{z}{\sqrt{2\tau}}\right), \end{aligned} \tag{D.11}$$

where we used

$$\lim_{u\to\infty} u^{-N} H_N\left(\frac{u}{\alpha}\right) = \left(\frac{2}{\alpha}\right)^N. \tag{D.12}$$

For the odd case, we use eq. (4.30), together with the following two relationships for Hermite polynomials

$$\begin{aligned} \frac{d^{n-1}}{dz^{n-1}} H_n(z) &= 2^n n!\, z, \\ H_{n+1}(z) &= 2zH_n(z) - 2nH_{n-1}(z) \qquad \text{for } n \geq 1, \end{aligned} \tag{D.13}$$

to show that

$$\begin{aligned} q_{2k+1}(z) = &\left(\sqrt{\frac{\tau}{2}}\right)^{2k+1} H_{2k+1}\left(\frac{z}{\sqrt{2\tau}}\right) - 2k\left(\sqrt{\frac{\tau}{2}}\right)^{2k-1} H_{2k-1}\left(\frac{z}{\sqrt{2\tau}}\right) \\ &+ c\left(\sqrt{\frac{\tau}{2}}\right)^{2k} H_{2k}\left(\frac{z}{\sqrt{2\tau}}\right), \end{aligned} \tag{D.14}$$

in which c is some arbitrary constant. If we define the scaled functions

$$C_k(z) \equiv \left(\frac{\tau}{2}\right)^{\frac{k}{2}} H_k\left(\frac{z}{\sqrt{2\tau}}\right) \tag{D.15}$$

then we reobtain the simple result from [For07; For08]

$$\begin{aligned} q_{2k}(z) &= C_{2k}(z), \\ q_{2k+1}(z) &= C_{2k+1}(z) - 2kC_{2k-1}(z) + cC_{2k}(z). \end{aligned} \tag{D.16}$$

We should note that our derivation of the skew-orthogonal polynomials does not involve an explicit calculation of the skew-inner product. However, in itself, it does not allow one to determine the norms for the skew-orthogonal polynomials.

Notes

Here we state precisely which parts of this thesis correspond to results that we have already published (and in which paper), which parts are new, and which are adaptations of known results.

Chapter 3 covers the derivation of the joint probability density function (JPDF) from the matrix representation. §3.1 for the quenched case is based primarily on [Ake10a], although in this thesis we have streamlined the presentation in some places, and added further detail and clarification in others. §3.2 is then an easy extension to the unquenched case.

Chapter 4 concerns the algebraic structure of the ensemble, and begins in §4.1 with a proof of the factorisation of the JPDF published in [Ake10b]. §4.2 is a new presentation of known material regarding skew-orthogonal polynomials and kernels; although we had not seen the important eqs. (4.29) and (4.30) elsewhere in the literature, it is unlikely that these are new results. §4.3 is new to this thesis, although (as indicated there) it is essentially an adaption of known results to the chGinOE. §4.4 is also new (with the exception of the generalisation of the de Bruijn formula in §4.4.1, which we published in [Ake10b]), giving an alternative proof of the results in §4.3. §4.5 contains the straightforward extension to the unquenched case.

Chapter 5 derives the finite-N building blocks. The proof of the partition function for $N_f = 2$ in §5.1.1 was given in [Ake10a], although the proof in this thesis has been adapted to use the factorised JPDF derived in [Ake10b]. §5.1.2 and §5.1.3 then extend this result to the cases of general even and odd N_f. These are new self-contained proofs, although we gave alternative proofs in [Ake10b]. §5.2 was published in [Ake09a], although §5.2.2 contains a new proof (using the saddle point method) of a result published in [Ake10a]. §5.3 and §5.4 present results on the unquenched kernel, and the derivation of the skew-orthogonal polynomials. These results were given in [Ake10b], although the proofs differ in places.

Chapter 6 looks at the quenched densities at finite N. §6.1.1 was published in [Ake10a], although the remainder of this chapter is entirely new to this thesis.

Chapter 7 covers the strongly non-Hermitian limit, and was published in [Ake10a], but the results on the heights of the plateaux in §7.3 are new to this thesis.

In Chapter 8 we consider the weakly non-Hermitian limit. §8.1 and §8.2 are based on [Ake10a], although §8.2.4 on the behaviour of the weak kernel is new. A much shortened version of §8.3 is to be found in [Ake11], although §8.3.3 on the Hermitian limit of the real density is new.

§9.1 is new, but the remainder of Chapter 9, on the results for the unquenched ensemble, is based on [Ake11]; we have, however, given substantially more detail in this thesis, especially on the weakly non-Hermitian case in §9.3.

The Monte Carlo results on universality in Chapter 10 are previously unpublished.

Appendix A is also previously unpublished, although it is unlikely that any of the results here are entirely original.

Appendix B does contain new results on expressing skew-orthogonal polynomials as matrix expectations, although we gave alternative proofs of the same results in [Ake10b].

Appendix C, which shows how the $\beta = 4$ ensemble can be written in the same algebraic form as the $\beta = 1$ case, is not new material; we refer to [Ake10b] for details.

Appendix D on the Ginibre $\beta = 1$ ensemble shows how known results can be rederived using our newly developed techniques, and this material was published in [Ake09a; Ake10b].

Throughout this thesis, we have made extensive use of Mathematica [Wol08] for performing numerical integrations, for plotting graphs and for the preparation of diagrams. However, the Monte Carlo code used for the results in Chapter 10 was implemented in custom-written C++ code, using third-party open source libraries for the generation of pseudo-random numbers with the Mersenne Twister algorithm [MT] and for performing the eigenvalue decomposition of matrices [ALGLIB].

References

[Adl99] M. Adler, P.J. Forrester, T. Nagao and P. van Moerbeke, arXiv:solv-int/9907001.

[Ake97] G. Akemann, P.H. Damgaard, U. Magnea and S. Nishigaki, *Nucl. Phys.* **B 487** (1997) 721; [arXiv:hep-th/9609174].

[Ake98a] G. Akemann and P.H. Damgaard, *Nucl. Phys.* **B 528** (1998) 411; [arXiv:hep-th/9801133].

[Ake98b] G. Akemann and P.H. Damgaard, *Phys. Lett.* **B 432** (1998) 390; [arXiv:hep-th/9802174].

[Ake00] G. Akemann and E. Kanzieper, *Phys. Rev. Lett.* **85** (2000) 1174; [arXiv:hep-th/0001188].

[Ake01a] G. Akemann and E. Kanzieper, *Nucl. Phys.* **B** *(Proc. Suppl.)* **94** (2001) 681; [arXiv:hep-lat/0010092].

[Ake01b] G. Akemann, *Phys. Rev.* **D 64** (2001) 114021; [arXiv:hep-th/0106053].

[Ake02a] G. Akemann, *Phys. Rev. Lett.* **89** (2002) 072002; [arXiv:hep-th/0204068].

[Ake02b] G. Akemann, *Phys. Lett.* **B 547** (2002) 100; [arXiv:hep-th/0206086].

[Ake03a] G. Akemann, *J. Phys.* **A 36** (2003) 3363; [arXiv:hep-th/0204246].

[Ake03b] G. Akemann, *Acta Phys. Polon.* **B 34** (2003) 4653; [arXiv:hep-th/0307116].

[Ake04a] G. Akemann and P.H. Damgaard, *Phys. Lett.* **B 583** (2004) 199; [arXiv:hep-th/0311171].

[Ake04b] G. Akemann, Y.V. Fyodorov and G. Vernizzi, *Nucl. Phys.* **B 694** (2004) 59; [arXiv:hep-th/0404063].

[Ake05a] G. Akemann, J.C. Osborn, K. Splittorff and J.J.M. Verbaarschot, *Nucl. Phys.* **B 712** (2005) 287; [arXiv:hep-th/0411030].

[Ake05b] G. Akemann, *Nucl. Phys.* **B 730** (2005) 253; [arXiv:hep-th/0507156].

[Ake07a] G. Akemann and F. Basile, *Nucl. Phys.* **B 766** (2007) 150; [arXiv:math-ph/0606060].

[Ake07b] G. Akemann, P.H. Damgaard, J.C. Osborn and K. Splittorff, *Nucl. Phys.* **B 766** (2007) 34; [arXiv:hep-th/0609059].

[Ake07c] G. Akemann, *Int. J. Mod. Phys.* **22** (2007) 1077; [arXiv:hep-th/0701175].

[Ake07d] G. Akemann and E. Kanzieper, *J. Stat. Phys.* **129** (2007) 1159; [arXiv:math-ph/0703019].

[Ake08a] G. Akemann, J. Bloch, L. Shifrin and T. Wettig, *Phys. Rev. Lett.* **100** (2008) 032002; [arXiv:0710.2865].

[Ake08b] G. Akemann and P.H. Damgaard, *JHEP* **0803** (2008) 073; [arXiv:0803.1171].

[Ake09a] G. Akemann, M.J. Phillips and H.-J. Sommers, *J. Phys.* **A 42** (2009) 012001; [arXiv:0810.1458].

[Ake09b] G. Akemann, M.J. Phillips and L. Shifrin, *J. Math. Phys.* **50** (2009) 063504; [arXiv:0901.0897].

[Ake09c] G. Akemann, E. Bittner, M.J. Phillips and L. Shifrin, *Phys. Rev.* **E 80** (2009) 065201 (R); [arXiv:0907.4195].

[Ake10a] G. Akemann, M.J. Phillips and H.-J. Sommers, *J. Phys.* **A 43** (2010) 085211; [arXiv:0911.1276].

[Ake10b] G. Akemann, M. Kieburg and M.J. Phillips, *J. Phys.* **A 43** (2010) 375207; [arXiv:1005.2983].

[Ake11] G. Akemann, T. Kanazawa, M.J. Phillips and T. Wettig, *JHEP* **1103** (2011) 066; [arXiv:1012.4461].

[ALGLIB] ALGLIB version 3.0.0 (C++ source code library for numerical analysis), `www.alglib.net`, [*Downloaded on 29th October 2010*].

[Ban80] T. Banks and A. Casher, *Nucl. Phys.* **B 169** (1980) 103.

[Bas07] F. Basile and G. Akemann, *JHEP* **0712** (2007) 043; [arXiv:0710.0376].

[Ber98] M.E. Berbenni-Bitsch, S. Meyer and T. Wettig, *Phys. Rev.* **D 58** (1998) 071502; [arXiv:hep-lat/9804030].

[Blo09a] J. Bloch and T. Wettig, *JHEP* **0903** (2009) 100; [arXiv:0812.0324].

[Blo09b] J. Bloch and T. Wettig, *PoS* **LAT2009** (2009) 186; [arXiv:0910.1206].

[Boh84] O. Bohigas, M.J. Giannoni and C. Schmit, *Phys. Rev. Lett.* **52** (1984) 1.

[Bor07] A. Borodin and C.D. Sinclair, arXiv:0706.2670.

[Bor09] A. Borodin and C.D. Sinclair, *Commun. Math. Phys.* **291** (2009) 177; [arXiv:0805.2986].

[Bou09] J.-P. Bouchaud and M. Potters, arXiv:0910.1205; to appear in *The Oxford Handbook of Random Matrix Theory*, eds. G. Akemann, J. Baik and P. Di Francesco, Oxford University Press, Oxford (2011).

[Bru09] W. Bruzda, V. Cappellini, H.-J. Sommers and K. Zyczkowski, *Phys. Lett.* **A 373** (2009) 320; [arXiv:0804.2361].

[Con00] J.B. Conrey, arXiv:math/0005300.

[Dam98a] P.H. Damgaard and S.M. Nishigaki, *Nucl. Phys.* **B 518** (1998) 495; [arXiv:hep-th/9711023].

[Dam98b] P.H. Damgaard, arXiv:hep-th/9807026.

[Dam99] P.H. Damgaard, J.C. Osborn, D. Toublan and J.J.M. Verbaarschot, *Nucl. Phys.* **B 547** (1999) 305; [arXiv:hep-th/9811212].

[Dam01] P.H. Damgaard and S.M. Nishigaki, *Phys. Rev.* **D 63** (2001) 045012; [arXiv:hep-th/0006111].

[Dam02] P.H. Damgaard, *Nucl. Phys. Proc. Suppl.* **106** (2002) 29; [arXiv:hep-lat/0110192].

[deB55] N.G. de Bruijn, *J. Indian Math. Soc.* **19** (1955) 133.

[Dei00] P. Deift, *Orthogonal Polynomials and Random Matrices: a Riemann-Hilbert Approach*, American Mathematical Society, Providence, USA (2000).

[desC73] J. des Cloizeaux and M.L. Mehta, *J. Math. Phys.* **14** (1973) 1648.

[DiF95] P. Di Francesco, P. Ginsparg and J. Zinn-Justin, *Phys. Rep.* **254** (1995) 1; [arXiv:hep-th/9306153].

[Dys62a] F.J. Dyson, *J. Math. Phys.* **3** (1962) 140.

[Dys62b] F.J. Dyson, *J. Math. Phys.* **3** (1962) 157.

[Dys62c] F.J. Dyson, *J. Math. Phys.* **3** (1962) 166.

[Dys62d] F.J. Dyson, *J. Math. Phys.* **3** (1962) 1191.

[Dys62e] F.J. Dyson, *J. Math. Phys.* **3** (1962) 1199.

[Dys70] F.J. Dyson, *Commun. Math. Phys.* **19** (1970) 235.

[Ede94] A. Edelman, E. Kostlan and M. Shub, *J. Amer. Math. Soc.* **7** (1994) 247.

[Ede97] A. Edelman, *J. Multivariate Anal.* **60** (1997) 203.

[Efe97a] K. Efetov, *Supersymmetry in Disorder and Chaos*, Cambridge University Press, London (1997).

[Efe97b] K.B. Efetov, *Phys. Rev. Lett.* **79** (1997) 491; [arXiv:cond-mat/9702091].

[Eyn01] B. Eynard, *J. Phys.* **A 34** (2001) 7591; [arXiv:cond-mat/0012046].

[For03] P.J. Forrester, N.C. Snaith and J.J.M. Verbaarschot, *J. Phys.* **A 36** (2003) R1; [arXiv:cond-mat/0303207].

[For07] P.J. Forrester and T. Nagao, *Phys. Rev. Lett.* **99** (2007) 050603; [arXiv:0706.2020].

[For08] P.J. Forrester and T. Nagao, *J. Phys.* **A 41** (2008) 375003; [arXiv:0806.0055].

[For09] P.J. Forrester and A. Mays, *J. Stat. Phys.* **134** (2009) 443; [arXiv:0809.5116].

[Fyo97a] Y.V. Fyodorov, B.A. Khoruzhenko and H.-J. Sommers, *Phys. Lett.* **A 226** (1997) 46; [arXiv:cond-mat/9606173].

[Fyo97b] Y.V. Fyodorov, B.A. Khoruzhenko and H.-J. Sommers, *Phys. Rev. Lett.* **79** (1997) 557; [arXiv:cond-mat/9703152].

[Fyo98] Y.V. Fyodorov, B.A. Khoruzhenko and H.-J. Sommers, *Ann. Inst. Henri Poincaré* **68** (1998) 449; [arXiv:chao-dyn/9802025].

[Fyo03] Y.V. Fyodorov and H.-J. Sommers, *J. Phys.* **A 36** (2003) 3303; [arXiv:nlin.CD/0207051].

[Gau61] M. Gaudin, *Nucl. Phys.* **25** (1961) 447.

[Gho02] S. Ghosh and A. Pandey, *Phys. Rev.* **E 65** (2002) 046221.

[Gho09] S. Ghosh, *Skew-orthogonal Polynomials and Random Matrix Theory*, American Mathematical Society, Providence, USA (2009).

[Gin65] J. Ginibre, *J. Math. Phys.* **6** (1965) 440.

[Gir84] V.L. Girko, *Russian Math. Surveys* **40** (1984) 77.

[Gra07] I.S. Gradshteyn and I.M. Ryzhik, *Table of Integrals, Series and Products*, 7th edition, Elsevier (2007).

[Guh98] T. Guhr, A. Müller-Groeling and H.A. Weidenmüller, *Phys. Rep.* **299** (1998) 189; [arXiv:cond-mat/9707301].

[Haa01] F. Haake, *Quantum Signatures of Chaos*, 2nd edition, Springer, Berlin (2001).

[Hal95] M.A. Halasz and J.J.M. Verbaarschot, *Phys. Rev.* **D 52** (1995) 2563; [arXiv:hep-th/9502096].

[Hal97] M.A. Halasz, J.C. Osborn and J.J.M. Verbaarschot, *Phys. Rev.* **D 56** (1997) 7059; [arXiv:hep-lat/9704007].

[Han08] J. Han and M.A. Stephanov, *Phys. Rev.* **D 78** (2008) 054507; [arXiv:0805.1939].

[Heu07] S. Heusler, S. Müller, A. Altland, P. Braun and F. Haake, *Phys. Rev. Lett.* **98** (2007) 044103.

[Hos01] A. Hosaka and H. Toki, *Quarks, Baryons and Chiral Symmetry*, World Scientific, Singapore (2001).

[Jan03] R.A. Janik and M.A. Nowak, *J. Phys.* **A 36** (2003) 3629; [arXiv:math-ph/0112017].

[Kana10] T. Kanazawa, T. Wettig and N. Yamamoto, *Phys. Rev.* **D 81** (2010) 081701; [arXiv:0912.4999].

[Kanz02] E. Kanzieper, *J. Phys.* **A 35** (2002) 6631; [arXiv:cond-mat/0109287].

[Kanz05] E. Kanzieper and G. Akemann, *Phys. Rev. Lett.* **95** (2005) 230201; [arXiv:math-ph/0507058].

[Kanz09] E. Kanzieper, arXiv:0909.3198; to appear in *The Oxford Handbook of Random Matrix Theory*, eds. G. Akemann, J. Baik and P. Di Francesco, Oxford University Press, Oxford (2011).

[Kea03] J.P. Keating and N.C. Snaith, *J. Phys.* **A 36** (2003) 2859.

[Kho09] B.A. Khoruzhenko and H.-J. Sommers, arXiv:0911.5645; to appear in *The Oxford Handbook of Random Matrix Theory*, eds. G. Akemann, J. Baik and P. Di Francesco, Oxford University Press, Oxford (2011).

[Kie10] M. Kieburg and T. Guhr, *J. Phys.* **A 43** (2010) 135204; [arXiv:0912.0658].

[Kle00] B. Klein and J.J.M. Verbaarschot, *Nucl. Phys.* **B 588** (2000) 483; [arXiv:hep-th/0004119].

[Kog04] J.B. Kogut and M.A. Stephanov, *The Phases of Quantum Chromodynamics*, Cambridge University Press, Cambridge (2004).

[Kwa06] J. Kwapien, S. Drozdz, A.Z. Gorski and P. Oswiecimka, *Acta Phys. Pol.* **B 37** (2006) 3039; [arXiv:physics/0605115].

[Lehm91] N. Lehmann and H.-J. Sommers, *Phys. Rev. Lett.* **67** (1991) 941.

[Lehn09] C. Lehner, M. Ohtani, J.J.M. Verbaarschot and T. Wettig, *Phys. Rev.* **D 79** (2009) 074016; [arXiv:0902.2640].

[Mag00] U. Magnea, *Phys. Rev.* **D 62** (2000) 016005; [arXiv:hep-th/9912207].

[Mah91] G. Mahoux and M.L. Mehta, *J. Phys. I France* **1** (1991) 1093.

[Meh60a] M.L. Mehta, *Nucl. Phys.* **18** (1960) 395.

[Meh60b] M.L. Mehta and M. Gaudin, *Nucl. Phys.* **18** (1960) 420.

[Meh04] M.L. Mehta, *Random Matrices*, 3rd edition, Elsevier, London (2004).

[Mon73] H.L. Montgomery, *Proc. Sympos. Pure Math.* **24** (1973) 181.

[MT] M. Matsumoto and T. Nishimura, Mersenne Twister (C++ code implementation), `www.math.sci.hiroshima-u.ac.jp/~m-mat/MT/MT2002/emt19937ar.html`, [*Downloaded on 29th October 2010*].

[Nag00a] T. Nagao and S.M. Nishigaki, *Phys. Rev.* **D 62** (2000) 065006; [arXiv:hep-th/0001137].

[Nag00b] T. Nagao and S.M. Nishigaki, *Phys. Rev.* **D 62** (2000) 065007; [arXiv:hep-th/0003009].

[Nag01] T. Nagao and S.M. Nishigaki, *Phys. Rev.* **D 63** (2001) 045011; [arXiv:hep-th/0005077].

[Nis96] S. Nishigaki, *Phys. Lett.* **B 387** (1996) 139; [arXiv:hep-th/9606099].

[Nis98] S.M. Nishigaki, P.H. Damgaard and T. Wettig, *Phys. Rev.* **D 58** (1998) 087704; [arXiv:hep-th/9803007].

[Now96] M.A. Nowak, M. Rho and I. Zahed, *Chiral Nuclear Dynamics*, World Scientific, Singapore (1996).

[Osb99] J.C. Osborn, D. Toublan and J.J.M. Verbaarschot, *Nucl. Phys.* **B 540** (1999) 317; [arXiv:hep-th/9806110].

[Osb04] J.C. Osborn, *Phys. Rev. Lett.* **93** (2004) 222001; [arXiv:hep-th/0403131].

[Osb05] J.C. Osborn, K. Splittorff and J.J.M. Verbaarschot, *Phys. Rev. Lett.* **94** (2005) 202001; [arXiv:hep-th/0501210].

[Osb08a] J.C. Osborn, K. Splittorff and J.J.M. Verbaarschot, *Phys. Rev.* **D 78** (2008) 065029; [arXiv:0805.1303].

[Osb08b] J.C. Osborn, K. Splittorff and J.J.M. Verbaarschot, *Phys. Rev.* **D 78** (2008) 105006; [arXiv:0807.4584].

[Rho08] M. Rho, *Chiral Nuclear Dynamics II*, World Scientific, Singapore (2008).

[Rip97] G. Ripka, *Quarks Bound by Chiral Fields*, Oxford University Press, Oxford (1997).

[Sen98] M.K. Sener and J.J.M. Verbaarschot, *Phys. Rev. Lett.* **81** (1998) 248.

[Shu93] E.V. Shuryak and J.J.M. Verbaarschot, *Nucl. Phys.* **A 560** (1993) 306; [arXiv:hep-th/9212088].

[Shu04] E.V. Shuryak, *The QCD Vacuum, Hadrons and Superdense Matter*, 2nd edition, World Scientific, Singapore (2004).

[Sin06] C.D. Sinclair, *Int. Math. Res. Not.* **2007** (2007) rnm015; [arXiv:math-ph/0605006].

[Sin09] C.D. Sinclair, *J. Stat. Phys.* **136** (2009) 17; [arXiv:0811.1276].

[Smi01] A. Smilga, *Lectures on Quantum Chromodynamics*, World Scientific, Singapore (2001).

[Somm88] H.-J. Sommers, A. Crisanti, H. Sompolinsky and Y. Stein, *Phys. Rev. Lett.* **60** (1988) 1895.

[Somm07] H.-J. Sommers, *J. Phys.* **A 40** (2007) F671; [arXiv:0706.1671].

[Somm08] H.-J. Sommers and W. Wieczorek, *J. Phys.* **A 41** (2008) 405003; [arXiv:0806.2756].

[Somp88] H. Sompolinsky, A. Crisanti and H.-J. Sommers, *Phys. Rev. Lett.* **61** (1988) 259.

[Spl06] K. Splittorff and J.J.M. Verbaarschot, *Nucl. Phys.* **B 757** (2006) 259; [arXiv:hep-th/0605143].

[Spl07] K. Splittorff and J.J.M. Verbaarschot, *Phys. Rev.* **D 75** (2007) 116003; [arXiv:hep-lat/0702011].

[Spl08] K. Splittorff and J.J.M. Verbaarschot, arXiv:0809.4503.

[Ste96] M.A. Stephanov, *Phys. Rev. Lett.* **76** (1996) 4472; [arXiv:hep-lat/9604003].

[Ste01] M.A. Stephanov, J.J.M. Verbaarschot and T. Wettig, in *Wiley Encyclopedia of Electrical and Electronics Engineering*, Supplement 1 (2001); [arXiv:hep-ph/0509286].

[Sto99] H.-J. Stöckmann, *Quantum Chaos*, Cambridge University Press, London (1999).

[Tou99] D. Toublan and J.J.M. Verbaarschot, *Nucl. Phys.* **B 560** (1999) 259; [arXiv:hep-th/9904199].

[Tra00] C.A. Tracy and H. Widom, in *Integrable Systems: From Classical to Quantum*, CRM Proceedings and Lecture Notes, **26**, eds. J. Harnad, G. Sabidussi and P. Winternitz, Amer. Math. Soc., Providence (2000) 251; [arXiv:math-ph/9909001].

[Ver93] J.J.M. Verbaarschot and I. Zahed, *Phys. Rev. Lett.* **70** (1993) 3852; [arXiv:hep-th/9303012].

[Ver94a] J. Verbaarschot, *Acta Phys. Polon.* **B 25** (1994) 133; [arXiv:hep-th/9310049].

[Ver94b] J. Verbaarschot, *Phys. Rev. Lett.* **72** (1994) 2531; [arXiv:hep-th/9401059].

[Ver94c] J. Verbaarschot, *Nucl. Phys.* **B 426** (1994) 559; [arXiv:hep-th/9401092].

[Ver94d] J. Verbaarschot, *Nucl. Phys.* **B 427** (1994) 534; [arXiv:hep-lat/9402006].

[Ver94e] J. Verbaarschot, *Phys. Lett.* **B 329** (1994) 351; [arXiv:hep-th/9402008].

[Ver94f] J.J.M. Verbaarschot and I. Zahed, *Phys. Rev. Lett.* **73** (1994) 2288; [arXiv:hep-th/9405005].

[Ver94g] J. Verbaarschot, arXiv:hep-th/9405006.

[Ver96] J.J.M. Verbaarschot, *Phys. Lett.* **B 368** (1996) 137; [arXiv:hep-ph/9509369].

[Ver00] J.J.M. Verbaarschot and T. Wettig, *Ann. Rev. Nucl. Part. Sci.* **50** (2000) 343; [arXiv:hep-ph/0003017].

[Ver04] J. Verbaarschot, arXiv:hep-th/0410211.

[Ver09] J.J.M. Verbaarschot, arXiv:0910.4134; to appear in *The Oxford Handbook of Random Matrix Theory*, eds. G. Akemann, J. Baik and P. Di Francesco, Oxford University Press, Oxford (2011).

[Wig51] E.P. Wigner, *Math. Proc. Cambr. Philos. Soc.* **47** (1951) 790.

[Wig55] E.P. Wigner, *Annal. Math.* **62** (1955) 548.

[Wig58] E.P. Wigner, *Annal. Math.* **67** (1958) 325.

[Wil98] T. Wilke, T. Guhr and T. Wettig, *Phys. Rev.* **D 57** (1998) 6486; [arXiv:hep-th/9711057].

[Wis28] J. Wishart, *Biometrika* **20A** (1928) 32.

[Wol08] Wolfram Research Inc., *Mathematica*, Version 7.0, Champaign, IL (2008).

[Ynd06] F.J. Yndurain, *The Theory of Quark and Gluon Interactions*, 4th edition, Springer, Berlin (2006).

[Zuk94] J.A. Zuk, arXiv:cond-mat/9412060.

`Version stamp: BURA-FINAL-20110327`